Hsp90 as a molecular target

By

Chinmay Munje

A thesis submitted to the University of Central Lancashire in partial fulfilment of the requirements for the degree of Doctor of Philosophy

Month Year submitted

Declaration

I declare that while registered as a candidate for this degree I have not been registered as a candidate for any other award from an academic institution. The work present in this thesis, except where otherwise stated, is based on my own research and has not been submitted previously for any other award in this or any other University.

Signed

Abstract

Heat shock protein 90 (Hsp90), a highly conserved molecular chaperone, has been proposed to play a vital role in tumorigenesis. Hsp90 has two isoforms, of which Hsp90α is the major isoform of the Hsp90 complex and has an inducible expression profile. The molecular chaperone Hsp90α has been recognized in different cancers and it is implicated to play a role in cell cycle progression, apoptosis, regulates invasion, angiogenesis and metastasis. It is being recognized as a promising target in cancer treatment. Previous studies in our laboratory have demonstrated *hsp90α* expression in both primary glioma tissue and cell lines, but not in normal healthy brain tissues and cell lines. Enhanced chemosensitivity was observed upon specific inhibition of *hsp90α* expression by siRNA, suggesting that inhibiting *hsp90α* expression could possibly be a favourable therapeutic approach compared to conventional chemotherapies. In this novel study, Hsp90 was inhibited by either treatment with 17AAG or shRNA oligonucleotide targeting *hsp90α* (sh*hsp90α*) in the U87-MG glioma cell line. The inhibition profile of Hsp90α was observed at the protein levels in control and treated cells by FACS analysis (quantitative) using a flow cytometer and Hsp90α ELISA kit. The results demonstrated a significant reduction of Hsp90α protein levels post treatment with 17AAG and sh*hsp90α*. The activity of Hsp90α was assayed by quantifying the levels of Akt/PKB in the samples. Significant reductions (>50 %) of Akt/PKB levels were observed post *hsp90α* inhibition. Cell cycle analysis carried out reported S and G2 phase arrest, post Hsp90 inhibition by either 17AAG or sh*hsp90α*. Interestingly, it was reported that 17AAG shows a better silencing profile compared to sh*hsp90α*.

To analyse the downstream effects of Hsp90 inhibition and to determine the client proteins affected, proteomic analysis was performed. Proteomic analysis identified several proteins which were either upregulated/downregulated post Hsp90 inhibition. IPA analysis further identified “cancer” as the top network significantly transformed post Hsp90 inhibition. Upregulated proteins include Hsp70 family members, Hsp27 and gp96, thereby suggesting the role of Hsp90 co-chaperones in compensating for Hsp90 function post Hsp90 inhibition. Moreover, members of the glycolysis/glucogenesis pathway were also upregulated, demonstrating increased dependency on glycolysis for

energy supply by the treated glioma cells. Considering Hsp70 and its role in anti-apoptosis, it was postulated that a combination therapy involving a multi-target approach could be carried out. Subsequently, inhibition of both Hsp90 and Hsp70 in U87-MG glioma cell line was carried out resulting in 60 % cell death along with S and G2 phase arrest. Thus, in the effective treatment of glioma, the inhibition of multiple targets needs to be taken into consideration.

Conclusion: It can be thus concluded that, combination therapy involving silencing of Hsp90 and Hsp70 could be of possible significance in glioma therapy.

To My Loving Family

Index

Declaration.....2

Abstract.....3

Index.....6

List of Figures.....10

List of Tables.....13

Acknowledgements.....15

Abbreviations..... 17

CHAPTER 1 INTRODUCTION.....23

1.1 Hsp90 protein.....30

1.2 Hsp90 ATPase Activity.....32

1.3 Hsp90 super chaperone.....33

1.4 Hsp90 isoforms.....35

1.5 Hsp90 the cancer chaperone 37

1.6 Glioma and Hsp90 38

1.6.1 Hsp90 in our laboratory 40

1.7 Hsp90 inhibitors 41

1.8 Summary.....45

1.9 Research question.....47

1.10 Aims and objectives.....47

CHAPTER 2 MATERIALS AND METHODS.....49

2.1 Cell Culture.....50

2.1.1 Cell lines.....50

2.1.2 Media and reagents.....50

2.1.3Resuscitation of frozen cells.....54

2.1.5 Cell Quantification.....56

2.2 mRNA ISOLATION.....57

2.3 Quantification of nucleic acid by spectrophotometer.....62
2.4 Analysis of nucleic acid (RNA and DNA) by agarose gel electrophoresis.....62
2.4.1 Alkaline (denatured) agarose gel electrophoresis for mRNA analysis.....63
2.4.2 Agarose gel electrophoresis for PCR amplicons.....64
2.4.3 Agarose gel documentation and analysis.....66
2.5 Complementary DNA synthesis (cDNA).....67
2.6 Quantitive real time polymerase chain reaction (qRT-PCR).....69
2.7 Analysis of qRT-PCR product.....73
2.7.1 Agarose gel electrophoresis.....73
2.7.2 Quantification analysis of qRT-PCR.....73
2.8 Antibody Information.....75
2.9 Akt/PKB Kinase activity assay.....77
2.9.1 Standard Curve.....78
2.9.2 Assay Procedure.....79
2.10 Hsp90α ELisa assay.....79
2.11 Cell viability assay.....81
2.12 Cell cycle analysis.....82
2.13 Flow cytometry.....83
2.13.1 Sample preparation.....83
2.13.2. Data analysis.....85
2.14 Statistical analysis.....86

CHAPTER 3 Hsp90α SILENCING BY RNAi.....87

3.1 Introduction.....88
3.1.1 RNA interference for cancer.....89
3.1.2 siRNA and shRNA.....91
3.2 Bioinformatics.....98
3.2.1 Gene mRNA Sequence.....99
3.2.2 Primer design.....100
3.2.3 shRNA Construct.....101
3.3 Materials and method.....101

3.3.1 Cell culture and shRNA treatment 102
3.3.2 Megatran 105
3.3.3 Puromycin 106
3.3.4 Statistical Analysis.....106
3.4 Results 107
3.4.1 Bioinformatics 107
3.4.2 Puromycin 114
3.4.3 mRNA, cDNA and qRT-PCR 115
3.4.4 Akt/PKB Kinase acitivity assay 121
3.5.Discussion 123
3.6 Conclusion 126

CHAPTER 4 PROTEOME CHANGE IN U87-MG POST Hsp90 SILENCING.....127
4.1 Introduction 128
4.1.1 Hsp90 and proteomic studies.....132
4.1.2 Summary.....134
4.2 Proteomics 136
4.2.1 Fluorescence difference gel electrophoresis (2D-DIGE) 137
4.2.2 Mass spectrophometry analysis 139
4.2.3 Database search 140
4.2.4 Ingenuity pathway analysis (IPA).....141
4.3 Materials and methods 142
4.3.1 Protein extraction for proteomic analysis.....142
4.3.2 Protein quantification.....143
4.3.3 Statistical Analysis 144
4.4 Results 145
4.4.1 Cell viability using 17AAG 145
4.4.2 Akt/PKB Kinase acitivity assay 146
4.4.3 Hsp90α Elisa assay.....147
4.4.4 Flow cytometery.....148
4.4.5 Cell cycle analysis 150

4.4.6 Proteomics analysis 152
4.4.8 Bioinformatic analysis 163
4.5 Discussion 166
4.6 Conclusion 186

CHAPTER 5 COMBINATION THERAPY TARGETING Hsp90 AND Hsp70 IN U87-MG GLIOMA CELL LINE.....187

5.1 Introduction 188
5.2. Materials and methods 192
5.3 Results 193
5.3.1 Cell viability using KNK437 193
5.3.2 Cell viability using 17AAG and KNK437 194
5.3.3 Cell cycle analysis 195
5.4 Discussion 199
5.5 Conclusion 201

CHAPTER 6 GENERAL DISCUSSION, CONCLUSION AND FUTURE WORK.....202

6.1 General discussion and conclusion 203
6.2 Future work 211

CHAPTER 7 References.....213
APPENDIX.....255

List of Figures

Figure 1.1: Protein folding pathways involving Hsp90 and Hsp70..... 26

Figure 1.2: The ATPase cycle of Hsp90..... 31

Figure 1.3: Equilibrium between latent and activated state..... 32

Figure 1.4: Hsp90 involved in apoptotic pathway..... 34

Figure 1.5: Hsp90 function..... 35

Figure 1.6: The intron/exon structure of Hsp90 isoforms..... 36

Figure 1.7: Chemical structures of Hsp90 inhibitors..... 42

Figure 1.8: Fixation sites of several inhibitors in case of Hsp90..... 44

Figure 2.1: Loading the haemocytometer and the middle square which is used for cell counting..... 56

Figure 2.2: Figure adapted from Roche Diagnostics, UK for mRNA isolation..... 58

Figure 2.3: Standards used to generate the copy numbers for each gene..... 74

Figure 2.4: A histogram graph demonstrating flow cytometric data..... 85

Figure 3.1: RNAi mechanism..... 90

Figure 3.2: siRNA and shRNA pathways..... 93

Figure 3.3: A comparison between siRNA and shRNA..... 96

Figure 3.4: Interaction of Hsp90 protein with Akt/PKB kinase..... 98

Figure 3.5: pGFP-V-RS vector map..... 103

Figure 3.5: Location of *hsp90α* denoted by red bar..... 107

Figure 3.6: Entrez gene database output on a gene search for *hsp90α*..... 108

Figure 3.7: Complete sequence of mRNA sequence of Hsp90α..... 109

Figure 3.8: The output file of Primer3 Plus provides an independent set of left and right primer and also shows the alignment of the primer on the sequence..... 110

Figure 3.9: shRNA oligonucleotides against Hsp90α mRNA transcript..... 114

Figure 3.10: Cell viability assessment of 1321N1, GOS-3 and U87-MG

with increasing concentrations of puromycin (0.2 – 1 µg/ml)..... 114

Figure 3.11: Alkaline gel electrophoresis mRNA isolated from glioma cell lines..... 116

Figure 3.12: Gene expression of *hsp90α* and *GAPDH* in glioma cell lines..... 117

Figure 3.13: shRNA construct 2..... 118

Figure 3.14: Gene expression of *hsp90α* and *GAPDH* in glioma cell lines treated with shRNA

constructs..... 120

Figure 3.15: Standard graph for Akt/PKB Kinase activity assay..... 121

Figure 4.1: Chemical structures of GA and its derivates..... 130

Figure 4.2: Hsp90 chaperone cycle..... 131

Figure 4.3: Overview of proteomic strategies..... 137

Figure 4.4: Typical workflow of 2D-DIGE using DeCyder..... 139

Figure 4.5: Standard graph for protein quantification..... 144

Figure 4.6: Cell viability assessment of U87-MG with increasing concentrations of 17AAG

(0.25 – 1.5 µM)..... 145

Figure 4.7: Standard graph for Hsp90α ELISA assay..... 147

Figure 4.8: Flow cytometric analysis of control and treated U87-MG cell line for Hsp90α

detection..... 149

Figure 4.9: Cell cycle analysis of U87-MG control and treated glioma cell line..... 151

Figure 4.10: Different stages of cell cycle affected post inhibition of Hsp90..... 152

Figure 4.11: 2D-DIGE protein profile..... 154

Figure 4.12: Functional network analysis by IPA..... 164

Figure 5.1: Structure of KNK437..... 191

Figure 5.2: Cell viability assessment of U87-MG with increasing concentrations of KNK437

(10 – 100 nM)..... 193

Figure 5.3: Cell viability assessment of U87-MG with 17AAG

and KNK437..... 194

Figure 5.4: Cell cycle analysis of U87-MG control and treated

glioma cell line..... 195

Figure 5.5: Different stages of cell cycle affected post inhibition of Hsp90 and Hsp70..... 197

Figure 6.1: Schematic model summarizing the main findings..... 210

List of Tables

Table 1.1: Examples of Hsp90 client proteins..... 27

Table 1.2: Differences in the function and expression of Hsp90 isoforms..... 37

Table 1.3: Hsp90 binding drugs..... 44

Table 1.4: Use of Hsp90 Inhibitors in cancers..... 45

Table 2.1: Media and supplements used in cell culture..... 51

Table 2.2: Reagents and chemicals used in cell culture..... 53

Table 2.3: Volume of reagents and buffer..... 59

Table 2.4: Materials and reagents adjusted for the number of cells for mRNA isolation..... 60

Table 2.5: Materials and reagents used for agarose gel electrophoresis..... 65

Table 2.6: Reagents provided with the kit for cDNA synthesis..... 68

Table 2.7: The composition and quantity of each reagent provided within the LightCycler® FastStart DNA MasterPLUS SYBR Green I kit..... 70

Table 2.8: The quantities of reagents required for each RT-PCR reaction using those provided within the LightCycler® FastStart DNA MasterPLUS SYBR Green I kit..... 70

Table 2.9: qRT-PCR conditions used as default conditions for all amplifications..... 72

Table 2.10: Genomic DNA corresponded to its average Ct values and equivalent copy number... 75

Table 2.11: Reagents and its concentration used for cell-cycle analysis..... 83

Table 3.1: The *hsp90α* and *GAPDH* primers [designed using Primer3 software and commercially synthesised by TIB MOLBIOL syntheselabor (Berlin, Germany)] used in qRT-PCR..... 111

Table 3.2: Spectrophotometry reading for three glioma cell lines..... 115

Table 3.3: Determination of kinase activity according to Akt/PKB Kinase Activity Assay Kit..... 122

Table 4.1: Determination of kinase activity according to Akt/PKB Kinase Activity Assay Kit..... 146

Table 4.2: Determination of Hsp90α protein level according to Hsp90α ELISA Kit..... 148

Table 4.3: Hsp90α quantification by flow cytometric analysis..... 150

Table 4.4: Cell cycle analysis of U87-MG control and treated glioma cell line..... 151

Table 4.5: Proteins identified by mass spectrophotometry..... 155

Table 4.6: Molecular and biological function with location of proteins identified by mass spectrophotometry using Human Protein Research Database..... 159

Table 4.8: Top biofunctions generated by IPA..... 165

Table 5.1: Cell cycle analysis of U87-MG control and treated glioma cell line..... 196

Acknowledgements

|| Adnyaanatimiraandhasya Dnyaanajanashalaakayaa ||

|| Chakshurunmiilitaan Yena Tasmai ShriGurave Namah ||

The above Sanskrit mantra stands for “Salutation to the noble Guru, who has opened the eyes blinded by darkness of ignorance with the collyrium-stick of knowledge” and with this, I would first and foremost like to thank my supervisor-my mentor-my guru, Dr. Amal Shervington for her constant support and guidance. She has been a pillar of inspiration and her willingness to motivate has contributed tremendously to this project. She has always encouraged me to not just grow as an experientialist but also as an independent thinker. I could not have imagined a better advisor and mentor for my PhD study and would always be grateful to her. For everything you have done for me, Dr. Amal Shervington, I thank you.

I would also like to thank Dr. Leroy Shervington for patiently reading through the countless draft copies and for commenting on this manuscript. He has always consoled me when things didn’t go the right way and has been a great support.

A special thanks to my colleagues, Zarine Khan, Dipti Thakkar, Adi Mehta and Dr. Rahima Patel for being with me whenever I needed them. They have always guided me and helped me overcome any hurdles that I faced.

I would also like to thank my friends who have stuck to me in my highs and lows and always provided me with the emotional and moral support that I needed. Special thanks to Shalmalee Aidoor, Saif Khan, Ninad Thavare, Krunal Khamkar, Dipti Thakkar and Zarine Khan for listening to all my cribbings with a patient ear and providing the much needed entertainment. I cannot thank them enough for always holding my hand during my weak moments and helping me see through the tunnel.

I would also like to thank late “John Cadbury” for providing the world with the most delicious chocolate which has helped me survive by keeping my sugar levels right through my PhD.

It is only in dictionary that success comes before work and as a child I was always taught this aphorism. I owe my deepest gratitude to my parents who have constantly guided and supported me in all walks of my life. My parents mean the world to me and I owe everything to them. They have always encouraged me to think out of the box and have brought the best out of me. I simply cannot thank them enough.

Last but definitely not the least; I would like to thank GOD for being the patient listener to my woes and for always showing me the right path. I would like to thank Him for making me fortunate and for giving me a chance to fulfil my ambitions. May His name be always glorified and honoured.

Abbreviations

0-9

1321N1 - Grade I astrocytoma with mutant p53

17AAG - 17-allylamino-17-demethoxygeldanamycin

17DMAG - 17-Dimethylaminoethylamino-17-demethoxygeldanamycin

2D-DIGE - Two dimensional fluorescence difference gel electrophoresis

A

A - Adenine

A-172, LA567 - Glioblastoma cell line

A431 - Human epidermoid carcinoma cells

ACDP - Advisory committee on dangerous pathogens

ADP - Adenosine diphosphate

Ad-stTRAIL - Adenovirus carrying the secretable trimeric tumour necrosis factor related apoptosis inducing ligand

Ago2 - Argonate 2

Aha1 - Aryl Hydrocarbon receptor Associated protein 1

ALK - Anaplastic lymphoma kinase

AMV - Avian myeloblastosis virus

Apaf-1 - Apoptotic protease activating factor 1

Arp2/3 - Actin related protein 2/3 complex subunit 2

ATCC - American type culture collection

ATP - Adenosine-5'-triphosphate

B

BCNU - 1,3-bis (2-chloroethyl)-1-nitrosoure

BCR-ABL - Breakpoint Cluster region-Abelson

Bid - BH3 interacting domain death agonist

bp - Base pair

BSA - Bovine serum albumin

C

C - Cytosine

$CD8^{+}T$ - Cytotoxic T cell

Cdc2 - Cell division control protein 2

Cdc37 - Cell division cycle 37 protein

Cdk4 - Cyclin-dependent kinase 4

Cdk6 - Cell division protein kinase 6

Cdk9 - Cyclin-dependent kinase 9

cDNA - complementary DNA

CML - Chronic myeloid leukemia

c-Mos - Proto-oncogene serine/threonine-protein kinase mos

c-myc - Myelocytomatosis cellular proto-oncogene

CNS - Central nervous system

c-RAF/Raf-1 - RAF proto-oncogene serine/threonine-protein kinase

c-src - Cellular sarcoma

Ct - Cycle threshold

C-terminus - carboxyl-terminus

Cy - Fluorescent cyanide

D

DAPI - 4',6-diamidino-2-phenylindole

DMSO - Dimethylsulphoxide

DNA - Deoxyribonucleic acid

E

ECACC - European collection of cell cultures

EDTA - ethylenediaminetetraacetic acid

eEF2 - Elongation factor 2

EGFR - Epidermal growth factor receptor

eIF3 - Eukaryotic translation initiation factor

eIF3K - Eukaryotic translation initiation factor 3 subunit K

ELISA - Enzyme linked immuno-absorbent assay

EMBL - European molecular biology laboratory

ER - Endoplasmic reticulum

ErbB2/ Her-2 - Human Epidermal growth factor Receptor 2

F

FACS - Fluorescence-activated cell sorting

FADD - Fas-Associated protein with Death Domain

FAK - Focal adhesion kinase

FBS - Foetal bovine serum

FITC - Fluorescein isothiocyanate

G

G - Guanine

GA - Geldanamycin

GAPDH - Glyceraldehyde 3-phosphate dehydrogenase

GBM - Glioblastoma multiforme

GOS-3 - Grade II/III astrocytoma/ oligodendroglioma

Grp94/ gp96/Hsp90B1/tumour rejection antigen - Heat shock protein 90kDa beta member 1

GTP - Guanosine-5'-triphosphate

xg - G-Force

H

HCC - Hepatocellular carcinoma

HCl - Hydrochloric acid

HCT116 - Colon cancer cells

HCV - Hepatitis C virus

HeLa - Cervical cancer cells taken from Henrietta Lacks

HIF-1 α - Hypoxia inducible factor-1α

HIV - Human immunodeficiency virus

HOP - Hsp70/Hsp90 organizing protein

HPRD - Human protein research database

HRP - Horseradish peroxidase

HSF-1 - Heat shock factor 1

Hsp - Heat shock protein

I

IC_{50} - Half maximal inhibitory concentration

IKK - Inhibitor of nuclear factor kappa-B kinase

IPA - Ingenuity pathway analysis

IPI-504 - 17-allylamino-17-demethoxygeldanamycin hydroquinone hydrochloride

K

K18 - Keratin 18

K8 - Keratin 8

KNK437 - N-formyl-3,4-methylenedioxy-benzylidene-gamma-butyrolactam

L

LN229 - Grade IV glioblastoma

M

MALDI-TOF - Matrix assisted laser desorption/ionization time-of-flight

MBG - Marburg virus

MCF7, T47D - Breast cancer cell lines

MDR1 - P-glycoprotein

MEK - methyl ethyl ketone

$MgCl_2$ - Magnesium chloride

MHC - Major histocompatibility complex

MnSOD - Manganese superoxide dismutase

MRI - Magnetic resonance imaging

mRNA - Messenger RNA

MS – Mass spectrometry

MS/MS - Tandem mass spectrometry

mTOR - Mammalian target of rapamycin

MW - Molecular weight

N

NaOH - Sodium hydroxide

NCBI - National centre for biotechnology information

NIH-3T3 - Mouse embryonic fibroblast cell line

nt - Nucleotides

N-terminus - Amino terminus

O

OD - Optical density

P

p23 - Prostaglandin E synthase 3 (cytosolic)

p53 - Protein 53/ Tumour protein 53

PBS - Phosphate buffer saline

PDPK1 - 3-Phosphoinositide-dependent kinase-1

PEP - Phosphoenolpyruvate

PGK1 - Phosphoglycerate kinase

pI - Isoelectric point

PI - Propidium iodide

Q

qRT-PCR - Quantitative RT-PCR

R

Ran - RAs-related Nuclear protein

RIP - Ribosome inactivating protein

RISC - RNA induced silencing complex

RNA - Ribonucleic acid

RNAi - RNA interference

RT-PCR - Reverse transcription polymerase chain reaction

S

SDS-PAGE - Sodium dodecyl sulfate polyacrylamide gel electrophoresis

shRNA - Short hairpin RNA

siRNA - Small interfering RNA

ss - Single strand

T

T - Thymine

TAE - Tris Acetate ethylenediaminetetraacetic acid

TBE - Tris borate EDTA

TF-1 - Erythroleukemia cell line

TMB - Tetramethylbenzidine substrate

TMZ - Temozolomide

TNF-α - Tumour necrosis factor α

tPA - Tissue plasminogen activator

TPM4 - Tropomyosin 4

TRBP/PACT - RISC-loading complex subunit TARBP2

U

U118, U118-9 – Grade III glioblastoma

U87-MG - Grade IV glioblastoma

UCHL1 - Ubiquitin carboxyl-terminal esterase L1

uPA - Urinary plasminogen activator

V

VEGF - Vascular endothelial growth factor

v-src - Viral sarcoma

W

WHO - World health organisation

WT - Wild type

CHAPTER 1

INTRODUCTION

Molecular chaperone proteins are responsible for maintenance of the correct folding, stability and function of several proteins. Following environmental insults, the cells in most of the tissues increase the production of a small group of proteins, which are collectively labelled as “heat shock proteins” or stress proteins (Li and Srivastava, 2004).

These heat shock proteins were first reported by Ritossa in the 1960s (Ritossa, 1962). Since then, there have been speculations regarding their roles and their expression profiles. Previous studies have shown that these heat shock proteins (Hsp’s) are actually molecular chaperones (Whitesell and Lindquist, 2005). Under normal conditions, the Hsp’s assist in normal protein folding and protect the proteome from perils of misfolding and aggregation. Many Hsp’s form multichaperone complexes which operate as molecular chaperones binding several proteins, labelled as client proteins (Takayama *et al*., 2003). Chaperones regulate several aspects of the protein structure including: folding of proteins in the endoplasmic reticulum, mitochondrial and cytoplasmic transport of proteins, repair or degradation of proteins, control several regulatory proteins and the refolding of misfolded proteins (Neidle, 2007).

Hsp’s are present in several cellular locations and each functions differently. The Hsp’s have been classified into families depending on their molecular weight (kDa) viz: Hsp90, Hsp70, Hsp60 and Hsp40 and Hsp27 (Li and Srivastava, 2004).

Either in stress or during environmental insults, the expression of Hsp’s activates in tissues an adaptive response that enhances cell survival. However, in case of tumours, the increased chaperone expression is a reflection of efforts of malignant cells to maintain homeostasis (Takayama *et al*., 2003). Thus, Hsp’s allow tumour cells to

tolerate several inner alterations and moreover, help to tolerate mutations in important signalling molecules. This drives the cells towards oncogenesis. Consequently, Hsp's can be aptly called biochemical buffers for the many genetic abrasions that are evident in most of the cancers (Sangster *et al*., 2004).

The heat shock protein 90 (Hsp90) is a highly conserved molecular chaperone present in eukaryotic cytosol and it has been proposed to play vital roles in tumorigenesis, maintenance of transformation and regulation of several key proteins involved in apoptosis, survival and growth pathways (Neckers, 2007). Hsp90 has been abundantly present both intracellularly and extracellularly in eukaryotic cells and has extensive influence in various cellular activities (Sreedhar *et al*., 2004; Richter and Buchner, 2001). In normal cells, Hsp90 consist of 1-2 % of the total cellular protein content. However, in the incidence of cancer, the malignant cells produce a 2-3 fold increase in the level of Hsp90 (Wong and Houry, 2006).

Hsp90 forms a multi-chaperone complex with various co-chaperones, in particular Hsp70, (Fig 1.1) and is involved in folding and maturation of several key proteins; some of which are involved in cancer progression (Kamal *et al*., 2003; Shervington *et al*., 2008; Gupta, 1995).

Several oncogenic proteins are dependent on Hsp90 since it plays a key role in the conformational maturation of proteins such as HER-2/ErbB2, Akt, Raf-1, BCR-ABL and mutated p53. Interstingly, most of the cancer cells are dependent on these oncogenic proteins (Kamal *et al*., 2003).

The Hsp90 chaperone is a specialized chaperone as it targets several client proteins that are involved in various signal transduction pathways. Hsp90 substrates include

various transcription factors and protein kinases (Table 1.1). It is very distinct from other chaperones as it binds to substrate proteins which are in a near native state i.e. proteins that are at the last stage of folding. Hsp90 does not directly fold non-native proteins (Wong and Houry, 2006).

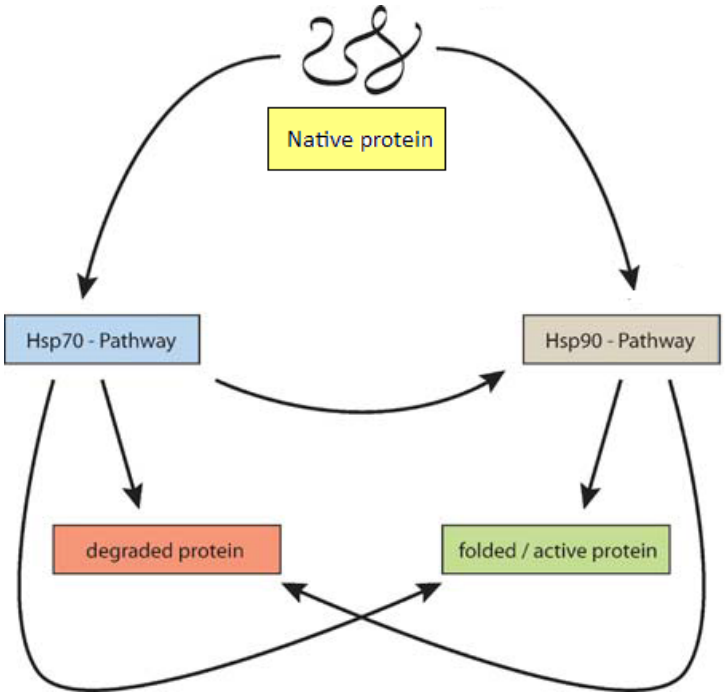

Figure 1.1: Protein folding pathways involving Hsp90 and Hsp70 (Modified from Wegele *et al.*, 2004)**.** Protein folding pathways for nascent proteins involving Hsp90 and Hsp70 with the transfer of some of the proteins from Hsp70 to Hsp90. The proteins get actively folded by molecular chaperones Hsp90 and Hsp70, with Hsp70 acting as co-chaperone to Hsp90 by transferring near-native proteins to Hsp90 for correct folding.

Table 1.1: Examples of Hsp90 client proteins (Adapted from Wegele *et al*., 2004; Goetz *et al*., 2003).

	Proteins	Client proteins
1	Transcription factors and Polymerases	Progesterone receptor Estrogen receptor Androgen receptor p53 mutant Hypoxia-inducible factor-1α
2	Signalling Proteins	Telomerase v-src, c-src c-Raf MEK Focal adhesion kinase (FAK) ErbB2 Cdk4 Epidermal growth factor receptor
3	Kinases	3-Phosphoinositide-dependent kinase-1 Akt Bcr-Abl Calmodulin-regulated eEF-2 kinase Casein kinase II Cdc2 Cdk4 Cdk6 Cdk9 c-Mos Her-2

1. Transcription Factors and Polymerases:

   i. Mutated p53: p53 is a known tumour suppressor protein which acts within the nucleus to affect cell cycle arrest and apoptosis. In most of the cancers, this protein is absent or mutated. Most mutated forms of p53 require interaction with Hsp90 complex to retain activity of the mutated protein (Blagosklonny *et al*, 1996).

   ii. Steroid hormone receptors: Steroid hormone receptors are complexed with Hsp90 to maintain a conformation capable of binding hormones (Smith and Toft, 1993).

   iii. Hypoxia inducible factor-1α (HIF-1 α): HIF-1 α controls the genetic expression of several genes. The proteins of which play an important role in tumour growth. HIF-1 α is expressed as being bound to Hsp90 in several metastases and late stage tumours (Gradin *et al*., 1999).

2. Signalling Proteins:

   i. Raf-1: Raf-1 is part of a conserved signal transduction pathway which transmits signals from tyrosine kinases in the cytosol and transmembrane, to mitogen activated protein kinases. Its association with Hsp90 complex and Hsp90N leads to the stabilization and inhibition of Raf-1's proteasome dependent degradation (Schulte *et al*., 1996).

   ii. v-src: Viral sarcoma protein (v-src) serves as a prototype of an oncogene family which is responsible to induce cellular transformation by non

regulated kinase activity. v-src is known to be complexed to Hsp90 (Uehara *et al*., 1986).

3. Kinases:

   i. Her-2: Human Epidermal growth factor Receptor 2 (Her-2) is a receptor kinase that binds to Hsp90. It is overexpressed in several cancers including breast, prostrate, gastric and ovarian cancers (Veltri *et al*., 1994).

   ii. Akt: Akt kinase plays a vital role in controlling pathways of proliferation and apoptosis. Akt has been implicated in cancer progression since it stimulates cell proliferation and suppresses apoptosis. In tumour cells the Akt activation is halted by ansamycin treatment. This is due to the occupancy of the Hsp90 pockets by ansamycin which results in the reduction of Akt half life and proteasomal degradation (Basso *et al*., 2002; Basso *et al*., 2002).

   iii. BCR-ABL: The BCR-ABL fusion protein is an unregulated tyrosine kinase which is responsible for the chronic phase in chronic myelogenous leukaemia (Lugo *et al*., 1990). The chimeric BCR-ABL is present in the complex with Hsp90 (Nimmanapalli *et al*., 2001).

1.1 Hsp90 PROTEIN:

The Hsp90 protein is a phosphorylated homodimer possessing two to three phosphate molecules covalently bonded to each monomer. It consists of three well defined domains, a highly conserved ATP binding domain at the N terminus (amino terminus), a middle domain that completes the ATPase site and which binds to several client proteins, and a C terminus (carboxyl terminus) dimerization domain. For the chaperoning activity of Hsp90, the binding and hydrolysis of ATP at this site is very important. Additionally, there is a second nucleotide binding site at the C terminus; however, it is not very well defined. (Richter and Buchner, 2006; Wong and Houry, 2006; Goetz *et al*., 2003).

Hsp90 interacts with various co-chaperones such as Hsp40, Hsp70 and several factors such as Hsp70/Hsp90 organizing protein (HOP) and prostaglandin E synthase 3 (cytosolic) (p23). These co-chaperones regulate Hsp90 ATPase activity, assist in protein folding or function as a scaffold for Hsp90 complex (Wong and Houry, 2006).

When ATP binds to the N terminal of Hsp90, it alters the conformational state and also affects the interactions with several client proteins and co-chaperones. During this ATPase cycle the three domains of Hsp90 move from an ATP-free open state to an ATP bound closed state (Fig 1.2). Several biochemical investigations have proved that, sets of conformational changes occur upon binding ATP, including the transient dimerization of N terminal domains and its association with the middle domain (Pearl and Prodromou, 2001).

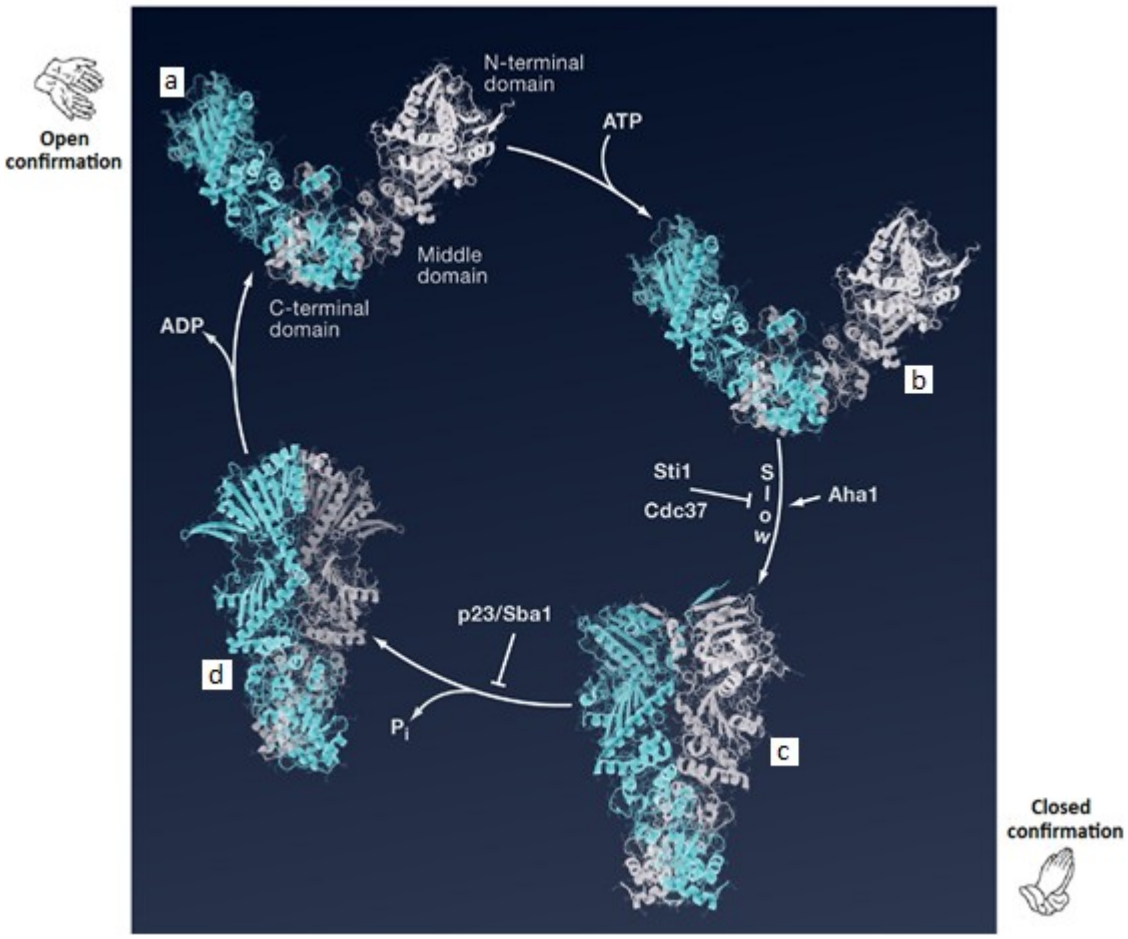

Figure 1.2: The ATPase cycle of Hsp90 (Adapted from Richter and Buchner, 2006).

The different stages of ATPase cycle of Hsp90 (a-d) wherein, a and b represents open conformation or inactive state whereas, c and d represents closed conformation or active state. The slow steps during the ATPase cycle are the conformational changes prior to ATP hydrolysis and are inhibited by Sti1 and/or Cdc37 and stimulated by Aha1. The co-chaperone p23/Sba1 binds to the active ATP complexed state and slows down ATP turnover.

Previous studies in various tumour cell lines have suggested that Hsp90 could possibly be exclusively complexed with several co-chaperones in a state of high affinity for ATP/ADP. In normal tissues, Hsp90 could possibly exist in a latent, uncomplexed and low affinity state (Kamal *et al*., 2003). Thus, it is suggested that Hsp90 is present in equilibrium between a “latent” state with low chaperoning activity and an increased chaperoning activity “activated” state with the shift in equilibrium depending upon the level of stress (Fig 1.3).

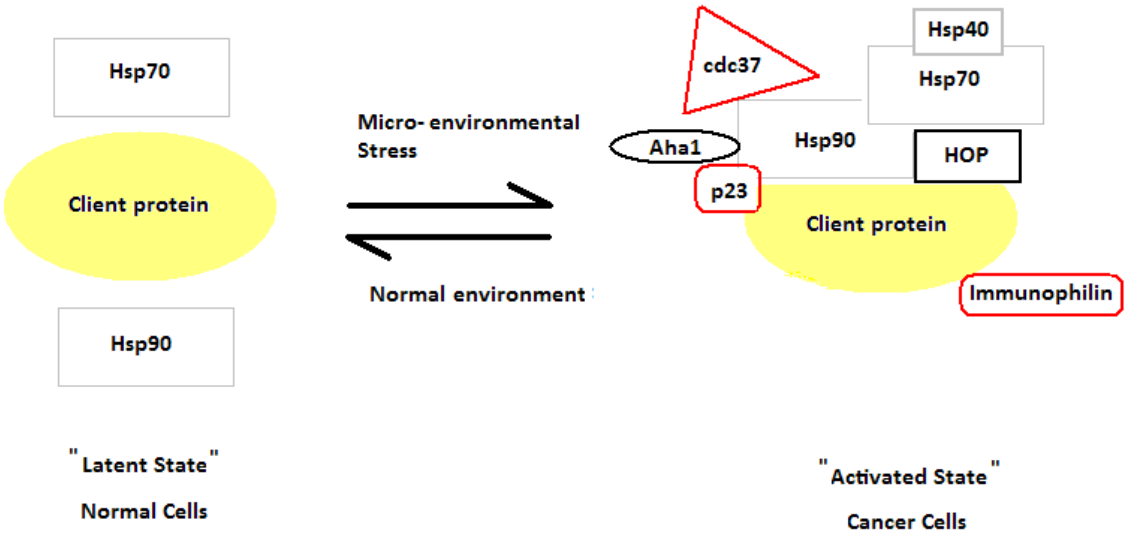

Figure 1.3: Equilibrium between latent and activated state (Adapted from Chiosis and Neckers, 2006).

The figure is a schematic representation of Hsp90 and its possible interactive partners which exists in equilibrium between the activated state and the latent state. The activated state is predominant in cancer cells while the latent state is predominant in normal cells. The activated state is regulated by the presence of several co-chaperones.

1.2 Hsp90 ATPase ACTIVITY:

As discussed earlier, hydrolysis of ATP is crucial for Hsp90 to function. Under normal conditions ATP binds in the N terminal pocket of Hsp90 by a weak bond. The ATPase activity is weak with ~ 0.3 ATP molecules hydrolyzed per minute at physiological temperature for yeast Hsp90. However, in humans it is detected in trace amounts with a Kcat of 0.089 ± 0.004 min^{-1} and a Km of 840 ± 60. It binds to the N terminal pocket in an unusually kinked conformation. The ribose unit and the adenosine ring are both buried deep in the binding pocket with the phosphate group pointing towards the surface, especially the γ phosphate (Wegele *et al*., 2004).

Kinetic analysis has revealed that Hsp90 regions outside the ATP binding domain are important for the efficient hydrolysis. Thus, it can be assumed that once ATP is bound,

the N terminal domain interacts with other parts of the Hsp90 molecule. Kinetic dissection of the ATPase mechanism has showed that the decisive state of the rate of hydrolysis is the slow conformational changes prior to hydrolysis and the rate is noted to be slow. These conformational changes help to lock in the ATP in the N terminal binding pocket and commit it to hydrolysis (Wegele *et al*., 2003).

During the ATPase cycle, a weak dimerization site amidst the N terminal part of Hsp90 becomes exposed. This leads to a transient dimerization of the N terminal domain. The hydrolysis of ATP leads to conformational changes in the protein, with two ATP molecules hydrolyzed, the N terminal domains causes' one round of association-dissociation. The dimeric nature of the Hsp90 is crucial not only for the hydrolyzing activity but also for the association of the N terminal domain through the ATPase cycle. This ensures maximum ATPase activity (Prodromou *et al*., 2000).

1.3 Hsp90 SUPER-CHAPERONE:

As mentioned previously, Hsp90 is required for the activity of several key regulators of apoptosis and through these associations the chaperone possibly leads to tumour cell survival. Survivin, a dual regulator of cell proliferation and cell death is overexpressed in most cancers. Survivin is known to be chaperoned by Hsp90 (Chiosis *et al*., 2004).

Several client proteins such as Akt and Raf-1 are regulated by Hsp90 which in turn regulate several pathways leading to cancer. Additionally, Hsp90 binds to ribosome inactivating protein (RIP) and the kinase domain of inhibitor of nuclear factor kappa-B kinase (IKK) subunit α/β and thus, plays an anti-apoptotic role (Fig 1.4). Moreover, Hsp90 can suppress the tumour necrosis factor α (TNF- α) by preventing the cleavage

of BH3 interacting domain death agonist (Bid) which is a client protein involved in the apoptosis pathway (Chiosis *et al*., 2004).

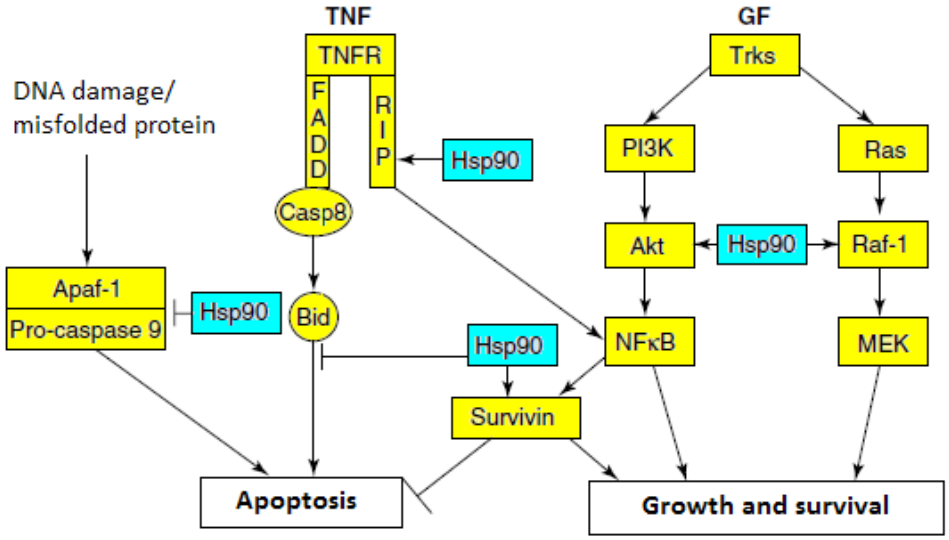

Figure 1.4: Hsp90 involved in apoptotic pathway (Adapted from Chiosis *et al*., 2004). Hsp90 regulates several proteins involved in both intrinsic and extrinsic apoptotic pathways.

Additional to its mutation buffering and survival promoting roles, Hsp90 helps to maintain the transformed cells. A wide list of client proteins to Hsp90 has been discussed and most of these proteins play vital roles in cell cycle, growth and apoptosis (Fig 1.5). Inhibition of Hsp90 leads to the degradation of these client proteins via the ubiquitin proteasome pathway. This in succession leads to growth arrest and apoptosis in cancer cells (Neckers, 2007).

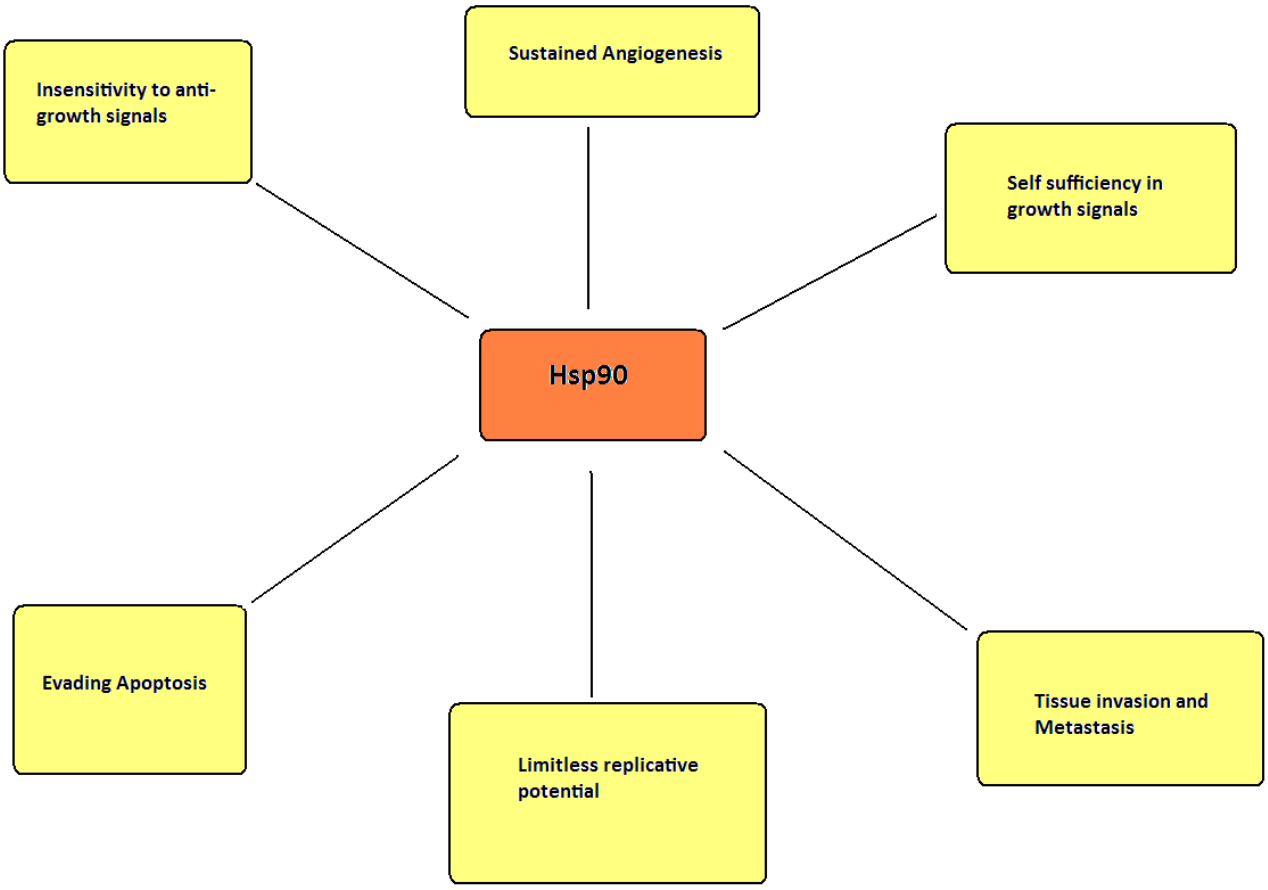

Figure 1.5: Hsp90 function (As modified from Neckers, 2007).

Implications of Hsp90 function in each of the hallmarks of cancer.

1.4 Hsp90 ISOFORMS:

There are two major isoforms of Hsp90, namely Hsp90α and Hsp90β. Although, *hsp90α* and *hsp90β* have dissimilar nucleotide sequences (Fig 1.6), their protein products are similar with a sequence homology of 85%. Hsp90α is the major isoform and is induced whereas, Hsp90β is the minor isoform and is constitutively expressed. Studies have shown that Hsp90 isoforms *α* and *β* occurred by gene duplication roughly 500 million years ago (Gupta, 1995). There is relatively high conservation observed

between these two isoforms. There is another isoform present, namely Hsp90N. Furthermore, Hsp90 analogues include heat shock protein 90kDa beta member 1 (Grp94/gp96) in the endoplasmic reticulum and Hsp75/TRAP1 in the mitochondrial matrix (Neidle, 2007). The *hsp90α* and *hsp90β* have been mapped onto chromosome 14q 32-33 and 12q24.2-q24.3, respectively. The nucleotide sequences of both genes are different in the 5' and 3' non-coding regions, the introns and the regulatory 5' flanking sequences. All the Hsp90 isoforms have five highly conserved regions, three of which are in the N terminal domain and the other two are in the middle domain. These conserved sequences are referred to as "signature sequence". (Sreedhar *et al*., 2004; Csermely *et al*., 1998; Shervington *et al*., 2008).

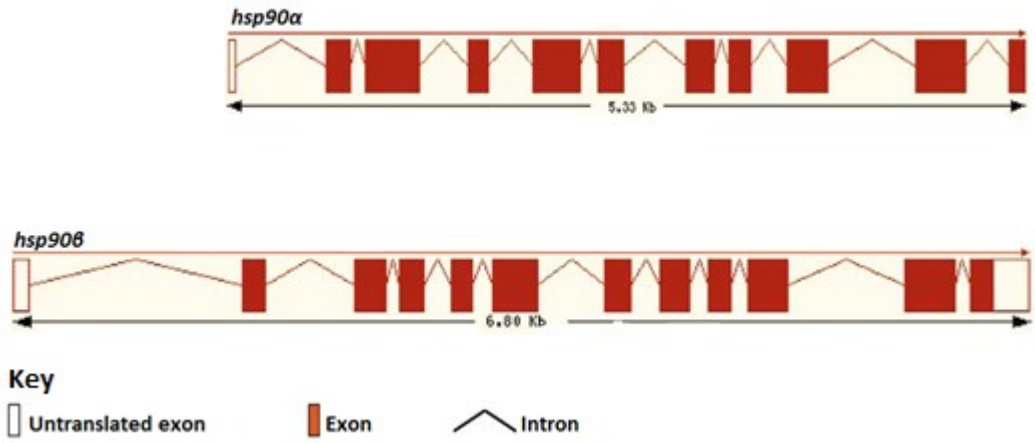

Figure 1.6: The intron/exon structure of Hsp90 isoforms. (Adapted from www.ensembl.org)

Hsp90α and Hsp90β have similar protein products however, their nucleotide sequences are dissimilar.

Hsp90 is mainly a constitutive dimer (αα or ββ), however, monomers (α or β) or even heterodimers (αβ) exists (Sreedhar *et al*., 2004). This dimerization potential is due to the C terminal of the Hsp90. Additionally, there are regions within the amino acid

sequence of α and β isoform that differ; suggesting isoform specific functions (Whitesell and Lindquist, 2005; Csermely *et al*., 1998).

Table 1.2: Differences in the function and expression of Hsp90 isoforms
(Adapted from Sreedhar *et al*., 2004).

Isoform	Function	Expression Status
Hsp90α	Growth promotion Cell cycle regulation Stress induced cytoprotection	Induced
Hsp90β	Early embryonic development Germ cell maturation Signal transduction Cellular transformation	Constitutive

1.5 Hsp90, THE CANCER CHAPERONE:

The structure of a protein determines its function and it is essential for proteins to maintain their specific structure in order to carry out their role(s) in the cell. These functions are achieved by molecular chaperones since they facilitate protein folding. The molecular chaperones binds to proteins and protects and control their three dimensional structure (Prodromou *et al*., 2000). As discussed earlier, Hsp90 plays a key role in the conformational maturation of various oncogenic proteins such as HER-2/ErbB2, Akt, Raf-1, Bcr-Abl and mutated p53. Hsp90 interacts with such client proteins to form a multichaperone complex (Kamal *et al*., 2003). This molecular chaperone is normally over expressed in breast tumours, lung cancers, leukaemias, and Hodgkin's disease (Ghobrial *et al*., 2005). It is also over expressed in B cell of non-

Hodgkin lymphomas in comparison with normal B cells. Poor prognosis of breast cancer is usually associated with overexpression of Hsp90 and also Hsp70 (Yano *et al*., 1996). Moreover, Hsp90 transcription is directly activated by the myelocytomatosis cellular proto-oncogene (c-myc) in several tumour models. It has been depicted that Hsp90 has a role in facilitating the emergence of polymorphisms and mutations supporting the evolution of resistant clones (Neckers and Lee, 2003; Kamal *et al*., 2003; Nimmanapalli, *et al*., 2001).

Furthermore, Hsp70 and Hsp90 have been identified as key regulators in the host's immune system. The Hsp90 chaperoned proteins were cross presented upon major histocompatibility complex (MHC) class I molecules and an antigen specific cytotoxic T cell ($CD8^+$ T) response was initiated *in vitro* in tumour mouse models. Such a cross presentation showed the transfer of exogenous peptides into the MHC class I pathway via an endosomal pathway and Hsp90 is responsible for cross presentation of tumour derived antigen peptides (Schmitt *et al*., 2007).

1.6 GLIOMA and Hsp90:

Glioma is a group of primary brain tumours of the cerebral hemisphere characterized into four types: astrocytoma, glioblastoma multiforme, oligodendroglioma and ependymomas. The grading of these malignant brain tumours is based on the WHO (World Health Organisation) classification system based on specific histological markers (Kleihues and Sobin, 2000). Gliomas originating from astrocytes, oligodendroglial and ependymal cells account for more than 70 % of all brain tumours while glioblastoma is the most frequent and malignant with a 65 % incidence rate (Ohgaki, 2005).

Astrocytoma is an important subtype of the glial tumours originating from the astrocytes. It is the most frequent form between the age of 40 and 60 years with males being more affected than females (Idowu *et al*., 2007). The survival period for astrocytoma is about 3 to 4 years. Diagnosis of astrocytoma can be carried out by obtaining tissue or can be inferred based on Magnetic Resonance Imaging (MRI). However, differentiation between grade II and grade III astrocytoma on the basis of these tests is difficult. They account for 10.3 % of all primary brain and central nervous system (CNS) tumours in the UK (http://www.cancerresearchuk.org/). Low grade astrocytomas usually grow slowly and are localised whereas high grade astrocytoma grow more rapidly and metastasize.

Glioblastoma multiforme (GBM) is a highly malignant and most frequently occurring lethal form of brain cancer (Ohgaki, 2005). It rarely metastasizes or invades into brain tissue and is resistant to current therapies (Rich *et al*., 2005). GBM occurs in patients with a mean age of 54 years with males having higher incident rates similar to astrocytoma. Less than 10 % of the cases are found in children. The survival period is approximately 9-12 months (Carter *et al*., 2008). GBM is classified into two distinct subtypes that are histologically identical but develop through different genetic pathways, thus being two separate entities (Ohgaki, 2005; Kleihues and Sobin, 2000; Rich *et al*., 2005). Hence, there is a need for a genetic marker to distinguish between these subtypes.

Oligodendroglioma are tumours of oligodendrocytes accounting for approximately 10 % of primary intracranial tumours. They are most frequent amongst patients of age 30 to 50 years of age. They usually show slow growth but sometimes may show

malignant changes that resemble glioblastoma multiforme. Incidence is more in males than females (Mork *et al*., 1985). Median survival period is 5 years.

Oligodendroglioma is of several types such as:

- Low grade oligodendroglioma
- Anaplastic oligodendroglioma
- Mixed oligodendroglioma – astrocytoma also termed as mixed glioma

The pathogenesis of these glial tumours is still unknown (Engelhard *et al*., 2002).

The current treatments available are surgery, radiotherapy and chemotherapy using drugs such as temozolomide (TMZ). In spite of recent advances, the prognosis and survival rates of patients with glioma are very poor (http://www.cancerresearchuk.org/). This calls for alternative targets to tackle glioma therapy.

1.6.1 Hsp90 IN OUR LABORATORY:

Previous studies within our laboratory have shown that *hsp90α* is expressed in both glioma tissue and in specific cell lines but was found to be absent in normal brain tissue and cell lines, indicating a possible role in sensitizing glioma cells to therapy by using anti-Hsp90*α* drugs. In the study, seven glioblastoma biopsy samples and a recurrent anaplastic ependymoma, together with three glioma cell lines, 1321N1, U87-MG and GOS-3, and controls including two normal brain tissues were analysed for *hsp90α* expression profiles (Shervington *et al*., 2008). Recent findings have shown that enhanced chemosensitivity is attained upon specific inhibition of *hsp90α* expression by siRNA, suggesting that inhibiting *hsp90α* expression by siRNA could possibly be a

favourable therapeutic approach compared to conventional chemotherapies as it is target specific and has reduced toxicity. Furthermore, a combination treatment of siRNA followed by TMZ (200-400 µM) after 48 hours was significantly more effective, suggesting it as a possible effective form of therapy (Cruickshanks *et al*., 2010). Given its functions as a molecular chaperone and its expression in gliomas, *hsp90α* may represent a promising target for the development of novel therapeutic strategies.

1.7 Hsp90 INHIBITORS:

Hsp90 is one of the most abundant molecular chaperones and it is expressed in several cancers, including glioma. It regulates several client proteins, some of which are even involved in cancer progression. Hence, the importance of blocking Hsp90 is being presently investigated.

RNAi system involves the use of either small interfering RNA's (siRNA's) or short hairpin RNA (shRNA) [Further discussion regarding RNAi can be found in Chapter 3].

Another approach to silence Hsp90 is by the application of Benzoquinone ansamycins.

Benzoquinone ansamycins are antibiotics, characterized by linkage of quinone moiety to a planar macrocyclic ansa bridge structure (Fig 1.7).

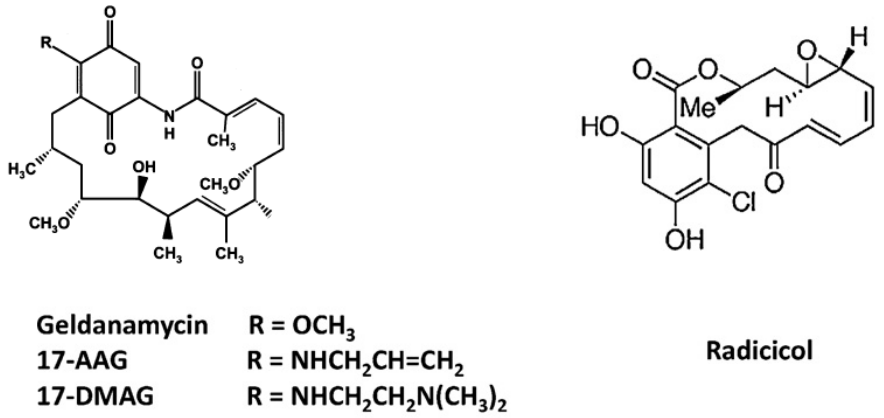

Figure 1.7: Chemical structures of Hsp90 inhibitors (Adapted from Messaoudi *et al*., 2008).

The chemical structure of geldanamycin (GA), 17-allylamino-17-demethoxygeldanamycin (17-AAG), 17-Dimethylaminoethylamino-17-demethoxygeldanamycin (17-DMAG) and Radicicol (RA).

Glendanamycin (GA) is the first prototype of the class of Bezoquinone ansamycins. It was purified from the broth of *Streptomyces hygroscopicus* (Solit and Rosen, 2006). Geldanamycin and herbimycin were initially identified as agents that revert transformation by v-src and demonstrate potent anti-tumour activity against human cancer cells and xenografts supposedly by directly inhibiting protein kinases. (Goetz *et al*., 2003).

The Hsp90 ATP/ADP pocket is hydrophobic and nucleotide binding to this pocket leads to conformational changes which bring about several characteristic changes in the client proteins. It can either form an assembly which protects and stabilizes client proteins or can lead towards their degradation. Thus, nucleotide binding determines the half life of the client proteins (Goetz *et al*., 2003). Consequently, it was found that GA has no inhibitory effect on protein kinases, however, it reduces their active levels in the cells and upholds their degradation. Moreover, the direct target for GA is Hsp90, as it binds onto the N terminal domain wherein ATP usually binds, with the affinity of GA

for Hsp90 being about 500 fold higher than that of ATP (K_D of 1.2) (Wegele *et al*., 2004).

Radicicol or monorden is an even more competitive inhibitor of ATP with a binding affinity of 19 nM. Radicicol is a fungal macrolactone which also binds to the N terminal domain (Messaoudi *et al*., 2008).

Recent advances have led to synthesis and evaluation of 17AAG, a glendamycin analogue with an allyl amino group instead of the methoxy group in the 17 position (Fig 1.7). Preclinical studies have demonstrated that 17AAG works in a similar manner to that of glendanamycin but with a radically improved toxicity profile. 17AAG is currently in phase I trials as a single agent (Goetz *et al*., 2003; Neckers, 2002).

Several small molecule inhibitors have been developed over the recent inhibiting Hsp90 function (Table 1.3 and Fig. 1.8).

Table 1.3: Hsp90 binding drugs (Adapted from Whitesell and Lindquist, 2005).

Binding Sites	Chemical Class	Selected Examples
N terminal ATP-binding pocket	Benzoquinone ansamycin	GA, 17AAG, 17DMAG
N terminal ATP-binding pocket	Macrolide	Radicicol and related oxime derivative.
N terminal ATP-binding pocket	Purine Scaffold	pU24FC1
N terminal ATP-binding pocket	Pyrazole	CCT018159
N terminal ATP-binding pocket	Hybrid	Randamycin, GA dimer, GA testosterone, GA oestrogen
C terminus	Novioslycoumarin	Novobiocin, coumermycin, cisplatin

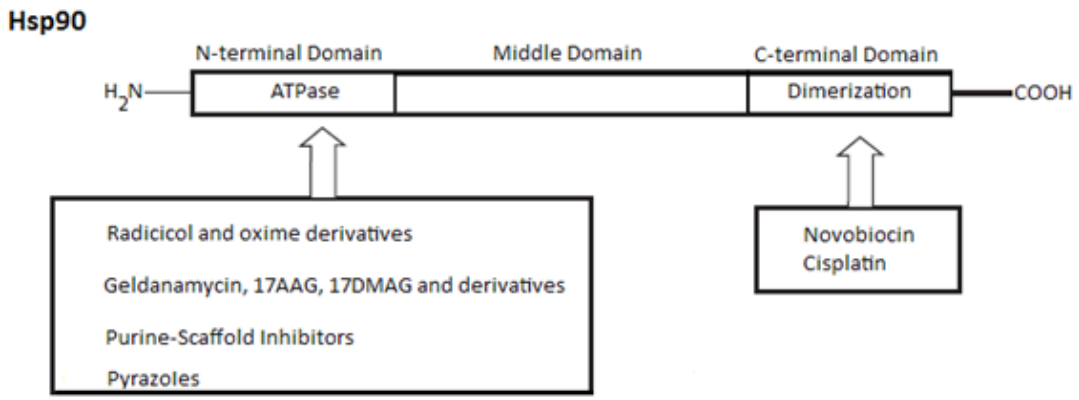

Figure 1.8: Fixation sites of several inhibitors in case of Hsp90 (Adapted from Didelot *et al.*, 2007).

Schematic representation of Hsp90 protein and the various binding sites for several drugs.

These Hsp90 inhibitors were used successfully in several cancer studies (Table 1.4).

A combination of the inhibitors along with cytotoxic, radiation and antiangiogenic agents can be used (Didelot *et al*., 2007).

Table 1.4: Use of Hsp90 Inhibitors in cancers (Adapted from Neckers, 2002).

Hsp90 inhibitors used to modify the response to standard chemotherapeutic agents
• Used with taxol or doxorubicin in ErB2 or Akt over-expressing tumours (breast, ovarian, prostate and lung cancer) • Used with Gleevec in Bcr-Abl positive leukemias

Study of Hsp90 biology has been broadened by the use of Hsp90 inhibitors. These Hsp90 inhibitors induce degradation of Hsp90 client proteins, many of which play a central role in tumour initiation and progression.

1.8 SUMMARY:

Because of Hsp90α inducible expression profile and its presence in several cancers to include glioma, it has the potential as an alternative therapeutic target and the feasibility of targeting Hsp90 for cancer therapy is well supported:

i. To begin with, Hsp90 is involved in the stabilization and maturation of a wide range of oncogenic client proteins vital for oncogenesis (Whitesell and Lindquist, 2005; Kamal *et al*., 2004; Powers and Workman, 2007), resulting in cancer cells predominantly dependent on Hsp90 function (Chiosis and Neckers, 2006).

ii. Furthermore, given the relatively harsh environmental conditions that exist in tumours such as: hypoxia, low pH and poor nutrition, could possibly destabilize proteins, thus rendering them even more dependent upon the activity of Hsp90 (Solit and Chiosis, 2008). Contrastingly, Hsp90 comprises of 4-6% of total proteins in tumour cells as opposed to 1-2% in normal cells. This itself shows dependence of tumour cells on the Hsp90 protein (Chiosis and Neckers, 2006).

iii. A further explanation of the high tumour selectivity of Hsp90 inhibitors comes from the fact that, in tumours Hsp90 primarily exists as a multi-chaperone complex with a very high affinity for both ATP and specific drugs, whilst in normal cells most of the Hsp90 present is in the latent/uncomplexed state (Chiosis and Neckers, 2006). Other reports have shown that Hsp90 isolated from tumour cells has approximately 100 fold greater binding affinity for 17-AAG than Hsp90 derived from normal cells (Kamal *et al*., 2003).

iv. A number of Hsp90 inhibitors such as 17-AAG, 17-DMAG, radicicol and purine scaffold inhibitors have shown tumour specific accumulation (Chiosis and Neckers, 2006). This selectivity could possibly be attributed to the properties of Hsp90 itself rather than the structural and/or physicochemical properties of a specific class of compounds. Though the mechanism of such tumour selectivity is not yet fully understood, Hsp90 has been validated as a potential target in cancer therapy (Solit and Chiosis, 2008).

v. Finally, preclinical and clinical trials of a plethora of Hsp90 inhibitors are underway with some already showing promising results as a single agent and/or in combination with chemotherapy (Solit and Chiosis, 2008).

1.9 RESEARCH QUESTION:

- Is it possible to take either a Molecular approach (shRNA) or Chemical approach (17AAG) in inhibiting Hsp90?
- Which client proteins are affected downstream during these approaches?

1.10 AIMS AND OBJECTIVES:

Main Aim

Hsp90α has been identified as a unique and a potential target in glioma therapy by previous findings within our laboratory. The main aim of the present research was to target Hsp90α using molecular and proteomic approches.

Specific Aim

1. To answer the research question
2. To develop the technique of tissue culture using U87-MG cells and to use the cells for further studies.
3. To treat cells with shRNA targeting *hsp90α* and 17AAG.
4. To undertake proteomic studies (Applied Biomics, U.S.A) and a series of supplementary experiments.
5. Cell cycle was performed upon silenced cells to study the effects of silencing.
6. To investigate the effect of both 17AAG and KNK437 on cell viability in U87-MG cell lines.

All the experiments involved an untreated cell sample as control.

The novelty of the research involved looking into the involvement of Hsp90α in glioma and to design a pathway which could possibly bridge the gap in glioma studies.

Additionally, the study compared the molecular approach with chemical approaches of treating glioma.

CHAPTER 2

MATERIALS AND METHODS

MATERIALS As listed in the relavant sections of Methods.

METHODS

2.1 CELL CULTURE:

2.1.1 Cell Lines:

Three glioma cell lines were primarily used, namely grade I astrocytoma, which expressed a mutant p53 (1321N1), grade II/III astrocytoma/ oligodendroglioma (GOS-3) and grade IV glioblastoma (U87-MG).

The glioma cell lines purchased from the European Collection of Cell Cultures (ECACC) and the American Type Culture Collection (ATCC) were of human origin with no evidence of the presence of infectious viruses or toxic products. ECACC stated that they should be handled as recommend by the Advisory Committee on Dangerous Pathogens (ACDP) for Category 2 containment.

All the cell lines were received as frozen ampoules in 1 ml plastic cryotubes which contained the cells present in a freezing medium which was an appropriate culture medium supplemented with 10 % Foetal bovine serum (FBS), 2 mM L-glutamine and 10 % (v/v) Dimethylsulphoxide (DMSO).

2.1.2 Media and Reagents:

A complete medium for cell growth was prepared in sterile conditions for each cell line. The mediums were prepared according to ECACC/ATCC recommendations by the addition of specific supplements.

Table 2.1: Media and supplements used in cell culture in this study.

Media	Abbreviations	Concentrations	Addition supplements
Dulbecco's Modified Eagle's Medium	DMEM	25 mM Hepes 1.0 g/l glucose 1.0 mM sodium bicarbonate 0.011 g/l phenol red	10 % FBS 2 mM L-glutamine
Eagle's Minimum Essential Medium	EMEM	2.2 g/l sodium bicarbonate 1 g/l glucose Earle's salt 0.0053 g/l phenol red	10 % FBS 2 mM L-glutamine 1% Non essential amino acids

Media were supplied in 500 ml aliquots and prepared for each cell line based on the ECACC/ATCC recommendations. In a 500 ml bottle of medium, 50 ml of FBS and 5 ml L-glutamine (200 mM) were aseptically added to achieve 10 % FBS and 2 mM L-glutamine, respectively. Each medium was mixed and labelled with the date of preparation. This was stored at 4 ˚C for 2-4 weeks.

To calculate the volumes of supplements added to the medium the following formula was used;

$$v = \frac{b \times c}{a}$$

where, a = stock concentration b= required final concentration

c= final reaction volume v= required volume

This formula has been used in all the calculations to resolve the volume and concentration of the reagents and chemicals used in this study.

Table 2.2: Reagents and chemicals used in this study for cell culture in this study.

Reagents	Suppliers	Components
Foetal bovine serum	Gibco BRL,UK	Heat inactivated foetal bovine serum
Non essential amino acid	Sigma, UK	100 x Non essential amino acids
L-glutamine	Sigma, UK	200 mM L-glutamine
Phosphatase buffer saline 0.10 M	Sigma, UK	8 g/l Sodium chloride 0.2 g/l Potassium chloride
DMSO	Sigma, UK	Dimethyl sulfoxide 99.5 %
Trypan blue (0.4%)	Sigma, UK	0.81 % Sodium chloride 0.06 % Potassium phosphate dibasic

2.1.3 Resuscitation of frozen cells:

Each medium was pre-warmed in a water bath at 37 ˚C before the frozen ampoules (containing the cells) were thawed. The following protocol was used as suggested by ECACC/ATCC:

1. Cells were thawed at 37 ˚C in a water bath for 1-2 min.
2. Cells were re-suspended into 2 ml medium in a centrifuge tube and an aliquot of 1 ml was added into two 25 cm^2 flasks, labelled with the name of the cell line, passage number and date.
3. Appropriate medium (5 ml) was added into each flask and then mixed manually by rocking the flask backward and forward.
4. Cells were incubated at 37 ˚C with 5 % CO_2 in filtered air.

2.1.4 Subculture and Cell Library Maintenance:

The cells were observed under a light microscope following overnight incubation. When a mono-layer growth of 70-80 % confluence was obtained the cells were scraped and subcultured as follows:

1. The culture medium was removed and the cells were washed with 1 x phosphate buffer saline (PBS) pH 7.4 to remove any remaining culture medium.
2. PBS (2-3 ml) was then added to the flask and the flask was scraped to remove any cells attached on the walls.

3. To ensure that all the cells were detached and floating, they were examined using a phase contrast microscope. The cells were then re-suspended in 2-3 ml of serum containing medium.
4. A 20 µl suspension of the cells was collected in an eppendorf tube for cell counting and the remaining suspension was centrifuged at 100 xg for 5 min. Approximately 1-2 x 10^6 cells were re-suspended in a cell freezing medium (complete culture medium with 10 % DMSO) in 1 ml cryoprotective ampoules, labelled with cell line name, passage number and date.
5. The ampoules were placed into a Mr Frosty passive freezer (Nalgene, UK) filled with isopropanol and stored at -80 ˚C overnight.
6. Following overnight storage the ampoules were then transferred into liquid nitrogen.
7. Cell information was kept in the data entry log book, specifying the position of storage in liquid nitrogen to ensure easy traceability at a later date for further use.

<u>Subculture:</u>

1. To maintain growth, the remaining cells were subcultured (approximately 2 x10^4 cells/cm^2) into a 75 cm^2 flask.
2. The flask was labelled with the cell line, passage number and date and incubated under standard culture conditions.
3. Following overnight incubation, the cells were checked for a sub confluent growth. When this was achieved, the cells were scraped and subcultured.

4. Cells (1 x 10^6) were frozen for stock maintenance as explained earlier, whilst 2×10^6 cells were frozen for mRNA isolation.
5. These cells were stored as pellets at -80 ˚C without freezing medium. For slow growing cells, the medium was changed after every 48 hours to maintain sufficient nutrients for the cells.

2.1.5 Cell Quantification:

The 20 µl aliquot of cells was diluted by adding Tryphan Blue to identify the number of live (glowing cells) and dead cells (stained blue). A haemocytometer was prepared by attaching a cover slip using applied pressure to produce Newton's refraction rings (Fig 2.1). Both sides of the chamber were filled with the stained cell suspension and the cells were counted by the use of a light microscope using 20 x magnification.

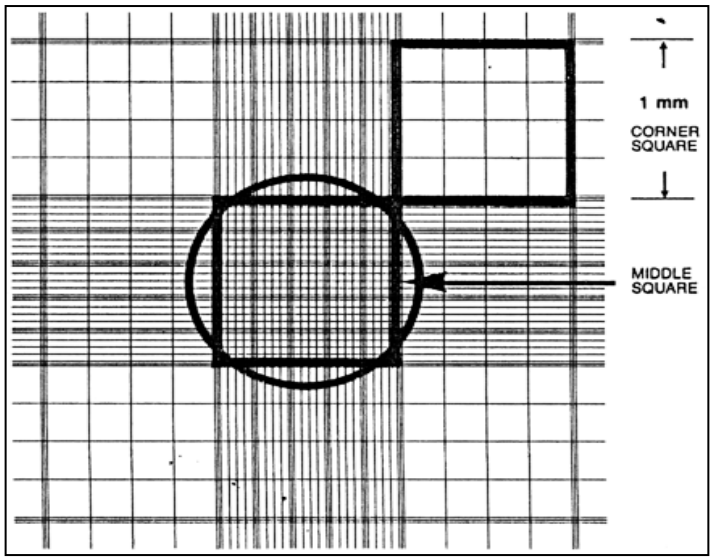

Figure 2.1: Loading the haemocytometer and the middle square which is used for cell counting. (http://www.uvm.edu/~wschaeff/BasicCulture1.html)

2.2 mRNA ISOLATION:

Messenger RNA (mRNA) was isolated using the mRNA isolation kit (Roche-Diagnostics, Germany). This kit used a straight forward and efficient procedure for isolating mRNA. This method helped to directly isolate mRNA without preparing total RNA. It was a safe method since no aggressive organic reagents were used and the mRNA isolated from this kit was of highest purity. [Roche Applied Science (2009) mRNA isolation kit, Roche Diagnostics-Germany]

The basis of the kit was that, the $(A)^+$ tail of mRNA hybridized to a biotin-labelled oligo$(dT)_{20}$ probe. Streptavidin-coated magnetic particles were then used to capture the biotinylated hybrids. A magnetic separator was then used to capture the magnetic particles. The fluid was removed by washing with PBS buffer and finally the mRNA was eluted from the particles by incubating with redistilled water.

The mRNA was then isolated from 2×10^6 cells following the manufacturer's protocol as shown in the schematic diagram (Fig 2.2). Table 2.3 showed the volumes of all reagents and buffers used in this study.

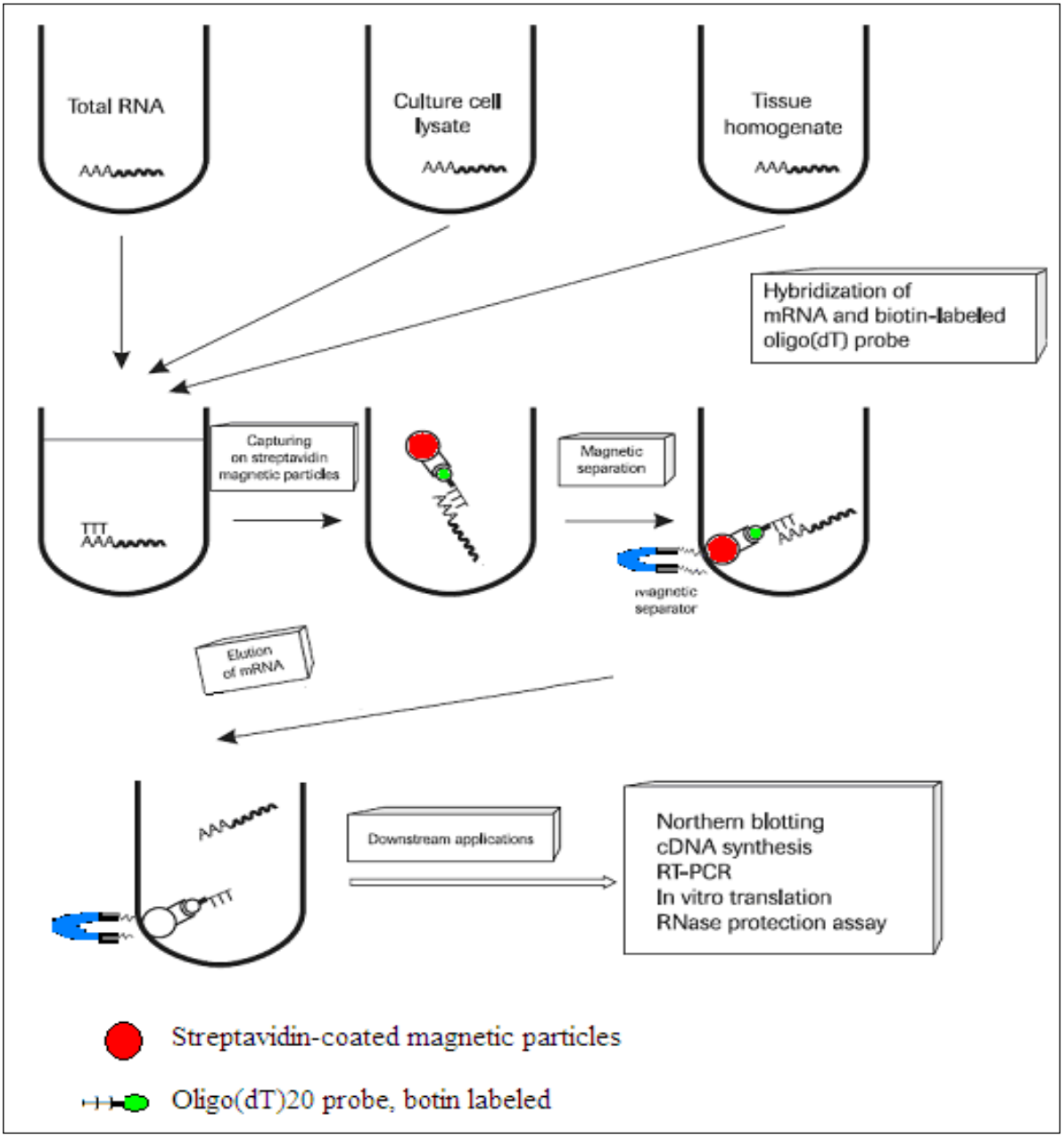

Figure 2.2: mRNA isolation using mRNA isolation kit (Adapted from Roche Diagnostics, UK).

The $(A)^+$ tail of mRNA isolated from the cells hybridizes with a biotin-labelled oligo$(dT)_{20}$ probe, which was then captured by streptavidin-coated magnetic particles. A magnetic separator was then used to capture the magnetic particles. The fluid was removed by washing with PBS buffer and finally the mRNA was eluted from the particles by incubating with redistilled water.

Table 2.3: Volume of reagents and buffer (This table is a modified form adapted from mRNA Isolation Kit catalogue by Roche Applied Science).

Number of cells	2×10^6
Volume of lysis buffer (bottle 1): cells/tissue	500 µl
Volume of streptavidin magnetic particles (cup 2)	50 µl (0.5 mg)
Volume of lysis buffer (bottle 1) for preparation of streptavidin magnetic particles	70 µl
Volume oligo$(dT)_{20}$ probe, biotin-labelled (cup 3)	0.5 µl
Volume of washing buffer (bottle 4)	3 x 200 µl
Volume of redistilled water (bottle 5)	10 µl

mRNA isolation was carried out following the manufacturers protocol. In this study about 2×10^6 cells were used to isolate mRNA following the recommended protocol found in Table 2.4.

Table 2.4: Materials and reagents adjusted for the number of cells for mRNA isolation. The shaded column is the number of cells and volumes of reagents used for this investigation.

Estimated number of cells	1×10^8	2×10^7	1×10^7	2×10^6	2×10^5
Volume of lysis buffer: cells	15 ml	3 ml	1.5 ml	0.5 ml	0.1 ml
Volume of streptavidin magnetic particles	1.5 ml	300 µl	150 µl	50 µl	50 µl
Volume of lysis buffer: streptavidin magnetic particle preparation	2.5 ml	500 µl	250 µl	70 µl	70 µl
Volume of Biotin-labelled oligo(dT)$_{20}$ probe	15 µl	3 µl	1.5 µl	0.5 µl	0.5 µl
Volume of washing buffer	3 x 2.5 ml	3 x 500 µl	3 x 250 µl	3 x 200 µl	3 x 200 µl
Volume of molecular biology-grade H_2O	250 µl	50 µl	25 µl	10 µl	5 µl

1. Cells were washed three times using ice cold PBS to remove excess medium.
2. Lysis buffer (500 µl) was added and the cells were mechanically sheared six times using 21G needle.
3. Streptavidin magnetic particles were prepared by thoroughly mixing and aliquoting 50 µl of streptavidin magnetic particles into a sterile Eppendorf tube. The streptavidin magnetic particles were separated from the storage buffer using the magnetic separator. Storage buffer was removed and discarded.
4. The magnetic particles were washed once by emulsifying in 75 µl of lysis buffer and separated to remove the buffer.
5. An aliquot 0.5 µl biotin labelled oligo $(dT)_{20}$ was added to the lysate, mixed and transferred into the prepared magnetic particles. It was then mixed and incubated at 37 ˚C for 5 min.
6. Following the incubation the lysate was separated from the magnetic particles using the magnetic separator and the lysate was then discarded.
7. Magnetic particles were washed three times with a washing buffer provided quantitatively (3 x 200 µl).
8. mRNA was eluted from the magnetic particles after the addition of 10 µl redistilled water and incubated at 65 ˚C for 2 min.
9. mRNA was separated from the magnetic beads using the magnetic separator and collected and stored at -20 ˚C in RNAse free eppendorf tubes ready for quantification and analysis. The used magnetic particles were emulsified in the storage buffer at a concentration of 10 mg/ml for further use and stored at 4 ˚C.

2.3 QUANTIFICATION OF NUCLEIC ACID BY SPECTROPHOTOMETER:

Spectrophotometry was used as a standard, fast and efficient method for determining quantity and the purity of mRNA (Thermospectronics, England). Optical density was applied at wavelengths of 260 nm and 280 nm to quantify isolated mRNA using gamma thermo Helios spectrophotometer (Thermospectronics, England). TAE (Tris Acetate Ethylenediaminetetraacetic acid) buffer was used as blank. mRNA (2 µl) was combined with 500 µl of 1X TAE buffer (400 mM Tris, 0.01 M EDTA; pH 8.3). The diluted sample was then measured using the spectrophotometer and the concentration determined at a wavelength of 260 nm. The standard formula used was: absorbance of one optical density (OD) = 50 µg/ml for dsDNA and 40 µg/ml for ssRNA. The purity of isolated nucleic acid was determined using the ratio of 260 nm to 280 nm. The presence of pure single-stranded (ss) RNA was indicated by a 1.8 – 2.0 ratio.

The concentrations of the isolated mRNA samples were calculated as follows:

A_{260} reading × 250 (dilution factor) × 40 (ssRNA) = Concentration (µg/ml)

* Dilution factor = total volume/ aliquot measured.

Total volume = volume added to cuvette = 500 µl

Aliquot measured = volume of sample added = 2µl. Therefore, the dilution factor = 250

2.4 ANALYSIS OF NUCLEIC ACID (RNA and DNA) BY AGAROSE GEL ELECTROPHORESIS:

Alkaline and neutral agarose gels were used to analyse isolated mRNA and reverse transcription polymerase chain reaction (RT-PCR) amplions prepared at a concentration of 2% using 0.6 – 2 g agarose powder to obtain 30 - 100 ml of gel.

2.4.1 Alkaline (denatured) agarose gel electrophoresis for mRNA analysis:

1. A gel of 2 % concentration was prepared by dissolving 0.6 g of agarose powder in 30 ml distilled water and heating it in a domestic microwave at maximum power (100 %) for 1-2 min. until a transparent molten solution was formed.
2. The solution was cooled to 50 ˚C before adding 150 µl of sodium hydroxide (NaOH) and 60 µl ethylenediaminetetraacetic acid (EDTA) (from the stock 10 N NaOH and 0.5 M EDTA) to give 50 mM NaOH and 1 mM EDTA final concentrations.
3. The solution was poured into the gel electrophoresis tray. A comb was placed and the gel was allowed to set for 30-45 min.
4. The running buffer with a final concentration of 50 nM NaOH and 1 mM EDTA was prepared by adding 2.5 ml and 1 ml of 10 N NaOH and 0.5 M EDTA in one litre of distilled water. This was mixed and poured in the gel tank containing solidified gel.
5. Samples were introduced in loading dye using 1:4 dilutions.
6. The comb was removed from the gel and the samples were loaded.
7. The gel was electrophoresed at 60 volts (V) for approximately 1 hour before being stained in fresh 0.4 µg/ml ethidium bromide for approximately 10 min. and then destained in distilled H_2O.
8. GENE GENIUS bioimaging system (Syngene, UK), a fully automated gel documentation and analysis system was then used to analyse the gel.

2.4.2 Agarose gel electrophoresis for PCR amplicons:

1. TAE buffer was diluted from a 10 x stock to make 1 x concentration by diluting 1:10 with distilled water.
2. 2 % concentration was made by dissolving 2 g agarose powder in 100 ml 1 x TAE
3. A domestic microwave was used for dissolving the agarose at maximum power for 3-4 min.
4. The solution was cooled to 50 ˚C and poured into the gel electrophoresis tray and the gel was allowed to set with the comb in place. After gel solidification, 1 x TAE running buffer was transferred to the tank.
5. The comb was removed and samples were loaded containing loading dye at a 1: 4 dilution.
6. A molecular marker of 100 bp was also loaded in order to identify the size of PCR product. The gel electrophoresis was carried out at 60 V for 2 hours.
7. The gel was analysed using GENE GENIUS bioimaging system (Syngene, UK).

Table 2.5: Materials and reagents used for agarose gel electrophoresis in this study.

Reagents	Suppliers	Preparation	Working concentration
Ultrapure agarose	Gibco BRL, UK	0.6 - 2 g Agarose 30 - 100 ml 1 x TBE. Solubilized by boiling in a microwave for 3-4 min.	2 % weight/volume
10 x TBE (Ultrapure 10 x Tris borate EDTA electrophoresis buffer)	Sigma, UK	1 M Trizma base 0.9 M 1 x Boric acid 0.01 M EDTA Diluted to 1 x concentration with distilled water	1 x
Alkaline buffer	BDH AnalaR, UK	10 N Sodium Hydroxide 0.5 M Ethylenediaminetetra acetic acid	1 x
Gel loading dye	Sigma, UK	0.25 % w/v Bromophenol blue 0.25 % w/v Xylene cyanole 40 % w/v Sucrose Supplied ready for use 4x concentration	1:4 sample:dye
Ethidium bromide 10 mg/ tablet	Amresco, UK	10 mg Ethidium bromide 10 ml Distilled water. Diluted to 0.5 µg/ml with distilled water	1:20
100 base pair (bp) molecular marker	Sigma, UK	100 µg supplied ready for use	1 µg/ml

2.4.3 Agarose gel documentation and analysis:

The Syngene gel analyser or Gene Genius (Syngene, Cambridge UK) was previously described as a comprehensive and fully automated system for all UV and white light fluorescence applications. The system along with the software Genesnap (Syngene, Cambridge UK) was used for all types of gel media, such as DNA, mRNA and PCR products stained with ethidium bromide. The bands presenting the DNA, mRNAs were observed, and molecular markers used to calculate the sizes were all documented in the system.

Staining of agarose gel with ethidium bromide (Sigma, UK) was needed so as to analyse nucleic acids (mRNA) from electrophoresis. A stock solution was prepared with a tablet of 10 mg ethidium bromide dissolved in 10 ml of distilled water to obtain a final concentration of 1 mg ml^{-1}. A staining working solution of 50 µg ml^{-1} was prepared by diluting 25 µl in 500 ml of distilled water. Syngene gel analyser was used after staining the gel for 15-30 min.

Since ethidium bromide was previously described as mutagenic and a suspected carcinogen, safety precautions were adopted to minimize risk to the user and the environment. A laboratory coat, gloves and safety goggles were worn during use of ethidium bromide and a special chamber located within the laminar hood was used to perform the process of staining. All gloves, pipette tips, and gels were disposed in special waste disposal containers for incineration. Staining solution was decontaminated using a charcoal filter funnel (Schleicher and Schuell Bioscience, UK). The funnel filter was disposed by incineration whilst the filtrate was poured down the drain with running water.

2.5 COMPLEMENTARY DNA SYNTHESIS (cDNA):

mRNA was reverse transcribed using the First strand cDNA synthesis kit using AMV enzymes isolated from Avian Myeloblastosis Virus (Roche Diagnostic, Germany). AMV Reverse Transcriptase is the enzyme which synthesizes the new cDNA strand at the 3'-end of the poly (A) - mRNA where oligo dT is used as a primer. RNAse contamination was minimized by using sterile vessels and pipette tips. The RNAse inhibitor and AMV reverse transcriptase were thawed on ice; all other solutions were thawed at room temperature and kept on ice after thawing. All reagents were vortexed and briefly centrifuged before carrying out the procedure.

After calculating the mRNA concentration, the volume of mRNA required for the conversion to cDNA was determined using the formula shown below:

Volume of mRNA for its conversion to cDNA (µl)	=	Required concentration (100 ng ml^{-1})/ calculated mRNA concentration

A master mix of 11.8 µl was prepared using the components as mentioned in Table 2.6.

Table 2.6: Reagents provided with the kit for cDNA synthesis. (Table adapted from 1st Strand cDNA synthesis Kit for RT-PCR (AMV)$^+$ by Roche Applied Science, Germany)

Reagents	Volumes	Final concentrations
10 x Reaction Buffer	2.0 µl	1 mM
25 mM Magnesium chloride ($MgCl_2$)	4.0 µl	5 mM
Deoxynucleotide Mix	2.0 µl	1 mM
Primer Oligo-p$(dT)_{15}$	2.0 µl	0.04 A260 units (1.6 µg)
RNAse inhibitor	1.0 µl	50 units
AMV reverse transcriptase	0.8 µl	≥20 units
Sterile water variable (depends on the quantity of mRNA added)		
RNA sample variable (depends on the concentration of isolated mRNA. 50 ng mRNA was added)		
Final volume for one sample = 20.0 µl		

1. The master mixture was briefly vortexed and centrifuged in order to collect the sample from the bottom of the microfuge tube.
2. Aliquots of 11.8 µl of the master mixture were added into the sterile microfuge tube.
3. mRNA was added to give a final concentration of 100 ng per volume.
4. Sterile water was added to give a final volume of 20 µl.
5. The mixture was briefly vortexed, centrifuged at 100 xg and incubated at 25 °C for 10 min. in order for the primer to anneal to the RNA.
6. The mixture was further incubated at 42 °C for 60 min. where mRNA was reversed transcribed to cDNA resulting in the synthesis of cDNA.
7. Following incubation, AMV Reverse Transcriptase was denatured by incubating the reaction at 99 °C for 5 min. and the cooled to 4 °C for 5 min.
8. The sample was then stored at -20 °C prior to amplification.

2.6 QUANTITIVE REAL TIME POLYMERASE CHAIN REACTION (qRT-PCR):

Polymerase Chain Reaction (PCR) was previously described as a process which allowed logarithmic amplification of short DNA sequences (usually 100-600 bases) within a longer stretch of the double stranded DNA molecule. qRT-PCR allows very low copies of mRNA to be amplified (Roche Applied Science, Germany).

The level of several gene expressions was calculated by using qRT-PCR using the LightCycler 2.0 system. (Roche Diagnostics, Germany) and LightCycler® FastStart DNA Master^{PLUS} SYBR Green I kit. The manufacturer's instructions were carried out to

perform the experiment. A master mix was prepared using the reagents from the kit provided.

Table 2.7: The composition and quantity of each reagent provided within the LightCycler® FastStart DNA Master^{PLUS} SYBR Green I kit.

Reagents	Reagent Compositions	Quantity
LightCycler® FastStart Enzyme (1a)	FastStart Taq DNA Polymerase	1 vial
LightCycler® FastStart Reaction Mix SYBR Green (1b)	Reaction buffer, dNTP mix (with dUTP instead of dTTP), SYBR Green I dye and 10 mM $MgCl_2$	3 vials
H_2O, PCR-grade	RNase-free H_2O	2 ml

Table 2.8: The quantities of reagents required for each RT-PCR reaction using those provided within the LightCycler® FastStart DNA Master^{PLUS} SYBR Green I kit.

Reagents	Quantity
Molecµlar biology-grade H_2O	12 µl
PCR primer mix	2 µl
Enzyme Master Mix	4 µl
Single-stranded cDNA template	2 µl

The enzyme master mix was prepared by transferring 14 µl of enzyme into the vial of reaction mix (Table 2.7)

1. The samples and reagents were kept on ice throughout the experiment.
2. Each capillary had a 20 µl total reaction volume comprising 12 µl of molecular biology-grade H_2O, 2 µl of 10 µM PCR primer mix, 4 µl of master mix and 2 µl of single-stranded cDNA template.
3. A volume of 20 µl template-free (molecular biology-grade H_2O substituted for cDNA) reaction mixture was also prepared as a negative control.
4. Before qRT-PCR was carried out for each gene in the cell line under examination, the annealing temperature was optimised using genomic DNA from a control kit as listed in table 1 in the method section.

The PCR protocol was: (See Table 2.9 below)

1. It involved a hot-start induction with the FastStart *Taq* DNA polymerase enzyme activated by pre-incubating the reaction mixture to 95 ^{o}C for 10 min.
2. The single-stranded cDNA template was then subjected to 35 amplification cycles composed of the following parameters:
    - Denaturation at 95 ^{o}C for 15 sec.
    - Annealing at the primer dependent temperature for 15 sec [63 ^{o}C for *hsp90α* and 56 ^{o}C for Glyceraldehyde 3-phosphate dehydrogenase (*GAPDH*)].
    - Extension at 72 ^{o}C for 25 bp sec^{-1} (amplicon dependent)

At the end of each cycle the emitted fluorescence was measured in a single step to acquire quantification analysis data. A slope of 20 $^{o}C\ s^{-1}$ was maintained for heating and cooling purposes.

On completion of the 35th cycle the produced amplicon was prepared for melting curve analysis and hence, it was heated to 95 ^{o}C (denaturation) and then rapidly cooled to the previously used annealing temperature (+10 ^{o}C) for 40 sec. For the melting curve analysis the temperature was raised to 95 ^{o}C with a slope of 0.1 $^{o}C\ s^{-1}$ and the emitted fluorescence was constantly measured.

Finally, the generated amplicon was cooled to 40 ^{o}C for 30 sec and stored at 20 ^{o}C until required.

Table 2.9: qRT-PCR conditions used as defaµlt conditions for all amplifications

Analysis Modes	Cycles	Segments	Target Temperatures (^{o}C)	Hold Times (min)
	Pre-Incubation			
None	1		95	10
	Amplification			
Quantification	35	Denaturation	95	1
		Annealing	variable	2
		Extension	72	1
			72	7
	Cooling			
None	1		4	∞

2.7 ANALYSIS OF qRT-PCR PRODUCT:

2.7.1 Agarose gel electrophoresis:

The amplicons from the qRT-PCR reaction were run on a 2% (w/v) agarose gel. Aliquots (10 µl) of each amplicon was mixed with 2 µl of loading dye while, 5 µl of a 100 bp molecular weight marker was mixed with 2 µl loading dye. The samples along with the molecular weight marker were loaded onto the gel and electrophoresed at 60 V. The banding patterns were visualised using a GENE GENIUS Bioimaging system, UK and Gensnap software.

2.7.2 Quantification analysis of qRT-PCR:

Copy numbers were used to express the absolute quantification of the target amplicon. In real time PCR a positive reaction was detected by the accumulation of a fluorescent signal. The number of cycles required for the fluorescent signal to cross the threshold was determined by the Ct (cycle threshold) value. Genomic DNA could be used as an external standard showing that 1 µg corresponded to 3.4×10^5 copies of a single gene (Wittwer *et al.*, 2004). In our laboratory (Shervington *et al.*, 2007; Mohammed, PhD Thesis, 2007), genomic DNA of known concentrations were used as a standard to amplify GAPDH gene using the LightCycler instrument. The Ct served as a tool for calculating the quantity of the starting template in order to plot a standard curve to aid the determination the of copy number in unknown samples. A standard curve was generated from five concentrations of genomic DNA in duplicate: 0.005, 0.05, 0.5, 5 and 50 ng (known copy numbers) and their corresponding average Ct's (Fig 2.3 and Table 2.10) were used to generate the copy number verses concentration.

A.

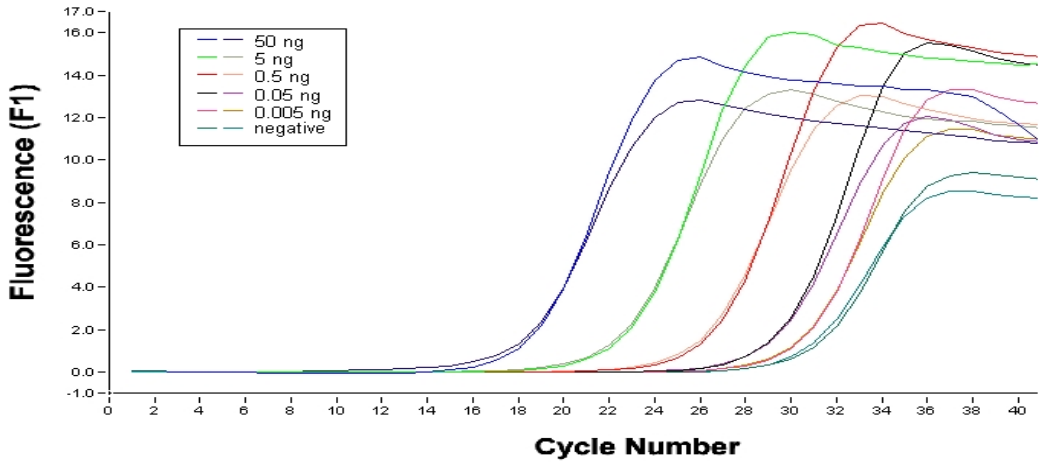

B.

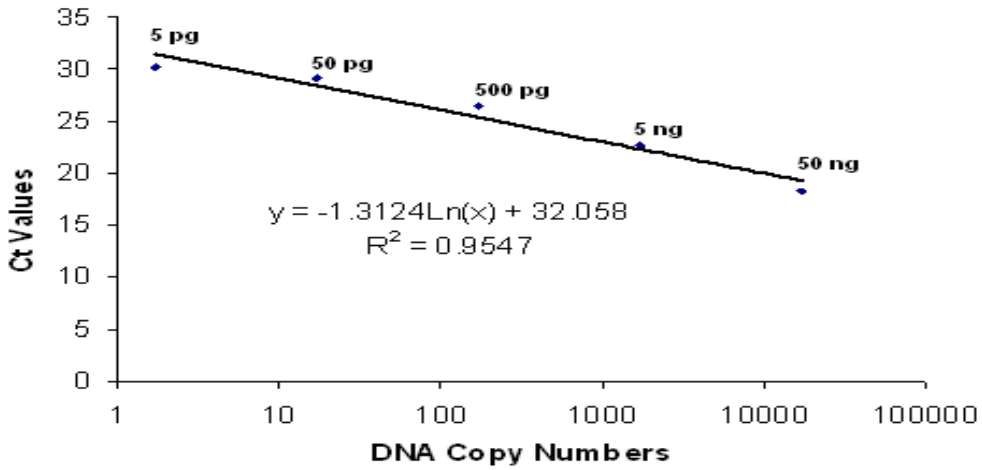

Figure 2.3: Standards used to generate the copy numbers for each gene. (A) LightCycler quantification curve generated using known concentration of genomic DNA was amplified, showing that the higher the concentration of DNA the lower the Ct values i.e. earlier the acquisition of florescence. The negative control (Primer alone, NTC) shows no florescence acquisition until after 30 Ct (straight line). (B) The standard generated from the crossing points indicating the relationship between Ct values and the copy numbers of the amplified genomic DNA using *GAPDH* reference gene (adapted from Mohammed, 2007). Data are mean ± standard deviation, n = 3.

Table 2.10: Genomic DNA corresponded to its average Ct values and equivalent copy number.

Concentrations of Genomic DNA (ng)	Average Ct	Copy numbers
0.005	30.15	1.7
0.05	29.10	17
0.5	26.42	170
5	22.60	1700
50	18.30	17000

The equation generated (y = -1.3124Ln(x) + 32.058) from this standard graph was rearranged to (=EXP ((Ct value-32.058)/-1.3124)) and used to determine copy numbers of the mRNA expression of all the genes used throughout this study.

2.8 ANTIBODY INFORMATION:

1) Hsp90α rat monoclonal antibody (PRIMARY)

This antibody detected a 90 kDa protein, corresponding to the apparent molecular mass of Heat Shock Protein 90 Alpha (Hsp90α) on sodium dodecyl sulfate polyacrylamide gel electrophoresis (SDS-PAGE) immunoblots. Company suggested that it was specific for Hsp90alpha (Hsp86) and did not cross react with Hsp90 beta (Hsp84) (Cambridge Bioscience, UK). It immunoprecipitated with both free and complexed Hsp90. This antibody recognized lower molecular weight Hsp90α degradation

fragments as well as the intact protein and was therefore useful for monitoring proteolytic degradation of Hsp90α.

Host Animal: Rat

Antibody Isotype: IgG2a

Species Reactivity: human, chicken

Immunogen: Human Hsp90 purified from therapeutic orchiectomy specimens

Applications: WB, IHC, Flow Cytometry

Stored: -20 ^{0}C

2) **Rabbit Anti-Rat IgG (H+L) (SECONDARY)**

Source: Pooled antisera from rabbit's hyperimmunized with rat IgG.

Cross Absorption: NA.

Purification: Affinity chromatography on pooled rat IgG covalently linked to agarose.

Specificity: Reacted with the heavy and light chains of rat IgG1, IgG2a, IgG2b and IgG2c, and with the light chains of rat IgM as demonstrated by ELISA and/or flow cytometry.

WORKING DILUTIONS

Immunofluorescence: Fluorescein isothiocyanate (FITC) conjugate ≤ 1 µg/10^6 cells

Stored: 2-8 ^{0}C

Both the antibodies were purchased from Cambridge Biosciences, UK.

2.9 Akt/PKB KINASE ACTIVITY ASSAY:

Akt/PKB Kinase Activity Assay Kit (Non-radioactive, Assay Designs, UK) was used to quantify the activity of Akt/PKB in the cell samples. The kit was based on a solid phase enzyme linked immuno-absorbent assay (ELISA) utilizing a synthetic peptide as a substrate for PKB along with a polyclonal antibody which recognized the phosphorylated form of the substrate. In this assay, the substrate which was readily phosphorylated by PKB was pre-coated onto the wells of the PKB substrate microtitre plate. Prior to the sample analysis, a standard curve was plotted using the purified active PKB supplied (20 µg/ml).

Following the addition of the samples to the appropriate wells, ATP was added to initiate the reaction. A phosphospecific substrate antibody was added to the well and which was specifically bound to the phosphorylated peptide substrate. Peroxidase conjugated secondary antibody was then added which was subsequently bound to the phosphospecific antibody. The assay was developed with tetramethylbenzidine substrate (TMB) and correspondingly, colour development observed was directly proportional to the PKB phosphotransferase activity. This colour development was quenched with acid stop solution and the intensity was measured in a microplate reader at 450 nm.

2.9.1 Standard Curve:

1. The following components of the kit: PKB substrate microtitre plate, Antibody dilution buffer, Kinase assay dilution buffer, TMB substrate and Stop solution 2, were adjusted to room temperature.
2. The desired number of wells from the PKB substrate microtitre plate was soaked with 50 µl of Kinase assay dilution buffer at room temperature for 10 min.
3. After carefully aspirating the liquid from each well, varying quantities of purified active PKB; 2.5, 5, 10, 20 and 40 ng were added to the appropriate wells of the PKB substrate microtitre plate.
4. The reaction was initiated by adding 10 µl of diluted ATP to each well except the blank.
5. The plate was then incubated for 60 min. at 30 ^{o}C in a rotating shaker set rotating 60 rpm.
6. The reaction was stopped by emptying the content of the well and then 40 µl of phosphospecific substrate antibody was added to each well except the blank.
7. The plate was then incubated for 60 min. at room temperature.
8. The wells were washed four times with 100 µl wash buffer.
9. A volume of 40 µl of diluted Anti-Rabbit IgG: HRP Conjugate was added to each well except the blank.
10. After incubating the plate at room temperature for 30 min, the wells were washed four times with 100 µl 1 x wash buffer.
11. An aliqot of 60 µl of TMB substrate was then added to each well.

12. The plate was then incubated at room temperature for 30-60 min. The incubation time was determined according to the development of the colour.
13. A volume of 20 µl of stop solution 2 was added to each well in a similar order to that of the TMB substrate.
14. Absorbance was measured at 450 nm using a microtitre plate reader.
15. The active PKB standard curve was plotted.

2.9.2 Assay Procedure:

1. The assay procedure was similar to the Standard Curve procedure (2.9.1), with a minor modification involving step 5 wherein, the microtitre plate was incubated for 90 min. at 30 ^{0}C in a rotating shaker at 0.6 xg.

2.10 Hsp90α ELISA ASSAY:

Assay Design's (UK) Hsp90α ELISA kit provided a sensitive, swift and steadfast method to detect and quantify Hsp90α in cell lysates, tissue extracts and serum samples from human origin.

Company recommended the kit to be specific for Hsp90α and involved a quantitative sandwich immunoassay. It used Hsp90α specific mouse monoclonal antibody pre-coated on the wells of the provided Anti-Hsp90α plates to capture Hsp90α in the sample or the standard. The captured protein was then detected using an Hsp90α antibody conjugated with horseradish peroxidase (HRP). The assay was developed with TMB substrate and the colour development was proportional to the quantity of Hsp90α captured. Acidic stop solution was then added to the wells which develops the

endpoint colour. The intensity of the colour was then measured in a microtitire plate reader at 450 nm.

1. The components of the kit: Anti-Hsp90α immunoassay plate, 20 x wash buffer, sample diluent, HRP conjugate diluent, TMB substrate and Stop Solution 2, were thawed until they achieve room temperature.
2. Recombinant Hsp90α standard (0.0625 - 4 ng ml^{-1}) and samples were prepared in sample diluent.
3. A volume of 100 µl of the prepared standards and samples were added to wells of Anti-Hsp90α immunoassay plate and then incubated at room temperature for 60 min.
4. The wells were washed 6 times using 1 x wash buffer.
5. An aliqot of 100 µl of diluted HRP conjugate was then added to the wells of the immunoassay plate and later incubated at room temperature for 60 min.
6. The wells were then washed 6 times with 1 x wash buffer.
7. A volume of 100 µl of TMB substrate was added to each well and the immunoassay plate was left to incubate at room temperature for 20 min.
8. An aliqot of 100 µl of Stop solution 2 was then added to each well in the same order that TMB substrate was added.
9. The absorbance was measured at 450 nm and an Hsp90α standard curve was plotted. The Hsp90α concentrations of samples were then calculated using the equation of the graph.

2.11 CELL VIABILITY ASSAY:

For cell viability assay, this study measured the levels of ATP in the cells using a luminescence assay kit as described below.

1. Cell viability was assessed using Celltiter-Glo® Luminescent cell viability assay (Promega, UK) according to the manufacturer's protocol.
2. Cultured cells were plated in flat-bottom 96 well plate; control wells containing medium without cells were prepared to obtain a value for background luminescence.
3. When the desired confluence was reached the test compound (drug) was added to the wells and incubated under standard cell culture conditions (varied according to experiment, usually 48 hours).
4. The contents of the 96 well plates were equilibrated at room temperature for 30 min.
5. CellTitre-Glo reagent was prepared by transferring the appropriate volume of CellTitre-Glo buffer and CellTitre-Glo substrate (1:1). Depending on the number of wells used, the CellTitre-Glo reagent was mixed 1:1 with cell media.
6. The contents of the 96 well plates were emptied and washed twice with PBS.
7. A volume of 200 µl of the prepared mixture of CellTitre-Glo reagent and cell media (1:1) was added to the appropriate wells of the 96 well plate.
8. The plate was then incubated at room temperature for 10 min. to allow stabilisation of the luminescent signal before the luminescent signal was detected using Tecan GENios Pro® (Tecan, Austria).

2.12 U87-MG CELL CYCLE ANALYSIS:

Cell cycle analysis of the cells treated with either drugs or shRNA was carried out. This analysis was performed to determine the different stages of cell cycle affected in U87-MG cells post treatment. Table 2.11 illustrated the reagents and their concentrations used for cell cycle analysis.

1. The cells (1 x 10^6 cells) were scraped and washed once with PBS (0.1M) and then centrifuged at 100 xg for 5 min.
2. The supernatant was discarded and the cells were fixed by re-suspending them in 2 ml of 70 % ice cold ethanol which was added drop wise to the cell pellet to avoid clumping of the cells.
3. The cell sample was then stored at -20 ^{o}C for a minimum of 24 hours.
4. The fixed samples were centrifuged at 100 xg for 5 min. and the supernatant was discarded and the cells were washed once with PBS (0.1 M).
5. The cells were re-suspended in PBS containing 50 μg ml^{-1} of PI and 100 μg ml^{-1} of RNAse and incubated at 37 ^{o}C for 30 min.
6. The stained samples were stored at 4 ^{o}C in the dark until subjected to flow cytometric analysis.

Table 2.11: Reagents and its concentration used for cell-cycle analysis

Reagents	Concentrations	Suppliers
PBS	0.1M	Sigma, UK
Ethanol	70%	Fisher Scientific, UK
PI	50 $\mu g\ ml^{-1}$	Sigma, UK
RNAse	100 $\mu g\ ml^{-1}$	Sigma, UK

2.13 FLOW CYTOMETRY:

Flow cytometer was previously described as an instrument that helps to measure the properties of an individual cell. The cells were labelled with a particular antibody conjugated to a fluorochrome and by means of hydrodynamic focusing. Each cell was passed through a single or multiple beams of light. The emitted fluorescence (light scattering) gave knowledge about the cellular properties. Fluorescence measurements taken at different wavelengths provided quantitative and qualitative data about fluorochrome-labelled cell surface receptors or intracellular molecules within a cell (e.g. DNA and cytokines).

2.13.1 Sample preparation: (adopted from Abcam, UK; modified according to the experimental requirement)

1. Untreated and treated cells (>1 x 10^6 cells) were collected by scraping. The cells were washed thrice with 0.1 % BSA made in (0.1 M) PBS.

2. After each wash the cells were centrifuged at 100 xg for 5 min. at 4 ^{o}C. The supernatant was carefully discarded with efforts to achieve a maximum number of cells for the analysis.
3. The cells were permeabilised by incubating with 0.1 % of Triton-X made up in (0.1 M) PBS for 15 min. in the dark. This was followed by three washes with 0.1 % BSA.
4. Blocking solution [made up in 5 % serum in (0.1 M) PBS based on the animal in which the antibody was raised] was added to the cells and incubated for 30 min. at 4 ^{o}C.
5. After 30 min. the cells were centrifuged and the blocking solution was discarded. This was followed by the addition of the specific primary antibody [made up in 5 % serum with (0.1 M) PBS] for 30 min.
6. The primary antibody was removed by washing thrice with 0.1 % BSA. The secondary antibody was then prepared in a similar fashion as the primary antibody and was added to the cell sample and incubated in the dark for 30 min.
7. Traces of secondary antibody were removed by washing thrice with 0.1 % BSA.
8. Finally, the cells were re-suspended in 250 µl 0.1 % BSA and then filtered to remove clumps using a sterile filter for flow cytometric sample preparation. The samples were stored at 4 ^{o}C in the dark until analysed on the flow cytometer.
9. The negative control was prepared by excluding the labelling with primary antibody. The rest of the treatment remained identical.

10. The cell sample and the reagents were kept on ice throughout the experiment to minimize cell death. Moreover, the samples were gently pipetted to achieve single cell suspension during each step.

2.13.2 Data analysis

The cells were gated selectively by eliminating cell debris or dead cells. For each sample a maximum of 10,000 events/sample was taken into consideration. Flow cytometric data were demonstrated by means of a density plot, contour diagrams and histograms. Throughout the studies, histogram graphs were used and which displayed relative fluorescence (single parameter) on the x-axis and the number of events on the y-axis. Figure 2.4 represented a typical histogram plot after flow cytometric analysis. A statistical view of the data could be achieved after acquiring 10,000 events/ sample to identify the exact number of positive cells in a given sample.

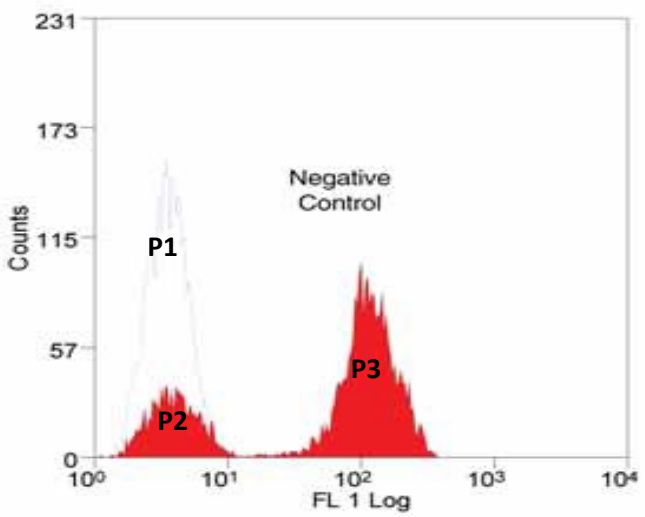

Figure 2.4: A histogram graph demonstrating flow cytometric data

[P1-negative control, P2- negative population of cells from sample and P3- positive population of the stained cells.

(Modified from http://keck.bioimaging.wisc.edu/Neuro670/Introduction %20to%20Flow%20Cytometry.pdf)]

2.14 STATISTICAL ANALYSIS:

Data have been analyzed using PASW package employing One-Sample Students T-test and Paired-Sample T-test. A value of $*p < 0.05$ and $**p < 0.001$ was taken as significant.

CHAPTER 3

Hsp90α SILENCING BY RNAi

3.1 INTRODUCTION:

Cancer is a class of disease which is mainly characterized by aberrant changes in the sequence and/or expression of several genes (Rao *et al*., 2009). Over the past decades, researchers have been studying these changes at the genetic and protein level to find strategies to block or prevent the progression of tumours. There are several sets of genes that are mutated in cancer which play a vital role in tumour progression and tumour cell stabilization (Rao *et al*., 2009). Numerous efforts to develop inhibitors against such genes and/or proteins have been investigated. RNA interference (RNAi) which inhibits transcription of particular gene(s) of interest has been underway with some of the small molecule inhibitors already undergoing clinical trials (www.cancerresearchuk.org).

RNAi is a natural process by which expression of the gene of interest could be knocked down with high specificity and selectivity (Rao *et al*., 2009). This involves enzymatic cleavage of target mRNA which leads to a decrease in the corresponding protein. With the current advanced technology together with the extensive understanding of bioinformatics, investigators could possibly identify relevant bio molecular tumour networks for knockdown. Gene specific RNAi agents can potentially knockdown key abnormally over and/or constitutively expressed molecular targets selectively in each patient's tumour in order to provide personalized tumour therapy. Additionally, these single agents can be combined with other small molecule inhibitors and be used in combination therapy for tumours (Rao *et al*., 2009).

3.1.1 RNA interference for cancer:

The discovery of the evolutionary gene silencing mechanism was reported more than 20 years ago (Stein and Cohen, 1988). RNAi is initiated by RNase Dicer which cleaves the double stranded RNA substrates into 21-25 nucleotide long RNA fragments (small interfering RNA/siRNA) (Fig 3.1). These siRNA duplexes become incorporated into a protein complex called RNA induced silencing complex (RISC) (Fig 3.1). RISC is an enzyme which catalyses hundreds or thousands of RNAi *in vivo* and it uses the antisense strand of the siRNA to bind and degrade corresponding mRNA thus, causing gene silencing (Sharp and Zamore, 2000; Bernstein *et al*., 2001). A member of the Argonate family, Argonate 2 (Ago2) is the protein in RISC responsible for cleavage of the sense strand of the siRNA duplex and also the target mRNA (Rand *et al*., 2004; Matranga *et al*., 2005; Rand *et al*., 2005).

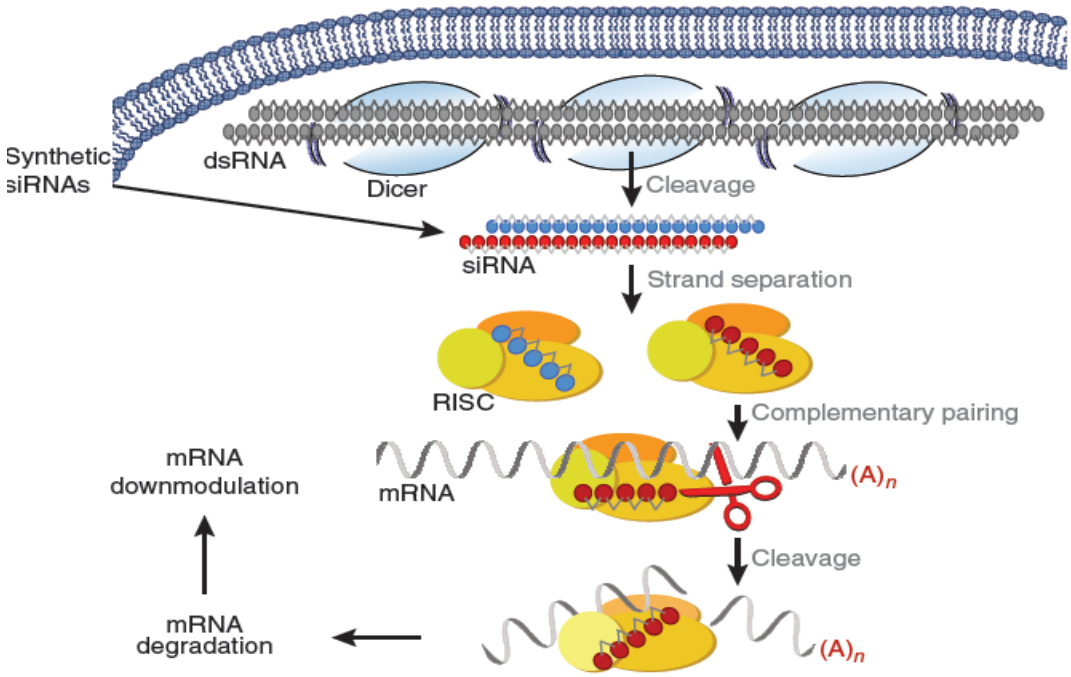

Figure 3.1: RNAi mechanism. (Adapted from Bumcrot *et al.,* 2006)

Long double stranded RNA (dsRNA) is cleaved by Dicer into siRNA (or synthetic siRNAs are added). These siRNAs bind to RISC where the strands are separated. The RISC complex with the antisense strand then binds to complementary mRNA sequences. mRNA is then cleaved by Ago2.

There has been significant progress in RNAi therapeutics, initiating from the discovery of RNAi being mediated by double stranded RNA in *C. elegans* in 1998 (Fire *et al*., 1998) and the use of synthetic siRNA's to silence target genes in mammalian cell line systems in 2001 (Elbashir *et al*., 2001). Several studies have demonstrated silencing of diseased genes by utilizing siRNA, with some studies showing promising *in vivo* results (Kumar *et al*., 2007; Dykxhoorn *et al.,* 2006).

In 2004, Soutschek *et al*. effectively silenced apolipoprotein apoB in mice by intravenously administering cholesterol conjugated siRNA duplexes. Three daily injections at a dose of 50 mg/kg resulted in silencing of the apoB mRNA in the liver and jejunum by 57 and 73 %, respectively (Soutschek *et al*., 2004). A study in human

prostate cancer xenograft model demonstrated the use of cardiolipin liposomes containing siRNA specific for Raf-1 to inhibit tumour growth (Pal *et al*., 2005).

The effects of RNAi are mediated by two types of molecules viz., chemically synthesized double stranded small interfering RNA (siRNA) or vector based short hairpin RNA (shRNA). Studies have shown that active siRNA produced *in vitro* by T7 RNA polymerase consisted of a hairpin structure which can be transcribed into cells by RNA polymerase III promoter on a plasmid construct (Yu *et al*., 2002; Miyagishi *et al*., 2003). Although both siRNA and shRNA have similar functional outcomes, they are actually two fundamentally different molecules and hence, their molecular mode of action together with their interference pathways, off target effects, and applications, are also different (Rao *et al*., 2009).

3.1.2 siRNA and shRNA:

Post delivery siRNA is observed to translocate within 15 min. in the nucleus and then gradually increase its quantity in the cytoplasm up to 4 hours before reaching a steady state level. The siRNA mediated RNAi activity usually peaks around 24 hours post delivery with a gradual decrease within 48 hours (Jarve *et al*., 2007; Grunweller *et al*., 2003). However, shRNA's is synthesized within the nucleus of the cells and is then transported to the cytoplasm where it is incorporated into the RISC for activity (Cullen, 2005). shRNA transcribed by the RNA polymerase II or III through the polymerase promoters on the expression cassette and the primary transcript form contains a hairpin like stem loop structure which is processed in the nucleus (Lee *et al*., 2003).

Inside the nucleus the complex containing RNase III enzyme Drosha and pasha protein (DGCR8), a double stranded RNA binding domain protein which measures the hairpin and permits the primary transcript to be processed into individual shRNA's with a 2 nucleotide 3' overhang (Zhang *et al*., 2002). This processed transcript is called pre-shRNA which is transported into the cytoplasm by exportin 5, a RA sarcoma-related nuclear protein guanosine-5'-triphosphate (Ran-GTP)-dependent mechanism (Lee *et al*., 2002; Cullen, 2004). Once inside the cytoplasm, the pre-shRNA is loaded to another RNase III complex containing the RNase III enzyme Dicer and RISC-loading complex subunit TARBP2 (TRBP/PACT), wherein, the loop of the pre-shRNA is processed to form a double stranded siRNA with 2 nucleotide 3' overhangs (Yi *et al*., 2003; Lund *et al*., 2004; Lee *et al*., 2004). This complex is then loaded to the RISC complex containing Ago2 protein as described previously. Once in the RISC complex, both siRNA and shRNA normally behave in a similar fashion (Fig 3.2).

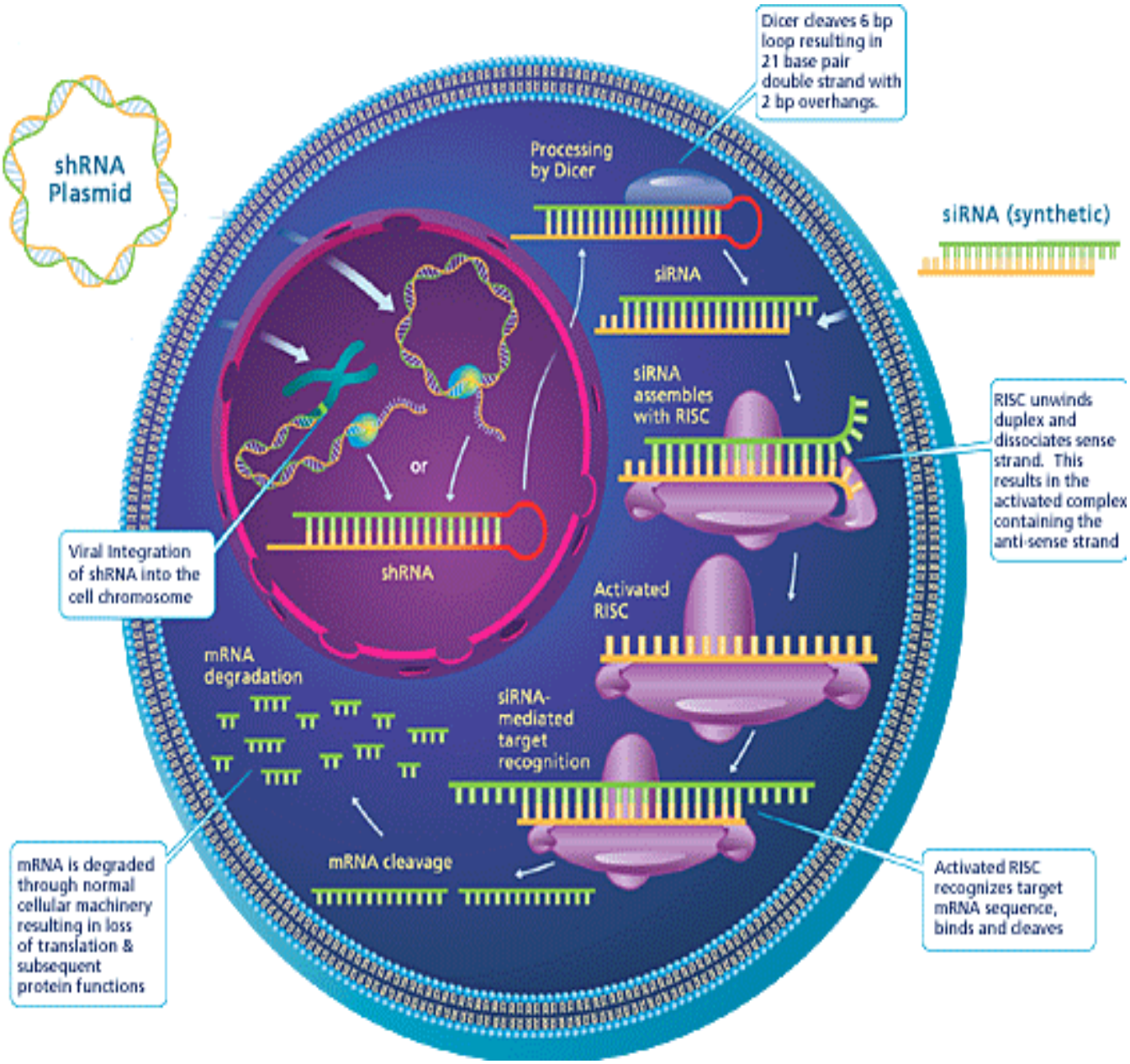

Figure 3.2: siRNA and shRNA pathways. Adapted from http://www.sigmaaldrich.com/united-kingdom.html. The siRNA/shRNA molecule is cleaved by Dicer resulting in 21 base pair double strand with 2 bp overhands. The siRNA strand then assembles with RISC which unwinds the duplex and dissociates sense strand. This results in an activated complex containing the anti-sense strand. The RISC-siRNA complex then recognizes target mRNA sequence and brings about mRNA degradation once bound. This result is loss of translation and subsequent protein functions.

RNA interference has rapidly become important in gene therapy since it enables the researcher to selectively target the gene of interest and knockdown its expression (Kumar *et al*., 2007; Xie *et al*., 2006). As previously described, the concept of antisense

oligonucelotides to regulate gene expression and its subsequent application in gene therapy for the treatment of tumours has been established for more than 20 years now (Stein *et al*., 1988). Preclinical studies have confirmed the use of RNAi techniques for the treatment of cancers. In 2003, Sherr *et al*., successfully demonstrated the use of siRNA to silence *bcr-abl* oncogene which causes chronic myeloid leukemia (CML) in BCR-ABL positive cell lines and in primary cell lines from patients (Scherr *et al*., 2003). Synthetic siRNAs have been used by Martinez and colleagues to specifically silence mutated p53 in a population of cells expressing both mutated and wild type (WT) p53, resulting in a total restoration of WT p53 protein function (Martinez *et al*., 2002). Furthermore, a study in 2004 demonstrated the use of siRNAs to silence *HER2*; *HER2* gene is supposed to play vital role in oncogenesis of several tumours including breast, ovarian, colon and gastric tumours. Treatment of tumour cell lines with *HER2* siRNA resulted in late arrest at the G (1)/S growth phase showing therapeutic importance (Choudhury *et al*., 2004). Moreover, Li *et al*., (2003) demonstrated the therapeutic potential in the treatment of hepatocellular carcinoma (HCC) by targeting overexpressed oncogenes such as cycline E with siRNAs targeted against it (Li *et al*., 2003).

Furthermore, *in vivo* studies involving the targeting of critical components for tumour cell growth (Li *et al*., 2003; Brummelkamp *et al*., 2002; Uchida *et al*., 2004) metastasis (Duxbury *et al*., 2004; Salisbury and Macaulay, 2003), angiogenesis (Takei *et al*., 2004) and chemoresistance (Singh *et al*., 2008; Nakahira *et al*., 2007) by siRNA have shown favourable usage of RNAi in the treatment of tumours. The silencing attained by siRNA is effective; however, it has certain disadvantages which are overcome by shRNA. Though siRNA's are stable and its delivery to the cytoplasm is much easily attained as

opposed to the shRNA's delivery into the nucleus, the shRNA hairpin is a better substrate to the dicer with improved RISC loading (Kim *et al*., 2005; Siolas *et al*., 2005). Furthermore, shRNA plasmids are amplified by transcription. siRNA's on the other hand are not amplified intracellularly and also are more susceptible to metabolism (McAnuff *et al*., 2007).

Some reports have further suggested that the loading efficiency of siRNA's is 10 times lower than that of shRNA's. Moreover, siRNA's have higher degradation with less than 1 % of siRNA remaining in the cell 48 hours post administration (Sano *et al*., 2008; Siolas *et al*., 2005; Vlassov *et al*., 2007). Interestingly, shRNA's are more durable with them being continuously synthesized in the host cells. Considering the potency of both siRNA and shRNA, it has been reported by McAnuff *et al*., (2007) using a luciferase expression system that shRNA is 250 times more effective than siRNA on a molar basis (McAnuff *et al*., 2007).

Siolas *et al.,* (2005) developed identical siRNA and shRNA stands and targeted firefly luciferase gene in HeLa cells, resulting in shRNA effectively inhibiting the gene better than siRNA (Siolas *et al*., 2005). In another study undertaken in 2007, the internal ribosome entry site of the hepatitis C virus (HCV) was targeted by both shRNA and siRNA to inhibit the site driven gene expression in cultured cells resulting in shRNA being more potent than the corresponding siRNA (Vlassov *et al*., 2007). Recent studies have also shown shRNA's to be effective *in vivo* (see Vorhies *et al*., 2007; Tong *et al*., 2009).

It has been reported that the 5' end of shRNA oligonucelotides are less immunogenic than the 5' ends of the siRNA oligonucelotides, thus it shows that shRNAs are less likely

to induce an inflammatory response as opposed to siRNAs. (Kim *et al*., 2005; Marques *et al*., 2006).

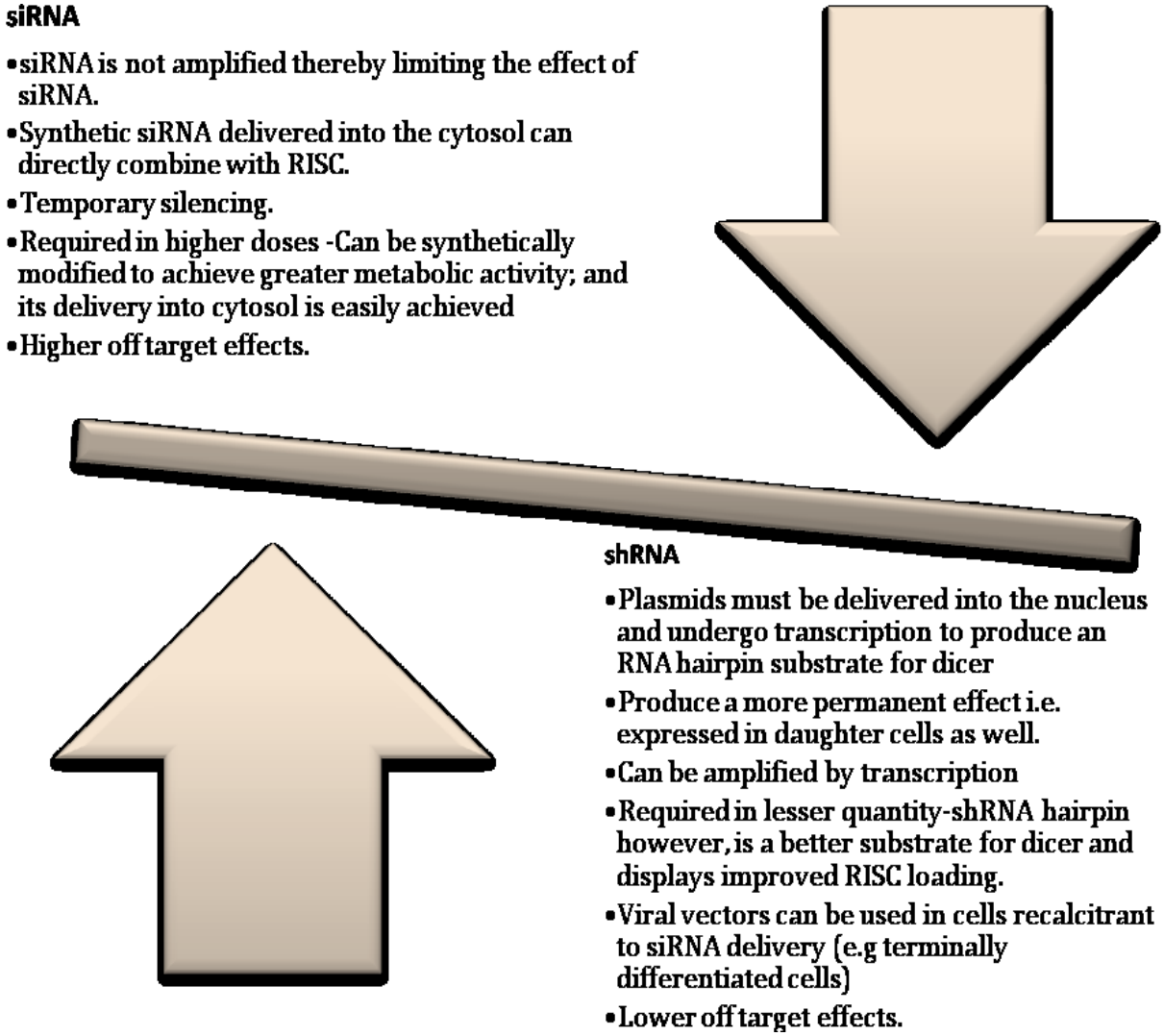

Figure 3.3: A comparison between siRNA and shRNA.

This figure summarises the advantages of using shRNA over siRNA.

A recent study carried out within our laboratory has deduced the presence of the inducible Hsp90α expression in glioma cell lines and tissue and its absence in normal cells and tissues (Shervington *et al*., 2008). *hsp90α* was downregulated in glioma cell

lines using siRNA targeted against *hsp90α* and the sensitivity of the cells to chemotherapeutic agents was checked. Inhibition of *hsp90α* using siRNA could possibly be adopted as a favourable therapeutic approach compared to conventional therapies owing to its specificity and reduced toxicity and also due to the enhanced chemosensitivity attained (Cruickshanks *et al*., 2010). Based on these findings, this study, evaluates the use of shRNA as opposed to siRNA to silence *hsp90α*.

The aim of this study *hsp90α* was silenced by using shRNA targeted against *hsp90α*. The silencing efficiency was validated by checking the mRNA level of *hsp90α* and *GAPDH* using qRT-PCR. Hsp90α ELISA assay was used to verify the level of Hsp90α expression. Additionally, the level of Akt/PKB kinase, which is a client protein to Hsp90, was also studied. Akt/PKB kinase is involved in the anti-apoptotic pathway however, in tumours, including glioma it stimulates cell proliferation and inhibits apoptosis, thus empowering the cancer cells the property of "immortality" (Basso *et al*., 2002). The Akt protein is directly regulated by Hsp90 as seen in Figure 3.4.

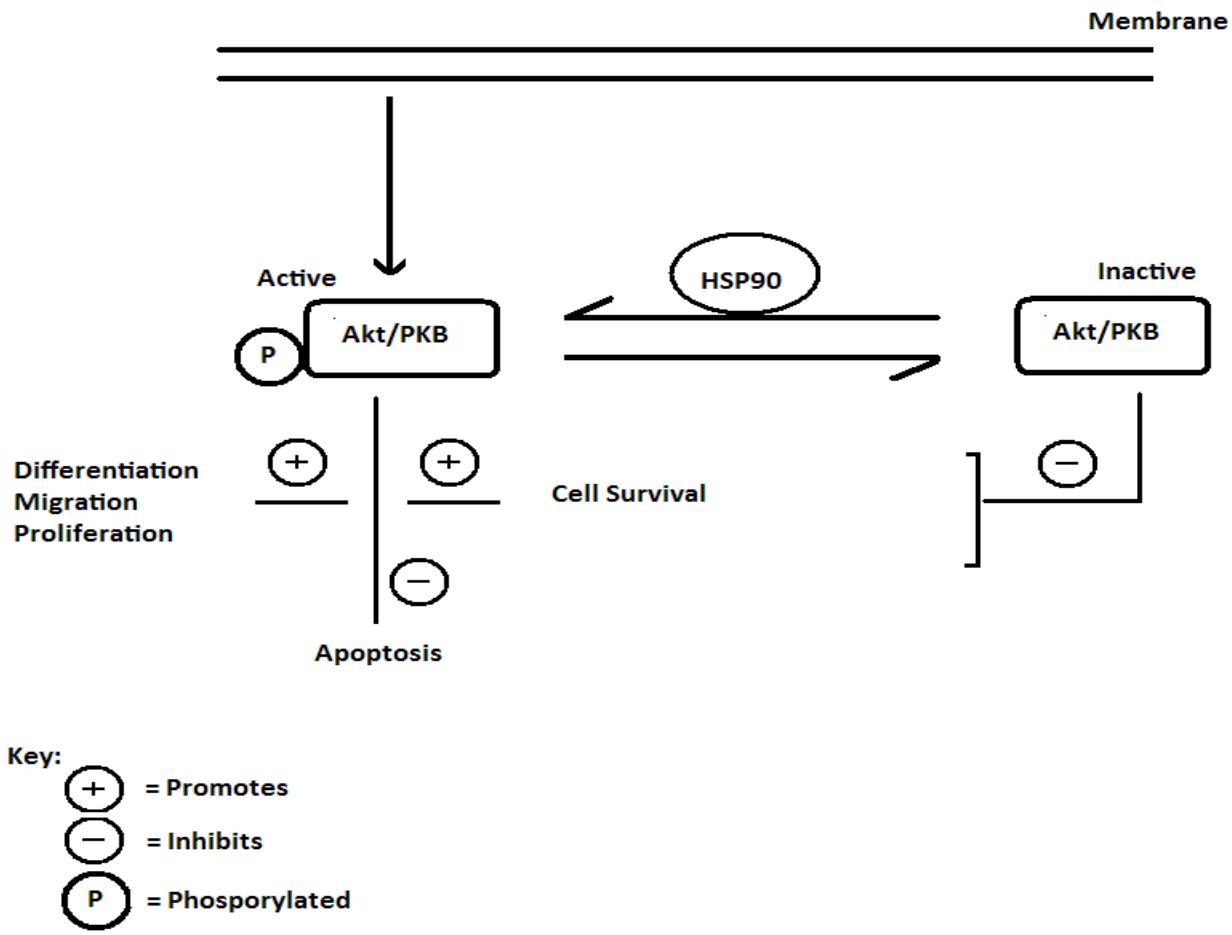

Figure 3.4: Interaction of Hsp90 protein with Akt/PKB kinase. Hsp90 shuttles Akt/PKB between phosphorylated (active) and dephosphorylated (inactive) states.

3.2 BIOINFORMATICS:

Bioinformatics is the computer-assisted mode of data management that helps us gather, analyze, and represent biological information in order to understand several processes involved in healthy and diseased states. The major research areas in which contribution of bioinformatics is significant are sequence analysis, genome annotation, computational evolutionary biology, prediction of protein structure, modelling biological systems and analysis of gene expression, protein expression and mutations in cancer (Fenstermacher, 2005).

The field of bioinformatics has evolved from molecular biology and the Human Genome Project. Several genome sequencing projects have recently been completed and the majority of human coding regions have been sequenced. Bioinformatics is an integral part of proteomic research. The recent developments and applications in proteomics have helped to easily access databases of genes and proteins. (Fenstermacher, 2005).

In addition, the World Wide Web has become an essential feature to the world of bioinformatics, as it makes DNA, RNA and protein data available to users throughout the world through databases such as National Centre for Biotechnology Information (NCBI, Unigene), GenBank (USA), European Molecular Biology Laboratory (EMBL, Europe), (Fenstermacher, 2005).

The location of *hsp90α* was found using public databases such as;

1) GeneCards (http://genome-www.stanford.edu/genecards/index.shtml)

2) NCBI (http://www.ncbi.nlm.nih.gov/entrez/query.fcgi?db=nucleotide&cmd=search&term).

3.2.1 GENE mRNA SEQUENCE:

The nucleotide sequence of the gene(s) of interest was obtained from NCBI. NCBI provides literature database, genomic database, sequence identification tools, protein structure tools and genome specific resources (http://www.ncbi.nlm.nih.gov/). NCBI provides with a detailed literature review, protein information and family information

along with the sequence of the gene. The gene search was used to gather general family information, protein function and mode of action of the protein coded by the gene. The nucleotide search on NCBI yields specific nucleotide information along with exon information for specific genes.

3.2.2 PRIMER DESIGN:

For a successful PCR, the design of synthetic primers suitable for the initiation of the polymerase reaction with the highest yield of the specific amplicon in question is of great importance. For RT-PCR, the primer should be approximately 20 nucleotides long and have a guanine/cytosine (G/C) and adenine/thymine (A/T) content similar to or higher than that of the sequence to be amplified. They usually have a melting temperature between 55 and 65 ^{o}C. For a primer which is 20 nucleotides long, this normally corresponds to 45-55 % GC content. Although long primers are more specific, they have higher annealing temperatures but are less efficient because thermodynamically the annealing takes longer (Dieffenbach *et al.,* 1993).

Several softwares to choose the primers of specific gene are available; in this study we have used Primer3 plus to determine appropriate primers for the extraction and amplification of amplicons. The sequence obtained from NCBI was pasted into Primer3 plus homepage (http://www.bioinformatics.nl/cgi-bin/primer3plus/primer3plus.cgi).

The output file included a main set of left and right primers and several sets of alternate primers. The output also indicated the alignment of the primers on the sequence, amplicon size, GC content and recommended annealing temperatures.

The primers obtained were utilized in PCR processes for further experimental procedures.

3.2.3 shRNA CONSTRUCT:

Pre-designed shRNA oligonucleotides targeted against *hsp90α* were obtained from Origene, USA. The shRNA oligonucleotides were tested against glioma cell lines and the best construct of the four constructs was selected and used for the study.

Furthermore, shRNA sequences were constructed against Hsp90α mRNA transcript sequence using ClustalW2 software. ClustalW2 software is a multiple sequence alignment programme used for both DNA and protein. It calculates the best match and aligns them (http://www.ebi.ac.uk/Tools/clustaw2/index.html).

3.3 MATERIALS AND METHODS:

In this study, 1321N1, GOS-3 and U87-MG cell lines were cultured as described in section 2.1 of chapter 2. mRNA was isolated using mRNA isolation kit (Roche Diagnostics, Germany) as described in section 2.2. The isolated mRNA was analysed using alkaline gel electrophoresis as explained in section 2.4. An amount of 100 ng of mRNA was then reverse transcribed to cDNA using cDNA synthesis kit (Roche, Diagnostics, Germany) as previously described in section 2.5. Quantitative real time PCR was performed to check the expression of *hsp90α* and *GAPDH* as described in section 2.6 using LightCycler 2.0 system (Roche Diagnostics Ltd, Germany), LightCycler® FastStart DNA Master^{PLUS} SYBR Green I and specific primers. PCR products were analysed using agarose gel electrophoresis as described in section 2.7. The Akt/PKB

kinase activity was assayed using Akt/PKB Kinase Activity Assay Kit (Assay Designs, UK) as described in section 2.9.

3.3.1 Cell culture and shRNA treatment:

The HuSH shRNA gene-specific expression cassettes were prepared using synthetic oligonucleotides. These oligonucleotide sequences were computer designed for optimal suppression of gene expression and minimal off-target effects. All shRNA sequences were verified through DNA sequencing analysis. The HuSH shRNA gene-specific expression cassettes were optimized to include both the termination signal for RNA Pol III and GC content to further improve the quality of the gene-specific shRNA expression vectors. Additionally, the shRNA expression cassette consisted of a 29 bp target gene specific sequence, a 7 bp loop, and another 29 bp reverse complementary sequence, all under the human U6 promoter. A termination sequence (TTTTTT) is located immediately downstream of the second 29 bp reverse complementary sequence to terminate the transcription by RNA Polymerase III. The gene-specific shRNA cassette was sequence-verified to ensure it was matched to the target gene.

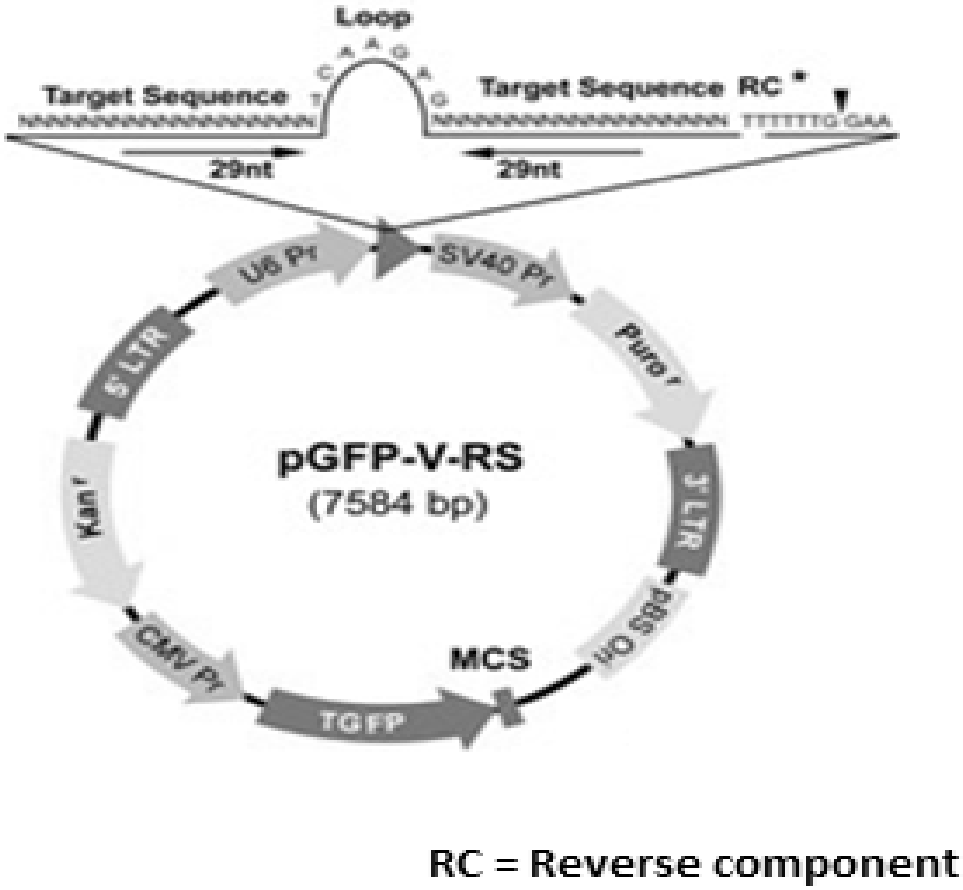

Figure 3.5: pGFP-V-RS vector map. (Adapted from www.origene.com)

Gene-specific shRNA transfection to glioma cell lines

1. dH_2O (50 µl) was added into each of the tubes containing shRNA expression plasmids. The tubes were then vortexed briefly to resuspend the DNA and to achieve a concentration of 100 ng μl^{-1}.

2. 1312N1, GOS-3 and U87-MG cells were plated into a 25 cm^3 flask for human shRNA validation at 3 x 10^5 cells. The cells were allowed to grow overnight in a 5 % CO_2 incubator to achieve 50 % confluence.

3. The following reagents were combined in the prescribed order to achieve optimal results:

   a) Serum-free DMEM 100 µl

   b) MegaTran 1.0 Solution 3 µl

   c) shRNA expression plasmid DNA 1 µg

      a. shRNA stock = 100 ng μl^{-1}

      b. Thus, for 1µg = 10 µl of shRNA.

4. The contents were carefully added to the sterile tube and mixed gently.

5. The tube containing the reagents was then incubated at room temperature for 15-45 min.

6. The DNA-MegaTran 1.0 mix was later directly added to the flasks containing the cells without the removal of the culture media. Gentle swirling of the flasks was carried out.

7. Upon transfection, the media were not changed in the flasks until the cells were ready to be passaged.

8. The transfected cells were passaged by scraping into a fresh flask containing growth medium and 0.5 - 1.0 µg ml^{-1} puromycin.

9. The cells were grown over a period and passaged when necessary, maintaining selection pressure by maintaining 0.5 - 1.0 µg ml^{-1} puromycin in the growth medium.

10. After 1-2 weeks, most of the cells were killed by the antibiotic which indicated that they did not take up or had lost the plasmid with the puromycin resistant cassette. The cells that were growing in the puromycin containing medium had retained the HuSH plasmid which integrated into the genome of the targeted cells.

11. The stably transfected cells were then grown in a selection medium for an additional 1-2 passages and at this time the selection pressure of the puromycin was reduced to 0.2 µg $µl^{-1}$.

12. These cell populations were then used in experiments and/or stored under liquid nitrogen in growth medium with 10% DMSO for future use.

3.3.2 Megatran:

MegaTran 1.0 was specifically designed as a new non-lipid polymer transfection reagent and manufactured for large volume DNA transfection, including large scale protein production via transient transfection, high-throughput screening using cDNA arrays or shRNA libraries, etc. (www.origene.com)

Advantages of using MegaTran;

1. Superior transfection efficiency compared to leading transfection reagents.

2. Improved protein production via transient transfection.
3. Reduced cytotoxicity.

3.3.3 Puromycin:

Puromycin (Calbiochem, UK) was dissolved in distilled water to provide a stock concentration of 25 mg/ml and then was further diluted in distilled water to achieve a final concentration of 2.5 µg/ml. To calculate the half maximal inhibitory concentration (IC_{50}) of puromycin, varying concentrations of puromycin (0.2 – 1 µg/ml) were added to untreated cells and incubated for 48 hours in order to determine the cell viability (as described in section 2.11) for all the three cell lines.

3.3.4 Statistical Analysis

As described in Chapter 2.

3.4 RESULTS:

3.4.1 Bioinformatics

Upon bioinformatic analysis it was observed that *hsp90α* is located on chromosome 14q32.33 (Fig 3.5).

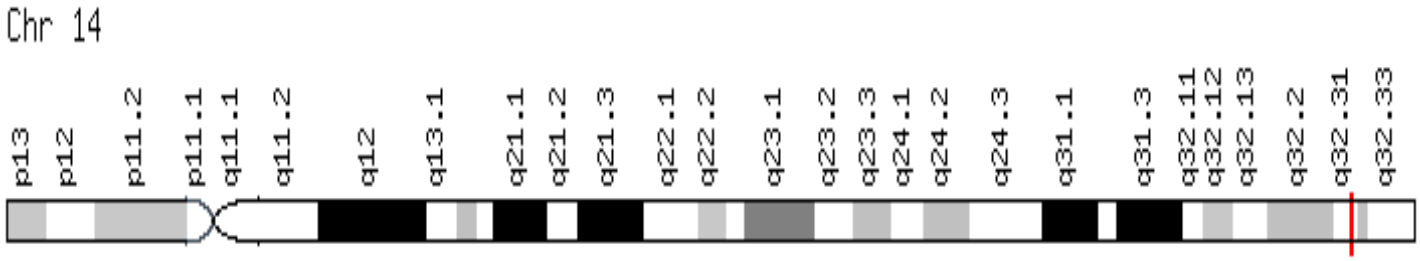

Figure 3.5: Location of *hsp90α* denoted by red bar. (Taken from GeneCards)

The above figure shows the typical location of *hsp90α* on chromosome 14q32.33. The location of *hsp90α* is denoted by the red bar in Figure 3.5.

Further, a gene search on NCBI yielded information on *hsp90α* as seen in Figure 3.6.

NCBI Entrez Gene

My NCBI [Sign In] [Register]

All Databases PubMed Nucleotide Protein Genome Structure OMIM PMC Journals Books

Search Gene for Go Clear

Limits Preview/Index History Clipboard Details

Display Full Report Send to

1: HSP90AA1 heat shock protein 90kDa alpha (cytosolic), class A member 1 [*Homo sapiens*]

GeneID: 3320 updated 30-Dec-2009

Summary

Official Symbol	HSP90AA1 provided by HGNC
Official Full Name	heat shock protein 90kDa alpha (cytosolic), class A member 1 provided by HGNC
Primary Source	HGNC:5253
See related	Ensembl:ENSG00000080824; HPRD:00777; MIM:140571
Gene type	protein coding
RefSeq status	VALIDATED
Organism	*Homo sapiens*
Lineage	*Eukaryota; Metazoa; Chordata; Craniata; Vertebrata; Euteleostomi; Mammalia; Eutheria; Euarchontoglires; Primates; Haplorrhini; Catarrhini; Hominidae; Homo*
Also known as	HSPN; LAP2; HSP86; HSPC1; HSPCA; Hsp89; Hsp90; HSP89A; HSP90A; HSP90N; HSPCAL1; HSPCAL4; FLJ31884; HSP90AA1
Summary	HSP90 proteins are highly conserved molecular chaperones that have key roles in signal transduction, protein folding, protein degradation, and morphologic evolution. HSP90 proteins normally associate with other cochaperones and play important roles in folding newly synthesized proteins or stabilizing and refolding denatured proteins after stress. There are 2 major cytosolic HSP90 proteins, HSP90AA1, an inducible form, and HSP90AB1 (MIM 140572), a constitutive form. Other HSP90 proteins are found in endoplasmic reticulum (HSP90B1; MIM 191175) and mitochondria (TRAP1; MIM 606219) (Chen et al., 2005 [PubMed 16269234]). [supplied by OMIM]

Entrez Gene Home

Table Of Contents

Summary
Genomic regions, transcripts, and products
Genomic context
Bibliography
HIV-1 protein interactions
Interactions
General gene info
General protein info
Reference sequences
Related sequences
Additional links

Links Explain

Order cDNA clone
BioAssay, by Gene target
BioSystems
CCDS
Conserved Domains
EST
Full text in PMC
GEO Profiles
Gene Genotype
GeneView in dbSNP
Genome
HomoloGene
Map Viewer
Nucleotide
OMIM

Figure 3.6: Entrez gene database output on a gene search for *hsp90α*. (Taken from NCBI).

The above figure shows a typical database output on a gene search for *hsp90α* on NCBI.

A nucleotide search was also carried out using NCBI to obtain specific nucleotide information as seen in Figure 3.7.

```
   1 gactgcgcag gcgtgctcac ctggcgtgct ccacccgact gggcgtccgc aggctcctcc
  61 cccgggtgtg gcctccgggc ggcatggctg cttcccaggt gatgccggct tcagctagtg
 121 gggtctagtt gaccgttccg cagccgccag ggccagcgga aagccggtca gggggaaccg
 181 cggcgggggct ggtgtcatga gcctgaggtg aacttgaggg tgcctcctca gcggtctccc
 241 gccctgccct gaggggcgcc gggaccccaa agagcggagg aagagcgcca ccccgacggc
 301 caccgcttcg gagccagcac gcggggtacc ctacggggag cgcggatgcc cccgtgttcg
 361 ggcggggacg gctccacccc tcctgggccc tcccttcggg acagggactg tcccgcccag
 421 agtgctgaat acccgcgcga ccgtctggat cccccccccag gaagcccctc tgaagcctcc
 481 tcgccgccgt ttctgagaag cagggcacct gttaactggt acccaagaaa ggcccaagtg
 541 tttctctggc atctgatggt gtctggatcc accactctac tctgtctctg gaaacagccc
 601 ttccacgtct ctgcattccc tgtcaccgcg tcactggcct tcagacagag ccaaggtgca
 661 gggcaacacc tctacaagga tctgcagcca tttatattgc ttaggctact gatgcctgag
 721 gaaacccaga cccaagacca accgatggag gaggaggagg ttgagacgtt cgcctttcag
 781 gcagaaattg cccagttgat gtcattgatc atcaatactt tctactcgaa caaagagatc
 841 tttctgagag agctcatttc aaattcatca gatgcattgg acaaaatccg gtatgaaagc
 901 ttgacagatc ccagtaaatt agactctggg aaagagctgc atattaacct tatccgaac
 961 aaacaagatc gaactctcac tattgtggat actggaattg gaatgaccaa ggctgacttg
1021 atcaataacc ttggtactat cgccaagtct gggaccaaag cgttcatgga agctttgcag
1081 gctggtgcag atatctctat gattggccag ttcggtgttg gttttattc tgcttatttg
1141 gttgctgaga aagtaactgt gatcaccaaa cataacgatg atgagcagta cgcttgggag
1201 tcctcagcag ggggatcatt cacagtgagg acagacacag gtgaacctat gggtcgtgga
1261 acaaaagtta tcctacacct gaaagaagac caaactgagt acttggagga acgaagaata
1321 aaggagattg tgaagaaaca ttctcagttt attggatatc ccattactct ttttgtggag
1381 aaggaacgtg ataaagaagt aagcgatgat gaggctgaag aaaaggaaga caaagaagaa
1441 gaaaaagaaa aagaagagaa agagtcggaa gacaaacctg aaattgaaga tgttggttct
1501 gatgaggaag aagaaaagaa ggatggtgac aagaagaaga agaagaagat taaggaaaag
1561 tacatcgatc aagaagagct caacaaaaca aagcccatct ggaccagaaa tcccgacgat
1621 attactaatg aggagtacgg agaattctat aagagcttga ccaatgactg ggaagatcac
1681 ttggcagtga agcatttttc agttgaagga cagttggaat tcagagccct tctatttgtc
1741 ccacgacgtg ctcttttga tctgtttgaa aacagaaaga aaaagaacaa catcaaattg
1801 tatgtacgca gagttttcat catggataac tgtgaggagc taatccctga atatctgaac
1861 ttcattagag gggtggtaga ctcggaggat ctccctctaa acatatcccg tgagatgttg
1921 caacaaagca aaattttgaa agttatcagg aagaatttgg tcaaaaaatg cttagaactc
1981 tttactgaac tggcggaaga taaagagaac tacaagaaat tctatgagca gttctctaaa
2041 aacataaagc ttggaataca cgaagactct caaaatcgga agaagcttcc agagctgtta
2101 aggtactaca catctgcctc tggtgatgag atggtttctc tcaaggacta ctgcaccaga
2161 atgaaggaga accagaaaca tatctattat atcacaggtg agaccaagga ccaggtagct
2221 aactcagcct ttgtggaacg tcttcggaaa catggcttag aagtgatcta tatgattgag
2281 cccattgatg agtactgtgt ccaacagctg aaggaatttg aggggaagac tttagtgtca
2341 gtcaccaaag aaggcctgga acttccagag gatgaagaag agaaaaagaa gcaggaagag
2401 aaaaaaacaa agtttgagaa cctctgcaaa atcatgaaag acatattgga gaaaaaagtt
2461 gaaaaggtgg ttgtgtcaaa ccgattggtg acatctccat gctgtattgt cacaagcaca
2521 tatggctgga cagcaaacat ggagagaatc atgaaagctc aagccctaag agacaactca
2581 acaatgggtt acatggcagc aaagaaacac ctggagataa acccctgacca ttccattatt
2641 gagaccttaa ggcaaaaggc agaggctgat aagaacgaca agtctgtgaa ggatctggtc
2701 atcttgcttt atgaaactgc gctcctgtct tctggcttca gtctggaaga tccccagaca
2761 catgctaaca ggatctacag gatgatcaaa cttggtctgg gtattgatga agatgaccct
2821 actgctgatg ataccagtgc tgctgtaact gaagaaatgc cacccccttga aggagatgac
2881 gacacatcac gcatggaaga agtagactaa tctctggctg agggatgact tacctgttca
2941 gtactctaca attcctctga taatatattt tcaaggatgt ttttctttat ttttgttaat
3001 attaaaaagt ctgtatggca tgacaactac tttaagggga agataagatt tctgtctact
3061 aagtgatgct gtgatacctt aggcactaaa gcagagctag taatgctttt tgagtttcat
3121 gttggtttat tttcacagat tggggtaacg tgcactgtaa gacgtatgta acatgatgtt
3181 aactttgtgg tctaaagtgt ttagctgtca agccggatgc ctaagtagac caaatcttgt
3241 tattgaagtg ttctgagctg tatcttgatg tttagaaaag tattcgttac atcttgtagg
3301 atctactttt tgaactttte attccctgta gttgacaatt ctgcatgtac tagtcctcta
3361 gaaataggtt aaactgaagc aacttgatgg aaggatctct ccacaggget tgttttccaa
3421 agaaaagtat tgtttggagg agcaaagtta aaagcctacc taagcatatc gtaaagctgt
3481 tcaaaaataa ctcagaccca gtcttgtgga tggaaatgta gtgctcgagt cacattctgc
3541 ttaaagttgt aacaaataca gatgagttaa aagatattgt gtgacagtgt cttatttagg
3601 gggaaagggg agtatctgga tgacagttag tgccaaaatg taaaacatga ggcgctagca
3661 ggagatggtt aaacactagc tgctccaagg gttgacatgg tcttcccagc atgtactcag
3721 caggtgtggg gtggagcaca cgtaggcaca gaaaacagga atgcagacaa catgcatccc
3781 ctgcgtccat gagttacatg tgttctctta gtgtccacgt tgttttgatg ttattcatgg
3841 aatacctctt gtgttaaata cagtcactta attccttggc cttaaaa
```

Figure 3.7: Complete sequence of mRNA sequence of Hsp90α. (Taken from NCBI)

The above figure shows a typical mRNA sequence for *hsp90α* taken from NCBI.

For qRT-PCR, primers for *hsp90α* and *GAPDH* were selected by using Primer3 Plus software. The sequence obtained from NCBI (Fig. 3.7) was pasted onto the Primer3 Plus homepage and the output file generated a main set of left and right primers and several sets of alternate primers. The output also indicated the alignment of the primers on the sequence, amplicon size, GC content and recommended annealing temperatures as seen in Figure 3.8.

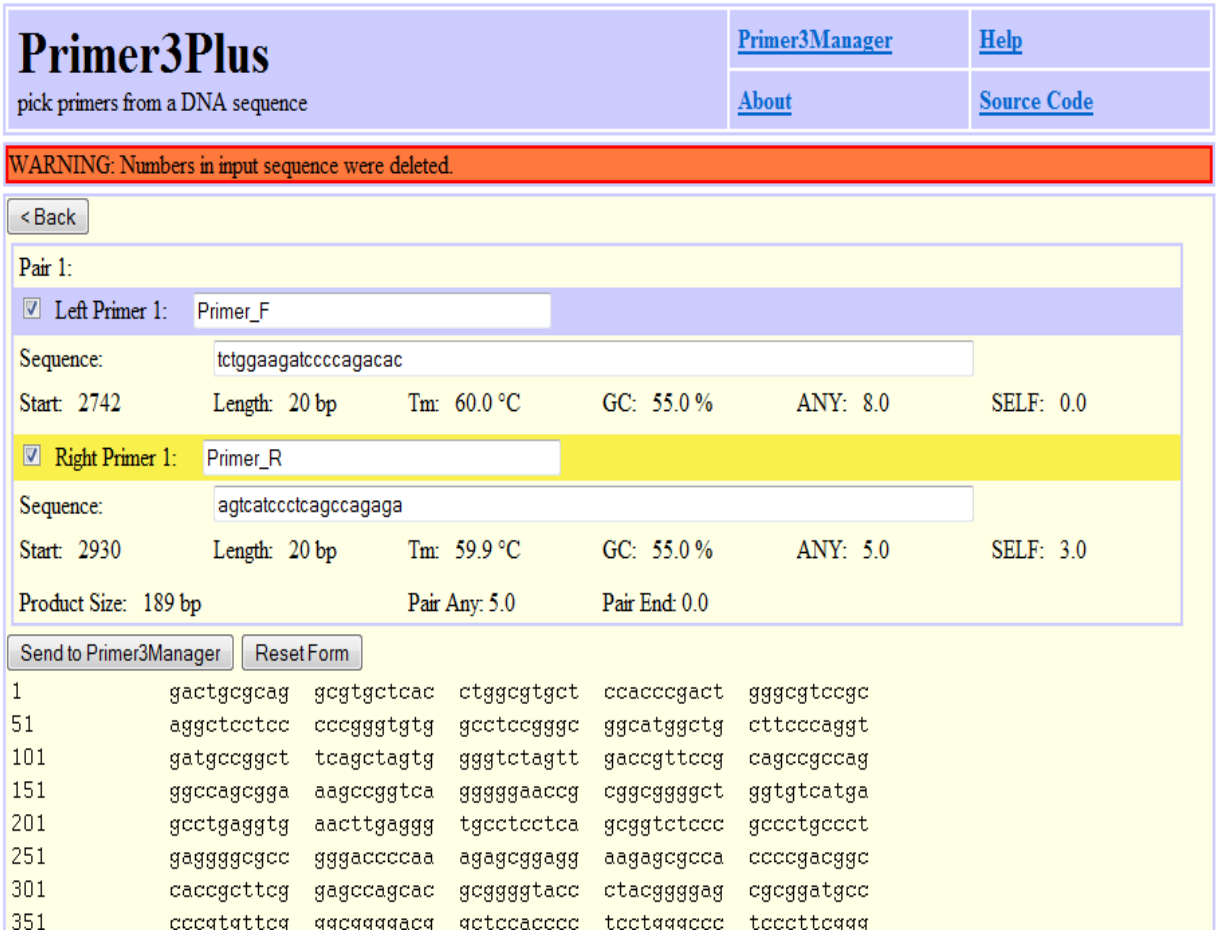

Figure 3.8: The output file of Primer3 Plus provides an independent set of left and right primer and also shows the alignment of the primer on the sequence. (Taken from Primer3 Plus)

The set of primers of the desired gene of interest were then used to measure the gene expression using qRT-PCR.

Table 3.1: The *hsp90α* and *GAPDH* primers [designed using Primer3 software and commercially synthesised by TIB MOLBIOL syntheselabor (Berlin, Germany)] used in qRT-PCR.

Gene	Primer Sequences	Annealing Temperature (^oC)				Expected amplicon size (bp)
		Primer3	TIB MOLBIOL	GC / AT rule*	Experimental temperature	
hsp90α	Sense: 5' – TCTGGAAGATCCCCAGACAC – 3' Antisense: 5' – AGTCATCCCTCAGCCAGAGA – 3'	60.00 59.90	55.40 55.60	62.00 62.00	63	189
GAPDH	Sense: 5' - GAGTCAACGGATTTGGTCGT - 3' Antisense: 5' - TTGATTTTGGAGGGATCTCG - 3'	59.97 60.01	56.20 54.80	60.00 58.00	56	238

* GC / AT rule: A method of calculating the primer annealing temperature using the formula: $T = 2^o (A + T) + 4^o (G + C)$, where A, C, G and T represent the number of adenine, cytosine, guanine and thymine bases respectively in the primer sequence concerned.

The shRNA oligonucleotides were blasted against Hsp90α mRNA transcript sequence using ClustalW2 software as seen in Figure 3.9.

```
GACTGCGCAGGCGTGCTCACCTGGCGTGCTCCACCCGACTGGGCGTCCGCAGGCTCCTCC 60

------------------------------------------------------------
CCCGGGTGTGGCCTCCGGGCGGCATGGCTGCTTCCCAGGTGATGCCGGCTTCAGCTAGTG 120
------------------------------------------------------------
GGGTCTAGTTGACCGTTCCGCAGCCGCCAGGGCCAGCGGAAAGCCGGTCAGGGGGAACCG 180
------------------------------------------------------------
CGGCGGGGCTGGTGTCATGAGCCTGAGGTGAACTTGAGGGTGCCTCCTCAGCGGTCTCCC 240
------------------------------------------------------------
GCCCTGCCCTGAGGGGCGCCGGGACCCCAAAGAGCGGAGGAAGAGCGCCACCCCGACGGC 300
------------------------------------------------------------
CACCGCTTCGGAGCCAGCACGCGGGGTACCCTACGGGGAGCGCGGATGCCCCCGTGTTCG 360
------------------------------------------------------------
GGCGGGGACGGCTCCACCCCTCCTGGGCCCTCCCTTCGGGACAGGGACTGTCCCGCCCAG 420
------------------------------------------------------------
AGTGCTGAATACCCGCGCGACCGTCTGGATCCCCGCCCAGGAAGCCCCTCTGAAGCCTCC 480
------------------------------------------------------------
TCGCCGCCGTTTCTGAGAAGCAGGGCACCTGTTAACTGGTACCAAGAAAAGGCCCAAGTG 540
------------------------------------------------------------
TTTCTCTGGCATCTGATGGTGTCTGGATCCACCACTCTACTCTGTCTCTGGAAACAGCCC 600
------------------------------------------------------------
TTCCACGTCTCTGCATTCCCTGTCACCGCGTCACTGGCCTTCAGACAGAGCCAAGGTGCA 660
------------------------------------------------------------
GGGCAACACCTCTACAAGGATCTGCAGCCATTTATATTGCTTAGGCTACTGATGCCTGAG 720
-----------------------------------TATTGCTTAGGCTACTGATGCCTGAG
                                   **************************
GAAACCCAGACCCAAGACCAACCGATGGAGGAGGAGGAGGTTGAGACGTTCGCCTTTCAG 780
GAA---------------------------------------------------------
*** shRNA construct 1
GCAGAAATTGCCCAGTTGATGTCATTGATCATCAATACTTTCTACTCGAACAAAGAGATC 840
------------------------------------------------------------
TTTCTGAGAGAGCTCATTTCAAATTCATCAGATGCATTGGACAAAATCCGGTATGAAAGC 900
------------------------------------------------------------
TTGACAGATCCCAGTAAATTAGACTCTGGGAAAGAGCTGCATATTAACCTTATACCGAAC 960
------------------------------------------------------------
AAACAAGATCGAACTCTCACTATTGTGGATACTGGAATTGGAATGACCAAGGCTGACTTG 1020
------------------------------------------------------------
ATCAATAACCTTGGTACTATCGCCAAGTCTGGGACCAAAGCGTTCATGGAAGCTTTGCAG 1080
------------------------------------------------------------
GCTGGTGCAGATATCTCTATGATTGGCCAGTTCGGTGTTGGTTTTTATTCTGCTTATTTG 1140
------------------------------------------------------------
GTTGCTGAGAAAGTAACTGTGATCACCAAACATAACGATGATGAGCAGTACGCTTGGGAG 1200
------------------------------------------------------------
TCCTCAGCAGGGGGATCATTCACAGTGAGGACAGACACAGGTGAACCTATGGGTCGTGGA 1260
------------------------------------------------------------
ACAAAAGTTATCCTACACCTGAAAGAAGACCAAACTGAGTACTTGGAGGAACGAAGAATA 1320
------------------------------------------------------------
AAGGAGATTGTGAAGAAACATTCTCAGTTTATTGGATATCCCATTACTCTTTTTGTGGAG 1380
------------------------------------------------------------
AAGGAACGTGATAAAGAAGTAAGCGATGATGAGGCTGAAGAAAAGGAAGACAAAGAAGAA 1440
------------------------------------------------------------
GAAAAAGAAAAAGAAGAGAAAGAGTCGGAAGACAAACCTGAAATTGAAGATGTTGGTTCT 1500
------------------------------------------------------------
GATGAGGAAGAAGAAAAGAAGGATGGTGACAAGAAGAAGAAGAAGAAGATTAAGGAAAAG 1560
------------------------------------------------------------
TACATCGATCAAGAAGAGCTCAACAAAACAAAGCCCATCTGGACCAGAAATCCCGACGAT 1620
------------------------------------------------------------
ATTACTAATGAGGAGTACGGAGAATTCTATAAGAGCTTGACCAATGACTGGGAAGATCAC 1680
------------------------------------------------------------
TTGGCAGTGAAGCATTTTTCAGTTGAAGGACAGTTGGAATTCAGAGCCCTTCTATTTGTC 1740
------------------------------------------------------------
```

```
CCACGACGTGCTCCTTTTGATCTGTTTGAAAACAGAAAGAAAAAGAACAACATCAAATTG 1800
------------------------------------------------------------
TATGTACGCAGAGTTTTCATCATGGATAACTGTGAGGAGCTAATCCCTGAATATCTGAAC 1860
------------------------------------------------------------
TTCATTAGAGGGGTGGTAGACTCGGAGGATCTCCCTCTAAACATATCCCGTGAGATGTTG 1920
------------------------------------------------------------
CAACAAAGCAAAATTTTGAAAGTTATCAGGAAGAATTTGGTCAAAAAATGCTTAGAACTC 1980
------------------------------------------------------------
TTTACTGAACTGGCGGAAGATAAAGAGAACTACAAGAAATTCTATGAGCAGTTCTCTAAA 2040
------------------------------------------------------------
AACATAAAGCTTGGAATACACGAAGACTCTCAAAATCGGAAGAAGCTTTCAGAGCTGTTA 2100
------------------------------------------------------------
AGGTACTACACATCTGCCTCTGGTGATGAGATGGTTTCTCTCAAGGACTACTGCACCAGA 2160
--------------------------------------CTCTCAAGGACTACTGCACCAGA
                                     ***********************
ATGAAGGAGAACCAGAAACATATCTATTATATCACAGGTGAGACCAAGGACCAGGTAGCT 2220
ATGAAG------------------------------------------------------
****** shRNA construct 2
AACTCAGCCTTTGTGGAACGTCTTCGGAAACATGGCTTAGAAGTGATCTATATGATTGAG 2280
------------------------------------------------------------
CCCATTGATGAGTACTGTGTCCAACAGCTGAAGGAATTTGAGGGGAAGACTTTAGTGTCA 2340
------------------------------------------------------------
GTCACCAAAGAAGGCCTGGAACTTCCAGAGGATGAAGAAGAGAAAAAGAAGCAGGAAGAG 2400
------------------------------------------------------------
AAAAAAACAAAGTTTGAGAACCTCTGCAAAATCATGAAAGACATATTGGAGAAAAAAGTT 2460
------------------------------------------------------------
GAAAAGGTGGTTGTGTCAAACCGATTGGTGACATCTCCATGCTGTATTGTCACAAGCACA 2520
------------------------------------------------------------
TATGGCTGGACAGCAAACATGGAGAGAATCATGAAAGCTCAAGCCCTAAGAGACAACTCA 2580
------------------------------------------------------------
ACAATGGGTTACATGGCAGCAAAGAAACACCTGGAGATAAACCCTGACCATTCCATTATT 2640
------------------------------------------------------------
GAGACCTTAAGGCAAAAGGCAGAGGCTGATAAGAACGACAAGTCTGTGAAGGATCTGGTC 2700
-----------------------GGCTGATAAGAACGACAAGTCTGTGAAGG--------
 shRNA construct 3     ****************************
ATCTTGCTTTATGAAACTGCGCTCCTGTCTTCTGGCTTCAGTCTGGAAGATCCCCAGACA 2760
------------------------------------------------------------
CATGCTAACAGGATCTACAGGATGATCAAACTTGGTCTGGGTATTGATGAAGATGACCCT 2820
------------------------------------------------------------
ACTGCTGATGATACCAGTGCTGCTGTAACTGAAGAAATGCCACCCCTTGAAGGAGATGAC 2880
-----------------------------------------------CTTGAAGGAGATGAC 15
                                shRNA construct 4  ***************
GACACATCACGCATGGAAGAAGTAGACTAATCTCTGGCTGAGGGATGACTTACCTGTTCA 2940
GACACATCACGCAT--------------------------------------------- 29
**************
GTACTCTACAATTCCTCTGATAATATATTTTCAAGGATGTTTTTCTTTATTTTTGTTAAT 3000
------------------------------------------------------------
ATTAAAAAGTCTGTATGGCATGACAACTACTTTAAGGGGAAGATAAGATTTCTGTCTACT 3060
------------------------------------------------------------
AAGTGATGCTGTGATACCTTAGGCACTAAAGCAGAGCTAGTAATGCTTTTTGAGTTTCAT 3120
------------------------------------------------------------
GTTGGTTTATTTTCACAGATTGGGGTAACGTGCACTGTAAGACGTATGTAACATGATGTT 3180
------------------------------------------------------------
AACTTTGTGGTCTAAAGTGTTTAGCTGTCAAGCCGGATGCCTAAGTAGACCAAATCTTGT 3240
------------------------------------------------------------
TATTGAAGTGTTCTGAGCTGTATCTTGATGTTTAGAAAAGTATTCGTTACATCTTGTAGG 3300
------------------------------------------------------------
ATCTACTTTTTGAACTTTTCATTCCCTGTAGTTGACAATTCTGCATGTACTAGTCCTCTA 3360
------------------------------------------------------------
GAAATAGGTTAAACTGAAGCAACTTGATGGAAGGATCTCTCCACAGGGCTTGTTTTCCAA 3420
------------------------------------------------------------
AGAAAAGTATTGTTTGGAGGAGCAAAGTTAAAAGCCTACCTAAGCATATCGTAAAGCTGT 3480
------------------------------------------------------------
TCAAAAATAACTCAGACCCAGTCTTGTGGATGGAAATGTAGTGCTCGAGTCACATTCTGC 3540
------------------------------------------------------------
TTAAAGTTGTAACAAATACAGATGAGTTAAAAGATATTGTGTGACAGTGTCTTATTTAGG 3600
------------------------------------------------------------
GGGAAAGGGGAGTATCTGGATGACAGTTAGTGCCAAAATGTAAAACATGAGGCGCTAGCA 3660
```

```
------------------------------------------------------------
GGAGATGGTTAAACACTAGCTGCTCCAAGGGTTGACATGGTCTTCCCAGCATGTACTCAG 3720
------------------------------------------------------------
CAGGTGTGGGGTGGAGCACACGTAGGCACAGAAAACAGGAATGCAGACAACATGCATCCC 3780
------------------------------------------------------------
CTGCGTCCATGAGTTACATGTGTTCTCTTAGTGTCCACGTTGTTTTGATGTTATTCATGG 3840
------------------------------------------------------------
AATACCTTCTGTGTTAAATACAGTCACTTAATTCCTTGGCCTTAAAA 3887

-----------------------------------------------
```

Figure 3.9: shRNA oligonucleotides against Hsp90α mRNA transcript. Accessed on http://www.ebi.ac.uk/Tools/clustalw2/index.html

3.4.2 Puromycin:

Cells treated with puromycin (0.2 – 1 µg/ml) showed decreased viability as the concentration of the drug increased (Fig. 3.10)

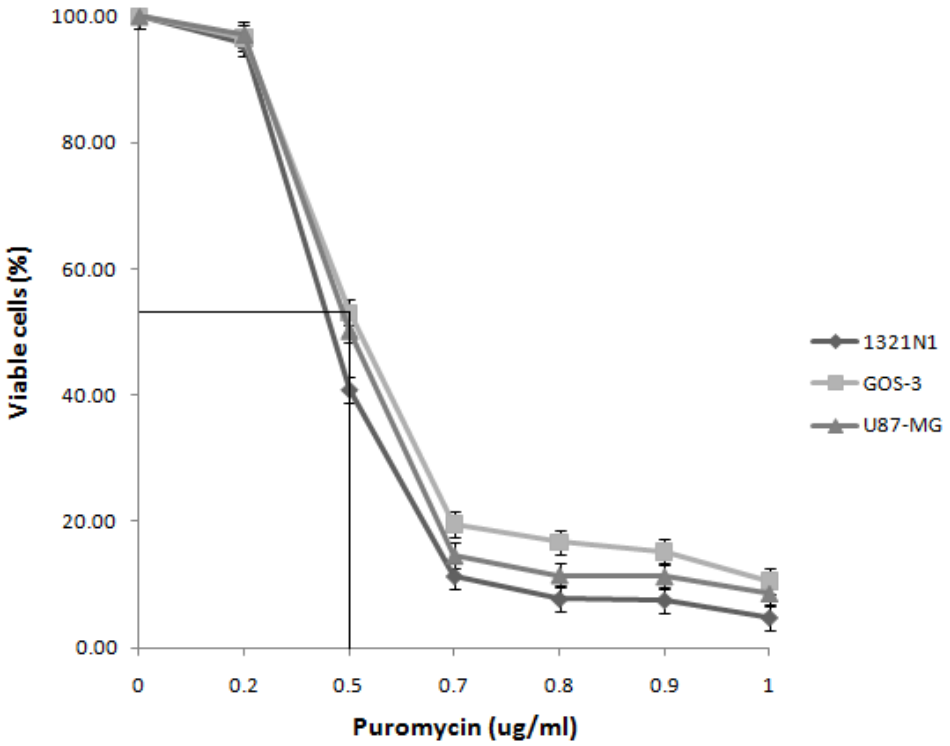

Figure 3.10: Cell viability assessment of 1321N1, GOS-3 and U87-MG with increasing concentrations of puromycin (0.2 – 1 µg/ml). Data values are mean ± standard error of the mean, n = 3.

The half maximal inhibitory rate (IC_{50}) for puromycin was achieved at a concentration of 0.5 µg/ml in all three glioma cell lines.

3.4.3 mRNA, cDNA and qRT-PCR:

Spectrophotometry was carried out on the extracted mRNA for checking the purity and quantification of the mRNA. Depending on the spectrophotmetry readings the concentration of mRNA varies which determined the quantity of mRNA required for converting it to cDNA. The absorbance was measured at 260 nm and 280 nm and the concentration of mRNA present in each cell line was calculated. Table 3.2 lists an example of the spectrophotometry results obtained for 1321N1, GOS-3 and U87-MG.

Table 3.2: Spectrophotometry reading for three glioma cell lines. Data are mean ± standard deviation, n = 3, *p < 0.05 and **p < 0.001 are considered significant.

Cell Lines	Ratio (A_{260}/A_{280})	mRNA concentrations (µg/ml)
1321N1	1.75	52 ± 2.8
GOS-3	1.86	70 ± 2.5 **
U87-MG	1.75	50 ± 1.5

The data show a significant decrease in GOS-3 cell line compared to 1321N1 and U87-MG cell line with **p < 0.01.

The isolated mRNA was analyzed using an alkaline gel electrophoresis.

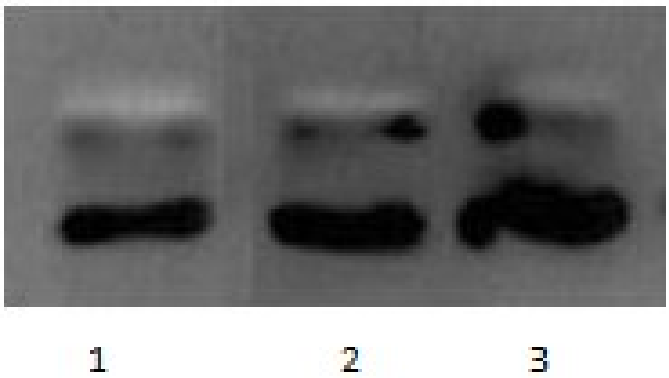

Figure 3.11: Alkaline gel electrophoresis mRNA isolated from glioma cell lines.

Lanes 1-3 represent 2µl of mRNA isolated from 1321N1, U87-MG, GOS-3, respectively ran on a denaturing alkaline agarose gel (2 %). Micrograph of gel is typical of 3 such different experiments.

Post successful isolation of mRNA, 100 ng of mRNA was reverse transcribed into cDNA and real time PCR was performed quantitatively to measure the expression of *hsp90α* and the housekeeping gene *GAPDH*. *hsp90α* was found to be present in all the three cell lines (Fig. 3.12), the highest expression was observed in the 1321N1 cell line.

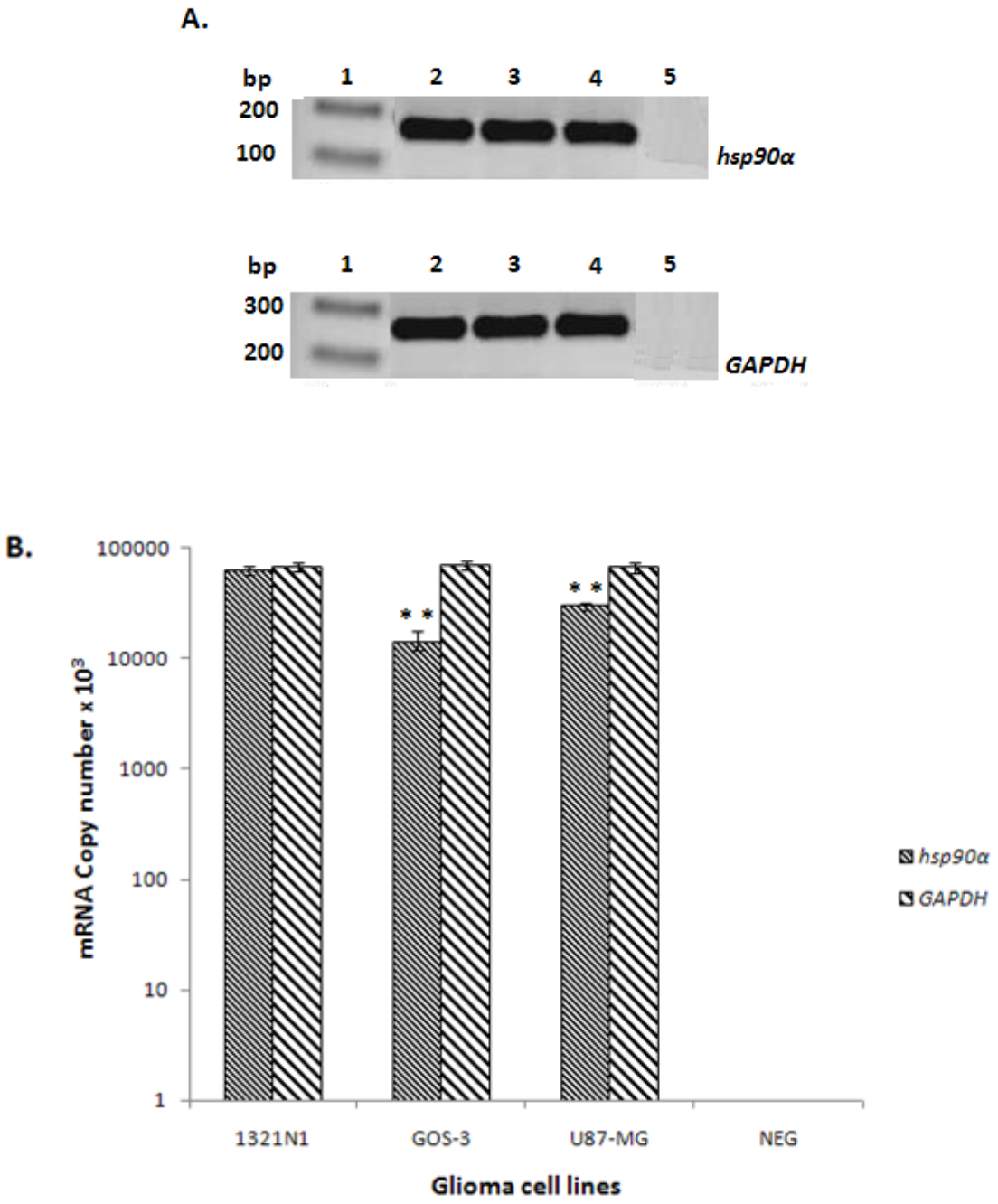

Figure 3.12: Gene expression of *hsp90α* and *GAPDH* in glioma cell lines. (A) Agarose gel electrophoresis: lane 1 represents the 100 bp molecular marker, lanes 2-4 represents 1321N1, GOS-3 and U87-MG, respectively, and lane 5 represents negative control (primer with no cDNA). (B) The respective mean values ± standard error of the copy number of *hsp90α* and *GAPDH* gene expressed in each cell line were included (obtained from 3 independent experiments, n = 3). *$p < 0.05$ and **$p < 0.01$ are considered statistically significant. The gel micrograph in A are typical of 3 such different experiments. Regarding Hsp90α expression, **$p < 0.001$ for 1321N1 compared to GOS-3 and U87-MG cell lines.

The qRT-PCR product analysis demonstrated induced expression of *hsp90α* in all three glioma cell lines. *GAPDH*, which is a housekeeping gene, was consistently expressed in all the three glioma cell lines and was used as a control in this study.

The cells were transfected with shRNA constructs targeted against *hsp90α* and post 48 hours were analysed for gene expression. 100 ng of mRNA was reverse transcribed to cDNA and real time PCR was performed quantitatively to measure the expression of *hsp90α* and *GAPDH* (Fig. 3.14).

As observed below, *hsp90α* is best silenced by using shRNA construct 2 (Fig. 3.9 and Fig. 3.13) and there is almost a 99 % decrease in the gene expression (Fig. 3.14).

```
                                    A   A
                                G       G
5'-CTCTCAAGGACTACTGCACCAGAATGAAG
3'-GAGAGTTCCTGATGACGTGGTCTTACTTC
                                G       C
                                    A   A
```

(TARGET mRNA SEQUENCE→ 2137-2166 bp)

Figure 3.13: shRNA construct 2. The sequence of shRNA construct further used in the study to silence *hsp90α*.

A.

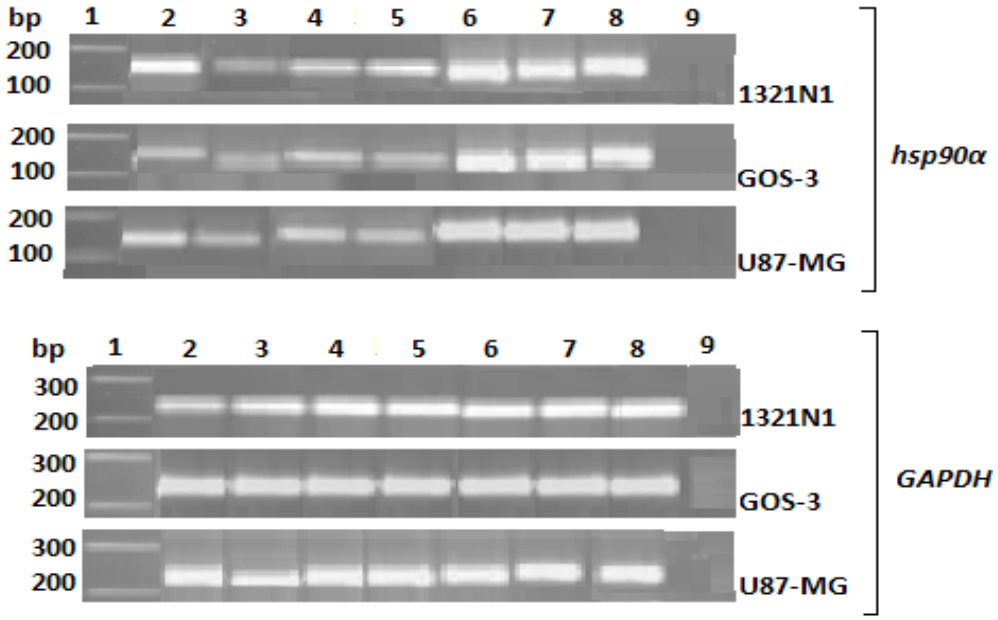

Figure 3.14 Contd.

Figure 3.14 Contd.

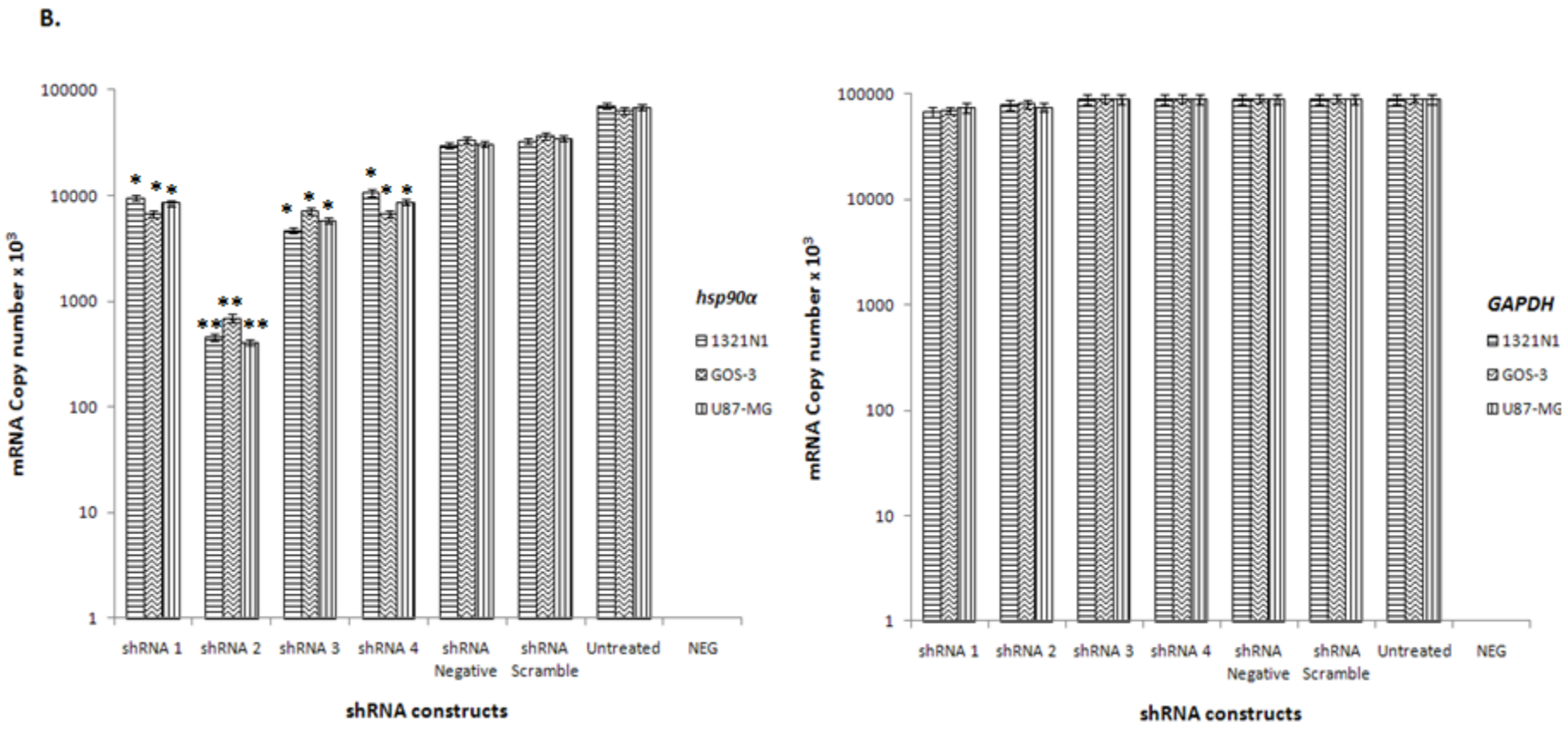

Figure 3.14: Gene expression of *hsp90α* and *GAPDH* in glioma cell lines treated with shRNA constructs. (A) Agarose gel electrophoresis: lane 1 represents 100 bp molecular size markers, lane 2-8 stands for shRNA construct 1, shRNA construct 2, shRNA construct 3, shRNA construct 4, shRNA negative control, shRNA scramble control and untreated cells, respectively. Lane 9 represents negative control (primer with no cDNA). (B) Copy numbers of *hsp90α* and *GAPDH* expression in glioma cell lines. Data values are mean ± standard error, n = 3, *$p < 0.05$ and **$p < 0.001$ are considered statistically significant. The gel micrograph in A are typical of 3 such different experiments.

Regarding *hsp90α* expression, **p < 0.01 for shRNA construct 2 compared to the other shRNA constructs in all three cell lines and thus it was statistically significant. Thus, shRNA construct 2 works better than the other constructs in silencing *hsp90α* and hence, it was used throughout the study.

3.4.4 Akt/PKB Kinase activity assay:

Commercially available Akt/PKB kinase activity assay kit (Assay Designs, UK) was used to measure the activity of Akt/PKB kinase in treated and untreated glioma cell lines (Fig. 3.15 and Table 3.3).

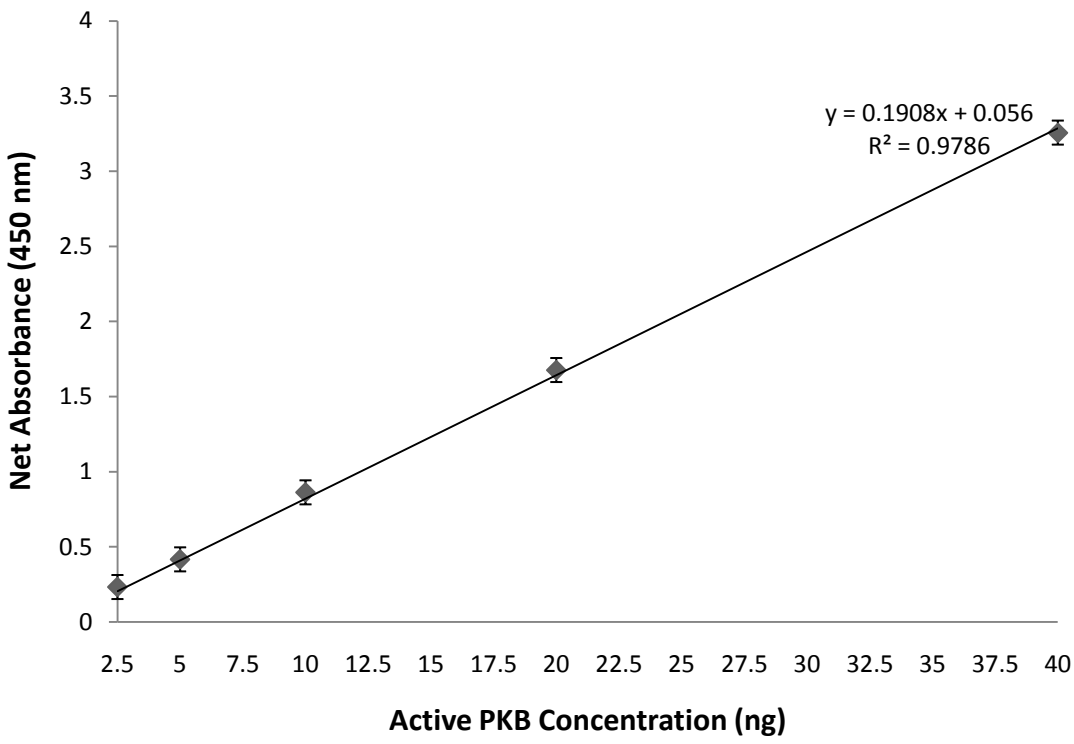

Figure 3.15: Standard graph for Akt/PKB Kinase activity assay. The standard graph was plotted with the active Akt/PKB provided. The equation for the graph was used to calculate the values of the samples based on their absorbance. This graph is typical of three such different experiments. Data are mean ± standard deviation, n = 3.

The kinase activity was calculated as:

Considering untreated 1321N1, the absorbance of the sample was = 1.838 nm, which was later substituted in the equation of the standard (y = 0.1908 x + 0.056).

Therefore, the kinase activity level for 1321N1 = 9.04 ng

The samples were diluted in the kinase buffer and subsequently the dilution factor for untreated 1321N1 sample = 78.95.

Thereby, the resulting kinase activity in 1321N1 control cells was calculated to be 713.30 ng (Table 3.3).

Table 3.3: Determination of kinase activity according to Akt/PKB Kinase Activity Assay Kit
Data values are mean ± standard deviation, n = 3, *p < 0.05 and **p < 0.001 are considered to be statistically significant.

Samples	Kinase activity for 1 ug Protein (ng)
1321N1	713.71 ± 2.5
1321N1-shRNA *hsp90α* 2	244.19 ± 1.7 **
GOS-3	149.80 ± 1.3
GOS-3-shRNA *hsp90α* 2	61.80 ± 1 **
U87-MG	367.89 ± 1.9
U87-MG-shRNA *hsp90α* 2	141.20 ± 1.7 **

Upon statisitical analysis, **p < 0.001 for treated cells compared to untreated cells in each cell line showing significant decrease in Akt kinase activity post *hsp90α* inhibition using shRNA construct 2.

3.5 DISCUSSION:

Hsp90 and its involvement in tumours have made it an attractive molecular target for cancer treatment by gene therapy. Hsp90 chaperones a vivid list of client proteins, several of which have been involved in apoptosis, cell survival and growth pathways (Chiosis *et al*., 2004). Recent studies in our laboratory have deduced the presence of the inducible Hsp90α protein and gene in glioma cell lines and tissue and its absence in normal cells and tissues (Shervington *et al*., 2008). Further, *hsp90α* was downregulated in glioma cell lines using siRNA targeted against *hsp90α* and the sensitivity of the cells to chemotherapeutic agents was confirmed. It was reported that, inhibition of *hsp90α* using siRNA could possibly be adopted as a favourable therapeutic approach compared to conventional therapies owing to its specificity and reduced toxicity and also due to the enhanced chemosensitivity attained (Cruickshanks *et al*., 2010).

Given the advantages of shRNA over siRNA, this study used shRNA to target *hsp90α* in glioma as opposed to the previous work (Cruickshanks *et al*., 2010). *hsp90α* was highly induced in three glioma cell lines. These results are in agreement with similar previous studies by Shervington *et al*., (2008) with *GAPDH* being consistently expressed. Pre-transfection with shRNA oligonucleotide the IC_{50} of puromycin in all three glioma cell lines was carried out in the study. The shRNA plasmids have a puromycin-N-acetyl transferase gene located downstream of the SV40 early promoter, thus transfecting the cells with shRNA plasmids which in turn resulted in them being resistant to antibiotic puromycin. The IC_{50} of puromycin for glioma cell lines was approximately 0.5 µg/ml and post transfection with shRNA plasmids, a selection pressure was maintained by adding 0.5 µg/ml of puromycin to the transfected cells. This was carried

out to selectively isolate the cells transfected with the plasmid from the cohort of cells. Yadav *et al*., in (2009) transfected human shRNA knockdown retroviral construct targeted against *ANXA7* in GBM cell lines, U87 and LN229 cell lines followed by 1 µg/ml of puromycin selection. Similarly, in another study, U87 and a mouse embryonic fibroblast (NIH-3T3) cell lines were transfected with Marburg virus (MBG) pseudotypes carrying a human immunodeficiency virus (HIV-1) vector containing a puromycin resistant gene. The IC_{50} level of puromycin was found to be 1 µg/ml for the cell lines used in the study (Chan *et al*., 2000). This difference in the IC_{50} level of puromycin for glioma cell lines could be attributed to different experimental conditions.

Post-treatment with shRNA oligonucleotides, mRNA was isolated from the three glioma cell lines after 48 hours of transfection. It was subsequently converted into cDNA and then was quantified using RT-PCR. Upon analysis, it was found that post-treatment with shRNA oligonucleotides, the *hsp90α* expression level was reduced significantly (*$p < 0.05$) with all the four shRNA constructs reducing the expression of *hsp90α* in glioma cell lines. Interestingly, amidst the four constructs, shRNA construct 2 silences *hsp90α* almost by 99 % compared to untreated cells (**$p < 0.001$). This was in accordance to the company's product specification (www.origene.com) which guaranteed at least one of the four constructs to inhibit the expression gene of interest (*hsp90α*) by > 90 %. Additionally, to rule out the potential non-specific effects induced by the shRNA oligonucleotides driven against *hsp90α*, the study used two sets of controls namely shRNA negative oligonucleotide (cloning plasmid) control. This is a purified and sequence verified plasmid construct without the shRNA cassette and shRNA scramble oligonucleotide (shGFP (29) non-effective plasmid) which was constructed by cloning a non-effective shGFP sequence cassette into the plasmid

vector. As expected, the controls, shRNA negative and shRNA scramble did not affect *hsp90α* expression and *GAPDH* was found to be expressed consistently in the samples.

It can thus be speculated that on genomic front, shRNA targeted against *hsp90α* works efficiently by reducing the activity of Hsp90α in all three glioma cell lines used in the study. In another study *hsp90α* was subjected to inhibition in breast cancer cell lines MCF7 and T47D with >30 shRNA constructs designed against *hsp90α*. It was reported that only one construct (sh11) was capable of reducing Hsp90α expression by approximately 80 % (Srirangam *et al*., 2006).

The level of Akt/PKB kinase, which is a client protein to Hsp90, was also checked. Akt/PKB kinase plays a major role in the anti-apoptotic pathway, however, in tumours, including glioma it stimulates cell proliferation and inhibits apoptosis, thus empowering the cancer cells the property of "immortality" (Basso *et al*., 2002). The Akt protein is directly regulated by Hsp90. Commercially available Akt/PKB kinase activity assay kit (Assay Designs, UK) was used to measure the activity of Akt/PKB kinase in glioma cell lines. The Akt/PKB kinase activity levels significantly decreased (**$p < 0.001$) by 65.8 %, 58.8 % and 61.7 % in 1321N1, GOS-3 and U87-MG treated cell lines, respectively, showing inactive Akt/PKB kinase in glioma cell lines thus, confirming the silencing of *hsp90α*. This reduced activity of Akt/PKB kinase is of therapeutic importance in glioma therapy. Furthermore, a report in 2010 suggested that silencing Hsp90 using deoxycholate, downregulates Akt pathway in a dose-dependent manner in human gastric epithelial cells with almost complete inhibition of Akt at a concentration of 100 µM deoxycholate (Redlak and Miller, 2010).

3.6 CONCLUSION:

Previous studies in our laboratory (Cruickshanks *et al*., 2010; Shervington *et al*., 2008) have shown that inhibition of *hsp90α* in glioma could be used as a future therapeutic approach. In this study, it can be concluded that shRNA works efficiently to silence *hsp90α* in glioma cell lines at a genetic level. Furthermore, it can also be stated that by using shRNA targeted against *hsp90α*, a significant reduction profile of the Akt/PKB kinase activity is observed. Given the role of Akt/PKB kinase, this may suggest that the glioma cells used in this study are no longer "immortal" and could thereby undergo apoptosis, which is of therapeutic importance. Thus, silencing of *hsp90α* using shRNA targeted against it could be used as a future therapeutic option in glioma studies.

CHAPTER 4

PROTEOME CHANGE IN U87-MG POST Hsp90 SILENCING

4.1 INTRODUCTION:

Gliomas are the most commonly diagnosed malignant adult primary brain tumours with a median survival rate for glioblastoma multiforme of 12 to 15 months. Treatment options include surgical resection followed by adjuvant radiotherapy and chemotherapy (Stupp *et al*., 2006). Despite technical advances, the prognosis and survival rate for gliomas is very poor. This demands alternative therapeutic aspects in the treatment of gliomas (Fulda *et al*., 2002). Heat shock protein Hsp90 is upregulated in several tumours including glioma and thus, targeting its function may provide new therapeutic aspects (Shervington *et al*., 2008; Altieri, 2004). The heat shock protein 90 (Hsp90) is a highly conserved molecular chaperone present in eukaryotic cytosol and it has been proposed to play a vital role in tumorigenesis, maintenance of transformation and regulation of several key proteins involved in apoptosis, survival and growth pathways (Neckers, 2007). These pathways are exploited in tumours where Hsp90 chaperoning contributes towards drug resistance (Cowen and Lindquist, 2005), metastasis (Eustace *et al*., 2004) and cell survival (Rodina *et al*., 2007). Hsp90 is abundantly present both intracellularly and extracellularly in eukaryotic cells and has extensive influence on v*a*rious cellular activities (Sreedhar *et al*., 2004; Richter and Buchner, 2001). The chaperoning function of Hsp90 is critical not only for normal cells but for transformed cells since it facilitates cell growth and cell cycle progression and thus, helps in their survival (Altieri, 2004). Hsp90 assists functional maturation for a diverse group of proteins particularly those involved in signalling pathways in several tumours (Picard, 2002). For an example, Hsp90 stabilizes Akt/PKB kinase and also oncogenic forms of mutant epidermal growth factor receptor (EGFR) both of which are responsible for the growth of several tumours including gliomas (Basso *et al*., 2002;

Lavictoire *et al*., 2003). The syntheses of several natural and chemical inhibitors along with RNAi using siRNA or shRNA to silence hsp90 have been undertaken.

Bensoquinone ansamycins were the first class of natural Hsp90 inhibitors to be studied and then subsequently used for tumour therapy (Workman *et al*., 2007). Benzoquinone ansamycins are antibiotics, characterized by the linkage of a quinone moiety to the planar macrocyclic ansa bridge structure (Messaoudi *et al*., 2008). Glendanamycin (GA) was the first prototype of the class of Bezoquinone ansamycins. It was purified from the broth of *Streptomyces hygroscopicus* as early as 1970 (Solit and Rosen, 2006). The structural and biochemical analysis showed GA to compete against ATP in binding to the Hsp90 N terminal pocket (Roe *et al*., 1999). Binding of GA to the N terminal pocket of Hsp90 restricts Hsp90 to remain in its ADP bound state and, thus, subsequently prevents Hsp90 binding to other client proteins (Blagg and Kerr, 2006; Neckers, 2006) resulting in degradation of the client proteins via the ubiquitin-proteasome pathway (Mimnaugh *et al*., 1996; Sharp and Workman, 2006; Whitesell and Lindquist, 2005). Although GA displayed potential anti-cancer activities, it was not seen as a prominent candidate due to the high levels of toxicity displayed in animal models (Neckers *et al*., 1999). This demanded the search for GA derivates with lower toxicity profiles. 17-allylamino-17-desmethoxygeldanamycin (17AAG) and more recently 17-dimethylaminoethylamino-17-demethoxygeldanamycin (17-DMAG) and 17-allylamino-17-demethoxygeldanamycin hydroquinone hydrochloride (IPI-504) were therefore synthesized for further evaluation (Fig. 4.1) (Pacey *et al*., 2006; Workman *et al*., 2007).

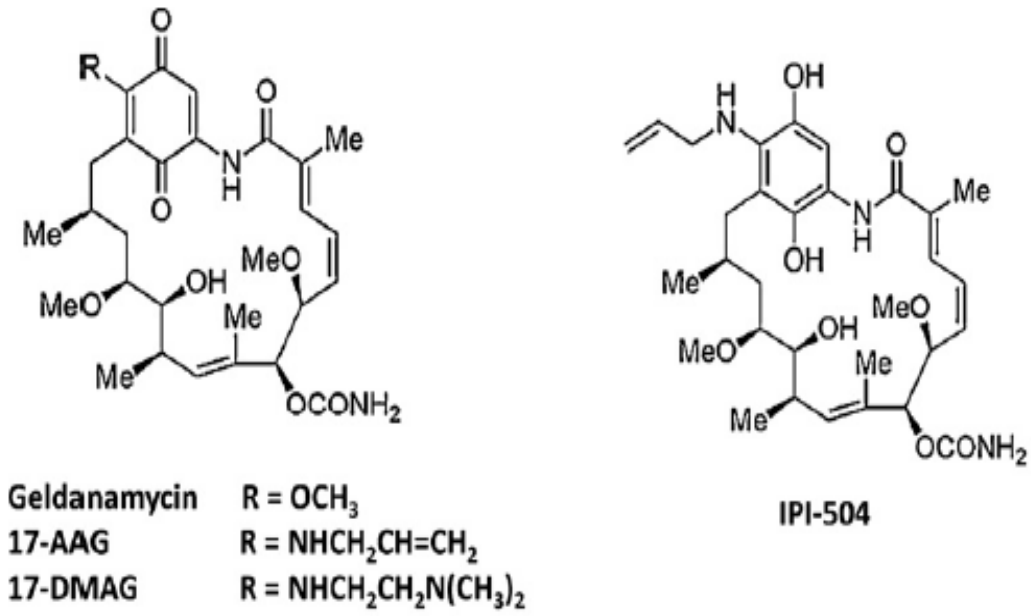

Figure 4.1: Chemical structures of GA and its derivates (Adapted from Messaoudi *et al*., 2008).

17AAG, an analogue of GA is less toxic and has the same mechanism of action to inhibit Hsp90 (Fig. 4.2) (Workman *et al*., 2007)

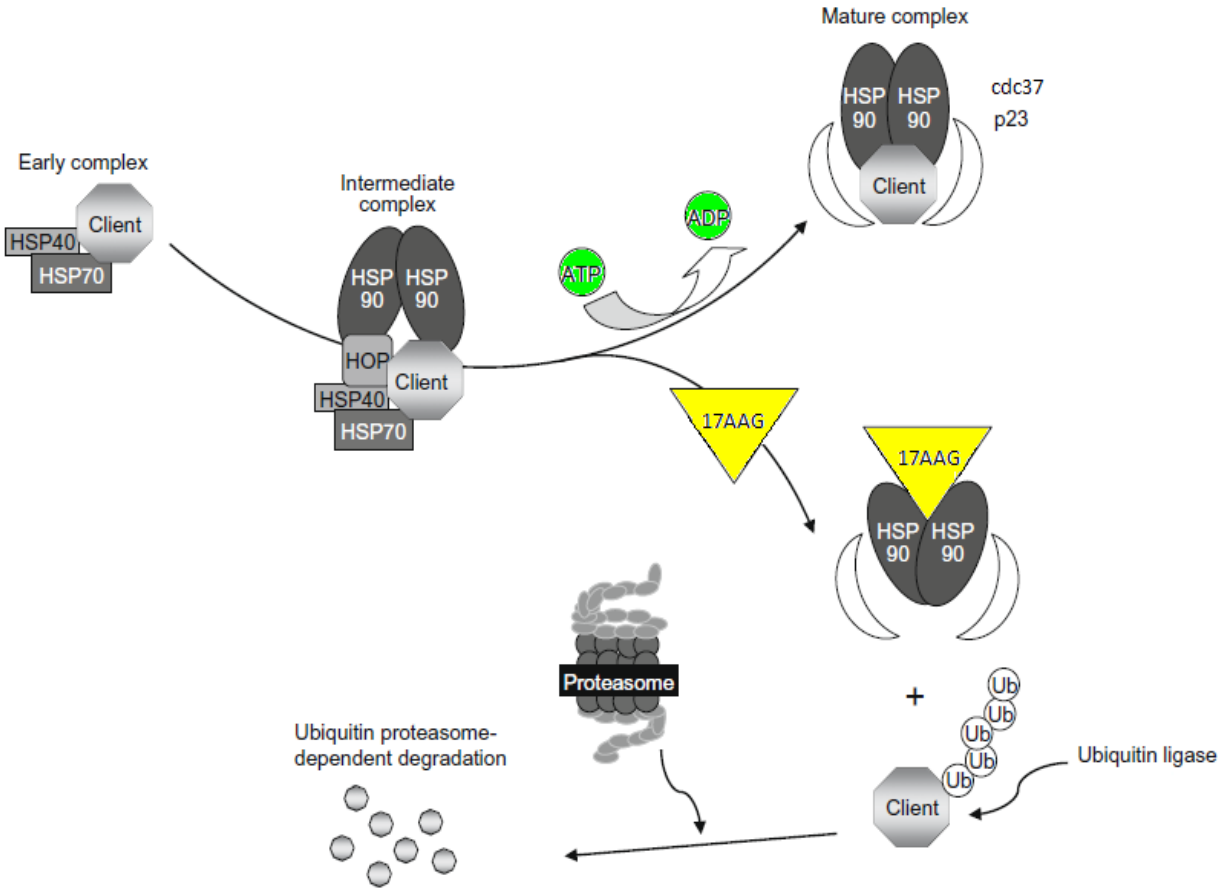

Figure 4.2: Hsp90 chaperone cycle. The client proteins bind to the Hsp70-Hsp40 early complex which then interacts with Hsp90 complex via HOP. Hydrolysis of ATP releases Hsp70-Hsp40 and HOP from the intermediate complex. The mature protein complex is formed by the association of Hsp90 along with its co-chaperons namely cdc37 p23 and/or client proteins. 17AAG blocks the formation of mature complex by actively binding to the ATP binding site of the Hsp90 protein leading to degradation of the client proteins via the ubiquitin proteasome pathway. (Adapted from Fukuyo *et al*., 2010)

17AAG was the first Hsp90 inhibitor to enter phase I clinical trials in 1999 (Banerji *et al*., 2005; Pacey *et al*., 2006). Clinical trials were carried out on patients with advanced tumours including metastatic prostate, melanoma, lung, colon, pancreatic, head and neck, ovarian and breast cancers (Goetz *et al*., 2005; Grem *et al*., 2005; Solit *et al*., 2007; Weigel *et al*., 2007; Heath *et al*., 2008; Solit *et al*., 2008). Phase II clinical trials for 17AAG are currently ongoing (Heath *et al*., 2005; Ronnen *et al*., 2006). In 2007, Modi

and his colleagues, successfully administered 17AAG in combination with trastuzumab in patients with breast cancer whose tumours had progressed during treatment with trastuzumab alone. It was found that a combination of trastuzumab and 17AAG was well tolerated in patients and has antitumour activity (Modi *et al*., 2007).

The ability of Hsp90 inhibitors to target several signal transduction pathways involved in proliferation and cell survival is of therapeutic importance in gliomas due to complex etiology of brain tumours (Siegelin *et al*., 2009). Additionally, the lipophilic nature of 17AAG enables it to penetrate through the blood brain barrier making it an ideal candidate for the treatment of gliomas (Siegelin *et al*., 2009).

4.1.1 Hsp90 and Proteomic Studies:

Genomic studies are edifying, however, they do not necessarily reveal the true picture of the condition of the cell. The levels of mRNA do not necessarily correlate with the cellular protein content as proteins often undergo proteolytic cleavage, alternative splicing and/or other post-translational modifications such as phosphorylation or glycosylation (Walsh *et al*., 2005). Proteome are proteins that are expressed in the cell in a particular condition at a particular time. Cancer proteome is estimated to be made of approximately 1.5 million proteins (Khalil and Madhamshetty, 2006; Alaoui-Jamali and Xu, 2006; Sun *et al*., 2007). Contrasting to the genome, the proteome is dynamic and in a state of unrest (Srinivas *et al*., 2002). Thus, it can be said that, genomic studies alone would not unravel the fate of Hsp90; in order to study the various regulatory and downstream effects and to determine the changes in the cell proteome at that instant in time, proteomic studies have to be carried out (Thakkar and Shervington, 2008).

Proteomic studies carried out on cervical cancer cells taken from Henrietta Lacks (HeLa) identified Hsp90 binding proteins which accumulated as ubiquityl tagged aggregates, post Hsp90 silencing (Falsone *et al*., 2007). HeLa cells were treated with a proteosomal inhibitor MG132 and then Hsp90 was silenced by treating the cells with radicicol. Post 16 hours detergent insoluble fractions were prepared and resolved on 2 dimensional gel electrophoresis (2-DE) gel. Of the 78 proteins identified, 48 proteins were ubiquitylated of which 30 proteins were previously unreported to be ubiquitylated in humans suggesting a significant effect of Hsp90 inhibition. Furthermore, a prominent degradation of proteins involved in signal transduction, transcription, metabolism and metabolic biosynthesis was observed post treatment with radicicol. These results suggest a multiple circuit breakdown of multiple networks post Hsp90 inhibition (Falsone *et al*., 2007).

A study in 2009 applied three complementary proteomics approaches (coimmunoprecipitation, purifying Hsp90 protein complexes with biotinylated Hsp90 inhibitor geldanamycin and immobilization of Hsp90β on sepharose) in human epidermoid carcinoma cells A431 to identify novel protein interactors of Hsp90. This study helped to increase current knowledge regarding Hsp90 interactors by identifying 42 proteins of which 18 proteins had not been characterized previously as Hsp90 interactors (Tsaytler *et al*., 2009).

It can be clearly observed that proteomic studies on Hsp90 shed light on Hsp90's role in regulating several signalling cascades in tumours (Falsone *et al*., 2007). Additionally, proteomic studies have helped expand our awareness of an ever increasing number of Hsp90 client proteins and provide further steps in understanding the Hsp90 chaperone system (Tsaytler *et al*., 2009).

Proteomic studies can therefore:

1. Shed light on downstream effects of Hsp90 silencing in the various biological processes.
2. Identify novel Hsp90 interactors and thereby further help understand the Hsp90 chaperone system.
3. Highlight post translational changes which were earlier not detected by genomic studies.

4.1.2 Summary:

U87-MG glioma cell line represents grade IV glioblastoma which is the most severe form of glioma and hence, would be used for further analysis. This study looks into Hsp90 inhibition with:

a) 17AAG, an analogue of GA and a potent Hsp90 inhibitor

and

b) shRNA oligonucleotide targeted against *hsp90α*

(sense: 5'CTCTCAAGGACTACTGCACCAGAATGAAG3'

antisense: 5'GAGAGTTCCTGATGACGTGGTCTTACTTC3')

Post inhibition with 17AAG or shRNA (*hsp90α*), proteins were extracted from the U87-MG cell lysate and further sent to Applied Biomics, U.S.A to characterize the changes made due to inhibition of Hsp90 by a differential proteomic analysis. The protein expressed in wild type U87-MG cells (control) were compared to the proteins expressed in U87-MG cells after silencing *hsp90α* (U87-MG-sh*hsp90α*) and the proteins expressed in U87-MG cells, post 17AAG treatment (U87-MG-17AAG). Additionally, the inhibition was compared by studying the protein level of Hsp90α in control and treated

cells using fluorescence-activated cell sorting (FACS) analysis (quantitative) with a flow cytometer. Furthermore, the Akt/PKB kinase activity levels were checked using the Akt/PKB Kinase Activity Assay kit (Assay Designs, UK) and Hsp90α protein levels were also quantified in the control and treated cells using Hsp90α ELISA kit (Assay Designs, UK).

This approach elucidates the changes caused in the Hsp90 chaperone system post inhibition using 17AAG or shRNA oligonucleotide targeting *hsp90α* in glioma. Though the significance of Hsp90's glioma regulation has been well documented, the downstream effect of Hsp90 inhibition at the various physiological and signalling pathways in glioma is still ambiguous. Silencing *hsp90α* at the genetic level (shRNA) and at the protein level (17AAG) to identify potential downstream pathways and protein affected and/or controlled by Hsp90 in glioma is a novel approach. Therefore, this study aims to silence Hsp90 either by using 17AAG or shRNA targeting *hsp90α* and tries to identify the potential downstream pathways and proteins affected by Hsp90 in glioma.

4.2 PROTEOMICS:

There are approximately 20,500 protein encoding genes in the human genome (Clamp *et al*., 2007) while close to a million protein products, including splice variants and essential post-translational modifications are present (Godovac *et al*., 1999).

Proteomics is the study and characterization of complete sets of proteins present in a cell, organ or organism at a given point in time (Wilkins *et al*., 1996) and it displays patterns of several proteins being differentially regulated at one time point post different treatments (Whiteley, 2006). Proteomic studies helps to analyze protein-protein interaction, compare different protein expression analysis under different conditions and monitors post-translational modifications (Whiteley, 2006). Proteomic analysis involves the use of a combination of sophisticated analytical techniques such as 2D gel electrophoresis for protein separation; image analysis, mass spectrophotometric analysis and bioinformatics tools to quantify and characterize complex proteins (Chandramouli and Quian, 2009).

Proteomic analysis for this study was carried out by Applied Biomics, U.S.A and an overview of the workflow is summarized in Figure 4.3.

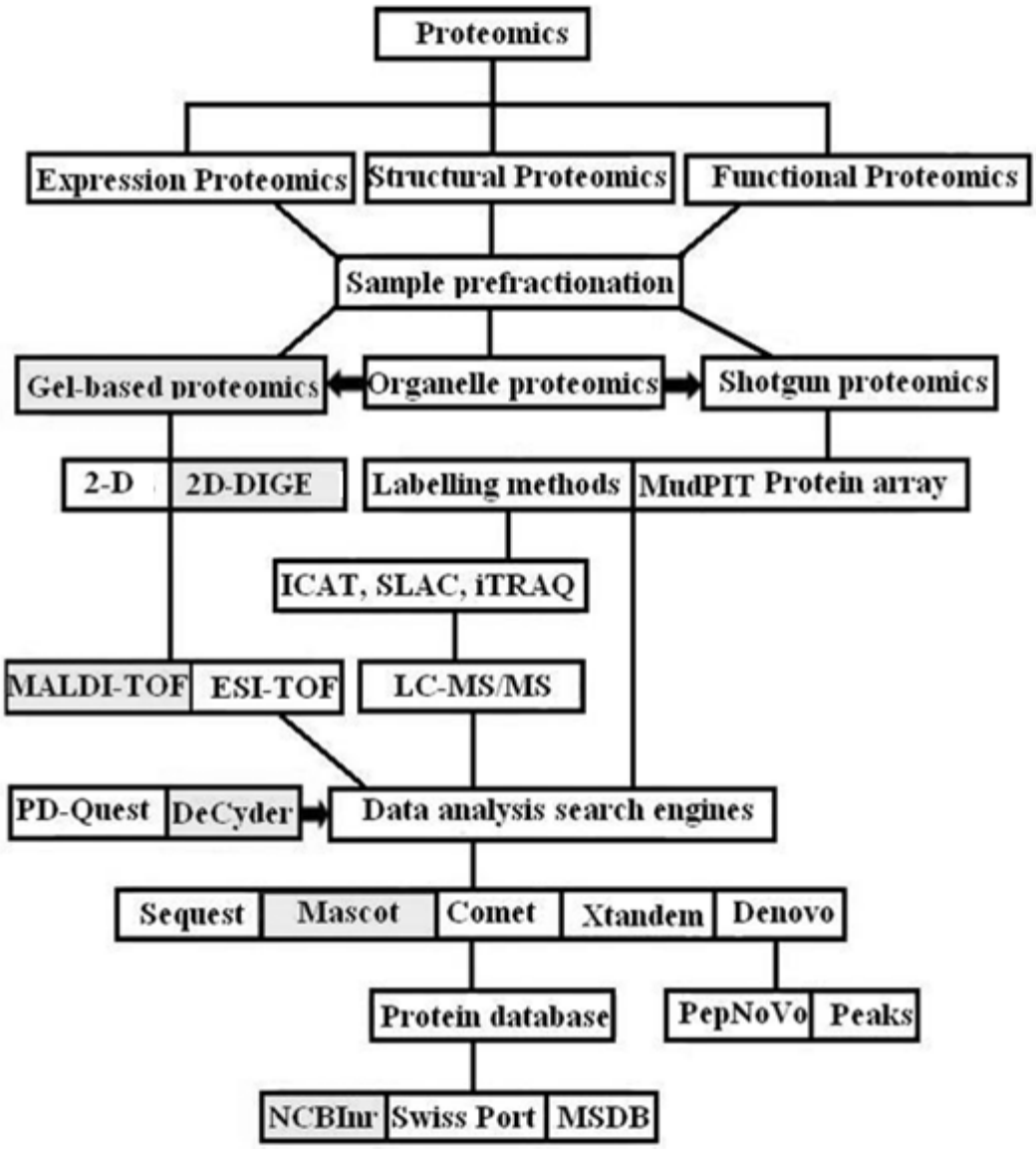

Figure 4.3: Overview of proteomic strategies. (Adapted from Chandramouli and Quian, 2009). Methods used in this study are highlighted.

4.2.1 Fluorescence difference gel electrophoresis (2D-DIGE):

In the 2D-DIGE experiment, the samples are covalently labelled with different fluorescent cyanide (Cy) dyes. Later, the samples are migration matched to ensure the protein labelled with different dyes migrate to the same position on the gel. The control/untreated sample serves as internal standard which is subsequently used for normalization and spot matching enabling inter and intra gel analysis (Minden, 2007;

Loeffler-Ragg *et al*., 2008). The gel is then scanned using a fluorescence imager at specific wavelengths for Cy2 (488 nm), Cy3 (532 nm) and Cy5 (633 nm). The gel image for each of the different samples obtained is then merged and analyzed using imaging software to analyze different regulations among the proteins (Minden, 2007).

Fully automated software such as DeCyder, which increases the accuracy of the DIGE, is specifically designed for 2D-DIGE analysis (Marouga *et al*., 2005). DeCyder being the only software to contain proprietary algorithms which helps in the co-detection of differently labelled samples within the same gel. It allows automated detection, background subtraction, normalization and inter-gel matching and spot picking (Marouga *et al*., 2005) which results in high output, minimum introduction of human error and high reproducibility (Fig. 4.4).

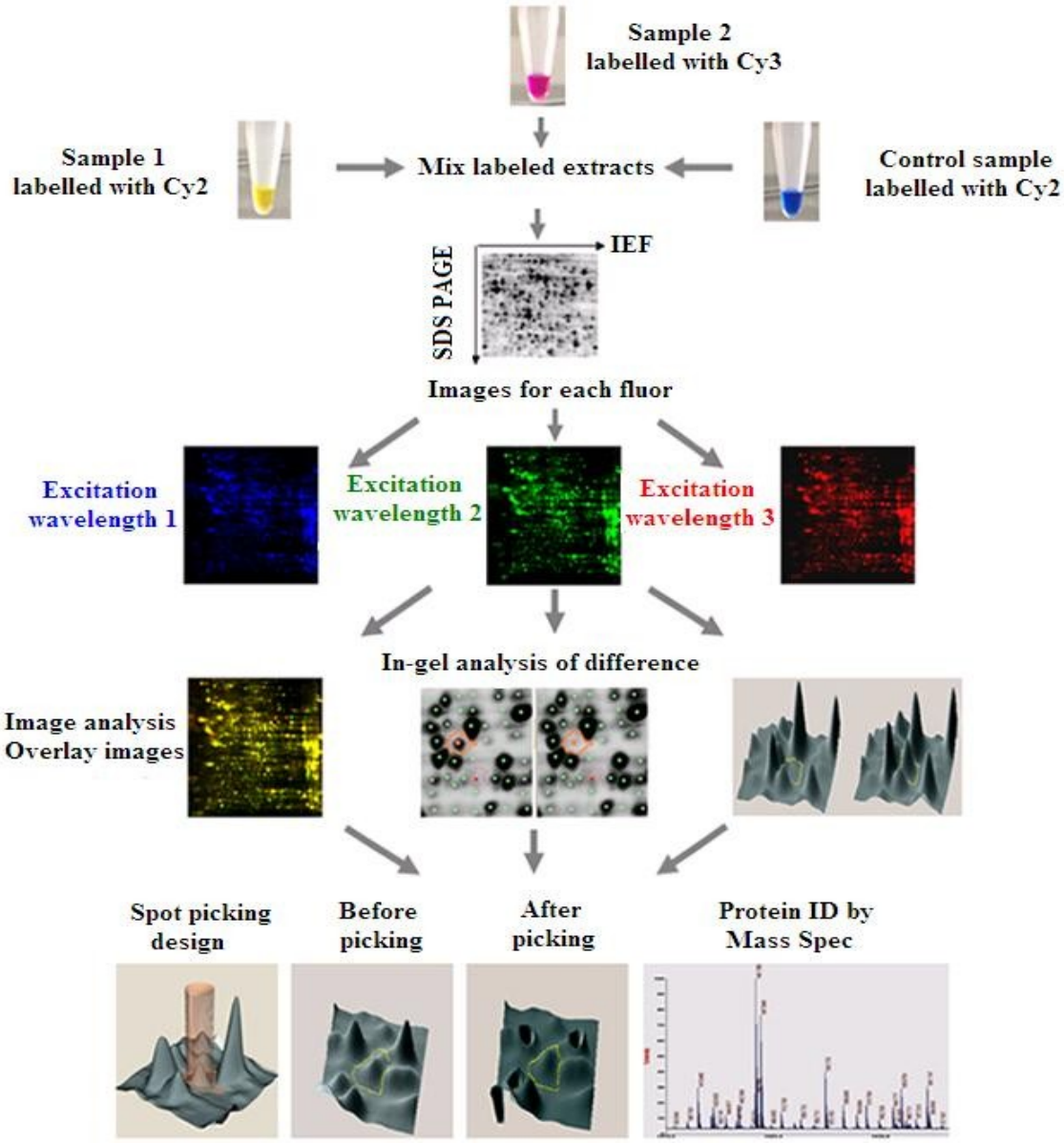

Figure 4.4: Typical workflow of 2D-DIGE using DeCyder (Adapted from Ettan DIGE user manual, 2002). Typical of one experiment based on cost.

4.2.2 Mass spectrophotometry analysis:

Protein identification is carried out by mass spectrophotometry (MS). A mass spectrophotometer consists of three major units namely, a) an ion source wherein proteins are ionized and gas phase ions are generated, b) a mass analyzer which

separates ions according to their mass to charge ratio and c) an ion detection system (Domon and Aebersold, 2006).

In matrix assisted laser desorption/ionization time-of-flight (MALDI-TOF) mass spectrophotometer, the samples of interest are crystallized with a chemical matrix which is mixed with the analyte and spotted on the MALDI plate reader. The molecules dissolve in their solvents (hydrophobic or hydrophilic) and then vaporize to leave a spreaded analyte in the recrystallized matrix. A nitrogen laser beam triggers the ionization of the samples. The matrix transfers some of its energy to the analyte when the light wavelength matches the absorbance maximum of the matrix and subsequently the analyte is released into the gas phase. MALDI measures the mass of peptides derived from the parent protein and generates a list of experimental peptide masses often referred as “mass fingerprints” (Vestling and Fenselau, 1994; Medzihradszky *et al*., 2000).

4.2.3 Database search:

Peptide masses derived from the mass spectrophotometer analysis are in correlation with peptide fingerprints of known proteins in a protein sequence database and are identified using search engines such as MASCOT, Sequest, Comet, X!tandem, MOWSE, PeptIdent-2 and Profound (Pappin *et al*., 1993; Mann *et al*., 1993; Yates *et al*., 1993; Colinge *et al*., 2003; Geer *et al*., 2004). These search engines provide a list of best matching peptide sequences for an individual tandem mass spectrum and also provide scores relating to the confidence level in the match. Each search engine has different algorithms and scoring functions and thereby do not provide identical results (Carr *et*

al., 2004; Bradshaw, 2005). This project used MASCOT search engine developed by Matric science.

4.2.4 Ingenuity Patway Analysis (IPA):

Knowledge-based software such as IPA (Ingenuity® Systems) was used to identify molecular functions and pathways relating to our dataset. The IPA system makes use of a knowledgebase derived from the literature to relate gene products based on their interaction and function. It helps to identify relationships, mechanisms, interaction networks, functions and global pathways of the proteins (Jimenez-Marin *et al*., 2009). IPA provides a platform where one can access information on genes and proteins implicated in tumour related processes and pathways generate hypothesis and discover new targets for tumour studies.

Biofunctions are grouped into three categories in IPA; a) diseases and disorders b) molecular and cellular functions and c) physiological systems development and functions. The canonical pathways on the other hand are grouped in metabolic and signalling pathways. The identified proteins are mapped to the existing networks based on their score. Two parameters are considered for the identification of the significant pathways namely a) ratio of the number of proteins that map to pathways divided by the total number of proteins that map to the canonical pathway and b) the p-value calculated by Fisher's exact test determines the association between the protein in the dataset and the canonical pathway (Skynner *et al*., 2006).

4.3 MATERIALS AND METHODS:

As described in chapter 2, the U87-MG cell line was cultured as described in section 2.1 of the study. The cells were treated with varying concentrations of 17AAG (0.25 – 1.5 µM) for 48 hours as described in section 2.11. Hsp90α ELISA assay was carried out to quantify Hsp90α in the cell lysate as described in section 2.10. The levels of Hsp90α protein were quantified by FACS analysis using a Flow Cytometer as described in section 2.13. The Akt/PKB kinase activity was assayed using Akt/PKB Kinase Activity Assay Kit (Assay Designs, UK) as described in section 2.9. The cell cycle analysis was carried out on the control and treated samples as described in section 2.12.

4.3.1 Protein extraction for proteomic analysis:

Proteins were extracted from the cell lysates of control and treated samples for proteomic analysis.

1. Cell pellets were freshly collected and washed thrice with washing Buffer (10 mM Tris-Hydrochloric acid (HCl), 5 mM magnesium acetate, pH 8.0) to remove culture medium.
2. For 10 mg of cultured cell pellet, 200 µl of 2D cell lysis buffer (400 mM Tris, 0.01 M EDTA; pH 8.3) was added.
3. The mixture was later sonicated at 4 °C followed by shaking for 30 min at room temperature.
4. The samples were centrifuged for 30 min at 14 x 10^3 rpm and the supernatant was collected.
5. Protein concentration was calculated using Bio-Rad protein assay method.

4.3.2 Protein quantification:

Bio-Rad protein assay based on Bradford method of protein quantification is a dye based assay which produces differential colour change based upon the protein concentration (Bradford, 1976). The dye reagent concentrate was purchased in a kit with BSA (Biorad, UK) which was used as a standard.

1. Lyophilized BSA standards were reconstituted by adding 20 ml of deionized water and were mixed thoroughly until dissolved.
2. The standard was aliquoted and stored at -20 °C when not used.
3. The dye reagent was prepared by diluting 1 part dye reagent concentrate with 4 parts of distilled deionized water and this was then filtered through Whatman #1 filter.
4. The protein solution to be tested was prepared by pipetting 100 µl of each standard and sample solution into a clean and dry test tube.
5. Diluted dye reagent (5 ml) was added to each tube.
6. The tubes were vortexed and incubated at room temperature for at least 5 min.
7. The absorbance was measured at 595 nm using gamma thermo Helios spectrophotometer (Thermospectronics, UK).
8. A standard curve was plotted and the value of the unknown protein was extrapolated (Fig 4.5).
9. Each protein was assayed at least 2-3 times and the mean values taken.

The protein samples from the control (wild type U87-MG cells) and treated cells (U87-MG-sh*hsp90α* and U87-MG-17AAG) were further sent to Applied Biomics, U.S.A for protein separation (2D-DIGE) and protein identification (MALDI-TOF).

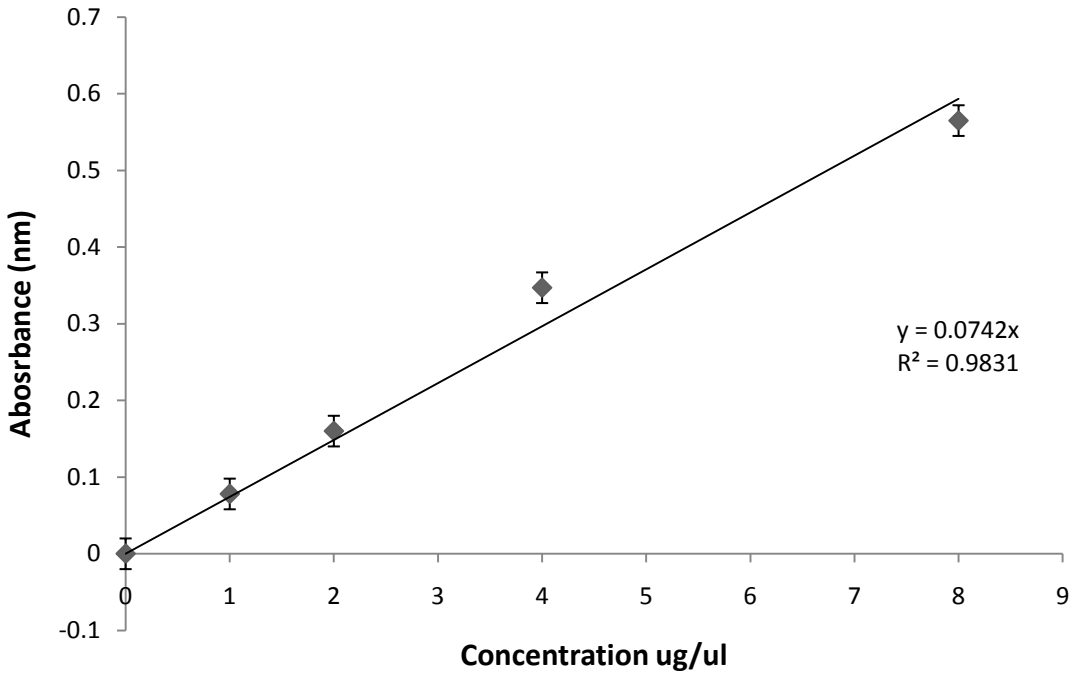

Figure 4.5: Standard graph for protein quantification. The standard graph was plotted with the lyophilized BSA standard supplied. The equation of the graph was used to calculate the values of the samples based on their absorbance. This is typical of 3 such different experiments. Data are mean ± standard deviation, n = 3.

4.3.4 Statistical Analysis

As described in Chapter 2.

4.4 RESULTS:

4.4.1 Cell viability using 17AAG:

Varying concentrations of 17AAG (0.25 – 1.5 µM) were added to the U87-MG glioma cell line and then incubated for 48 hours to check the IC_{50} of 17AAG (Fig. 4.6).

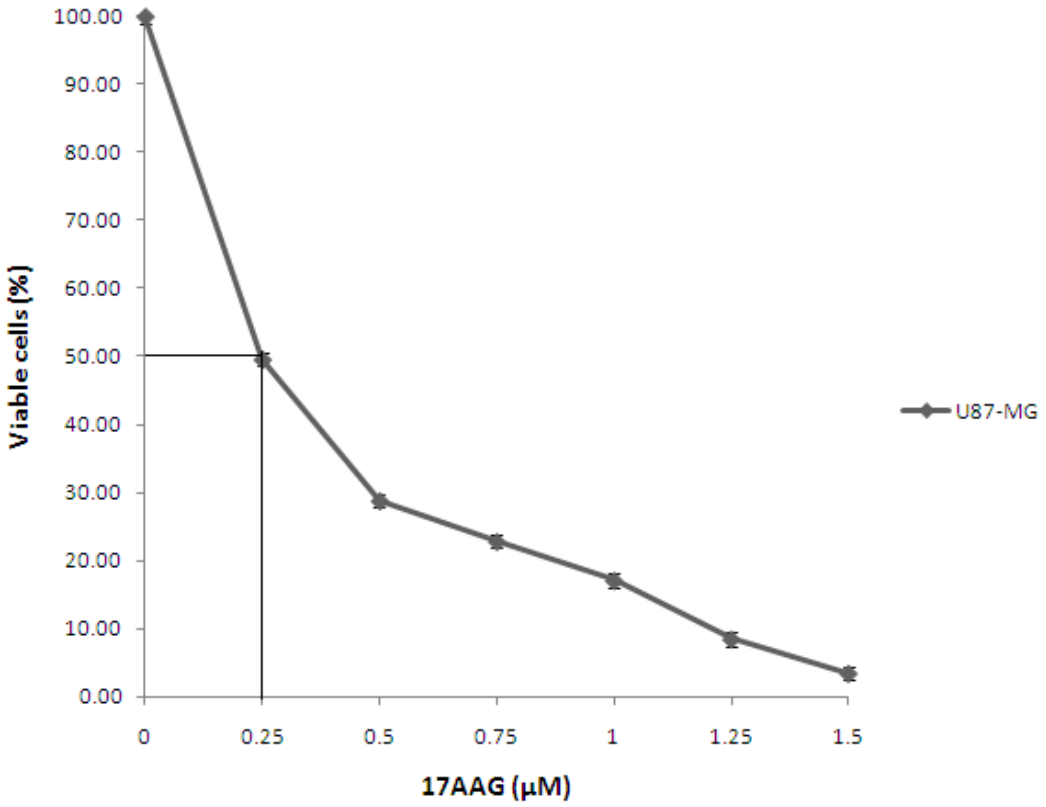

Figure 4.6: Cell viability assessment of U87-MG with increasing concentrations of 17AAG (0.25 – 1.5 µM). Data values are mean ± standard error, n = 3.

The IC_{50} of 17AAG is 0.25 µM in case of the U87-MG glioma cell line.

4.4.2 Akt/PKB kinasae activity assay:

Commercially available Akt/PKB kinase activity assay kit (Assay Designs, UK) was used to measure the activity of Akt/PKB kinase in the control (wild type U87-MG cells) and treated cells (U87-MG-sh*hsp90α* and U87-MG-17AAG) (Table 4.1). The standard graph was plotted as shown in figure 3.15, in chapter 3 and the equation of the graph was used to calculate the values of the samples based on their absorbance.

Table 4.1: Determination of kinase activity according to Akt/PKB Kinase Activity Assay Kit
Data values are mean ± standard deviation, n=3, *p < 0.05 and **p < 0.001 are considered to be statistically significant.

Samples	Kinase activity for 1 ug Protein
U87-MG (CONTROL)	234.51 ± 4
U87-MG-17AAG	44.53 ± 0.1 **
U87-MG-shRNA *hsp90α*	95.16 ± 1.9 **

It can be clearly seen that the Akt/PKB kinase activity was significantly reduced upon inhibition of Hsp90 by 17AAG and shRNA oligonucleotide targeted against *hsp90α.* Moreover, statitisical analysis using Paired-Sample T-Test demonstrated **p < 0.001 for treated cells compared to untreated cells in U87-MG cell line showing significant decrease in Akt kinase activity post *hsp90α* inhibition using 17AAG and sh*hsp90α*. Note that sh*hsp90α* was less effective compared to 17AAG.

4.4.3 Hsp90α ELISA assay:

Commercially available Hsp90α Elisa Kit (Assay Designs, UK) was used to measure the Hsp90α protein level in treated and untreated glioma cell lines (Table 4.2).

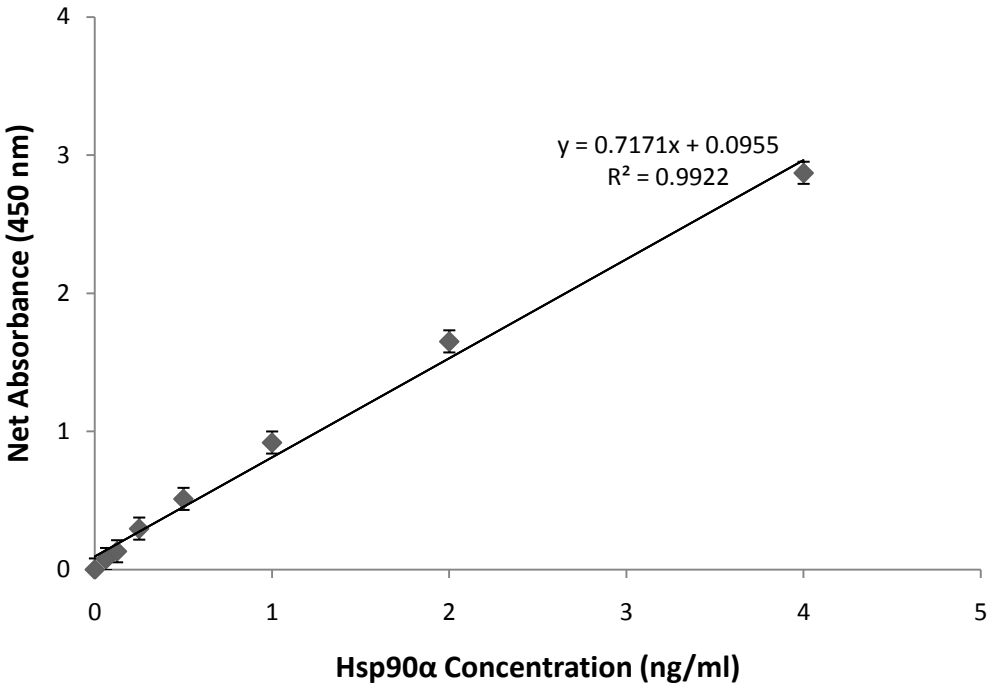

Figure 4.7: Standard graph for Hsp90α ELISA assay. The standard graph was plotted with the recombinant Hsp90α standard supplied. The equation of the graph was used to calculate the values of the samples based on their absorbance. This is typical of 3 such different experiments. Data are mean ± standard deviation, n = 3.

<u>Hsp90α protein levels were calculated as:</u>

Considering U87-MG cells treated with 17AAG, absorbance obtained was 1.873 nm. Substituting this value in the equation of graph (y = 0.7171x + 0.0955), the Hsp90α level was = 2.36 ng/ml.

However, the samples were diluted in the sample diluent and the resulting dilution factor for U87-MG-17AAG was 14.71.

Therefore, the Hsp90α protein level in U87-MG-17AAG cells was obtained to be 34.72 mg/ml (Table 4.2).

Table 4.2: Determination of Hsp90α protein level according to Hsp90α ELISA kit

Data values are mean ± standard deviation, n=3,

Samples	Hsp90α protein level (ng/ml)
U87-MG (CONTROL)	100 ± 3.6
U87-MG-17AAG	34.72 ± 2.9 **
U87-MG-shRNA *hsp90α*	55.12 ± 1.7 **

The results show that, Hsp90α protein level was significantly (**$p < 0.001$) reduced upon inhibition of Hsp90 by 17AAG or shRNA oligonucleotide targeted against *hsp90α* (Table 4.2).

4.4.4 Flow cytometry:

A flow cytometer was used to quantify Hsp90α protein levels in control (wild type U87-MG cells) and treated cells (U87-MG-sh*hsp90α* and U87-MG-17AAG). Hsp90α antigen was detected with fluorescein isothiocyanate (FITC) conjugated secondary antibody which was detected upon flow cytometric analysis (Fig. 4.8 and Table 4.3).

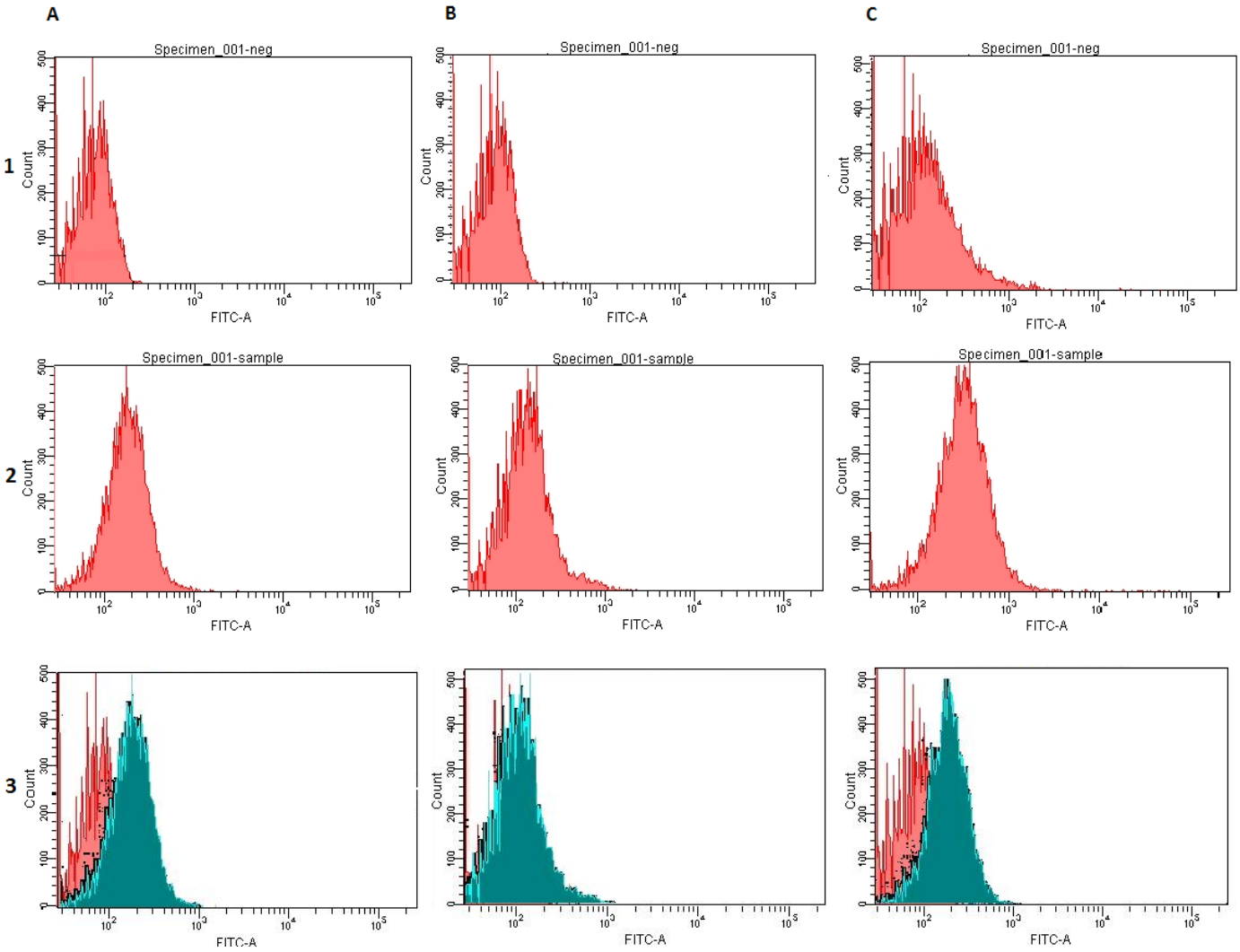

Figure 4.8: Flow cytometric analysis of control and treated U87-MG cell line for Hsp90α detection. Hsp90α antigen is detected with FITC conjugated secondary antibody upon flow cytometric analysis; A) Control (wild type U87-MG cells) B) U87-MG cells treated with 17AAG and C) U87-MG cells treated with shRNA targeted against hsp90α and; 1) Cells stained negative to Hsp90α secondary antibody 2) Gated cell population stained with FITC showing positive cells 3) Overlay image of negative(red) with the positive (blue). These flow cytometric readings are typical of 3 such different experiments.

Table 4.3: Hsp90α quantification by flow cytometric analysis (data values are mean ± standard deviation, n=3).

Samples	Hsp90α expression (%)
U87-MG (CONTROL)	76 ± 0.7
U87-MG-17AAG	42.7 ± 0.2 **
U87-MG-shRNA *hsp90α*	64.1 ± 1.4 **

The results showed that both treatments can significantly (**$p < 0.001$) inhibit the expression of Hsp90α in the U87-MG glioma cell line. These results also show that, 17AAG was much more effective than shRNA.

4.4.5 Cell cycle analysis:

Cell cycle analysis was carried out to compare control cells (wild type U87-MG) and treated cells (U87-MG-sh*hsp90α* and U87-MG-17AAG) based on the cohort of cells found at different stages of cell cycle. As shown in Figure 4.8, the P2 represents the cohort of cells in the G1 phase of the cell cycle, P3 represents for the cohort of cells in the S phase of the cell cycle and P4 represents the cohort of cells in the G2 phase of the cell cycle (Figures 4.9 and 4.10; Table 4.4).

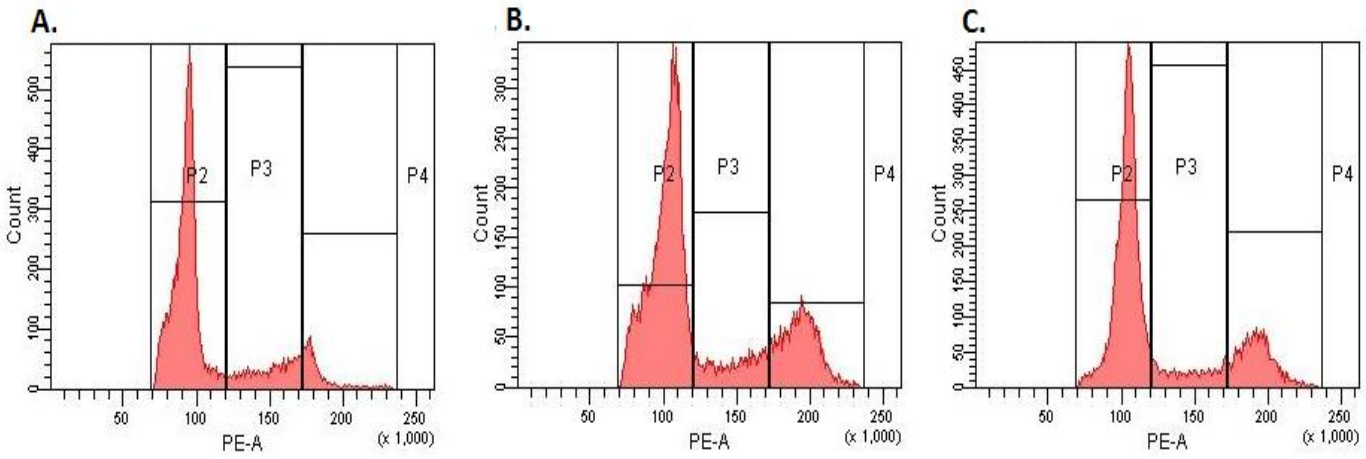

Figure 4.9: Cell cycle analysis of U87-MG control and treated glioma cell line. Cohort of U87-MG cells stained with PI upon cell cycle analysis in A) Control (wild type U87-MG cells) B) U87-MG cells treated with 17AAG and C) U87-MG cells treated with shRNA targeted against *hsp90α*. These flow cytometric readings are typical of 3 such different experiments.

Table 4.4: Cell cycle analysis of U87-MG control and treated glioma cell line (data values are mean ± standard deviation, n=3).

Samples	Cell Cycle (%)		
	G1	**S**	**G2**
WT U87-MG	61.15 ± 0.6	14.4 ± 0.2	14.3 ± 0.7
U87-MG-17AAG	54.65 ± 0.3 *	17.1 ± 0.8*	19.95 ± 0.5
U87-MG-sh*hsp90α*	60.95 ± 0.2	19.6 ± 0.3	15.05 ± 0.3 *

Different stages of the cell cycle affected upon inhibiting Hsp90.

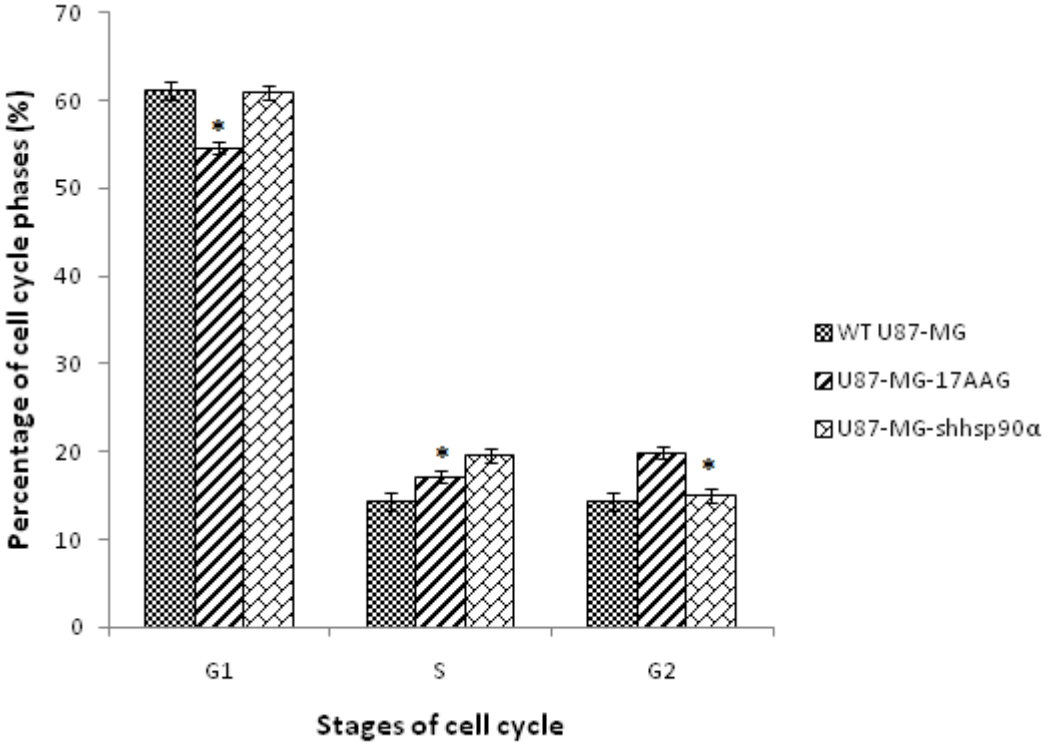

Figure 4.10: Different stages of the cell cycle affected post inhibition of Hsp90. Data are mean ± standard deviation, n = 3, *p < 0.05 and **p < 0.001 are considered to be statistically significant.

Statistical analysis confirmed a significant decrease (*p < 0.05) in G1 and S phase of U87-MG cell cycle upon treatment with 17AAG while a significant decrease (*p < 0.05) was observed in G2 phase of U87-MG cell cycle upon treatment with shRNA targeting *hsp90α*.

4.4.6 Proteomic analysis:

U87-MG glioma cells were treated with 17AAG or were transfected with shRNA targeting *hsp90α* to inhibit Hsp90 function. Proteins were isolated from the samples and were then sent for proteomic analysis (Applied Biomics, U.S.A). A comprehensive

proteomic study was further performed on control (wild type U87-MG) and treated (U87-MG-17AAG and U87-MG-sh*hsp90α*) samples using 2D-DIGE and MALDI-TOF. Proteomic analysis revealed 96 spots to be differentially expressed by a volume ratio of 1.5 fold or greater post treatment across the three samples tested (Fig. 4.10). The spots were selected upon DeCyder analysis and some of the spots were differentially modified between the three treated groups to show a slight shift in molecular weights. Mass spectrophotometric analyses was carried out using MALDI-TOF and for protein identification, 36 spots showing ≥ 2 fold change were selected (Table 4.5). The identification of the proteins was carried out on the basis of peptide fingerprint mass mapping (MS data) and peptide fragmentation mapping [tandem mass spectrometry (MS/MS) data]. For identification of proteins from their primary sequence databases, MASCOT search engine was used. Of the 36 spots identified, 33 were identified as human proteins while the other 3 were not elucidated (identified). More than one spot was identified as the same protein upon protein identification. This could have been attributed to the presence of different isoforms of the same protein following post-translational modifications such as phosphorylation or methylation which changes the proteins isoelectric point (pI) and/or molecular weight (MW) causing the spots to shift along with protein fragmentation.

The biological significance and molecular functions of the proteins identified have been analysed using the public database, Human Protein Research Database (HPRD) (Table 4.6).

A. B.

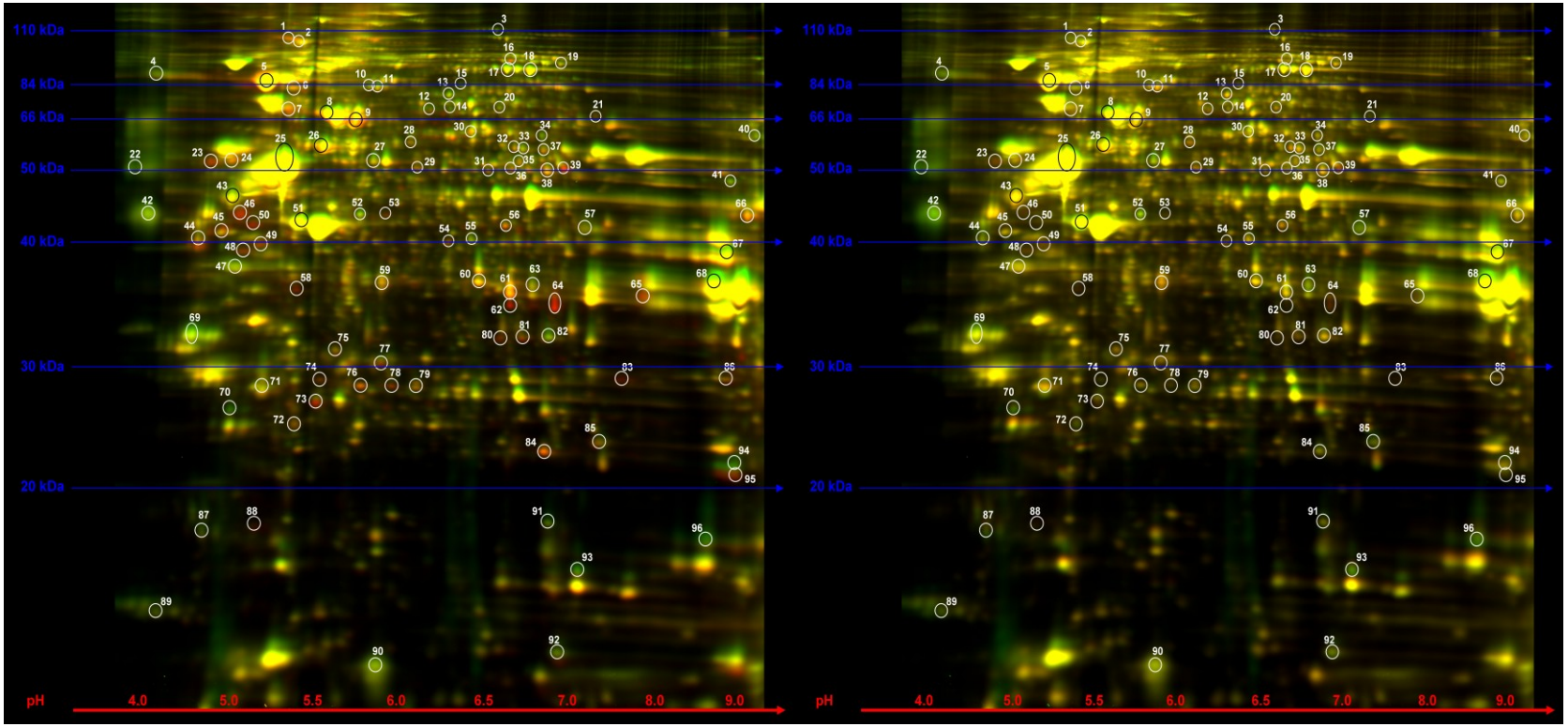

Figure 4.11: 2D-DIGE protein profile. Representation of the 2D-DIGE gel showing, A) Control U87-MG and U87-MG-17AAG and B) Control U87-MG and U87-MG-sh*hsp90α*. Spots were picked automatically by Spots Vol Ratio ≥ 2. Typical of one experiment due to cost.

Table 4.5: Proteins identified by mass spectrophotometry.

The lists of identified peptide having ≥ 2 fold change were searched against MASCOT database for the corresponding proteins. Proteins were categorized according to their change in expression post treatment with 17AAG and shRNA targeting *hsp90α* in U87-MG glioma cell line.

Top Ranked Protein Name	Accession No.	Protein MW	Protein PI	Peptide Count	Protein Score	Protein Score C. I. %	Total Ion Score	Total Ion C. I. %	U87-MG-17AAG/ U87-MG	U87-MG-sh*hsp90α* /U87-MG
A. Up-regulated proteins										
unnamed protein product [Homo sapiens]	gi|28193108	49327.3	5.33	12	203	100	157	100	2.3	1.3
HSP70-1 [Homo sapiens]	gi|4529893	69995.0	5.5	17	297	100	199	100	7.8	1.3
hexokinase 1, isoform CRA_d [Homo sapiens]	gi|119574708	108001.9	6.4	29	357	100	190	100	4.5	1.9
tumor rejection antigen (gp96) 1 variant [Homo sapiens]	gi|62088648	65912.3	5.1	20	417	100	269	100	3.1	1.7
vimentin variant 3 [Homo sapiens]	gi|167887751	49623.1	5.2	18	192	100	64	100	2	1.2
Pyruvate kinase, muscle [Homo sapiens]	gi|127795697	57921.1	8.4	19	291	100	158	100	6.6	2.9
vimentin variant 3 [Homo sapiens]	gi|167887751	49623.1	5.19	29	839	100	523	100	3.9	1.4
unnamed protein product [Homo sapiens]	gi|194379798	54543.4	4.9	17	332	100	217	100	2.6	1.2
unnamed protein product [Homo sapiens]	gi|194379798	54543.4	4.9	15	252	100	153	100	2.7	1.7
heat shock 70kDa protein 8 isoform 2 [Homo sapiens]	gi|24234686	53484.4	5.6	9	223	100	178	100	4.2	1.2
Chain A, Crystal Structure of Aldose Reductase complexed with Dichlorophenylacetic Acid	gi|119390284	35700.4	6.4	16	349	100	206	100	2.8	1.2
annexin I [Homo sapiens]	gi|4502101	38690.0	6.6	18	544	100	380	100	16.8	1.7

Table 4.5 (contd)

glyceraldehyde-3-phosphate dehydrogenase [Homo sapiens]	gi|31645	36031.4	8.3	12	329	100	233	100	8	1.9
ubiquitin carboxyl-terminal esterase L1 (ubiquitin thiolesterase), isoform CRA_c [Homo sapiens]	gi|119613387	24508.3	5.2	3	73	99	60	100	2.2	1
heat shock protein 27 [Homo sapiens]	gi|662841	22313.3	7.8	13	489	100	367	100	2.7	1.1
heat shock protein 27 [Homo sapiens]	gi|662841	22313.3	7.8	11	224	100	131	100	2.7	1.2
actin related protein 2/3 complex subunit 2 [Homo sapiens]	gi|5031599	34311.5	6.8	18	384	100	220	100	2.9	1
heat shock 70kDa protein 8 isoform 2 variant [Homo sapiens]	gi|62896815	53466.4	5.62	12	147	100	80	100	4.5	1.3

Top Ranked Protein Name	Accession No.	Protein MW	Protein PI	Peptide Count	Protein Score	Protein Score C. I. %	Total Ion Score	Total Ion C. I. %	U87-MG-17AAG / U87-MG	U87-MG-sh*hsp90α* /U87-MG
B. Down-regulated proteins										
X-ray repair complementing defective repair in Chinese hamster cells 6 (Ku autoantigen, 70kDa) [Homo sapiens]	gi|169145198	64035.1	6.4	7	92	100	70	100	-3.7	-1.2
vimentin [Homo sapiens]	gi|62414289	53619.1	5.1	29	421	100	137	100	-2.3	-3.4

Table 4.5 (contd)

vimentin [Homo sapiens]	gi|62414289	53619.1	5.1	30	851	100	523	100	-2.1	-1.3
SERPINE1 mRNA binding protein 1 isoform 1	gi|66346679	44938.5	8.7	11	204	100	142	100	-2.2	-1.4
calumenin isoform a precursor [Homo sapiens]	gi|4502551	37083.5	4.5	16	364	100	203	100	-1.9	-2.5
phosphoglycerate kinase 1 [Homo sapiens]	gi|4505763	44586.1	8.3	20	376	100	217	100	-1.2	-2
aldolase A, fructose-bisphosphate, isoform CRA_b	gi|119600342	39792.5	8.3	13	143	100	36	86	-2	-1.6
PREDICTED: glyceraldehyde-3-phosphate dehydrogenase-like 6 [Homo sapiens]	gi|169208088	37668.4	9.2	1	108	100	108	100	-2.5	-1.8
tropomyosin 4-anaplastic lymphoma kinase fusion protein [Homo sapiens]	gi|13274400	36564.6	4.9	17	302	100	193	100	-2	-1.4
eukaryotic translation initiation factor 3, subunit 12	gi|10801345	25043.4	4.8	6	73	99	38	93	-2.7	-1.6
transgelin 2 [Homo sapiens]	gi|4507357	22377.2	8.4	18	589	100	386	100	-3	-1
Chain A, Cyclophilin B complexed with [d-(Cholinylester)ser8]-Cyclosporin	gi|1310882	19648.2	9.2	15	181	100	31	56	-3.7	-1.8

Table 4.5 (contd)

Top Ranked Protein Name	Accession No.	Protein MW	Protein PI	Peptide Count	Protein Score	Protein Score C. I. %	Total Ion Score	Total Ion C. I. %	U87-MG-17AAG/ U87-MG	U87-MG-sh*hsp90α* /U87-MG
C. Differentially regulated proteins										
collagen, type VI, alpha 1 precursor [Homo sapiens]	gi|87196339	108462.0	5.3	12	92	100	58	100	2.1	-1.5
Chain A, Structure of human Annexin A2 in the presence of calcium ions	gi|56967118	36459.8	8.3	17	405	100	254	100	2.1	-1.1
heat shock protein beta-1 [Homo sapiens]	gi|4504517	22768.5	6.0	6	196	100	159	100	2.3	-1.2
Chain A, Human Manganese Superoxide Dismutase Mutant Q143n	gi|2780818	22176.2	6.9	12	399	100	277	100	2.7	-1.2
Chain A, Crystal structure of Ca2+-bound form of Des3-23alg-2	gi|211939086	19773.8	5.0	10	208	100	104	100	2.3	-1.1
transgelin 2 [Homo sapiens]	gi|4507357	22377.2	8.4	17	461	100	275	100	2.4	-1.1

Table 4.6: Molecular and biological function with location of proteins identified by mass spectrophotometry using Human Protein Research Database.

Protein	Molecular function	Biological process	Location
Proteins upregulated by inhibition of Hsp90 by 17AAG and shRNA targeted towards *hsp90α*			
HSP70-1 [Homo sapiens]	Chaperone activity	Protein metabolism	Cytoplasm
hexokinase 1, isoform CRA_d [Homo sapiens]	Catalytic activity	Metabolism, Energy pathways	Cytoplasm
tumor rejection antigen (gp96) 1 variant [Homo sapiens]	Heat shock protein activity	Protein metabolism	Cytoplasm
vimentin variant 3 [Homo sapiens]	Structural constituent of cytoskeleton	Cell growth and/or maintenance	Intermediate filament
Pyruvate kinase, muscle [Homo sapiens]	Kinase activity	Metabolism, Energy pathways	Cytoplasm
vimentin variant 3 [Homo sapiens]	Structural constituent of cytoskeleton	Cell growth and/or maintenance	Intermediate filament
heat shock 70kDa protein 8 isoform 2 [Homo sapiens]	Heat shock protein activity	Protein metabolism	Cytoplasm, Nucleolus
Chain A, Crystal Structure of Aldose Reductasecomplexed with Dichlorophenylacetic Acid	Oxidoreductase activity	Metabolism, Energy pathway	Cytoplasm
annexin I [Homo sapiens]	Calcium ion binding	Cell communication, Signal transduction	Plasma membrane
glyceraldehyde-3-phosphate dehydrogenase [Homo sapiens]	Catalytic activity	Metabolism, Energy pathway	Cytoplasm

Table 4.6 (contd)

ubiquitin carboxyl-terminal esterase L1 (ubiquitin thiolesterase), isoform CRA_c [Homo sapiens]	Ubiquitin specific protease activity	Protein metabolism	-
heat shock protein 27 [Homo sapiens]	Chaperone activity	Protein metabolism	Cytoplasm
heat shock protein 27 [Homo sapiens]	Chaperone activity	Protein metabolism	Cytoplasm
actin related protein 2/3 complex subunit 2 [Homo sapiens]	Cytoskeletal protein binding	Cytoskeleton organization and biogenesis	Actin cytoskeleton
heat shock 70kDa protein 8 isoform 2 variant [Homo sapiens]	Heat shock protein activity	Protein metabolism	Cytoplasm, Nucleolus

Table 4.6 (cont)

Proteins downregulated by inhibition of Hsp90 by 17AAG and shRNA targeted towards *hsp90α*

X-ray repair complementing defective repair in Chinese hamster cells 6 (Ku autoantigen, 70kDa) [Homo sapiens]	DNA binding	Regulation of nucleobase, nucleoside, nucleotide and nucleic acid metabolism, DNA repair.	Nucleus
vimentin [Homo sapiens]	Structural constituent of cytoskeleton	Cell growth and/or maintenance	Intermediate filament
vimentin [Homo sapiens]	Structural constituent of cytoskeleton	Cell growth and/or maintenance	Intermediate filament
SERPINE1 mRNA binding protein 1 isoform 1	RNA binding	Regulation of nucleobase, nucleoside, nucleotide and nucleic acid metabolism.	Cytoplasm
calumenin isoform a precursor [Homo sapiens]	Calcium ion binding	Cell communication, Signal transduction	Endoplasmic reticulum
phosphoglycerate kinase 1 [Homo sapiens]	Catalytic activity	Metabolism, Energy pathways	Cytoplasm
aldolase A, fructose-bisphosphate, isoform CRA_b	Lyase activity	Metabolism, Energy pathways	Cytoplasm
PREDICTED: glyceraldehyde-3-phosphate dehydrogenase-like 6 [Homo sapiens]	Catalytic activity	Metabolism, Energy pathways	Cytoplasm
tropomyosin 4-anaplastic lymphoma kinase fusion protein [Homo sapiens]	Structural constituent of cytoskeleton	Cell communication, Signal transduction	Cytoskeleton
eukaryotic translation initiation factor 3, subunit 12	Translation regulator activity	Protein metabolism	Cytoplasm
transgelin 2 [Homo sapiens]	Unknown	Unknown	Unknown
Chain A, Cyclophilin B complexed with [d-(Cholinylester)ser8]-Cyclosporin	Unknown	Unknown	Unknown

Proteins differentially expressed by inhibition of Hsp90 by 17AAG and shRNA targeted towards *hsp90α*			
collagen, type VI, alpha 1 precursor [Homo sapiens]	Extracellular matrix structural constituent	Cell growth and/or maintenance	Extracellular
Chain A, Structure of human Annexin A2 in the presence Of Calcium ions	Calcium ion binding	Signal transduction, Cell communication	Nucleus
heat shock protein beta-1 [Homo sapiens]	Chaperone activity	Protein metabolism	Cytoplasm
Chain A, Human Manganese Superoxide Dismutase Mutant Q143n	Superoxide dismutase activity	Cell proliferation, Anti-apoptosis, Cell growth and/or maintenance	Mitochondrion
Chain A, Crystal structure of Ca2+-bound form of Des3-23alg-2	Unknown	Apoptosis	Cytoplasm
transgelin 2 [Homo sapiens]	Unknown	Unknown	Unknown

- Three of the proteins identified were unknown protein products and hence have been excluded from the table.

4.4.8 Bioinformatic analysis:

IPA knowledge-based software was used to identify molecular functions with pathways correlating proteins identified by mass spectrophotometry post Hsp90 inhibition. The programme correlated the proteins (Table 4.6) with each other based on their interaction and function. In IPA, the biofunctions are categorized according to: A) Diseases and disorder B) Molecular and cellular function C) Physiological system development and functions while canonical pathways are grouped into metabolic and signalling pathways.

Significant functional pathways and networks were identified from the IPA library of canonical pathways based on two parameters taken into consideration i.e. A) ratio of the number of proteins mapping to the pathway the total number of proteins that map to the canonical pathway and B) Fisher's exact test was used to calculate the p-value which determined the probability of association of proteins between the dataset and the canonical pathways by chance alone.

The networks generated were ranked on the basis of a score based on the negative log of p-value. The top four networks are shown in Figure 4.12.

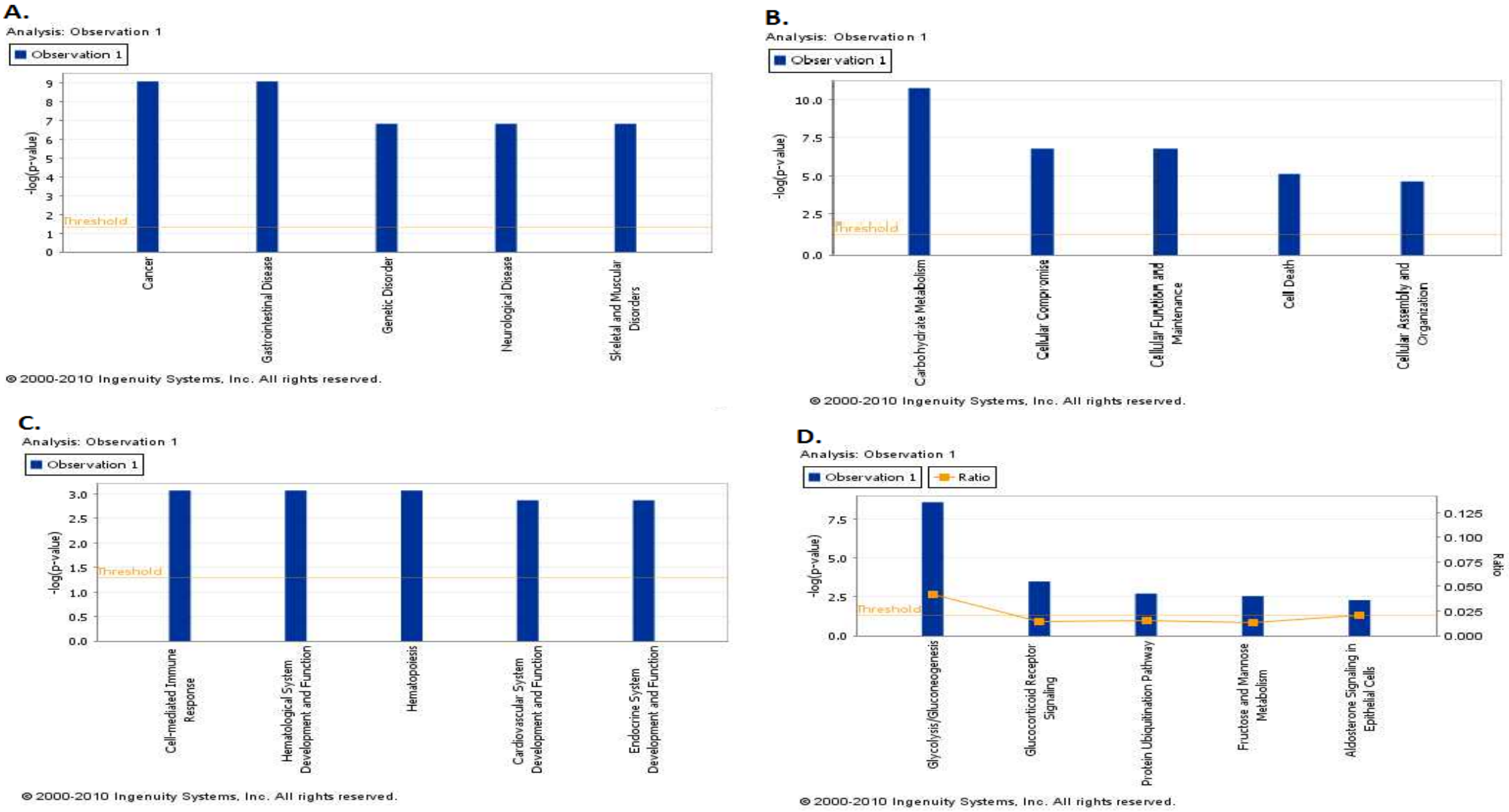

Figure 4.12: Functional-network-analysis-by-IPA. Top 4 A) Diseases and disorders; B) Molecular and cellular functions and C) Physiological System Development and Function and D) Pathways selected from a total of 96 canonical pathways relevant to the dataset defined by Ingenuity Pathway Analysis program.

The networks were ranked on a score based on the negative log of p-value computed using a right tailed Fisher's exact test (Table 4.8).

Table 4.8: Top biofunctions generated by IPA.

The values are calculated using right tailed Fisher's exact test based on the negative log of p-value.

Top Biofunctions		
Diseases and Disorders		**p-value**
1	Cancer	1.14×10^{-9} - 4.21×10^{-2}
2	Gastrointestinal disease	1.14×10^{-9} - 2.08×10^{-2}
3	Genetic disorder	9.53×10^{-8} - 4.21×10^{-2}
4	Neurological disease	9.53×10^{-8} - 4.86×10^{-2}
5	Skeletal and muscular disorders	9.53×10^{-8} - 1.62×10^{-2}
Molecular and Cellular Functions		
1	Carbohydrate Metabolism	1.88×10^{-11} - 3.61×10^{-2}
2	Cellular Compromise	1.98×10^{-7} - 3.21×10^{-2}
3	Cellular Function and Maintenance	1.98×10^{-7} - 4.65×10^{-2}
4	Cell Death	7.51×10^{-6} - 4.00×10^{-2}
5	Cellular Assembly and Organization	2.38×10^{-5} - 4.26×10^{-2}
Physiological System Development and Function		
1	Cell-mediated Immune Response	8.44×10^{-4} - 1.35×10^{-2}
2	Hematological System Development and Function	8.44×10^{-4} - 4.65×10^{-2}
3	Hematopoiesis	8.44×10^{-4} - 4.13×10^{-2}
4	Cardiovascular System Development and Function	1.36×10^{-3} - 2.15×10^{-2}
5	Endocrine System Development and Function	1.36×10^{-3} - 1.48×10^{-2}
Top Cannonical Pathways		
1	Glycolysis/Glucogenesis	2.68×10^{-9}
2	Glucocorticoid Receptor Signaling	3.23×10^{-4}
3	Protein Ubiquitination Pathway	1.99×10^{-3}
4	Fructose and Mannose Metabolism	2.86×10^{-3}
5	Aldosterone Signaling in Epithelial Cells	4.95×10^{-3}

IPA analysis did not generate any pathways from amongst the proteins identified and this could have been attributed to the small number of proteins deteced by mass spectrophotometry.

4.5 DISCUSSION:

Hsp90 is upregulated in several human cancers and targeting its function could be of therapeutic importance (Altieri, 2004). Recent studies have shown the presence of Hsp90 activity in glioma cell lines and tissues but not in normal brain cell lines or tissues (Shervington *et al*., 2008; Siegelin *et al*., 2009). Hsp90 inhibitors exhibit anti-tumour activity by binding to Hsp90 and inducing proteosomal degradation of Hsp90 (Schulte *et al*., 1997; An *et al*., 2000; Whitesell *et al*., 1994; Miller *et al*., 1994; Mimnaugh *et al*., 1996; Schulte *et al*., 1995). 17AAG, a benzoquinone antibiotic derived from GA is a potent Hsp90 inhibitor and has been reported to inhibit tumour growth in tumour cell line and it is presently being examined in pre-clinical trials (Burger *et al*., 2004; Bagatell *et al*., 2001; Nguyen *et al*., 2001; Nimmanapalli *et al*., 2001; Yang *et al*., 2001; Braga-Basaria *et al*., 2004; Bisht *et al*., 2003; Munster *et al*., 2002; Hostein *et al*., 2001; Solit *et al*., 2002).

Varying concentrations of 17AAG (0.25 – 1.5 µM) were added to U87-MG cells. The cells were incubated for 48 hours before the viability of the drug was assessed. It was noted that 0.25 µM of 17AAG killed nearly half of the cells (IC_{50}) post 48 hours. Consistent to these findings, Sauvageot *et al.,* (2009) inhibited Hsp90 in several glioma cell lines and reported the IC_{50} of 17AAG to lie between 0.05 – 0.5 µM concentrations. In another study the IC_{50} of 17AAG was reported to be approximately 10 µM in U87-MG glioma cell line (Siegelin *et al*., 2009).The variation in the levels of 17AAG could have been attributed to the difference in cell line growth conditions, passage number of the cell lines and also differing experimental conditions.

Cohorts of U87-MG cells were treated with either 17AAG or shRNA to target *hsp90α*. The efficacy of Hsp90 inhibition was analysed by measuring the protein levels of Hsp90α in control and treated cells by FACS analysis (quantitative) using a flow cytometer. The Akt/PKB kinase activity levels were also measured using the Akt/PKB Kinase Activity Assay kit (Assay Designs, UK) and Hsp90α levels were also quantified in control and treated cells using Hsp90α ELISA kit (Assay Designs, UK).

In the post treatment, the level of Akt/PKb, a client protein for Hsp90 (Basso *et al*., 2002) was assayed using commercially available Akt/PKB kinase activity assay kit (Assay Designs, UK) in U87-MG cells. The Akt/PKB kinase activity was significantly reduced (**$p < 0.001$) by 81 and 59.4 %, post 17AAG and sh*hsp90α* treatment, respectively in U87-MG glioma cells, suggesting that Hsp90 inhibition could be of therapeutic significance. The reduction of Akt/PKB kinase protein was in agreement with previous studies which reported a dose dependent decrease in Hsp90 client proteins, namely Akt post exposure to 17AAG in murine neural stem cells and glioma stem cells (Sauvageot *et al*., 2008). Furthermore, Hsp90α ELISA assay using commercially available Hsp90α ELISA kit (Assay Designs, UK) showed that Hsp90α protein levels were reduced significantly by approximately 65 % and 45 %, post treatment with 17AAG and sh*hsp90α*, respectively, in U87-MG cells. Moreover, flow cytometric analysis showed a reduction in Hsp90α protein levels by approximately 44 % and 16% post 17AAG and sh*hsp90α* treatment respectively (**$p < 0.001$). This variation between the two results could be due to flow cytometry not being able to distinguish between active and inactive protein i.e. dying or apoptotic cells can influence the results (Nusse and Marx, 1997). Thus, it can be suggested that in post

Hsp90 inhibition, most of the treated cells could be apoptotic and hence, a false negative result could be obtained.

Cell cycle analysis was carried out to compare control cells (wild type U87-MG) and treated cells (U87-MG-sh*hsp90α* and U87-MG-17AAG) based on the cohort of cells found at different stages of cell cycle. The S phase arrest and the G2 phase arrest was observed post Hsp90 inhibition in treated cells compared to control cells, suggesting that Hsp90 inhibition affects DNA replication and cell growth which is of therapeutic importance while treating tumours such as glioma. 17AAG inhibits the Chk1, a protein kinase essential for G2/M cell cycle checkpoint (Tse and Schwartz, 2004). HCT116 colon cancer cells were treated with 0.5 µM 17AAG and it was observed that treatment with 17AAG resulted in a time and dose dependent depletion of Chk1, suggesting a G2/M cell cycle phase arrest (Tse and Schwartz, 2004). Statistical analysis showed a significant decrease ($*p < 0.05$) in G1 and S phase of U87-MG cell cycle upon treatment with 17AAG while a significant decrease ($*p < 0.05$) was observed in G2 phase of U87-MG cell cycle upon treatment with sh*hsp90α*.

Treatment with either 17AAG or shRNA targeting *hsp90α*, effectively reduced Hsp90α activity and subsequently reduced the Akt/PKB kinase activity along with the S and G2 phase arrest in the U87-MG glioma cell line. These results suggest that inhibition of Hsp90 activity could be used for GBM therapy.

Based on these reports and also the laboratory findings, the inhibition of Hsp90 protein is a more effective therapeutic approach than silencing *hsp90* i.e. though shRNA targeting *hsp90α* did silence Hsp90, 17AAG showed a better silencing profile.

Inhibition of Hsp90 as discussed above is of therapeutic importance in glioma therapy. However, to understand the mechanisms involved or to characterize the changes caused at the cellular protein levels by inhibition of Hsp90 a differential proteomic analysis comparing control cells (wild type U87-MG) and treated cells (U87-MG-sh*hsp90α* and U87-MG-17AAG) was performed. The 2D-DIGE technique was carried out to separate the proteins while MALDI-TOF was used for protein identification. Based on a 2 fold cut off, the analysis identified 36 proteins while MALDI-TOF analysis identified 33 proteins with altered expressions showing >99 % confidence levels (3 protein being listed as unknown proteins).

IPA analysis identified dynamically regulated biological networks and canonical pathways correlating cellular response to Hsp90 inhibition. The top network significantly transformed upon Hsp90 inhibition was identified as “cancer”. The top diseases and disorders modulated upon Hsp90 inhibition were cancer, gastrointestinal disease, genetic disorder, neurological disease and skeletal and muscular disorders. This confirmed that altering Hsp90 levels significantly alters the cancer proteome including neurological and genetic disorders. The IPA analysis also showed that by inhibiting Hsp90 molecular and cellular functions such as; carbohydrate metabolism, cellular compromise, cellular function and maintenance, cell death and cellular assembly and organization, are affected. The IPA library of canonical pathways indicated that most of the proteins altered upon Hsp90 inhibition are involved in glycolysis/glucogenesis pathways. These results highlight the downstream effects of Hsp90 in different molecular and cellular functions besides its normal role as a chaperone.

Proteins upregulated by Hsp90 inhibition

Previous studies have reported that inhibition of Hsp90 alters the multi-chaperone complexes associated with heat shock factor 1 (HSF-1) (Luo *et al*., 2010). HSF-1 is a transcription factor regulating the stress response and it is stimulated upon Hsp90 inhibition (Zou *et al*., 1998). Subsequently, stimulation of HSF-1 leads to induction of heat shock response which in turn provides protection to the non-transformed cells from the toxicity of Hsp90 inhibitors, whereas the tumour cells are particularly sensitive to Hsp90 inhibition (Voellmy and Boellmann, 2007; Ali *et al*., 1998). Induction of Hsp72 and Hsp27 act as molecular signatures proving Hsp90 inhibition (McCollum *et al*., 2006). Thus, it could be postulated that several co-chaperones of Hsp90 such as Hsp72 (Hsc70) and Hsp27 would be upregulated along with other client proteins upon Hsp90 inhibition.

Inhibition of Hsp90 by either 17AAG or shRNA to target *hsp90α* in this study resulted in the upregulation of several proteins such as Hsp70 isoform 1, hexokinase 1 isoform CRA_d, tumour rejection antigen (gp96) 1 variant, vimentin variant 3, pyruvate kinase, vimentin, Hsp70 protein 8 isoform 2, aldose reductase complexed with dicholorophenyacetic acid, annexin 1, GAPDH, ubiquitin thiolesterase isoform CRA_d, Hsp27 and actin related protein 2/3 complex subunit 2. The proteins in questiion are involved in protein metabolism, energy pathways, cell growth and/or maintenance, metabolism, cell communication, signal transduction and cytoskeleton organization and biogenesis.

Hsp70 and Hsc70 (Hsp70 protein 8 isoform 2 variant) represent the inducible and constitutively expressed isoforms of Hsp70 family, respectively. Members of the Hsp70 family were found to be upregulated post Hsp90 inhibition. Additionally, Hsp90

inhibition by 17AAG induced Hsp70 family members to a greater extent than that seen with Hsp90 inhibition with sh*hsp90α*. Previous studies have shown a relation between Hsp90 and Hsp70, wherein Hsp70 acts as a co-chaperone to Hsp90 for recruiting substrates (Wegele *et al*., 2004). Hsp70 is the most predominant and conserved class of the Hsps (Oehler *et al*., 2000) and it functions as an anti-apoptotic protein (Kang *et al*., 2009; Lanneau *et al*., 2007). Hsp70 is involved in folding and refolding of newly synthesized or misfolded proteins (Kang *et al*., 2009; Lanneau *et al*., 2007; Beckmann *et al*., 1990; Seidberg *et al*., 2003; Mayer and Bukau, 2005). Similar to Hsp90, Hsp70 has two domains namely an N terminal ATPase domain and a C terminal domain chaperoning denatured proteins and peptides. Both the domains play a vital role in tumour immunity by preventing apoptosis and regulating the generation of stable complexes with cytoplasmic tumour antigens bestowing anti-tumour immunity (Calderwood *et al*., 2005; Schmitt *et al*., 2007). Under normal conditions, Hsp70 functions as a molecular chaperone whereas in tumours including glioma, it is over expressed and is associated with cell proliferation, metastasis, invasion and cell death (Nylandsted *et al*., 2000). The over expression of Hsp70 has been associated with poor prognosis and reduced response to tumour therapeutics (Calderwood *et al*., 2006). Members of the Hsp70 family act at multiple points in the apoptotic pathway and inhibit cell death (Mosser and Morimoto, 2004; Calderwood *et al*., 2006; Garrido *et al*., 2006). Following Hsp90 inhibition, the glioma cells undergo apoptosis, and as a survival mechanism induced Hsp70 family members. Supporting the findings, previous studies of the Hsp70 isoforms (Hsp70 and Hsc70) reported increases in their expression post exposure to Hsp90 inhibitors in colon and ovarian cancer cell lines (Clarke *et al*., 2000;

Maloney *et al*., 2007). Thus, it could be further postulated that inhibition of the Hsp70 family members could inhibit Hsp90 chaperone function in glioma.

Another member of the chaperone family, Hsp27 was also induced post Hsp90 inhibition. Hsp27 is a molecular chaperone and it plays a role in protein metabolism, cytoskeletal reorganization and apoptosis-inhibition (Huot *et al*., 1997; Concannon *et al.,* 2003; Nakagomi *et al*., 2003; Arrigo *et al.,* 2005). Hsp27 has been involved in the regulation of cell death by interacting with cytochrome c (Bruey *et al*., 2000) and it can also activate protein kinase B and Akt to inhibit cell death by phosphorylating procaspase-9 (Mehlen *et al*., 1996). Hsp27 is over expressed in ovarian, gastric, liver and prostate tumours (Cardone *et al*., 1995; Harrison *et al*., 1991; King *et al*., 2000; Cornford *et al*., 2000) and has been down regulated in human glioma tissues (Shen *et al*., 2010). Proteomic analysis revealed that Hsp27 was induced post Hsp90 inhibition in glioma and this could possibly be to increase the survival ability of glioma cells. Previous studies supported this finding and reported the induction of Hsp27 post Hsp90 inhibition (Shen *et al*., 2010).

Hsp90 beta member 1 referred to as tumour rejection antigen 1 and gp96 is a molecular chaperone. It is involved in protein folding and also been implicated as an essential immune chaperone regulating both innate and adaptive immunity (Schild and Rammensee, 2000). The gp96 is to be highly expressed in several tumours such as lung, adenocarcinoma and esophageal squamous cell carcinoma (Wang *et al*., 2010). Its expression is abundant in the glial cells (Graham *et al*., 2009). Though its expression in glioma is not yet known, studies have shown that vitespen, a gp96 peptide complex purified from resected tumours is being used in Phase I and II clinical trials to capture the antigenic fingerprint of a specific tumour and is also used as a patient specific

vaccine for the treatment of several tumours including GBM (Wood and Mulders, 2009). It is unclear as to why inhibition of Hsp90 leads to both induction and differential expression of gp96. A possible reason for the upregulation of gp96 post Hsp90 inhibition could be to confer tumour immunity to the glioma cells so as to evade apoptosis. However, further studies need to be carried out to address this issue.

As observed from IPA analysis that the top canonical pathway upon Hsp90 inhibition was glycolysis/glucogenesis, several key enzymes of the pathway namely, hexokinase 1, GAPDH and pyruvate kinase were reportedly upregulated upon Hsp90 inhibition. Hexokinase is an enzyme which phosphorylates glucose to glucose-6-phosphate in the glycolysis pathway while pyruvate kinase is an enzyme which catalyzes the transfer of a phosphate group from phosphoenolpyruvate (PEP) to ADP forming ATP molecules. GAPDH is an enzyme which breaks down glucose to give energy and carbon molecules. The expression of Hexokinase 1 is lower in gliomas (Oudard *et al*., 1996). The pyruvate kinase expression is correlated with the grade of gliomas (van Veelen *et al*., 1998). Interestingly, the protein expression of *GAPDH* which is a house keeping gene whose expression is constitutive in glioma is induced upon Hsp90 silencing. This contradicts the gene expression profile of *GAPDH* post Hsp90 inhibition. A possible reason could be attributed to the fact that gene expression does not necessarily correlates to the protein expression. Moreover, increased levels of proteins involved in glycolysis post Hsp90 inhibition suggests an increased dependency on glycolysis for energy supply by the treated glioma cells. This phenomenon is called the Warburgs effect and it is an important concept during malignant transformation (Warburg, 1956).

Increased dependency on glycolysis and induction of Hsp70 isoforms post Hsp90 inhibition suggests that targeting Hsp90 is sub-lethal and a multi-target approach should be considered for future glioma therapy.

Vimentin is a major intermediate filament cytoskeletal protein and is involved in maintaining structural constituency of the cytoskeleton (Katsumoto *et al*., 1990). It plays a role in cell motility and movement, responding to mechanical stress, stabilizes cytoskeletal interactions and maintains the integrity of the cytoplasm (Thoumine *et al*., 1995). It is associated with mechanosensitive signalling, apoptosis, regulating genomic DNA and providing immunity (Wang *et al*., 1993; Ingber, 2003). Vimentin has several isoforms and it can be present either in phosphorylated or non-phosphorylated form (Ando *et al*., 1989; Chou *et al*., 1991; Huang *et al*., 1994).

Vimentin is involved in tumour development and progression (Ngan *et al*., 2007; Zajchowski *et al*., 2001; Penuelas *et al*., 2005). Studies have suggested phosphorylated vimentin to be an indicator of non-aggressiveness and/or non-invasiveness in certain tumours (Shirahata *et al*., 2009). Vimentin is found in the extracellular matrix component and is involved in neo-vascularisation and invasion of malignant glioma cells (Zhang *et al*., 2006). Four spots were identified by MALDI-TOF as vimentin protein products post Hsp90 inhibition. Two upregulated spots identified were vimentin variant 3, while two downregulated spots were identified as vimentin. Studies have reported vimentin as a novel client protein for Hsp90α with Hsp90α-vimentin binding inhibition resulting in an increase in apoptosis induced stimulus making cells more chemosensitive (Trog *et al*., 2006). Thus, the downregulation of vimentin protein could be attributed to Hsp90 inhibition. A possible reason in the upregulation status of vimentin variant 3 could be that post Hsp90 inhibition vimentin variant 3 is

upregulated to compensate for the downregulation of vimentin as a cell survival mechanism.

Aldose reductase is an oxidoredutase catalyzing the reduction of several aldehydes and carbonyls. It primarily catalyzes the reduction of glucose to sorbitol, the first step in polyol pathway of glucose metabolism (Petrash, 2004). The expression of the aldose reductase gene has been reported in several tumours such as liver, breast, cervix and rectal and even gliomas (Saraswat *et al*., 2006; Dan *et al*., 2003). It has been reported that, in hepatocarcinoma induction of aldose reductase gene expression renders tumour cells resistant to toxic compounds produced during metabolism or when administered as drugs (Takahashi *et al*., 1996). Thus, it can be suggested that induction of aldose reductase is associated with drug resistance in tumours. Proteomic analysis revealed aldose reductase complexed with dicholorophenylacetic acid suggesting a post-translational modification. The compound was reported to be upregulated post Hsp90 inhibition, suggesting that inhibition of Hsp90 could possibly induce aldose reductase expression conferring drug resistance to the glioma cell line.

Annexin 1 is a class of proteins involved in cell communication and signal transduction, and is involved in several physiological pathways such as cell growth, membrane trafficking, phagocytosis, chaperone activity, tumour suppression, apoptosis differentiation, proliferation and inflammation (Lim and Parvaiz, 2007). Annexin 1 shows differential expression in tumours with it being downregulated in certain tumours such as prostrate and oesophageal, whereas, it is upregulated in other tumours such as neck, head and breast tumours (Lim and Parvaiz, 2007). The over expression of annexin 1 was found in gliomas with primary glioblastomas having a higher expression of annexin 1 compared to secondary glioblastomas (Schittenhelm *et*

al., 2009). In post Hsp90 inhibition, an increased expression of annexin 1 was observed and this could possibly be explained by the antiproliferative and/or proapoptotic function of annexin 1. The induction in annexin 1 expression on Hsp90 inhibition could possibly be adapted by the U87-MG glioma cells for their survival.

UCHL1 encodes for ubiquitin carboxyl-terminal esterase L1 (UCHL1) which is also commonly referred to as ubiquitin thiolesterase. UCHL1 is reported to be involved in ubiquitin specific protease activity (http://ghr.nlm.nih.gov/gene/UCHL1). Damaged or unwanted proteins are tagged with ubiquitin molecules which further move these proteins into proteosomes where the proteins are degraded. The ubiquitin-proteasome pathway thus acts as the cells quality control system (http://ghr.nlm.nih.gov/gene/UCHL1). UCHL1 is predominantly present in neurons and associated tumours (Doran *et al*., 1983). It has been reported that UCHL1 interacts with Hsp90 causing an increase in α-synuclein and GAPDH (Kabuta *et al*., 2008).

Considering glioma UCHL1 expression is inversely proportional to the grades of glioma (Park *et al*., 2009). The present results show that in U87-MG cells, a decrease in Hsp90 activity was associated with an increase in UCHL1 levels. A possible explanation for this reciprocal change could be the involvement of UCHL1 in ubiquitin specific protease activity.

ARPC2 encodes for actin related protein 2/3 complex subunit 2 (Arp2/3). Arp2/3 protein complex regulates actin polymerization in cells (http://www.ncbi.nlm.nih.gov/gene/10109). Arp2/3 has been over expressed in certain tumours such as leukaemia (Ross *et al*., 2003; Yeoh *et al*., 2002). Its role in glioma or with Hsp90 is unclear although a study has reported that Arp2/3 is downregulated in glioma cell lines post treatment with chemotherapeutic drug, BCNU

(1,3-bis (2-chloroethyl)-1-nitrosoure) (Bandres *et al*., 2005). It is unclear as to why Hsp90 inhibition would result in the down regulation of a protein with such properties and further investigations are necessary to address this phenomenon.

Considering the types of proteins found to be upregulated post Hsp90 inhibition it could be postulated that, Hsp90 inhibition is sub-lethal and there is a need for a multi-target approach in glioma therapy. Furthermore, as discussed earlier, it can be seen that 17AAG inhibits Hsp90 better than shRNA targeting *hsp90α*. A significant difference between the increased fold observed in some of the key proteins namely; Hsp70-1, Hsc70, hexokinase 1, pyruvate kinase, GAPDH and annexin 1 was observed. The increased changes observed post 17AAG treatment could possibly be attributed towards a more profound Hsp90 inhibition attained with 17AAG than shRNA targeting *hsp90α*.

Proteins downregulated by Hsp90 inhibition

A vast number of proteins involved in cell signalling, apoptosis and cell survival are chaperoned by Hsp90. Thus, it could be postulated that, a wide range of proteins involved in cell cycle, apoptosis, signal transduction and other metabolic pathways could be downregulated post Hsp90 inhibition. Proteomic studies have reported that inhibition of Hsp90 activity leads to a downregulation of several proteins such as Ku autoantigen, vimentin, serpine1 mRNA binding protein 1, calumenin, phosphoglycerate kinase, aldolase A, tropomyosin 4-anaplastic lymphoma kinase fusion protein, eukaryotic translation initiation factor 3, transgelin 2, cyclophilins B complexed with [d-(cholinyester)ser8]-cyclosporin. Another protein detected was predicted to be GAPDH.

X-ray repair complementing defective repair in Chinese hamster cells 6 also referred as Ku70 is an autoantigen. The Ku protein is a heterodimer of Ku70 and Ku86 proteins. It binds to double stranded DNA and is involved in nucleic acid metabolism (Rathmell and Chu, 1994). The Ku70 protein is involved in DNA recombination and DNA repair pathways. It has been found to be associated with a DNA dependent protein kinase and could possibly initiate a signalling pathway for a cell cycle arrest upon DNA damage (Rathmell and Chu, 1994). Additionally, the Ku protein has also been reported to play a vital role in apoptosis and telomere fusion (Ayene *et al*., 2005). The Ku70 protein is over expressed in several tumours such as colon, breast, skin, renal cell carcinoma and glioma (Wang *et al*., 2009; Pucci *et al*., 2004; Parrella *et al*., 2006). The expression of the Ku70 protein has been linked to tumour progression and tumour proliferation rate (Pucci *et al*., 2004; Parrella *et al*., 2006). Ku70 was inhibited in human cervical epithelioid (HeLa) and colon cancer cells (HCT116) and its inhibition lead to sensitization towards radiation in HeLa and HCT116 cells by several folds and to decrease in tumour cell survival (Ayene *et al*., 2005). No direct relation between Ku70 protein and Hsp90 has yet been made, however, this studies illustrates that Hsp90 inhibition leads to downregulation of Ku70 protein. This downregulation of Ku70 could be of possible therapeutic importance in glioma therapy.

SERPINE1 codes for SERPINE1 which is a member of serine proteinase inhibitor (serpin) superfamily. It acts as an inhibitor to fibrinolysis and acts by inhibiting tissue plasminogen activator (tPA) and urinary plasminogen activator (uPA)

(http://www.ncbi.nlm.nih.gov/sites/entrez?db=gene&cmd=Retrieve&dopt=full_report&list_uids=5054). Previous studies have shown that a high level of SERPINE1 is

correlated with poor prognosis in several tumours. Although it has been reported that SERPINE1 is over expressed in tumours the rationale behind the altered levels of SERPINE1 expression in tumours is still unknown (Gao *et al*., 2010). In glioma, SERPINE1 has been reported to play a role in regulating glioma cell motility and invasion (Martin *et al*., 2009). Currently, the link between Hsp90 and SERPINE1 is has not been found; however, post Hsp90 inhibition in U87-MG glioma cell line it was observed that SERPINE1 protein is downregulated. This could be of therapeutic importance in glioma therapy as SERPINE1 downregulation possibly suggests inhibition of glioma cell motility and invasion. Though the mechanism is unclear, it would be interesting to further investigate the potential of SERPINE1 inhibition in glioma therapy.

Calumenin is a calcium binding protein localized in the endoplasmic reticulum (ER). It is reported to be differentially expressed in cardiomyopathy; cell induced apoptosis and in squamous tumour cells (Cho *et al*., 2009). Though it has been implicated in several diseases, the *in vivo* functions of calumenin are largely unknown (Cho *et al*., 2009). Additionally, calumenin is highly expressed in neoplastic cells which have developed resistance to chemotherapeutic drugs. Research is presently focussed on utilizing calumenin as a diagnostic and therapeutic tool in the treatment of tumours (Georges and Prinos, 2007). Moreover, it has been reported that calumenin is downregulated in invasive glioma cells compared to stationary glioma cells (Holtkamp *et al*., 2005). Thus, in the U87-MG glioma cell line, the expression of calumenin should be downregulated when compared to the stationary glioma cell line. In post Hsp90 inhibition in U87-MG glioma cell line, it was reported that calumenin levels decreased with treatment. Owing to the ambiguity in calumenin functions, it would be difficult to suggest the

implications of these findings and further work should be undertaken to clarify the role of calumenin.

Phosphoglycerate kinase (PGK1) is a glycolytic enzyme that catalyses the formation of ATP from ADP and vice versa (http://www.ncbi.nlm.nih.gov/gene/5230). A study in ovarian cancer cells demonstrated that PGK1 can induce multidrug resistance through p- glycoprotein (MDR-1) independent mechanism (Duan *et al*., 2002). Another study involving gastric cancer illustrated that PGK1 could be used as a prognostic marker and/or could possibly be a potential therapeutic target by preventing dissemination of gastric carcinoma cells into the peritoneum (Zieker *et al*., 2010). PGK1 is over expressed in both high and low grade astrocytomas (Kreth *et al*., 2010; Khatua *et al*., 2003). This study has demonstrated that post Hsp90 inhibition U87-MG glioma cells exhibit low levels of PGK1. Thus, U87-MG glioma cells could possibly be prone to chemotherapeutics upon PGK1 downregulation, therefore being of therapeutic importance in glioma therapy.

Proteomic analysis on U87-MG glioma cell line exhibited downregulation of aldolase A post Hsp90 inhibition. Aldolase A also referred to as fructose-bisphosphate aldolase is a glycolytic enzyme catalyzing fructose 1,6-diphosphate to glyceraldehyde-3-phosphate and dihydroxyacetone phosphate. Aldolase A physically interacts with tubulin and actin filaments contributing towards regulation of cytoskeletal structures and cell mobility. Furthermore, it can modulate transcriptional activity by interacting with the DNA sequence (Hua *et al*., 2000). Aldolase C is a more potential biomarker than aldolase A for not just cerebrovascular diseases but also glia cells and their differentiation (Asaka *et al*., 1990; Sato *et al*., 1972). Aldolase A is also a useful

biomarker for renal cell carcinoma (Takashi *et al*., 1992). Considering the role of aldolase A in glioma and Hsp90, no specific correlation has yet been reported.

Anaplastic lymphoma kinase (ALK) fused with tropomyosin 4 (TPM4) results in the formation of TPM4-ALK fusion protein. The homodimerization through the TPM coiled-coil domain with ALK leads to the autophosphorylation and activation of ALK (Chiarle *et al*., 2008). Such fusion has been previously reported to occur in anaplastic large cell lymphoma, inflammatory myofibroblastic tumours and oesophageal squamous cell carcinomas (Chiarle *et al*., 2008). ALK has been reported to be overexpressed in gliomas and its downregulation prevents anti-apoptotic signalling and reduced tumour growth (Chiarle *et al*., 2008). This study, thereby for the first time, demonstrates the downregulation of TPM4-ALK fusion protein post Hsp90 inhibition in glioma which could hold therapeutic significance. However, a more mechanistic insight is required to gain a complete understanding of the effect of TPM4-ALK downregulation post Hsp90 inhibition for glioma studies.

During post Hsp90 inhibition, the protein level of eukaryotic translation initiation factor 3 subunit 12 is downregulated in the U87-MG glioma cell line. Eukaryotic translation initiation factor 3 subunit 12 also known as eukaryotic translation initiation factor 3 subunit K (eIF3K) is a component of eukaryotic translation initiation factor 3 (eIF3) complex which plays a role in the initiation of protein synthesis (http://www.uniprot.org/uniprot/Q9UBQ5). A study of simple epithelial cell demonstrated apoptosis promoting function of the eIF3K complex by reducing the caspase sequestration effect of kertains 8 and 18 (K8/K18), thereby increasing the bio availability of caspases to non-keratin residing substrates (Lin *et al*., 2008). However, no direct link between eIF3K and gliomas has yet been reported.

Transgelin 2 is a homologue to the protein transgelin which is a marker for smooth muscle differentiation. The precise function of this protein is yet to be determined (http://www.ncbi.nlm.nih.gov/sites/entrez?db=protein&cmd=Link&LinkName=protein_gene&from_uid=4507357). Transgelin 2 is frequently observed in tumour cells, precancerous lesions and hepatatic metastases while its expression in normal epithelia is rarely observed. A study in colorectal cancer displayed transgelin 2 to be over expressed and the over expression was associated with lymph node metastasis. Thereby, transgelin 2 can be a potential biomarker for the prognosis and to predict progression of colorectal cancer (Zhang *et al*., 2010). Transgelin 2 is reportedly upregulated in gliomas (Mehrian *et al*., 2005; Shirahata *et al*., 2007), subsequently, post Hsp90 inhibition transgelin 2 was downregulated post Hsp90 silencing using shRNA targeting *hsp90α* and was differentially expressed post Hsp90 inhibition using 17AAG in U87-MG glioma cell line. This study for the first time demonstrates a link between Hsp90 and transgelin 2. It is unclear as to why a differential expression was observed in trangelin 2 protein levels, post Hsp90 inhibition and it would be interesting to study the interaction between Hsp90α and transgelin 2 in order to achieve a better understanding of glioma therapy.

Another protein downregulated post Hsp90 inhibition in U87-MG glioma cell line was identified as chain A, cyclophilins B complexed with[d-(cholinylester)ser8]-cyclosporin. Proteomic studies in head and neck cancer (HNC) identified chain A, cyclophilins B complexed with [d-(cholinylester) ser8]-cyclosporin to be potentially involved in radioresistance phenotype (Lin *et al*., 2010).

The inhibition of Hsp90 by either 17AAG or shRNA to target *hsp90α* in U87-MG glioma cell line resulted in subsequent downregulation of several proteins such as Ku70,

SERPINE 1 and PGK 1 which could possibly be of therapeutic importance in glioma therapy. Moreover, considering the difference in the changes between proteins downregulated by 17AAG and shRNA targeting *hsp90α*, it could be postulated that Hsp90 inhibition with 17AAG is more effective. Furthermore, an understanding of the interactions between Hsp90 and other downregulated proteins such as transgelin, calumenin, aldolase A, TPM4-ALK and eIF3K would be interesting and it would certainly clarify the working of the Hsp90 chaperoning system in glioma studies.

Proteins differentially regulated by Hsp90 inhibition

Inhibition of Hsp90 using 17AAG and shRNA targeting *hsp90α* in the U87-MG glioma cell line resulted in the differential expression of specific proteins such as type IV collagen, annexin A2 with calcium ions, Hsp90 beta-1, manganese superoxide dismutase, Des3-23alg-2 bound to calcium and transgelin 2. Interestingly, all the proteins differentially expressed were upregulated upon 17AAG treatment and downregulated upon shRNA treatment. The differential expression of these proteins could be attributed to the inhibition of Hsp90 by different mechanisms i.e. 17AAG targeting Hsp90 protein and shRNA targeting *hsp90α* gene. *COL4A1* gene encodes for collagen alpha-1 (IV) chain which is a major type IV collagen chain of basement membranes (http://www.ncbi.nlm.nih.gov/sites/entrez?Db=gene&Cmd=ShowDetailView&TermToSearch=1282). Molecular genetics have enabled the identification of six evolutionary related mammalian genes that encode six different polypeptide chains of collagen IV. Each gene is differentially expressed during embryonic development, thus, providing a tissue specific collagen IV network. The α-chains further assemble themselves in ER

forming unique heterotrimers in a chain specific manner (Khoshnoodi *et al*., 2008). Type IV collagen is strictly an exclusive member of the basement membrane and forms supramolecular networks influencing cell adhesion, migration and differentiation (Khoshnoodi *et al*., 2008). Studies have linked collagen IV to rare genetic diseases such as cererbral haemorrhage, porencephaly in infants, haemorrhagic strokes in adults and several tumours (Khoshnoodi *et al*., 2008). The human glioma cell line, U87-MG has the ability to degrade type IV collagen intracellularly for tumour invasion (Sameni *et al*., 2001).

Annexin A2 also referred to as annexin II is encoded by *ANXA2* gene. It is a calcium and phospholipid ion binding protein and acts as a substrate for tyrosine kinases. Increased levels of annexin II have been observed in various tumours including gliomas (Nygaard *et al*., 1998). Earlier studies have demonstrated the presence of annexin II as a marker for malignancy in glioma cell lines (Nygaard *et al*., 1998). Annexin II is also involved in glioma invasion and its subsequent silencing using RNAi reportedly decreased the migration of human glioma cell lines *in vitro* (Tatenhorst *et al*., 2006).

Manganese superoxide dismutase (MnSOD) is a mitochondrial protein which forms homotetramer and binds to one manganese per subunit. It further binds to superoxide by-products of oxidative phosphorylation and converts them to hydrogen peroxide and diatomic oxygen (http://www.genecards.org/cgi-bin/carddisp.pl?gene=Sod2). Mutations of the gene encoding MnSOD are associated with several diseases including tumours. MnSOD has been found to be increased in several tumours including glioma (Zhong *et al*., 1997). In one particular study, MnSOD was over expressed in wild type U118 and U118-9 glioma cell lines and interestingly, it was noted that the MnSOD over expressed cell lines became less malignant and had a slower tumour growth. Thus, the

present findings suggest MnSOD to be a tumour suppressor gene in a several tumours (Zhong *et al*., 1997).

The N terminal truncated apoptosis linked gene-2 (des3-23alg-2) was found to be differentially regulated upon Hsp90 inhibition. *ALG-2* gene encodes for ALG-2 protein belonging to the penta-EF-hand protein family. It is reportedly bound to calcium and this calcium binding enables homodimerization and brings about conformational changes which are required for binding to other proteins. The ALG-2 protein is also reportedly involved in T cell receptor-Fas-and glucocorticoid-induced cell death (http://www.genecards.org/cgi-bin/carddisp.pl?gene=Pdcd6; Jang *et al*., 2002). A study reported that, ALG-2 deficiency in mice failed to block apoptosis induced by T cell receptor-Fas-and/or glucocorticoid signals indicating that ALG-2 is not essential for apoptotic responses and other functionally redundant proteins might be present in mammalian cells (Jang *et al*., 2002). Contradictory to the above findings, the expression of ALG-2 was reportedly upregulated in lung and mesenchymal tumours. Further *ALG-2* expression was silenced in HeLa cells using siRNA targeting *ALG-2*. A significant reduction in the viability of HeLa cells was observed suggesting a possible role of ALG-2 in tumour development and expansion (Ia Cour *et al*., 2008).

Although Hsp90 was inhibited, proteomic analysis could not identify Hsp90 to be one the proteins affected. This could have been attributed to post translational modifications and/or alteration of the Hsp90 protein complex post treatment with 17AAG and sh*hsp90α*.

4.6 CONCLUSION:

In conclusion, the present results have shown that the treatment of U87-MG glioma cells with either 17AAG or shRNA to target *hsp90α* effectively reduced Hsp90α activity and subsequently reduced the Akt/PKB kinase activity along with S and G2 phase arrest in the cell line. These results suggest that inhibition of Hsp90 activity could be used for GBM therapy. Based on the application of proteomics and the laboratory findings, it was observed that the inhibition of the Hsp90 is achieved far greater with 17AAG than with shRNA targeting *hsp90α*.

Proteomic analysis post Hsp90 inhibition in the U87-MG glioma cell line revealed a clearer picture of the role of Hsp90 in glioma. However, there are still certain areas where further work should be carried out in order to understand the multifaceted nature of gliomas. With post proteomic analysis, it may be suggested that Hsp90 inhibition is sub-lethal and a multi-target approach involving the targeting of Hsp70 and/or members of the glycolysis pathway should be undertaken for enhanced glioma therapy.

CHAPTER 5

COMBINATION THERAPY TARGETING Hsp90 AND Hsp70 IN U87-MG GLIOMA CELL LINE

5.1 INTRODUCTION:

Glioma is resistant to standard treatment modalities such as surgery, radiation and chemotherapy with a mean survival rate of approximately 12-15 months (Carter *et al*., 2007). Recent studies have shown significant progress in understanding the molecular pathogenesis of GBM (Furnari *et al*., 2007) which has increased an interest in molecular therapies for the treatment of gliomas (Idbaih *et al*., 2008; Chi and Wen, 2007). Several single agents have been tried unsuccessfully in therapeutics (Idbaih *et al*., 2008; Chi and Wen, 2007). Co-activation of multiple tyrosine kinases and superfluous signalling pathways are some of the reasons for poor therapeutic response towards signal agents (Stommel *et al*., 2007). Furthermore, passage of several agents via the blood brain barrier has been poor followed by active efflux of the drugs via P-glycoprotein and other pumps. To improve the effectiveness of molecular therapies there has been an increased interest in using multiple agents that target kinases, combining agents inhibiting complementary targets such as EGFR and mammalian target of rapamycin (mTOR), followed by the combination of several single agents with radiotherapy and/or chemotherapy (Wen, 2009). Previous preliminary results have shown good response in:

1. A clinical study involving seventeen patients with advanced solid tumours was carried out. The patients were treated with a combination of chemotherapeutic drugs such as sorafenib and bevacizumab. Partial responses (12 %) or disease stabilization occurred in most of the patients, thus, showing promising clinical activity along with sorafenib dose reduction and lowered side effects (Lee *et al*., 2010).

2. A monoclonal antibody against vascular endothelial growth factor (VEGF) called as bevacizumab has shown promising activity in malignant glioma therapeutics. Six patients with malignant glioma were treated with bevacizumab alongwith chemotherapy (temozolomide, irinotecan or topotecan). Five of six patients showed a radiographic response. Thus, combining bevacizumab with chemotherapy could be an effective strategy to treat patients with malignant gliomas (Zhang *et al*., 2009). Additionally, bevacizumab combined with irinotecan showed promising activity in relapsed, heavily pre-treated population of patients with high grade malignant glioma. Of the thirteen patients treated, ten patients showed partial response (Ali *et al*., 2008).
3. Adenovirus carrying the secretable trimeric tumour necrosis factor-related apoptosis inducing ligand (Ad-stTRAIL) was injected in human glioma tumours *in vivo*. It was observed that gene therapy obtained with Ad-stTRAIL illustrated potent anti-tumour activity with no toxic side effects at therapeutically effective doses. In comparison with 1,3-bis(2-chloroethyl)-1-nitrosourea (BCNU), a conventional therapeutic for malignant glioma, Ad-stTRAIL demonstrated potent tumour growth suppression. Furthermore, the combination of Ad-stTRAIL with BCNU showed a significant increase in survival compared to control mice or mice treated with Ad-stTRAIL alone, thereby suggesting possible therapeutic aspects of Ad-stTRAIL combined with BCNU in the treatment of gliomas (Jeong *et al*., 2009).
4. Human GBM cell lines (A-172 and LA567) were treated with a combination of TMZ and tamoxifen or hypericin and cell survival was analysed. It was observed that both tamoxifen and hypericin were able to enhance the growth inhibition

and apoptosis stimulatory response of TMZ by down regulating essential components of cell cycle and survival pathways (inhibiting protein kinase C, a growth stimulatory kinase) both *in vivo* and *in vitro* (Gupta *et al*., 2006).

5. Inhibitor of Akt pathway, LY294002 in combination with 17AAG showed enhanced cytotoxicity in malignant glioma cell lines. Furthermore, the cells exposed to LY294002 and 17AAG demonstrated a significant reduction in cell cycle regulatory proteins. Taken together, these findings postulate the use of targeting the Akt pathway in combination with 17AAG to achieve enhanced effects on downstream signalling pathways on treating patients with malignant gliomas (Premkumar *et al*., 2006).

Proteomic analysis in the present study reported the induction of molecular chaperone Hsp70 family members post Hsp90 inhibition. This induction was in agreement with the literature (McCollum *et al*., 2006). In tumours, Hsp70 is upregulated and plays a key role in the regulation of several pathways such as cell proliferation, metastasis, invasion and death (Nylandsted *et al*., 2000). Members of Hsp70 family are involved in the apoptotic pathway and inhibit cell death (Frese *et al*., 2003; Pocaly *et al*., 2007; Kaur *et al*., 2000; Zhao *et al*., 2005). Thus, even though Hsp90 was inhibited, the induction of Hsp70 post inhibition resulted in survival of the glioma cells (U87-MG). It can be postulated that inhibition of Hsp70 along with Hsp90 could be of therapeutic importance in glioma therapy. Based on this hypothesis, U87-MG glioma cells were treated with both Hsp90 inhibitor i.e 17AAG and Hsp70 inhibitor i.e. N-formyl-3,4-methylenedioxy-benzylidene-gamma-butyrolactam (KNK437). KNK437 is a benzylidene lactam compound which inhibits Hsp70 (Yokota *et al*., 2000). Along with

Hsp70, KNK437 inhibits the activity of Hsp40 and Hsp105. However, little is known about KNK437 and its mechanisms (Yokota *et al*., 2000).

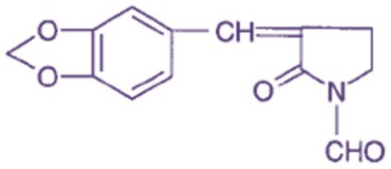

Figure 5.1: Structure of KNK437 (*N*-formyl-3,4-methylenedioxy-benzylidene-gamma-butyrolactam)

KNK437 was first reported in 2000 by Yokota *et al*., (2000) where in they showed inhibition of Hsp70 and inhibition of thermotolerance acquisition post KNK437 treatment in human colon carcinoma (Yokota *et al*., 2000). Furthermore, Lui and Kong (2007) observed DNA defragmentation when Hsp70 was inhibited by KNK437 in erythroleukemic cell line, TF-1 (Lui and Kong, 2007). However, studies are still ongoing to determine the exact mechanisms of action of KNK437.

This study, in the light of these previous findinup, examined the combined effect of inhibiting Hsp90 and Hsp70 with 17AAG and KNK437 respectively, in U87-MG glioma cell line. Cell cycle analysis was carried out to determine the effect of combining 17AAG and KNK437 on various stages of cell cycle. Additionally, U87-MG glioma cells were checked for viability post treatment with both 17AAG and KNK437.

5.2 MATERIALS AND METHODS:

In this study, U87-MG glioma cell line was cultured as described in section 2.1. The cells were treated with varying concentrations of KNK437 (10 – 100 nM) for 48 hours to assess its IC_{50} as described in section 2.11. The cells were then treated with both 17AAG and KNK437 in combination and assessed for viability as described in section 2.11. Moreover, cell cycle analysis was carried out on control (wild type U87-MG cell line) and treated (1. U87-MG cells treated with 17AAG, 2. U87-MG cells treated with KNK437 and 3. U87-MG cells treated with both 17AAG and KNK437) as described in section 2.12. Statistical analysis were performed as described in chapter 2, section 2.14.

5.3 RESULTS:

5.3.1 U87-MG cell viability using KNK437:

Varying concentrations of KNK437 (10 – 100 nM) were added to U87-MG glioma cell line and then incubated for 48 hours to determine the IC_{50} for KNK437 (Fig. 5.2).

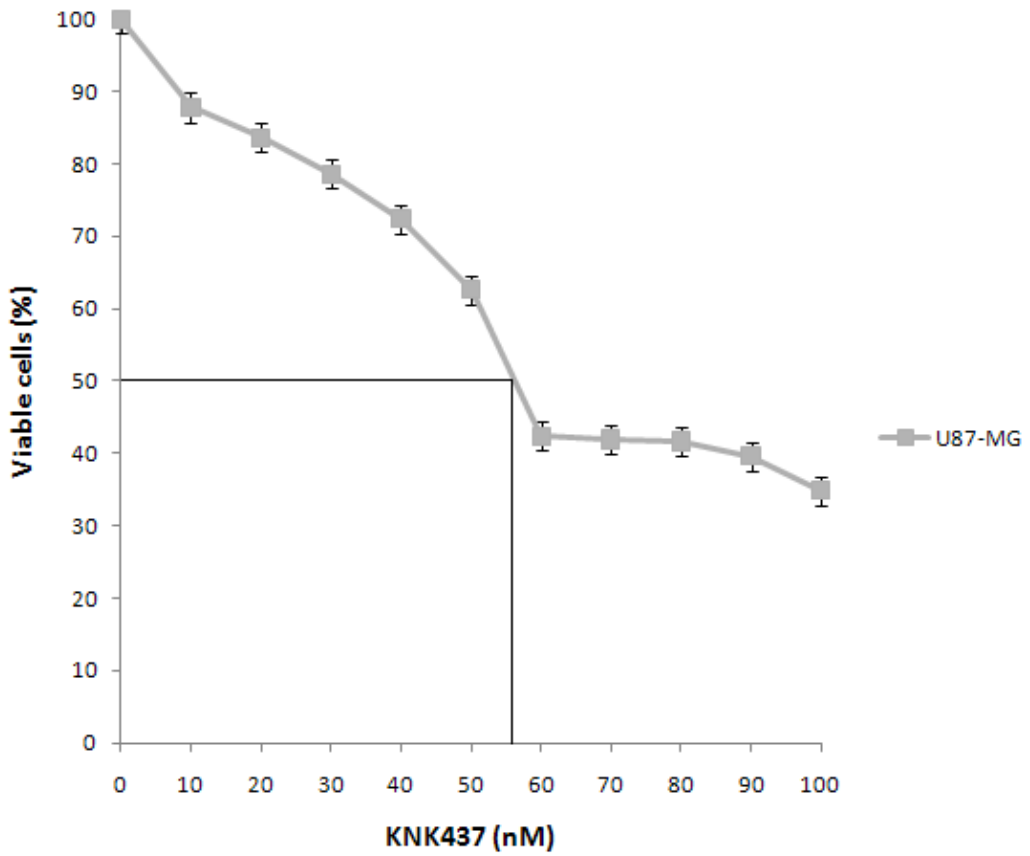

Figure 5.2: Cell viability assessment of U87-MG with increasing concentrations of KNK437 (10 – 100 nM). Data values are mean ± standard error, n = 3.

The results presented in figure 5.2 show that KNK437 can evoke a gradual inhibition in cell viability upto 50 nM. Further concentrations evoked only small decreses in cell viability with maximal effect observed with 100 nM. Typically, 100 nM produced an inhibition of 65 %. Following an analusos of the data the IC_{50} of KNK437 was calculated to be 55 nM.

5.3.2 Cell viability using 17AAG AND KNK437:

U87-MG glioma cells were treated with IC_{50} values of 17AAG (0.25 µM), KNK437 (55 nM) and then with a combination of IC_{50} values of 17AAG and KNK437 (Fig. 5.3).

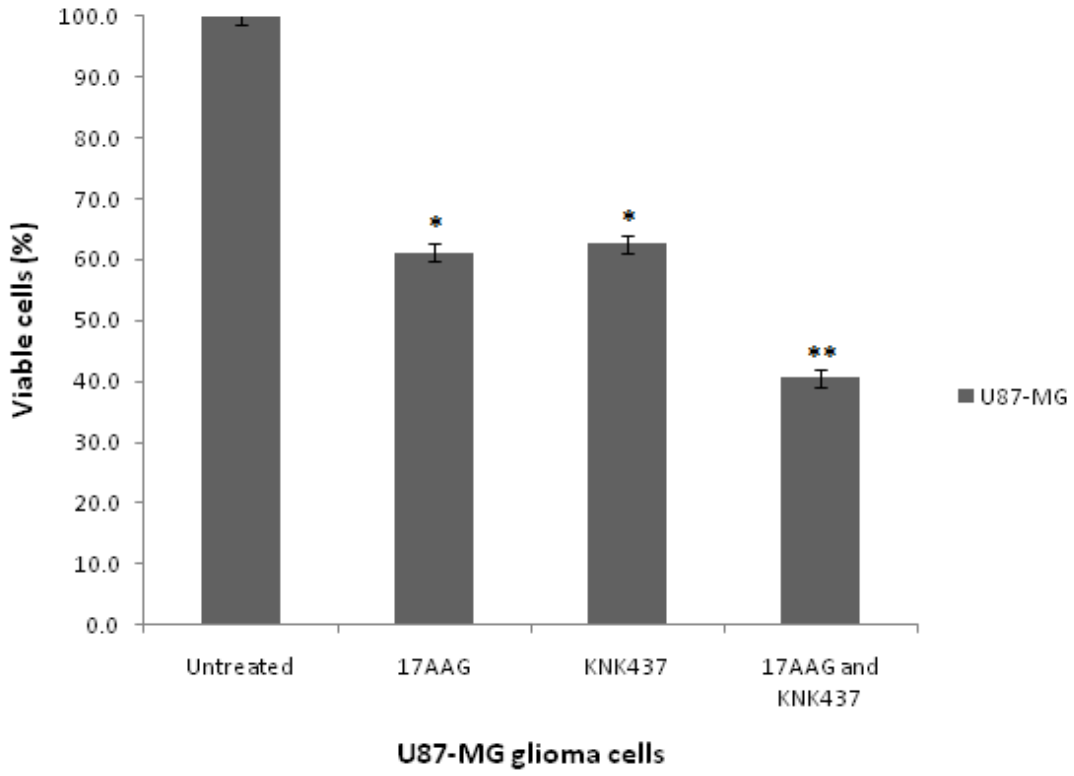

Figure 5.3: Cell viability assessment of U87-MG with 17AAG and KNK437. Data values are mean ± standard error, n = 3, *p < 0.05 and **p < 0.001 are considered to be statistically significant.

The results show that, combining 17AAG and KNK437 (**p < 0.001) resulted in an increased cell death rate of U87-MG glioma cells. Though IC_{50} values of 17AAG and KNK437 were used, the percentage of viable cells observed, post 17AAG and KNK437 treatment were 61.2 (*p < 0.05) and 62.6 (*p < 0.05), respectively. This flux could have been possibly attributed to changes in passage number of the U87-MG cells used.

5.3.3 Cell cycle analysis:

Cell cycle analysis was carried out to compare control cells (wild type U87-MG) and treated cells [U87-MG-17AAG, U87-MG-KNK437 and U87-MG-(17AAG + KNK437)] based on the cohort of cells found at different stages of the cell cycle. As seen below, the P2 represents the cohort of cells at the G1 phase of the cell cycle, P3 stands for the cohort of cells in the S phase of the cell cycle and P4 represents the cohort of cell in the G2 phase of cell cycle (Fig. 5.4 and 5.5; Table 5.1).

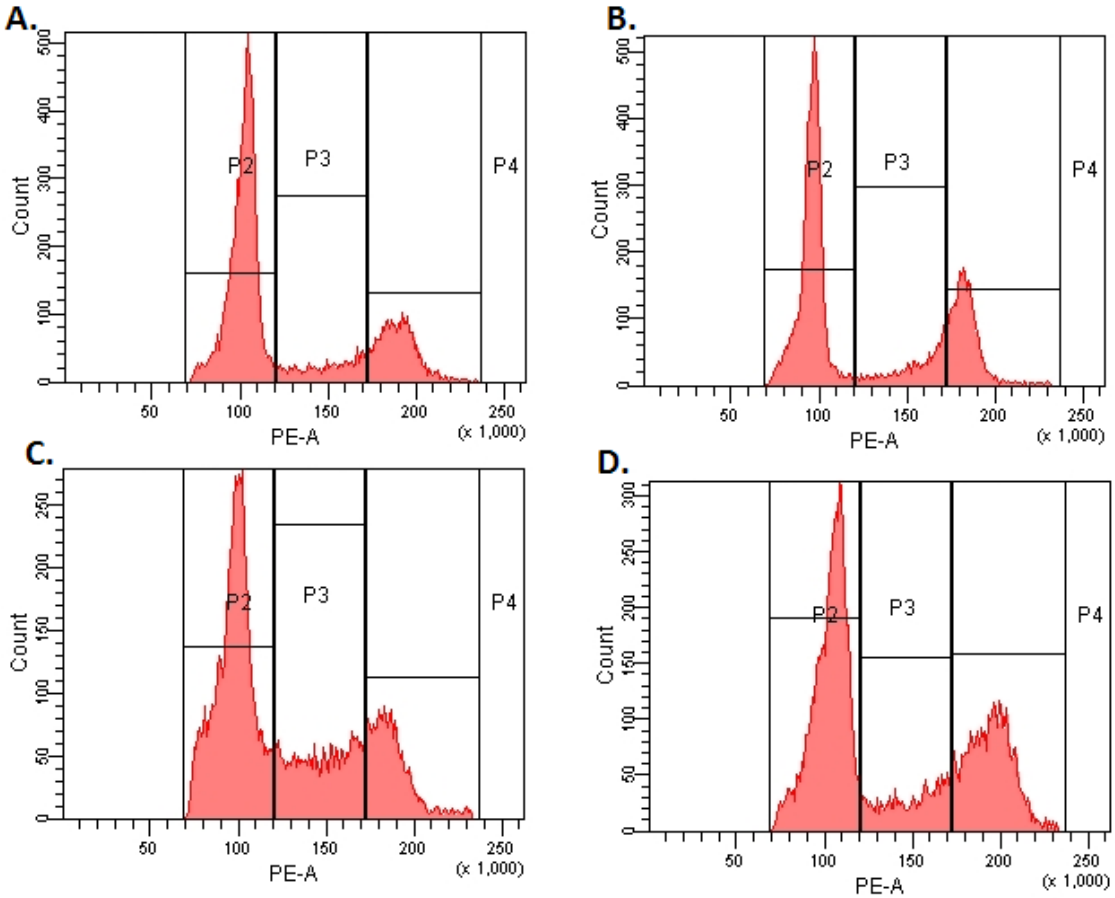

Figure 5.4: Cell cycle analysis of U87-MG control and treated glioma cell line. Cohort of U87-MG cells stained with PI upon cell cycle analysis in A) Control (wild type U87-MG cells) B) U87-MG cells treated with 17AAG C) U87-MG cells treated with KNK437 and D) U87-MG cells treated with a combination of 17AAG and KNK437. These flow cytometric readings are typical of 3 such different experiments.

Table 5.1: Cell cycle analysis of U87-MG control and treated glioma cell line.

Data values are mean ± standard deviation, n=3, *p < 0.05 and **p < 0.001 are considered to be statistically significant.

Sample	Cell Cycle (%)		
	G1	S	G2
WT U87-MG	60.5 ± 0.6	14.2 ± 0.1	15.6 ± 3.4
U87-MG-17AAG	54.8 ± 0.1	17.9 ± 0.6*	18 ± 5
U87-MG-KNK437	45.5 ± 2.2	25.8 ± 2.9*	20 ± 3.1 *
U87-MG-(17AAG + KNK437)	48.5 ± 0.7 *	16 ± 0.7	20.5 ± 3 *

Different stages of the cell cycle are affected upon inhibiting Hsp90 and Hsp70.

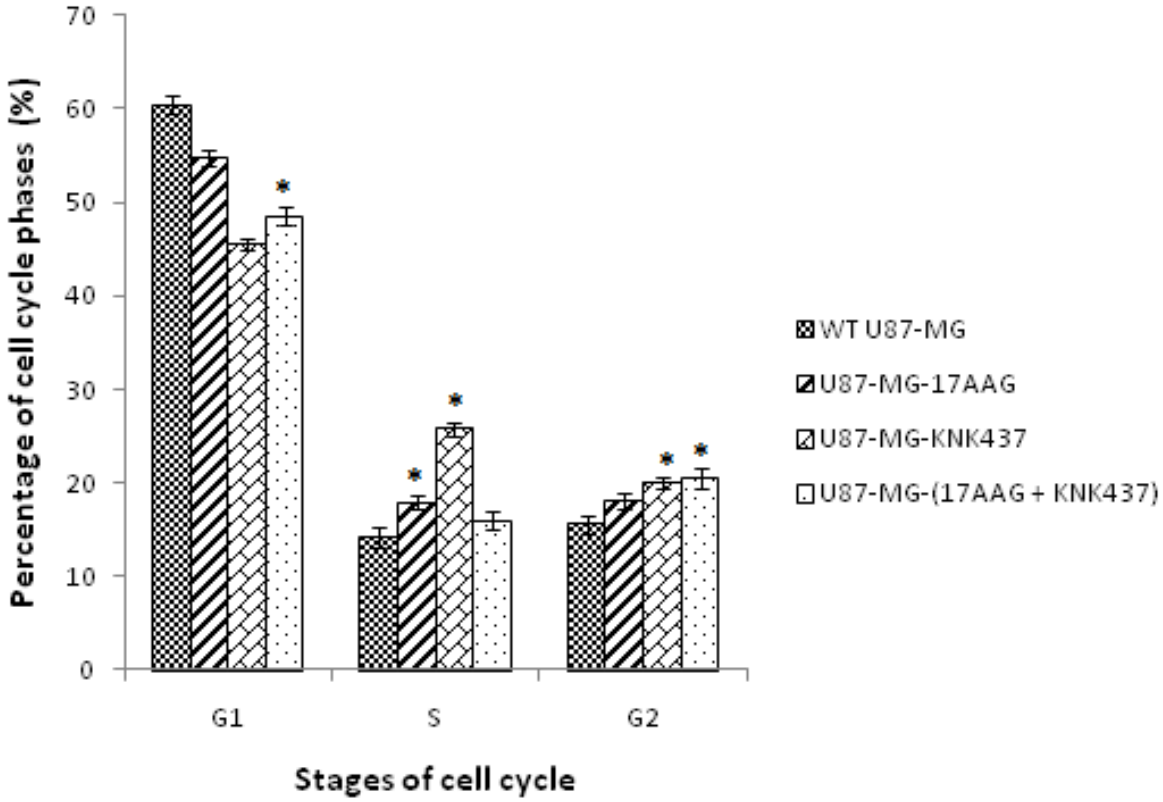

Figure 5.5: Different stages of the cell cycle affected post inhibition of Hsp90 and Hsp70. Data are mean ± standard deviation, n = 3, *p < 0.05 and **p < 0.01 are considered to be statistically significant.

Thus, it can be observed that various stages of the cell cycle are affected post inhibition of Hsp90 and Hsp70 using 17AAG and KNK437, respectively. Also, upon statistical analysis there was a significant decrease (*p < 0.05) when KNK437 was used in combination with 17AAG on G1 and G2 phases of U87-MG cell cycle.

5.4 DISCUSSION:

Heat shock proteins are a group of molecular chaperones responsible for protein folding, assisting re-folding of denatured proteins and preventing proteins from aggregation and other cellular processes (Hartl *et al*., 2002; Young *et al*., 2004). Hsp90 and Hsp70 act as co-chaperones to each other (Dittmar and Prat, 1997; Morishima *et al*., 2000). Hsp90 has emerged as a molecular target due to its role in maturation and regulation of key oncogenic client proteins (Workman *et al*., 2007; Whitesell and Lindquist, 2005). Over the past few years, several small molecular inhibitors such as radicicol and 17AAG have been utilized to inhibit Hsp90 function in an attempt to be of therapeutic importance. One of the inhibitors of Hsp90, 17AAG is currently in clinical trials for the treatment of several tumours (Goetz *et al*., 2003; Neckers, 2002). Though Hsp90 works on multiple oncogenic, proliferative and survival pathways, inhibition of Hsp90 does not completely inhibit the rate of tumour cell growth or tumour invasion. This could be attributed to the heat shock response generated post Hsp90 inhibition which attenuates cell death (Guo *et al*., 2005; Gabai *et al*., 2005; Zaarur *et al*., 2006). Post Hsp90 inhibition, HSF-1 transcription factor monomers are released from the Hsp90 complexes and results in HSF-1 trimerization followed by its translocation inside the nucleus, wherein, it binds to the promoter elements of heat shock genes (Zou *et al*., 1998; Ali *et al*., 1998; Voellmy and Boellmann *et al*., 2007). Regulators of apoptotic pathways such as members of Hsp70 family are predominantly induced along with Hsp27 post Hsp90 inhibition causing reduced sensitivity amongst tumour cells towards Hsp90 inhibition (Powers *et al*., 2008). Previous studies have noted induction of Hsp70 isoforms i.e. Hsp72 and Hsc70 post Hsp90 inhibition in colon and ovarian tumours (Clarke *et al*., 2000; Maloney *et al*., 2007). Proteomic analysis of the present research

showed a similar pattern. Members of the Hsp70 family were induced post Hsp90 inhibition using 17AAG or shRNA targeting *hsp90α*. Taking this into consideration, experiments were conducted to inhibit both Hsp90 and Hsp70 in U87-MG glioma cell line.

Varying concentrations (10 – 100 nM) of KNK437, an Hsp70 inhibitor were pre-incubated with U87-MG cells. The cells were treated for 48 hours before the viability of the cells were assessed. The results have indicated that approximately 55 nM of KNK437 was required to kill 50 % of the cells (IC_{50}) post 48 hours. Previous studies in the erythroleukemia cell line (TF-1) showed that 100 nM of KNK437 was required to kill 50 % of the cells post 24 hours of treatment (Lui and Kong 2007). Thus, it could be inferred that if maintained for 48 hours, the IC_{50} of KNK437 in TF-1 cells could possibly then be 50 nM which is in consistency to our findings. Additionally, this flux of IC_{50} levels in KNK437 could be due to differences in cell lines and the experimental conditions used.

Furthermore, U87-MG cells were treated with either 17AAG, KNK437 or a combination of the two inhibitors. The combination of 17AAG with KNK437 resulted in a higher percentage (~ 60 %) of U87-MG glioma cell death rate compared to treatment with 17AAG (~ 39 %) or KNK437 (~ 37 %) alone. Statistic analysis using paired-sample T-test confirmed that the combination of 17AAG with KNK437 produced a significant decrease (**$p < 0.001$) of U87-MG glioma cells. Thus, it may be suggested that combination therapy involving inhibition of both, Hsp90 and Hsp70 could be used in glioma therapy. Interestingly, arsenic trioxide (ATO) is used as a promising therapeutic agent in leukemia as it can induce apoptosis (Wu *et al*., 2009). Wu *et al*., (2009)

demonstrated that co-treatment of human adenocarcinoma cell line, HeLa-S3 with ATO, with either 17-DMAG (Hsp90 inhibitor) or KNK437 significantly increased ATO-induced cell death and apoptosis along with ATO-induced mitotic arrest (Wu *et al*., 2009).

Cell cycle analysis was carried out to compare control (wild type U87-MG cell line) and treated cells (U87-MG cells treated with 17AAG and U87-MG cells treated with KNK437 and U87-MG cells treated with both 17AAG and KNK437). Consistent with previous findings, it was observed that Hsp90 inhibition with 17AAG resulted in S and G2 phase arrest. Additionally, inhibition of Hsp70 with KNK437 also resulted in S and G2 phase arrest. Similarly, inhibition of both Hsp90 and Hsp70 resulted in G1 and G2 phase arrest in the U87-MG glioma cell line (*$p < 0.05$). Previous work on the A-172 glioma cell line demonstrated that post KNK437 treatment, the A-172 cells entered into G2/M phase arrest post 48 hours of treatment (Ohnishi *et al*., 2006). Though the data obtained are preliminary, the results do look promising. Previous studies have illustrated the use of a multi-target approach combining different therapeutic drugs/inhibitors for tumour therapy (Ali *et al*., 2008; Gupta *et al*., 2006; Premkumar *et al*., 2006; Jeong *et al*., 2009). Thus, it could be hypothesized that a combination treatment involving the simultaneous inhibition of both, Hsp90 and Hsp70 could be possible strategy for the treatment of glioma.

5.5 CONCLUSION:

The efficacy of Hsp90 inhibitors can be compromised by the induction of anti-apoptotic Hsp70 isoforms as an off-target effect of Hsp90 inhibition. Similar findings were observed when Hsp90 was inhibited in U87-MG glioma cells. Subsequently, Hsp90 and Hsp70 were both inhibited by treating U87-MG cells with 17AAG and KNK437, respectively. An induced U87-MG cell death rate was observed when both Hsp90 and Hsp70 were simultaneously inhibited. Additionally, S and G2 phase arrest was observed in U87-MG cells post Hsp90 and Hsp70 inhibition. It can thus be postulated that, combination therapy targeting multiple pathways could be a future strategy in glioma therapy.

CHAPTER 6

GENERAL DISCUSSION, CONCLUSION AND

FUTURE WORK.

6.1 GENERAL DISCUSSION AND CONCLUSION:

Heat shock protein 90 (Hsp90), a highly conserved molecular chaperone, has two isoforms of which, Hsp90α is the major inducible isoform (Gupta, 1995). Hsp90 plays a vital role in tumorigenesis, maintenance of transformation and regulation of several proteins involved in apoptosis, survival and growth pathways (Shervington *et al*., 2008). Hsp90 also has an active role in the transformation and maturation of several "oncogenic" client proteins such as Akt (Kamal *et al*., 2003). Akt, a protein kinase is involved in anti-apoptotic pathways. However, in tumours including glioma, it stimulates cell proliferation and inhibits apoptosis thus empowering cancer cells the property of "immortality" (Basso *et al*., 2002; Basso *et al*., 2002). Hsp90 is over-expressed in breast tumours, lung cancers, leukaemias and Hodgkin's disease (Neckers, 2007). Previous studies in our laboratory have reported *hsp90α* over expression in both glioma tissue and cell lines but not in normal brain tissues and cell lines, suggesting a possible role in sensitizing glioma cells to therapy by using anti-Hsp90*α* drugs (Shervington *et al*., 2008). Inhibiting *hsp90α* expression can possibly be a favourable therapeutic approach compared to conventional chemotherapies since it is target-specific and has a reduced toxicity profile (Cruickshanks *et al*., 2010). Given the advantages of silencing achieved using shRNA as opposed to siRNA, this study used shRNA oligonucleotides targeting *hsp90α*. shRNA olignucleotide 2 was mRNA effective by silencing *hsp90α* upto approximately 99 % (**$p < 0.001$). The activity of the Hsp90α protein was assayed by quantifying the levels of Akt/PKB in these samples. Significant reductions (> 50 %) (**$p < 0.001$) of Akt/PKB levels were observed post *hsp90α* inhibition. Due to the anti-apoptotic role of Akt in gliomas, it can be suggested that the

reduction of Akt levels post Hsp90α inhibition would be of therapeutic importance in glioma therapy.

Hsp90 was inhibited using 17AAG, a potent Hsp90 inhibitor which has shown significant results so far in clinical trials. The IC_{50} level of 17AAG was found to be 0.25 µM following 48 hours incubation in the case of the U87-MG cell line. Cohorts of the U87-MG cells were treated with either 17AAG or shRNA to target *hsp90α*. The efficacy of Hsp90 inhibition was analysed by assessing the protein level of Hsp90α in control and treated cells by FACS analysis (quantitative) using a flow cytometer. Furthermore, the Akt/PKB kinase activity levels were checked using the Akt/PKB kinase activity assay kit (Assay Designs, UK) and Hsp90α levels were also quantified in control and treated cells using Hsp90α ELISA kit (Assay Designs, UK). Upon FACS analysis Hsp90α protein levels were found to be reduced (**$p < 0.001$) by approximately 44 % and 16 %, post treatment with 17AAG and shRNA oligonucleotide targeting *hsp90α*, respectively. ELISA analysis quantified Hsp90α protein levels in control (wild type U87-MG) and treated (U87-MG-17AAG and U87-MG-sh*hsp90α*) and it was observed that the Hsp90α protein levels were reduced significantly (**$p < 0.001$) by more than 65 % and 45 %, post treatment with 17AAG and sh*hsp90α,* respectively, in U87-MG cells. The activity of Hsp90α protein was determined by assaying the quantity of Akt in the samples. It was observed that the Akt/PKB kinase activity was reduced significantly (**$p < 0.001$) by 81 % and 59 %, post 17AAG and sh*hsp90α* treatment, respectively in U87-MG glioma cells, suggesting that Hsp90 inhibition could be of therapeutic significance. Furthermore, cell cycle analysis demonstrated S and G2 phase arrest in the U87-MG cell line, post Hsp90 inhibition.

Interestingly, it was observed that the inhibition of the Hsp90 protein is a more effective therapeutic approach than silencing *hsp90α* i.e. though shRNA targeting *hsp90α* did silence Hsp90, the 17AAG showed a better silencing profile. These results thereby illustrate the importance of Hsp90 inhibition for glioma therapy.

A major drawback of RNAi therapy is the effects of silencing by RNAi being only partial and results in incomplete knockout of phenotype (Yamada *et al*., 2007). Such a phenotype might contribute in the production of a spliced/altered Hsp90 isoforms which could compensate the function of Hsp90α and thereby diminish the effects of post treatment with sh*hsp90α*. The mRNA transcripts are processed by several post-translational events such as alternative splicing or RNA editing. These events generate different mRNA strands from the same gene resulting in an increase of the transcriptome and subsequently the proteome (Gallo and Galardi, 2008). Thus, it could be suggested that RNA editing generates RNA diversity through the post-transcriptional modification of single nucleotides in pre-Hsp90α mRNA and subsequently hampering the effect of Hsp90α inhibition, post sh*hsp90α* treatment.

Though such an edited/altered isoform of Hsp90α has yet to be reported, recent studies have reported that adenosine (A) to inosine (I) editing widely occurs in human trancriptome (at least 2 % of available mRNAs), with most of the editing sites residing in Alu repetitive elements. Alu sequences are typically 300 nucleotides (nt) long and comprise > 10% of the human genome (Athanasiadis *et al.,* 2004; Kim *et al*., 2004; Levanon *et al*., 2004; Levanon *et al.,* 2005; Eisenberg *et al.,* 2005).

Tumour cells have a high dependence on stress response pathways compared to normal cells. As a result, Hsp90 has been found to be present in an activated superchaperone complex in tumour cells while in normal cells it is present in an

uncomplexed state. Hsp90 present in the activated superchaperone complex (tumour cells) is highly sensitive to pharmacological Hsp90 inhibitors than the Hsp90 present in an uncomplexed state (normal cells) (Workman *et al*., 2007). Considering 17AAG, it targets the Hsp90 protein reducing the effects of RNA editing. Furthermore, the binding affinity of Hsp90 to 17AAG is 100 folds higher in tumour cells than normal cells which enables selective drug targeting of tumours (Kamal *et al*., 2003). Moreover, 17AAG's ability to target tumour cells over normal cells and its ability to cross the blood brain barrier is of therapeutic importance in glioma therapy (Sauvageot *et al*., 2009).

To understand the downstream effects of Hsp90 inhibition and to determine the client proteins affected, proteomic analysis was performed on U87-MG cells. Proteins were extracted from the control and treated samples and then were analyzed by Applied Biomics; 2D-DIGE for separation and MALDI-TOF for protein identification. Based on a 2 fold cut off, the analysis identified 36 proteins while MALDI-TOF analysis identified 33 proteins with altered expression with a confidence levels > 99 %. Three proteins were classified as unknown proteins. IPA analysis demonstrated dynamically regulated biological networks and canonical pathways, post Hsp90 inhibition. The top network transformed post Hsp90 inhibition identified as "cancer" while the top diseases and disorders transformed upon Hsp90 inhibition were cancer, gastrointestinal disease, genetic disorder, neurological disease and skeletal and muscular disorders. These results confirm that by altering Hsp90 levels, the cancer proteome including neurological and genetic disorders is affected. The IPA library of canonical pathways further demonstrate that most of the proteins affected post Hsp90 inhibition belong to glycolysis/glucogenesis pathways.

During post Hsp90 inhibition, several proteins were upregulated, and these included members of Hsp70 family together with Hsp27 and member of the Hsp90 family, i.e. gp96. These molecular chaperones are also upregulated and they serve as co-chaperones to Hsp90 function (Dittmar and Pratt, 1997; Morishima *et al*., 2000) there by suggesting the role of Hsp90 co-chaperones in compensating for Hsp90 function post Hsp90 inhibition. However, further research needs to be carried out to confirm these postulations. Moreover, members of the glycolysis/glucogenesis pathways are also upregulated, demonstrating increased dependency on glycolysis for energy supply by the treated glioma cells. This phenomenon is called the "Warburgs effect" and it is an important phenomenon during malignant transformation (Warburg, 1956). Other proteins such as vimentin, aldose reductase complexed with dicholorophenyacetic acid, annexin 1, ubiquitin thiolesterase isoform CRA_d and actin related protein 2/3 complex subunit 2. Most of the proteins upregulated are involved in protein metabolism, energy pathways, cell growth and/or maintenance, metabolism, cell communication, signal transduction, and cytoskeleton organization and biogenesis. Their upregulation could be attributed to their functions which could have helped U87-MG glioma cells survive post Hsp90 inhibition. Thus, Hsp90 inhibition may be sub-lethal and there is a need for a multi-target approach in glioma therapy. As discussed earlier, it was observed that 17AAG inhibits Hsp90 better than shRNA targeting *hsp90α*. A significant difference between the increase observed in some the key proteins namely, Hsp70-1, Hsc70, hexokinase 1, pyruvate kinase, GAPDH and annexin 1 could be seen between the two treatments i.e. 17AAG and shRNA targeting *hsp90α*.

Several proteins such as Ku autoantigen, vimentin, serpine1 mRNA binding protein 1, calumenin, phosphoglycerate kinase, aldolase A, tropomyosin 4-anaplastic lymphoma

kinase fusion protein, eukaryotic translation initiation factor 3, transgelin 2, cyclophilins B complexed with [d-(cholinyester)ser8]-cyclosporin and GAPDH (predicted) were downregulated. Some of the proteins downregulated post Hsp90 inhibition are involved in various cellular responses such as DNA repair, protein synthesis and cell mobility. Most of the proteins downregulated such as Ku70, SERPINE1, PGK1 and transgelin post Hsp90 inhibition are normally upregulated in several tumours including gliomas (Wang *et al*., 2009; Martin *et al*., 2009; Kreth *et al*., 2010; Shirahata *et al*., 2007). Thus, their subsequent downregulation post Hsp90 inhibition could be of therapeutic importance. However, further work should be carried out to understand the interactions between the downregulated proteins and Hsp90 in the treatment of gliomas.

Proteomic analysis in this study also showed induction of the Hsp70 family members post Hsp90 inhibition. This induction is in agreement with the literature (McCollum *et al*., 2006). Members of Hsp70 family act at multiple points in the apoptotic pathway and inhibit cell death (Frese *et al*., 2003; Pocaly *et al*., 2007; Kaur *et al*., 2000; Zhao *et al*., 2004). Thus, even though Hsp90 was inhibited, the induction of Hsp70 post inhibition could have resulted in survival of the glioma cells (U87-MG). It can therefore be postulated that inhibition of Hsp70 and Hsp90 would be of therapeutic importance in glioma therapy. Based on this hypothesis, U87-MG glioma cells were treated with both the Hsp90 inhibitor i.e 17AAG and the Hsp70 inhibitor i.e. KNK437. The IC_{50} level of KNK437 was reported to be 55 nM, post 48 hours in the U87-MG cell line. Cell viability analysis demonstrated a higher percentage of U87-MG glioma cell death (~ 60 %)(**$p < 0.001$) when treated with a combination of 17AAG and KNK437 compared to treatment with 17AAG alone which resulted in ~ 39 % cell death. When U87-MG

glioma cells were treated with only KNK437 there was ~ 37 % cell death. However, the effects of 17AAG and KNK437 are not synergetic but rather additive in nature. Thus, it could be suggested that combination therapy involving inhibition of both Hsp90 and Hsp70 could be used in glioma therapy. Cell cycle analysis was also carried out to compare control (wild type U87-MG cell line) and treated cells (U87-MG cells treated with 17AAG, U87-MG cells treated with KNK437 and U87-MG cells treated with both 17AAG and KNK437). It was observed that Hsp90 inhibition with 17AAG resulted in S and G2 phase arrest. Inhibition of Hsp70 with KNK437 also resulted in S and G2 phase arrest. Similarly, inhibition of both Hsp90 and Hsp70 resulted in S and G2 phase arrest in U87-MG glioma cell line. Figure 6.1 summarizes the main findings of this study.

General conclusion: Together, the above findings have demonstrated the effect of combination therapy involving Hsp90 and Hsp70 for glioma therapy. However, more work needs to be undertaken to fully understand the Hsp90-Hsp70 chaperoning of glioma for effective glioma therapy. Further work needs to be carried out to understand the role of the proteins affected downstream post Hsp90 inhibition in glioma therapeutics. Members of the glycolysis pathway should also be extensively studied as a possible therapeutic option for glioma therapy. It is also equally important to determine the cellular and subcellular mechanism whereby KNK437 and 17AAG can induce cell death.

A

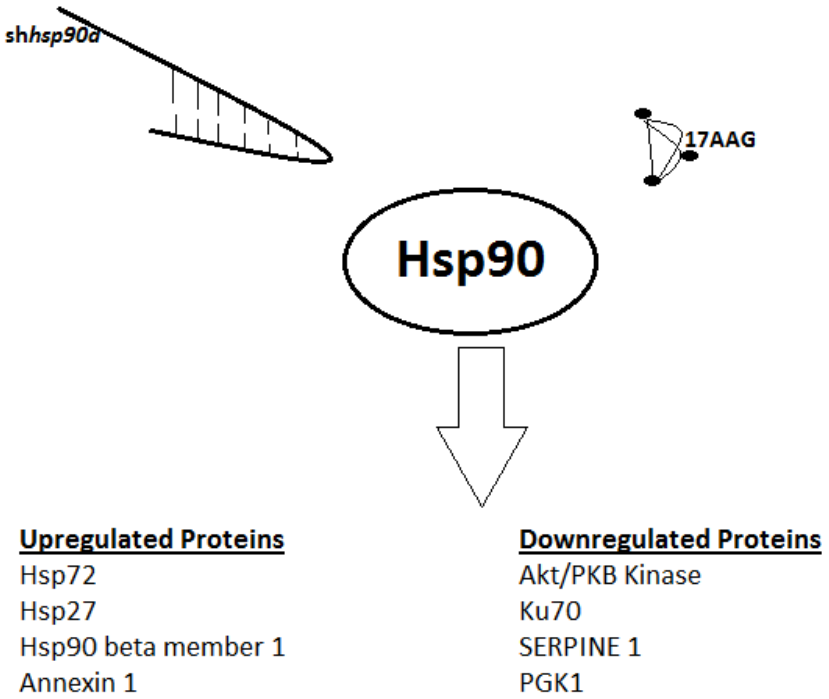

B

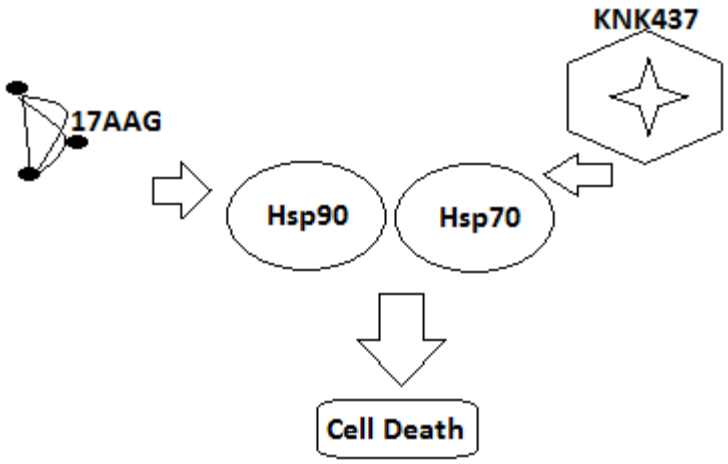

Figure 6.1: Schematic model summarizing the main findings. A) Hsp90 inhibition by either 17AAG or shRNA targeting *hsp90α* is of significant importance in glioma therapy. Proteomic analysis highlighted several proteins regulated post Hsp90 inhibition and further work needs to be undertaken to understand the chaperoning activity of Hsp90 in glioma therapy. B) Combination therapy involving 17AAG and KNK437 to inhibit Hsp90 and Hsp70 respectively, showed enhanced U87-MG glioma cell death.

6.2 FUTURE WORK:

Given the role of Hsp90 and its subsequent involvement in several tumours including gliomas, it has been an attractive target in tumour therapy. Several Hsp90 inhibitors have been used over the past decades in an attempt to treat tumours. In recent years, 17AAG has emerged as an attractive Hsp90 inhibitor and has shown to be a promising candidate in clinical trials carried out so far. It inhibits Hsp90 ATPase activity; shuts down the chaperone function and induces client protein degradation. Furthermore, the results from our laboratory also illustrate that 17AAG is a better inhibitor for Hsp90 function compared with shRNA oligonucleotide targeting *hsp90α*. However, there are some drawbacks in using 17AAG in clinical studies (Kang and Altieri, 2009). There is therefore a need to understand other aspects of Hsp90 biology to unlock the full therapeutic potential of these inhibitors.

Cancer is a complex disorder and is usually caused by more than one oncogenic factor. Targeting a single agent or a single protein (in this case Hsp90) would be sub-lethal and subsequently, it demands a need to target multiple proteins/factors in the treatment therapy of tumours. Post Hsp90 inhibition, Hsp70 was induced, assiting the glioma cells survive by evading apoptosis. Upon subsequent inhibition of both Hsp90 and Hsp70 in U87-MG glioma cell line, a high percentage of cell death was observed along with S and G2 phase arrest. Taking this into considerations, it could be postulated that targeting multiple targets, such as inhibiting Hsp90 and Hsp70, could be of therapeutic importance in glioma studies. However, further work needs to be undertaken to understand the role of Hsp90-Hsp70 in the chaperoning of glioma and its implication on glioma therapy.

Hsp90 chaperones a vivid list of client proteins and there is an ever increasing list of proteins that are being discovered that appear to play a role with Hsp90. In this particular study, several novel client proteins of Hsp90 such as transgelin 2, Ku70, SERPINE1, calumenin and TPM4-ALK fusion protein were identified. However, work needs to be undertaken to establish a direct link between Hsp90 and the proteins mentioned above to categorize them as novel Hsp90 client proteins.

Members of the glycolysis/glucogenesis pathways were upregulated, post Hsp90 inhibition, suggesting an increased dependency on glycolysis for energy supply by the treated glioma cells. Thus, more work needs to be undertaken to establish the link between Hsp90 and members of glycolysis pathway. The identified proteins should then be analyzed and studied for their role in the treatment of glioma. Work needs to be done illustrating the cellular and subcellular mechanism of action of 17AAG and KNK437 in inducing glioma cell death by measuring cellular Ca^{+2} homeostatis, p53 and caspase 3/9 and several other kinases which are involved with cell death.

CHAPTER 7

REFERENCES

Alaoui-Jamali MA & Xu YJ (2006). Proteomic technology for biomarker profiling in cancer: an update. *J Zhejiang Univ Sci B* **7**, 411-420.

Ali A, Bharadwaj S, O'Carroll R, & Ovsenek N (1998). HSP90 interacts with and regulates the activity of heat shock factor 1 in Xenopus oocytes. *Mol Cell Biol* **18**, 4949-4960.

Ali SA, McHayleh WM, Ahmad A, Sehgal R, Braffet M, Rahman M, Bejjani G, & Friedland DM (2008). Bevacizumab and irinotecan therapy in glioblastoma multiforme: a series of 13 cases. *J Neurosurg* **109**, 268-272.

Altieri DC (2004). Coupling apoptosis resistance to the cellular stress response: the IAP-Hsp90 connection in cancer. *Cell Cycle* **3**, 255-256.

An WG, Schulte TW, & Neckers LM (2000). The heat shock protein 90 antagonist geldanamycin alters chaperone association with p210bcr-abl and v-src proteins before their degradation by the proteasome. *Cell Growth Differ* **11**, 355-360.

Ando S, Tanabe K, Gonda Y, Sato C, & Inagaki M (1989). Domain- and sequence-specific phosphorylation of vimentin induces disassembly of the filament structure. *Biochemistry* **28**, 2974-2979.

Arrigo AP, Virot S, Chaufour S, Firdaus W, Kretz-Remy C, & Diaz-Latoud C (2005). Hsp27 consolidates intracellular redox homeostasis by upholding glutathione in its reduced form and by decreasing iron intracellular levels. *Antioxid Redox Signal* **7**, 414-422.

Asaka M, Kimura T, Nishikawa S, Saitoh M, Miyazaki T, Takatori T, & Alpert E (1990). Serum aldolase isozyme levels in patients with cerebrovascular diseases. *Am J Med Sci* **300**, 291-295.

Athanasiadis A, Rich A, & Maas S (2004). Widespread A-to-I RNA editing of Alu-containing mRNAs in the human transcriptome. *PLoS Biol* **2**, e391.

Ayene IS, Ford LP, & Koch CJ (2005). Ku protein targeting by Ku70 small interfering RNA enhances human cancer cell response to topoisomerase II inhibitor and gamma radiation. *Mol Cancer Ther* **4**, 529-536.

Bagatell R, Khan O, Paine-Murrieta G, Taylor CW, Akinaga S, & Whitesell L (2001). Destabilization of steroid receptors by heat shock protein 90-binding drugs: a ligand-independent approach to hormonal therapy of breast cancer. *Clin Cancer Res* **7**, 2076-2084.

Bandres E, Andion E, Escalada A, Honorato B, Catalan V, Cubedo E, Cordeu L, Garcia F, Zarate R, Zabalegui N, & Garcia-Foncillas J (2005). Gene expression profile induced by BCNU in human glioma cell lines with differential MGMT expression. *J Neurooncol* **73**, 189-198.

Banerji U, O'Donnell A, Scurr M, Pacey S, Stapleton S, Asad Y, Simmons L, Maloney A, Raynaud F, Campbell M, Walton M, Lakhani S, Kaye S, Workman P, & Judson I (2005). Phase I pharmacokinetic and pharmacodynamic study of 17-allylamino, 17-demethoxygeldanamycin in patients with advanced malignancies. *J Clin Oncol* **23**, 4152-4161.

Basso AD, Solit DB, Chiosis G, Giri B, Tsichlis P, & Rosen N (2002). Akt forms an intracellular complex with heat shock protein 90 (Hsp90) and Cdc37 and is destabilized by inhibitors of Hsp90 function. *J Biol Chem* **277**, 39858-39866.

Beckmann RP, Mizzen LE, & Welch WJ (1990). Interaction of Hsp 70 with newly synthesized proteins: implications for protein folding and assembly. *Science* **248**, 850-854.

Bernstein E, Caudy AA, Hammond SM, & Hannon GJ (2001). Role for a bidentate ribonuclease in the initiation step of RNA interference. *Nature* **409**, 363-366.

Bisht KS, Bradbury CM, Mattson D, Kaushal A, Sowers A, Markovina S, Ortiz KL, Sieck LK, Isaacs JS, Brechbiel MW, Mitchell JB, Neckers LM, & Gius D (2003). Geldanamycin and 17-allylamino-17-demethoxygeldanamycin potentiate the in vitro and in vivo radiation response of cervical tumor cells via the heat shock protein 90-mediated intracellular signaling and cytotoxicity. *Cancer Res* **63**, 8984-8995.

Blagg BS & Kerr TD (2006). Hsp90 inhibitors: small molecules that transform the Hsp90 protein folding machinery into a catalyst for protein degradation. *Med Res Rev* **26**, 310-338.

Blagosklonny MV, Toretsky J, Bohen S, & Neckers L (1996). Mutant conformation of p53 translated in vitro or in vivo requires functional HSP90. *Proc Natl Acad Sci (U S A)* **93**, 8379-8383.

Bradford MM (1976). A rapid and sensitive method for the quantitation of microgram quantities of protein utilizing the principle of protein-dye binding. *Anal Biochem* **72**, 248-254.

Bradshaw RA (2005). Revised draft guidelines for proteomic data publication. *Mol Cell Proteomics* **4**, 1223-1225.

Braga-Basaria M, Hardy E, Gottfried R, Burman KD, Saji M, & Ringel MD (2004). 17-Allylamino-17-demethoxygeldanamycin activity against thyroid cancer cell lines correlates with heat shock protein 90 levels. *J Clin Endocrinol Metab* **89**, 2982-2988.

Bruey JM, Ducasse C, Bonniaud P, Ravagnan L, Susin SA, Diaz-Latoud C, Gurbuxani S, Arrigo AP, Kroemer G, Solary E, & Garrido C (2000). Hsp27 negatively regulates cell death by interacting with cytochrome c. *Nat Cell Biol* **2**, 645-652.

Brummelkamp TR, Bernards R, & Agami R (2002). Stable suppression of tumorigenicity by virus-mediated RNA interference. *Cancer Cell* **2**, 243-247.

Bumcrot D, Manoharan M, Koteliansky V, & Sah DW (2006). RNAi therapeutics: a potential new class of pharmaceutical drugs. *Nat Chem Biol* **2**, 711-719.

Burger AM, Fiebig HH, Stinson SF, & Sausville EA (2004). 17-(Allylamino)-17-demethoxygeldanamycin activity in human melanoma models. *Anticancer Drugs* **15**, 377-387.

Calderwood SK, Khaleque MA, Sawyer DB, & Ciocca DR (2006). Heat shock proteins in cancer: chaperones of tumorigenesis. *Trends Biochem Sci* **31**, 164-172.

Calderwood SK, Theriault JR, & Gong J (2005). Message in a bottle: role of the 70-kDa heat shock protein family in anti-tumor immunity. *Eur J Immunol* **35**, 2518-2527.

Cardone MH, Roy N, Stennicke HR, Salvesen GS, Franke TF, Stanbridge E, Frisch S, & Reed JC (1995). Expression of heat shock protein HSP27 in human ovarian cancer. *Clin Cancer Res* **1**, 1603-1609.

Carr S, Aebersold R, Baldwin M, Burlingame A, Clauser K, & Nesvizhskii A (2004). The need for guidelines in publication of peptide and protein identification data: Working Group on Publication Guidelines for Peptide and Protein Identification Data. *Mol Cell Proteomics* **3**, 531-533.

Carter AN, Cole CL, Playle AG, Ramsay EJ, & Shervington AA (2008). GPR26: a marker for primary glioblastoma? *Mol Cell Probes* **22**, 133-137.

Chan SY, Speck RF, Ma MC, & Goldsmith MA (2000). Distinct mechanisms of entry by envelope glycoproteins of Marburg and Ebola (Zaire) viruses. *J Virol* **74**, 4933-4937.

Chandramouli K & Qian PY (2009). Proteomics: Techniques and Possibilities to Overcome Biological Sample Complexity. *Human Genomics and Proteomics* 2009, 1-23.

Chi AS & Wen PY (2007). Inhibiting kinases in malignant gliomas. *Expert Opin Ther Targets* **11**, 473-496.

Chiarle R, Voena C, Ambrogio C, Piva R, & Inghirami G (2008). The anaplastic lymphoma kinase in the pathogenesis of cancer. *Nat Rev Cancer* **8**, 11-23.

Chiosis G & Neckers L (2006). Tumor selectivity of Hsp90 inhibitors: the explanation remains elusive. *ACS Chem Biol* **1**, 279-284.

Chiosis G, Vilenchik M, Kim J, & Solit D (2004). Hsp90: the vulnerable chaperone. *Drug Discov Today* **9**, 881-888.

Cho JH, Song HO, Singaravelu G, Sung H, Oh WC, Kwon S, Kim dH, & Ahnn J (2009). Pleiotropic roles of calumenin (calu-1), a calcium-binding ER luminal protein, in Caenorhabditis elegans. *FEBS Lett* **583**, 3050-3056.

Chou YH, Ngai KL, & Goldman R (1991). The regulation of intermediate filament reorganization in mitosis. p34cdc2 phosphorylates vimentin at a unique N-terminal site. *J Biol Chem* **266**, 7325-7328.

Choudhury A & Kiessling R (2004). Her-2/neu as a paradigm of a tumor-specific target for therapy. *Breast Dis* **20**, 25-31.

Clamp M, Fry B, Kamal M, Xie X, Cuff J, Lin MF, Kellis M, Lindblad-Toh K, & Lander ES (2007). Distinguishing protein-coding and noncoding genes in the human genome. *Proc Natl Acad Sci U S A* **104**, 19428-19433.

Clarke PA, Hostein I, Banerji U, Stefano FD, Maloney A, Walton M, Judson I, & Workman P (2000). Gene expression profiling of human colon cancer cells following inhibition of signal transduction by 17-allylamino-17-demethoxygeldanamycin, an inhibitor of the hsp90 molecular chaperone. *Oncogene* **19**, 4125-4133.

Colinge J, Masselot A, Giron M, Dessingy T, & Magnin J (2003). OLAV: towards high-throughput tandem mass spectrometry data identification. *Proteomics* **3**, 1454-1463.

Concannon CG, Gorman AM, & Samali A (2003). On the role of Hsp27 in regulating apoptosis. *Apoptosis* **8**, 61-70.

Cornford PA, Dodson AR, Parsons KF, Desmond AD, Woolfenden A, Fordham M, Neoptolemos JP, Ke Y, & Foster CS (2000). Heat shock protein expression independently predicts clinical outcome in prostate cancer. *Cancer Res* **60**, 7099-7105.

Cowen LE & Lindquist S (2005). Hsp90 potentiates the rapid evolution of new traits: drug resistance in diverse fungi. *Science* **309**, 2185-2189.

Cruickshanks N, Shervington L, Patel R, Munje C, Thakkar D, & Shervington A (2010). Can hsp90alpha-targeted siRNA combined with TMZ be a future therapy for glioma? *Cancer Invest* **28**, 608-614.

Csermely P, Schnaider T, Soti C, Prohaszka Z, & Nardai G (1998). The 90-kDa molecular chaperone family: structure, function, and clinical applications. A comprehensive review. *Pharmacol Ther* **79**, 129-168.

Cullen BR (2004). Transcription and processing of human microRNA precursors. *Mol Cell* **16**, 861-865.

Cullen BR (2005). RNAi the natural way. *Nat Genet* **37**, 1163-1165.

Dan S, Shirakawa M, Mukai Y, Yoshida Y, Yamazaki K, Kawaguchi T, Matsuura M, Nakamura Y, & Yamori T (2003). Identification of candidate predictive markers of anticancer drug sensitivity using a panel of human cancer cell lines. *Cancer Sci* **94**, 1074-1082.

Didelot C, Lanneau D, Brunet M, Joly AL, De TA, Chiosis G, & Garrido C (2007). Anti-cancer therapeutic approaches based on intracellular and extracellular heat shock proteins. *Curr Med Chem* **14**, 2839-2847.

Dieffenbach CW, Lowe TM, & Dveksler GS (1993). General concepts for PCR primer design. *PCR Methods Appl* **3**, S30-S37.

Dittmar KD & Pratt WB (1997). Folding of the glucocorticoid receptor by the reconstituted Hsp90-based chaperone machinery. The initial hsp90.p60.hsp70-dependent step is sufficient for creating the steroid binding conformation. *J Biol Chem* **272**, 13047-13054.

Domon B & Aebersold R (2006). Mass spectrometry and protein analysis. *Science* **312**, 212-217.

Doran JF, Jackson P, Kynoch PA, & Thompson RJ (1983). Isolation of PGP 9.5, a new human neurone-specific protein detected by high-resolution two-dimensional electrophoresis. *J Neurochem* **40**, 1542-1547.

Duan Z, Lamendola DE, Yusuf RZ, Penson RT, Preffer FI, & Seiden MV (2002). Overexpression of human phosphoglycerate kinase 1 (PGK1) induces a multidrug resistance phenotype. *Anticancer Res* **22**, 1933-1941.

Duxbury MS, Ito H, Zinner MJ, Ashley SW, & Whang EE (2004). Focal adhesion kinase gene silencing promotes anoikis and suppresses metastasis of human pancreatic adenocarcinoma cells. *Surgery* **135**, 555-562.

Dykxhoorn DM, Schlehuber LD, London IM, & Lieberman J (2006). Determinants of specific RNA interference-mediated silencing of human beta-globin alleles differing by a single nucleotide polymorphism. *Proc Natl Acad Sci U S A* 103, 5953-5958.

Eisenberg E, Nemzer S, Kinar Y, Sorek R, Rechavi G, & Levanon EY (2005). Is abundant A-to-I RNA editing primate-specific? *Trends Genet* **21**, 77-81.

Elbashir SM, Harborth J, Lendeckel W, Yalcin A, Weber K, & Tuschl T (2001). Duplexes of 21-nucleotide RNAs mediate RNA interference in cultured mammalian cells. *Nature* **411**, 494-498.

Engelhard HH, Stelea A, & Cochran EJ (2002). Oligodendroglioma: pathology and molecular biology. *Surg Neurol* **58**, 111-117.

Ettan DIGE user manual (2002). Amersham Biosciences, UK, pp 88.

Eustace BK, Sakurai T, Stewart JK, Yimlamai D, Unger C, Zehetmeier C, Lain B, Torella C, Henning SW, Beste G, Scroggins BT, Neckers L, Ilag LL, & Jay DG (2004).

Functional proteomic screens reveal an essential extracellular role for hsp90 alpha in cancer cell invasiveness. *Nat Cell Biol* **6**, 507-514.

Falsone SF, Gesslbauer B, Rek A, & Kungl AJ (2007). A proteomic approach towards the Hsp90-dependent ubiquitinylated proteome. *Proteomics* **7**, 2375-2383.

Fenstermacher D (2005). Introduction to bioinformatics. *Journal of American Society for Science and Technology* **56**, 440-446

Fire A, Xu S, Montgomery MK, Kostas SA, Driver SE, & Mello CC (1998). Potent and specific genetic interference by double-stranded RNA in Caenorhabditis elegans. *Nature* 391, 806-811.

Frese S, Schaper M, Kuster JR, Miescher D, Jaattela M, Buehler T, & Schmid RA (2003). Cell death induced by down-regulation of heat shock protein 70 in lung cancer cell lines is p53-independent and does not require DNA cleavage. *J Thorac Cardiovasc Surg* **126**, 748-754.

Fukuyo Y, Hunt CR, & Horikoshi N (2010). Geldanamycin and its anti-cancer activities. *Cancer Lett* **290**, 24-35.

Fulda S, Wick W, Weller M, & Debatin KM (2002). Smac agonists sensitize for Apo2L/T. *Nat Med* **8**, 808-815.

Furnari FB, Fenton T, Bachoo RM, Mukasa A, Stommel JM, Stegh A, Hahn WC, Ligon KL, Louis DN, Brennan C, Chin L, DePinho RA, & Cavenee WK (2007). Malignant astrocytic glioma: genetics, biology, and paths to treatment. *Genes Dev* **21**, 2683-2710.

Gabai VL, Budagova KR, & Sherman MY (2005). Increased expression of the major heat shock protein Hsp72 in human prostate carcinoma cells is dispensable for their viability but confers resistance to a variety of anticancer agents. *Oncogene* **24**, 3328-3338.

Gallo A & Galardi S (2008). A-to-I RNA editing and cancer: from pathology to basic science. *RNA Biol* **5**, 135-139.

Gao S, Nielsen BS, Krogdahl A, Sorensen JA, Tagesen J, Dabelsteen S, Dabelsteen E, & Andreasen PA (2010). Epigenetic alterations of the SERPINE1 gene in oral squamous cell carcinomas and normal oral mucosa. *Genes Chromosomes Cancer* **49**, 526-538.

Garrido C, Brunet M, Didelot C, Zermati Y, Schmitt E, & Kroemer G (2006). Heat shock proteins 27 and 70: anti-apoptotic proteins with tumorigenic properties. *Cell Cycle* **5**, 2592-2601.

Geer LY, Markey SP, Kowalak JA, Wagner L, Xu M, Maynard DM, Yang X, Shi W, & Bryant SH (2004). Open mass spectrometry search algorithm. *J Proteome Res* **3**, 958-964.

Georges E & Prinos P (2007). Calumenin directed diagnostics and therapeutics for cancer and chemotherapeutic drug resistance. *United States Patent Application Publication* 1-37.

Ghobrial IM, McCormick DJ, Kaufmann SH, Leontovich AA, Loegering DA, Dai NT, Krajnik KL, Stenson MJ, Melhem MF, Novak AJ, Ansell SM, & Witzig TE (2005). Proteomic analysis of mantle-cell lymphoma by protein microarray. *Blood* **105**, 3722-3730.

Godovac-Zimmermann J, Soskic V, Poznanovic S, & Brianza F (1999). Functional proteomics of signal transduction by membrane receptors. *Electrophoresis* **20**, 952-961.

Goetz MP, Toft D, Reid J, Ames M, Stensgard B, Safgren S, Adjei AA, Sloan J, Atherton P, Vasile V, Salazaar S, Adjei A, Croghan G, & Erlichman C (2005). Phase I trial of 17-allylamino-17-demethoxygeldanamycin in patients with advanced cancer. *J Clin Oncol* **23**, 1078-1087.

Goetz MP, Toft DO, Ames MM, & Erlichman C (2003). The Hsp90 chaperone complex as a novel target for cancer therapy. *Ann Oncol* **14**, 1169-1176.

Gradin K, Toftgard R, Poellinger L, & Berghard A (1999). Repression of dioxin signal transduction in fibroblasts. Identification Of a putative repressor associated with Arnt. *J Biol Chem* **274**, 13511-13518.

Graham G, Sharp PJ, Li Q, Wilson PW, Talbot RT, Downing A, & Boswell T (2009). HSP90B1, a thyroid hormone-responsive heat shock protein gene involved in photoperiodic signaling. *Brain Res Bull* **79**, 201-207.

Grem JL, Morrison G, Guo XD, Agnew E, Takimoto CH, Thomas R, Szabo E, Grochow L, Grollman F, Hamilton JM, Neckers L, & Wilson RH (2005). Phase I and pharmacologic study of 17-(allylamino)-17-demethoxygeldanamycin in adult patients with solid tumors. *J Clin Oncol* **23**, 1885-1893.

Grunweller A, Gillen C, Erdmann VA, & Kurreck J (2003). Cellular uptake and localization of a Cy3-labeled siRNA specific for the serine/threonine kinase Pim-1. *Oligonucleotides* **13**, 345-352.

Guo F, Rocha K, Bali P, Pranpat M, Fiskus W, Boyapalle S, Kumaraswamy S, Balasis M, Greedy B, Armitage ES, Lawrence N, & Bhalla K (2005). Abrogation of heat shock protein 70 induction as a strategy to increase antileukemia activity of heat shock

protein 90 inhibitor 17-allylamino-demethoxy geldanamycin. *Cancer Res* **65**, 10536-10544.

Gupta RS (1995). Phylogenetic analysis of the 90 kD heat shock family of protein sequences and an examination of the relationship among animals, plants, and fungi species. *Mol Biol Evol* **12**, 1063-1073.

Gupta V, Su YS, Wang W, Kardosh A, Liebes LF, Hofman FM, Schonthal AH, & Chen TC (2006). Enhancement of glioblastoma cell killing by combination treatment with temozolomide and tamoxifen or hypericin. *Neurosurg Focus* **20**, E20 (An Abstract).

Harrison JD, Jones JA, Ellis IO, & Morris DL (1991). Oestrogen receptor D5 antibody is an independent negative prognostic factor in gastric cancer. *Br J Surg* **78**, 334-336.

Hartl FU & Hayer-Hartl M (2002). Molecular chaperones in the cytosol: from nascent chain to folded protein. *Science* **295**, 1852-1858.

Heath EI, Gaskins M, Pitot HC, Pili R, Tan W, Marschke R, Liu G, Hillman D, Sarkar F, Sheng S, Erlichman C, & Ivy P (2005). A phase II trial of 17-allylamino-17-demethoxygeldanamycin in patients with hormone-refractory metastatic prostate cancer. *Clin Prostate Cancer* **4**, 138-141.

Heath EI, Hillman DW, Vaishampayan U, Sheng S, Sarkar F, Harper F, Gaskins M, Pitot HC, Tan W, Ivy SP, Pili R, Carducci MA, Erlichman C, & Liu G (2008). A phase II trial of 17-allylamino-17-demethoxygeldanamycin in patients with hormone-refractory metastatic prostate cancer. *Clin Cancer Res* **14**, 7940-7946.

Holtkamp N, Afanasieva A, Elstner A, van Landeghem FK, Konneker M, Kuhn SA, Kettenmann H, & von DA (2005). Brain slice invasion model reveals genes differentially regulated in glioma invasion. *Biochem Biophys Res Commun* **336**, 1227-1233.

Hostein I, Robertson D, DiStefano F, Workman P, & Clarke PA (2001). Inhibition of signal transduction by the Hsp90 inhibitor 17-allylamino-17-demethoxygeldanamycin results in cytostasis and apoptosis. *Cancer Res* **61**, 4003-4009.

Hua LV, Green M, Warsh JJ, & Li PP (2000). Lithium regulation of aldolase A expression in the rat frontal cortex: identification by differential display. *Biol Psychiatry* **48**, 58-64.

Huang TJ, Lee TT, Lee WC, Lai YK, Yu JS, & Yang SD (1994). Autophosphorylation-dependent protein kinase phosphorylates Ser25, Ser38, Ser65, Ser71, and Ser411 in vimentin and thereby inhibits cytoskeletal intermediate filament assembly. *J Protein Chem* **13**, 517-525.

Huot J, Houle F, Marceau F, & Landry J (1997). Oxidative stress-induced actin reorganization mediated by the p38 mitogen-activated protein kinase/heat shock protein 27 pathway in vascular endothelial cells. *Circ Res* **80**, 383-392.

Idbaih A, Ducray F, Sierra Del RM, Hoang-Xuan K, & Delattre JY (2008). Therapeutic application of noncytotoxic molecular targeted therapy in gliomas: growth factor receptors and angiogenesis inhibitors. *Oncologist* **13**, 978-992.

Idowu O, Akang E, & Malomo A (2007). Symptomatic primary intracranial neoplasms in Nigeria, West Africa. *J Neuro Sci* **24**, 212-218

Ingber DE (2003). Tensegrity I. Cell structure and hierarchical systems biology. *J Cell Sci* **116**, 1157-1173.

Jang IK, Hu R, Lacana E, D'Adamio L, & Gu H (2002). Apoptosis-linked gene 2-deficient mice exhibit normal T-cell development and function. *Mol Cell Biol* **22**, 4094-4100.

Jarve A, Muller J, Kim IH, Rohr K, MacLean C, Fricker G, Massing U, Eberle F, Dalpke A, Fischer R, Trendelenburg MF, & Helm M (2007). Surveillance of siRNA integrity by FRET imaging. *Nucleic Acids Res* **35**, e124 (An Abstract).

Jeong M, Kwon YS, Park SH, Kim CY, Jeun SS, Song KW, Ko Y, Robbins PD, Billiar TR, Kim BM, & Seol DW (2009). Possible novel therapy for malignant gliomas with secretable trimeric TRAIL. *PLoS One* **4**, e4545 (An Abstract).

Jimenez-Marin A, Collado-Romero M, Ramirez-Boo M, Arce C, & Garrido JJ (2009). Biological pathway analysis by ArrayUnlock and Ingenuity Pathway Analysis. *BMC Proc* 3 Suppl **4**, S6 (An Abstract).

Kabuta T, Furuta A, Aoki S, Furuta K, & Wada K (2008). Aberrant interaction between Parkinson disease-associated mutant UCH-L1 and the lysosomal receptor for chaperone-mediated autophagy. *J Biol Chem* **283**, 23731-23738.

Kamal A, Boehm MF, & Burrows FJ (2004). Therapeutic and diagnostic implications of Hsp90 activation. *Trends Mol Med* **10**, 283-290.

Kamal A, Thao L, Sensintaffar J, Zhang L, Boehm MF, Fritz LC, & Burrows FJ (2003). A high-affinity conformation of Hsp90 confers tumour selectivity on Hsp90 inhibitors. *Nature* **425**, 407-410.

Kang BH & Altieri DC (2009). Compartmentalized cancer drug discovery targeting mitochondrial Hsp90 chaperones. *Oncogene* **28**, 3681-3688.

Kang EH, Kim DJ, Lee EY, Lee YJ, Lee EB, & Song YW (2009). Downregulation of heat shock protein 70 protects rheumatoid arthritis fibroblast-like synoviocytes from nitric oxide-induced apoptosis. *Arthritis Res Ther* **11**, R130 (An Abstract).

Katsumoto T, Mitsushima A, & Kurimura T (1990). The role of the vimentin intermediate filaments in rat 3Y1 cells elucidated by immunoelectron microscopy and computer-graphic reconstruction. *Biol Cell* **68**, 139-146.

Kaur J, Kaur J, & Ralhan R (2000). Induction of apoptosis by abrogation of HSP70 expression in human oral cancer cells. *Int J Cancer* **85**, 1-5.

Khalil AA & Madhamshetty J (2006). Proteome analysis of whole cell lysates of human glioblastoma cells during passages. *Res J Med Med Sci* **1**, 120-131

Khatua S, Peterson KM, Brown KM, Lawlor C, Santi MR, LaFleur B, Dressman D, Stephan DA, & MacDonald TJ (2003). Overexpression of the EGFR/FKBP12/HIF-2alpha pathway identified in childhood astrocytomas by angiogenesis gene profiling. *Cancer Res* **63**, 1865-1870.

Khoshnoodi J, Pedchenko V, & Hudson BG (2008). Mammalian collagen IV. *Microsc Res Tech* **71**, 357-370.

Kim DD, Kim TT, Walsh T, Kobayashi Y, Matise TC, Buyske S, & Gabriel A (2004). Widespread RNA editing of embedded alu elements in the human transcriptome. *Genome Res* **14**, 1719-1725.

Kim DH, Behlke MA, Rose SD, Chang MS, Choi S, & Rossi JJ (2005). Synthetic dsRNA Dicer substrates enhance RNAi potency and efficacy. *Nat Biotechnol* **23**, 222-226.

King KL, Li AF, Chau GY, Chi CW, Wu CW, Huang CL, & Lui WY (2000). Prognostic significance of heat shock protein-27 expression in hepatocellular carcinoma and its relation to histologic grading and survival. *Cancer* **88**, 2464-2470.

Kleihues P & Sobin LH (2000). World Health Organization classification of tumors. *Cancer* **88**, 2887 (Electronic Article).

Kreth S, Heyn J, Grau S, Kretzschmar HA, Egensperger R, & Kreth FW (2010). Identification of valid endogenous control genes for determining gene expression in human glioma. *Neuro Oncol* **12**, 570-579.

Kumar P, Wu H, McBride JL, Jung KE, Kim MH, Davidson BL, Lee SK, Shankar P, & Manjunath N (2007). Transvascular delivery of small interfering RNA to the central nervous system. *Nature* **448**, 39-43.

la Cour JM, Hoj BR, Mollerup J, Simon R, Sauter G, & Berchtold MW (2008). The apoptosis linked gene ALG-2 is dysregulated in tumors of various origin and contributes to cancer cell viability. *Mol Oncol* **1**, 431-439.

Lanneau D, De TA, Maurel S, Didelot C, & Garrido C (2007). Apoptosis versus cell differentiation: role of heat shock proteins HSP90, HSP70 and HSP27. *Prion* **1**, 53-60.

Lavictoire SJ, Parolin DA, Klimowicz AC, Kelly JF, & Lorimer IA (2003). Interaction of Hsp90 with the nascent form of the mutant epidermal growth factor receptor EGFRvIII. *J Biol Chem* **278**, 5292-5299.

Lee JM, Sarosy GA, Annunziata CM, Azad N, Minasian L, Kotz H, Squires J, Houston N, & Kohn EC (2010). Combination therapy: intermittent sorafenib with bevacizumab yields activity and decreased toxicity. *Br J Cancer* **102**, 495-499.

Lee Y, Ahn C, Han J, Choi H, Kim J, Yim J, Lee J, Provost P, Radmark O, Kim S, & Kim VN (2003). The nuclear RNase III Drosha initiates microRNA processing. *Nature* **425**, 415-419.

Lee Y, Jeon K, Lee JT, Kim S, & Kim VN (2002). MicroRNA maturation: stepwise processing and subcellular localization. *EMBO J* **21**, 4663-4670.

Levanon EY, Eisenberg E, Yelin R, Nemzer S, Hallegger M, Shemesh R, Fligelman ZY, Shoshan A, Pollock SR, Sztybel D, Olshansky M, Rechavi G, & Jantsch MF (2004). Systematic identification of abundant A-to-I editing sites in the human transcriptome. *Nat Biotechnol* **22**, 1001-1005.

Levanon K, Eisenberg E, Rechavi G, & Levanon EY (2005). Letter from the editor: Adenosine-to-inosine RNA editing in Alu repeats in the human genome. *EMBO Rep* **6**, 831-835.

Li K, Lin SY, Brunicardi FC, & Seu P (2003). Use of RNA interference to target cyclin E-overexpressing hepatocellular carcinoma. *Cancer Res* **63**, 3593-3597.

Li Z & Srivastava P (2004). Heat-shock proteins. *Curr Protoc Immunol* **Appendix 1**, Appendix 1T.

Lim LH & Pervaiz S (2007). Annexin 1: the new face of an old molecule. *FASEB J* **21**, 968-975.

Lin TY, Chang JT, Wang HM, Chan SH, Chiu CC, Lin CY, Fan KH, Liao CT, Chen IH, Liu TZ, Li HF, & Cheng AJ (2010). Proteomics of the radioresistant phenotype in head-and-neck cancer: Gp96 as a novel prediction marker and sensitizing target for radiotherapy. *Int J Radiat Oncol Biol Phys* **78**, 246-256.

Lin YM, Chen YR, Lin JR, Wang WJ, Inoko A, Inagaki M, Wu YC, & Chen RH (2008). eIF3k regulates apoptosis in epithelial cells by releasing caspase 3 from keratin-containing inclusions. *J Cell Sci* **121**, 2382-2393.

Loeffler-Ragg J, Sarg B, Muller D, Auer T, Linder H, & Zwierzina H (2008). Proteomics, a new tool to monitor cancer therapy? *Memo* **1**, 129-136.

Lugo TG, Pendergast AM, Muller AJ, & Witte ON (1990). Tyrosine kinase activity and transformation potency of bcr-abl oncogene products. *Science* **247**, 1079-1082.

Lui JC & Kong SK (2007). Heat shock protein 70 inhibits the nuclear import of apoptosis-inducing factor to avoid DNA fragmentation in TF-1 cells during erythropoiesis. *FEBS Lett* **581**, 109-117.

Lund E, Guttinger S, Calado A, Dahlberg JE, & Kutay U (2004). Nuclear export of microRNA precursors. *Science* **303**, 95-98.

Luo W, Sun W, Taldone T, Rodina A, & Chiosis G (2010). Heat shock protein 90 in neurodegenerative diseases. *Mol Neurodegener* **5**, 24 (An Abstract).

Maloney A, Clarke PA, Naaby-Hansen S, Stein R, Koopman JO, Akpan A, Yang A, Zvelebil M, Cramer R, Stimson L, Aherne W, Banerji U, Judson I, Sharp S, Powers M, deBilly E, Salmons J, Walton M, Burlingame A, Waterfield M, & Workman P (2007). Gene and protein expression profiling of human ovarian cancer cells treated with the heat shock protein 90 inhibitor 17-allylamino-17-demethoxygeldanamycin. *Cancer Res* **67**, 3239-3253.

Mann M, Hojrup P, & Roepstorff P (1993). Use of mass spectrometric molecular weight information to identify proteins in sequence databases. *Biol Mass Spectrom* **22**, 338-345.

Marouga R, David S, & Hawkins E (2005). The development of the DIGE system: 2D fluorescence difference gel analysis technology. *Anal Bioanal Chem* **382**, 669-678.

Marques JT, Devosse T, Wang D, Zamanian-Daryoush M, Serbinowski P, Hartmann R, Fujita T, Behlke MA, & Williams BR (2006). A structural basis for discriminating between self and nonself double-stranded RNAs in mammalian cells. *Nat Biotechnol* **24**, 559-565.

Martin S, Cosset EC, Terrand J, Maglott A, Takeda K, & Dontenwill M (2009). Caveolin-1 regulates glioblastoma aggressiveness through the control of alpha(5)beta(1) integrin expression and modulates glioblastoma responsiveness to SJ749, an alpha(5)beta(1) integrin antagonist. *Biochim Biophys Acta* **1793**, 354-367.

Martinez LA, Naguibneva I, Lehrmann H, Vervisch A, Tchenio T, Lozano G, & Harel-Bellan A (2002). Synthetic small inhibiting RNAs: efficient tools to inactivate oncogenic mutations and restore p53 pathways. *Proc Natl Acad Sci U S A* **99**, 14849-14854.

Matranga C, Tomari Y, Shin C, Bartel DP, & Zamore PD (2005). Passenger-strand cleavage facilitates assembly of siRNA into Ago2-containing RNAi enzyme complexes. *Cell* **123**, 607-620.

Mayer MP & Bukau B (1998). Hsp70 chaperone systems: diversity of cellular functions and mechanism of action. *Biol Chem* **379**, 261-268.

McAnuff MA, Rettig GR, & Rice KG (2007). Potency of siRNA versus shRNA mediated knockdown in vivo. *J Pharm Sci* **96**, 2922-2930.

McCollum AK, Teneyck CJ, Sauer BM, Toft DO, & Erlichman C (2006). Up-regulation of heat shock protein 27 induces resistance to 17-allylamino-demethoxygeldanamycin through a glutathione-mediated mechanism. *Cancer Res* **66**, 10967-10975.

Medzihradszky KF, Campbell JM, Baldwin MA, Falick AM, Juhasz P, Vestal ML, & Burlingame AL (2000). The characteristics of peptide collision-induced dissociation using a high-performance MALDI-TOF/TOF tandem mass spectrometer. *Anal Chem* **72**, 552-558.

Mehlen P, Kretz-Remy C, Preville X, & Arrigo AP (1996). Human hsp27, Drosophila hsp27 and human alphaB-crystallin expression-mediated increase in glutathione is essential for the protective activity of these proteins against TNFalpha-induced cell death. *EMBO J* **15**, 2695-2706.

Mehrian SR, Reichardt JK, Ya-Hsuan H, Kremen TJ, Liau LM, Cloughesy TF, Mischel PS, & Nelson SF (2005). Robustness of gene expression profiling in glioma specimen samplings and derived cell lines. *Brain Res Mol Brain Res* **136**, 99-103.

Messaoudi S, Peyrat JF, Brion JD, & Alami M (2008). Recent advances in Hsp90 inhibitors as antitumor agents. *Anticancer Agents Med Chem* **8**, 761-782.

Miller P, DiOrio C, Moyer M, Schnur RC, Bruskin A, Cullen W, & Moyer JD (1994). Depletion of the erbB-2 gene product p185 by benzoquinoid ansamycins. *Cancer Res* **54**, 2724-2730.

Mimnaugh EG, Chavany C, & Neckers L (1996). Polyubiquitination and proteasomal degradation of the p185c-erbB-2 receptor protein-tyrosine kinase induced by geldanamycin. *J Biol Chem* **271**, 22796-22801.

Minden J (2007). Comparative proteomics and difference gel electrophoresis. *Biotechniques* **43**, 739, 741, 743.

Miyagishi M, Hayashi M, & Taira K (2003). Comparision of the suppressive effects of antisense oligonucleotides and siRNAs directed against the same targets in mammalian cell lines. *Antisense Nucleic Acid Drug Dev.* **13**, 1-7

Modi S, Stopeck AT, Gordon MS, Mendelson D, Solit DB, Bagatell R, Ma W, Wheler J, Rosen N, Norton L, Cropp GF, Johnson RG, Hannah AL, & Hudis CA (2007). Combination of trastuzumab and tanespimycin (17-AAG, KOS-953) is safe and

active in trastuzumab-refractory HER-2 overexpressing breast cancer: a phase I dose-escalation study. *J Clin Oncol* **25**, 5410-5417.

Mohammed, K. (2007) A study of gene expression in human normal and carcinogenic cell lines using qRT-PCR. Theses Collection 572.865/MOH University of Central Lancashire theses collection.

Morishima Y, Murphy PJ, Li DP, Sanchez ER, & Pratt WB (2000). Stepwise assembly of a glucocorticoid receptor.hsp90 heterocomplex resolves two sequential ATP-dependent events involving first hsp70 and then hsp90 in opening of the steroid binding pocket. *J Biol Chem* **275**, 18054-18060.

Mork SJ, Lindegaard KF, Halvorsen TB, Lehmann EH, Solgaard T, Hatlevoll R, Harvei S, & Ganz J (1985). Oligodendroglioma: incidence and biological behavior in a defined population. *J Neurosurg* **63**, 881-889.

Mosser DD & Morimoto RI (2004). Molecular chaperones and the stress of oncogenesis. *Oncogene* **23**, 2907-2918.

Munster PN, Marchion DC, Basso AD, & Rosen N (2002). Degradation of HER2 by ansamycins induces growth arrest and apoptosis in cells with HER2 overexpression via a HER3, phosphatidylinositol 3'-kinase-AKT-dependent pathway. *Cancer Res* **62**, 3132-3137.

Nakagomi S, Suzuki Y, Namikawa K, Kiryu-Seo S, & Kiyama H (2003). Expression of the activating transcription factor 3 prevents c-Jun N-terminal kinase-induced neuronal death by promoting heat shock protein 27 expression and Akt activation. *J Neurosci* **23**, 5187-5196.

Nakahira S, Nakamori S, Tsujie M, Takahashi Y, Okami J, Yoshioka S, Yamasaki M, Marubashi S, Takemasa I, Miyamoto A, Takeda Y, Nagano H, Dono K, Umeshita K, Sakon M, & Monden M (2007). Involvement of ribonucleotide reductase M1

subunit overexpression in gemcitabine resistance of human pancreatic cancer. *Int J Cancer* **120**, 1355-1363.

Neckers L & Lee YS (2003). Cancer: the rules of attraction. *Nature* **425**, 357-359.

Neckers L (2002). Hsp90 inhibitors as novel cancer chemotherapeutic agents. *Trends Mol Med* **8**, S55-S61.

Neckers L (2006). Chaperoning oncogenes: Hsp90 as a target of geldanamycin. *Handb Exp Pharmacol* **172**, 259-277.

Neckers L (2007). Heat shock protein 90: the cancer chaperone. *J Biosci* **32**, 517-530.

Neckers L, Schulte TW, & Mimnaugh E (1999). Geldanamycin as a potential anti-cancer agent: its molecular target and biochemical activity. *Invest New Drugs* **17**, 361-373.

Neidle S, (2007). *Cancer drug design and discovery*. Academic Press, London, 336-343.

Ngan CY, Yamamoto H, Seshimo I, Tsujino T, Man-i M, Ikeda JI, Konishi K, Takemasa I, Ikeda M, Sekimoto M, Matsuura N, & Monden M (2007). Quantitative evaluation of vimentin expression in tumour stroma of colorectal cancer. *Br J Cancer* **96**, 986-992.

Nguyen DM, Desai S, Chen A, Weiser TS, & Schrump DS (2000). Modulation of metastasis phenotypes of non-small cell lung cancer cells by 17-allylamino 17-demethoxy geldanamycin. *Ann Thorac Surg* **70**, 1853-1860.

Nimmanapalli R, O'Bryan E, & Bhalla K (2001). Geldanamycin and its analogue 17-allylamino-17-demethoxygeldanamycin lowers Bcr-Abl levels and induces apoptosis and differentiation of Bcr-Abl-positive human leukemic blasts. *Cancer Res* **61**, 1799-1804.

Nusse M & Marx K (1997). Flow cytometric analysis of micronuclei in cell cultures and human lymphocytes: advantages and disadvantages. *Mutat Res* 392, 109-115.

Nygaard SJ, Haugland HK, Kristoffersen EK, Lund-Johansen M, Laerum OD, & Tysnes OB (1998). Expression of annexin II in glioma cell lines and in brain tumor biopsies. *J Neurooncol* **38**, 11-18.

Nylandsted J, Brand K, & Jaattela M (2000). Heat shock protein 70 is required for the survival of cancer cells. *Ann N Y Acad Sci* **926,** 122-125.

Oehler R, Schmierer B, Zellner M, Prohaska R, & Roth E (2000). Endothelial cells downregulate expression of the 70 kDa heat shock protein during hypoxia. *Biochem Biophys Res Commun* **274**, 542-547.

Ohgaki H (2005). Genetic pathways to glioblastomas. *Neuropathology* **25**, 1-7.

Ohnishi K, Yokota S, Takahashi A, & Ohnishi T (2006). Induction of radiation resistance by a heat shock protein inhibitor, KNK437, in human glioblastoma cells. *Int J Radiat Biol* **82**, 569-575.

Oudard S, Arvelo F, Miccoli L, Apiou F, Dutrillaux AM, Poisson M, Dutrillaux B, & Poupon MF (1996). High glycolysis in gliomas despite low hexokinase transcription and activity correlated to chromosome 10 loss. *Br J Cancer* **74**, 839-845.

Pacey S, Banerji U, Judson I, & Workman P (2006). Hsp90 inhibitors in the clinic. *Handb Exp Pharmacol* **172**, 331-358.

Pal A, Ahmad A, Khan S, Sakabe I, Zhang C, Kasid UN, & Ahmad I (2005). Systemic delivery of RafsiRNA using cationic cardiolipin liposomes silences Raf-1 expression and inhibits tumor growth in xenograft model of human prostate cancer. *Int J Oncol* **26**, 1087-1091.

Pappin DJ, Hojrup P, & Bleasby AJ (1993). Rapid identification of proteins by peptide-mass fingerprinting. *Curr Biol* **3**, 327-332.

Park CK, Jung JH, Park SH, Jung HW, & Cho BK (2009). Multifarious proteomic signatures and regional heterogeneity in glioblastomas. *J Neurooncol* **94**, 31-39.

Parrella P, Mazzarelli P, Signori E, Perrone G, Marangi GF, Rabitti C, Delfino M, Prencipe M, Gallo AP, Rinaldi M, Fabbrocini G, Delfino S, Persichetti P, & Fazio VM (2006). Expression and heterodimer-binding activity of Ku70 and Ku80 in human non-melanoma skin cancer. *J Clin Pathol* **59**, 1181-1185.

Pearl LH & Prodromou C (2001). Structure, function, and mechanism of the Hsp90 molecular chaperone. *Adv Protein Chem* **59**, 157-186.

Penuelas S, Noe V, & Ciudad CJ (2005). Modulation of IMPDH2, survivin, topoisomerase I and vimentin increases sensitivity to methotrexate in HT29 human colon cancer cells. *FEBS J* **272**, 696-710.

Petrash JM (2004). All in the family: aldose reductase and closely related aldo-keto reductases. *Cell Mol Life Sci* **61**, 737-749.

Picard D (2002). Heat-shock protein 90, a chaperone for folding and regulation. *Cell Mol Life Sci* **59**, 1640-1648.

Pocaly M, Lagarde V, Etienne G, Ribeil JA, Claverol S, Bonneu M, Moreau-Gaudry F, Guyonnet-Duperat V, Hermine O, Melo JV, Dupouy M, Turcq B, Mahon FX, &

Pasquet JM (2007). Overexpression of the heat-shock protein 70 is associated to imatinib resistance in chronic myeloid leukemia. *Leukemia* **21**, 93-101.

Powers MV & Workman P (2007). Inhibitors of the heat shock response: biology and pharmacology. *FEBS Lett* **581**, 3758-3769.

Powers MV, Clarke PA, & Workman P (2008). Dual targeting of HSC70 and HSP72 inhibits HSP90 function and induces tumor-specific apoptosis. *Cancer Cell* **14**, 250-262.

Premkumar DR, Arnold B, Jane EP, & Pollack IF (2006). Synergistic interaction between 17-AAG and phosphatidylinositol 3-kinase inhibition in human malignant glioma cells. *Mol Carcinog* **45**, 47-59.

Prodromou C, Panaretou B, Chohan S, Siligardi G, O'Brien R, Ladbury JE, Roe SM, Piper PW, & Pearl LH (2000). The ATPase cycle of Hsp90 drives a molecular 'clamp' via transient dimerization of the N-terminal domains. *EMBO J* **19**, 4383-4392.

Pucci S, Bonanno E, Pichiorri F, Angeloni C, & Spagnoli LG (2004). Modulation of different clusterin isoforms in human colon tumorigenesis. *Oncogene* **23**, 2298-2304.

Rand TA, Ginalski K, Grishin NV, & Wang X (2004). Biochemical identification of Argonaute 2 as the sole protein required for RNA-induced silencing complex activity. *Proc Natl Acad Sci U S A* **101**, 14385-14389.

Rand TA, Petersen S, Du F, & Wang X (2005). Argonaute2 cleaves the anti-guide strand of siRNA during RISC activation. *Cell* **123**, 621-629.

Rao DD, Vorhies JS, Senzer N, & Nemunaitis J (2009). siRNA vs. shRNA: similarities and differences. *Adv Drug Deliv Rev* **61**, 746-759.

Rathmell WK & Chu G (1994). Involvement of the Ku autoantigen in the cellular response to DNA double-strand breaks. *Proc Natl Acad Sci U S A* **91**, 7623-7627.

Redlak MJ & Miller TA (2010). Targeting PI3K/Akt/HSP90 Signaling Sensitizes Gastric Cancer Cells to Deoxycholate-Induced Apoptosis. *Dig Dis Sci* **56**, 323-329.

Rich JN, Hans C, Jones B, Iversen ES, McLendon RE, Rasheed BK, Dobra A, Dressman HK, Bigner DD, Nevins JR, & West M (2005). Gene expression profiling and genetic markers in glioblastoma survival. *Cancer Res* **65**, 4051-4058.

Richter K & Buchner J (2001). Hsp90: chaperoning signal transduction. *J Cell Physiol* **188**, 281-290.

Richter K & Buchner J (2006). Hsp90: twist and fold. *Cell* **127**, 251-253.

Ritossa P (1962). [Problems of prophylactic vaccinations of infants.]. *Riv Ist Sieroter Ital* **37**, 79-108.

Rodina A, Vilenchik M, Moulick K, Aguirre J, Kim J, Chiang A, Litz J, Clement CC, Kang Y, She Y, Wu N, Felts S, Wipf P, Massague J, Jiang X, Brodsky JL, Krystal GW, & Chiosis G (2007). Selective compounds define Hsp90 as a major inhibitor of apoptosis in small-cell lung cancer. *Nat Chem Biol* **3**, 498-507.

Roe SM, Prodromou C, O'Brien R, Ladbury JE, Piper PW, & Pearl LH (1999). Structural basis for inhibition of the Hsp90 molecular chaperone by the antitumor antibiotics radicicol and geldanamycin. *J Med Chem* **42**, 260-266.

Ronnen EA, Kondagunta GV, Ishill N, Sweeney SM, Deluca JK, Schwartz L, Bacik J, & Motzer RJ (2006). A phase II trial of 17-(Allylamino)-17-demethoxygeldanamycin in patients with papillary and clear cell renal cell carcinoma. *Invest New Drugs* **24**, 543-546.

Ross ME, Zhou X, Song G, Shurtleff SA, Girtman K, Williams WK, Liu HC, Mahfouz R, Raimondi SC, Lenny N, Patel A, & Downing JR (2003). Classification of pediatric acute lymphoblastic leukemia by gene expression profiling. *Blood* **102**, 2951-2959.

Salisbury AJ & Macaulay VM (2003). Development of molecular agents for IGF receptor targeting. *Horm Metab Res* **35**, 843-849.

Sameni M, Dosescu J, & Sloane BF (2001). Imaging proteolysis by living human glioma cells. *Biol Chem* **382**, 785-788.

Sangster TA, Lindquist S, & Queitsch C (2004). Under cover: causes, effects and implications of Hsp90-mediated genetic capacitance. *Bioessays* **26**, 348-362.

Sano M, Sierant M, Miyagishi M, Nakanishi M, Takagi Y, & Sutou S (2008). Effect of asymmetric terminal structures of short RNA duplexes on the RNA interference activity and strand selection. *Nucleic Acids Res* **36**, 5812-5821.

Saraswat M, Mrudula T, Kumar PU, Suneetha A, Rao Rao TS, Srinivasulu M, & Reddy B (2006). Overexpression of aldose reductase in human cancer tissues. *Med Sci Monit* **12**, CR525-CR529.

Sato S, Shimizu K, Sugimura T, Takaoka T, & Katsuta H (1972). Aldolase C in cultured mouse glioblastoma cells. *Cancer Res* **32**, 1290-1292.

Sauvageot CM, Weatherbee JL, Kesari S, Winters SE, Barnes J, Dellagatta J, Ramakrishna NR, Stiles CD, Kung AL, Kieran MW, & Wen PY (2009). Efficacy of the HSP90 inhibitor 17-AAG in human glioma cell lines and tumorigenic glioma stem cells. *Neuro Oncol* **11**, 109-121.

Scherr M, Battmer K, Winkler T, Heidenreich O, Ganser A, & Eder M (2003). Specific inhibition of bcr-abl gene expression by small interfering RNA. *Blood* **101**, 1566-1569.

Schild H & Rammensee HG (2000). gp96--the immune system's Swiss army knife. *Nat Immunol* **1**, 100-101.

Schittenhelm J, Trautmann K, Tabatabai G, Hermann C, Meyermann R, & Beschorner R (2009). Comparative analysis of annexin-1 in neuroepithelial tumors shows altered expression with the grade of malignancy but is not associated with survival. *Mod Pathol* **22**, 1600-1611.

Schmitt E, Gehrmann M, Brunet M, Multhoff G, & Garrido C (2007). Intracellular and extracellular functions of heat shock proteins: repercussions in cancer therapy. *J Leukoc Biol* **81**, 15-27.

Schulte TW, An WG, & Neckers LM (1997). Geldanamycin-induced destabilization of Raf-1 involves the proteasome. *Biochem Biophys Res Commun* **239**, 655-659.

Schulte TW, Blagosklonny MV, Ingui C, & Neckers L (1995). Disruption of the Raf-1-Hsp90 molecular complex results in destabilization of Raf-1 and loss of Raf-1-Ras association. *J Biol Chem* **270**, 24585-24588.

Schulte TW, Blagosklonny MV, Romanova L, Mushinski JF, Monia BP, Johnston JF, Nguyen P, Trepel J, & Neckers LM (1996). Destabilization of Raf-1 by geldanamycin leads to disruption of the Raf-1-MEK-mitogen-activated protein kinase signalling pathway. *Mol Cell Biol* **16**, 5839-5845.

Seidberg NA, Clark RS, Zhang X, Lai Y, Chen M, Graham SH, Kochanek PM, Watkins SC, & Marion DW (2003). Alterations in inducible 72-kDa heat shock protein and

the chaperone cofactor BAG-1 in human brain after head injury. *J Neurochem* **84**, 514-521.

Sharp PA & Zamore PD (2000). Molecular biology. RNA interference. *Science* **287**, 2431-2433.

Sharp S & Workman P (2006). Inhibitors of the HSP90 molecular chaperone: current status. *Adv Cancer Res* **95**, 323-348.

Shen G, Liang S, Xu Z, Zhou L, Xiao S, Xia X, Li R, Liao Y, You C, & Wei Y (2010). Downregulated expression of HSP27 in human low-grade glioma tissues discovered by a quantitative proteomic analysis. *Proteome Sci* **8**, 17 (An Abstract).

Shervington A, Cruickshanks N, Lea R, Roberts G, Dawson T, & Shervington L (2008). Can the lack of HSP90alpha protein in brain normal tissue and cell lines, rationalise it as a possible therapeutic target for gliomas? *Cancer Invest* **26**, 900-904.

Shervington A, Mohammed K, Patel R, & Lea R (2007). Identification of a novel co-transcription of P450/1A1 with telomerase in A549. *Gene* **388**, 110-116.

Shirahata A, Sakata M, Sakuraba K, Goto T, Mizukami H, Saito M, Ishibashi K, Kigawa G, Nemoto H, Sanada Y, & Hibi K (2009). Vimentin methylation as a marker for advanced colorectal carcinoma. *Anticancer Res* **29**, 279-281.

Shirahata M, Iwao-Koizumi K, Saito S, Ueno N, Oda M, Hashimoto N, Takahashi JA, & Kato K (2007). Gene expression-based molecular diagnostic system for malignant gliomas is superior to histological diagnosis. *Clin Cancer Res* **13**, 7341-7356.

Siegelin MD, Habel A, & Gaiser T (2009). 17-AAG sensitized malignant glioma cells to death-receptor mediated apoptosis. *Neurobiol Dis* **33**, 243-249.

Singh A, Boldin-Adamsky S, Thimmulappa RK, Rath SK, Ashush H, Coulter J, Blackford A, Goodman SN, Bunz F, Watson WH, Gabrielson E, Feinstein E, & Biswal S (2008). RNAi-mediated silencing of nuclear factor erythroid-2-related factor 2 gene expression in non-small cell lung cancer inhibits tumor growth and increases efficacy of chemotherapy. *Cancer Res* **68**, 7975-7984.

Siolas D, Lerner C, Burchard J, Ge W, Linsley PS, Paddison PJ, Hannon GJ, & Cleary MA (2005). Synthetic shRNAs as potent RNAi triggers. *Nat Biotechnol* **23**, 227-231.

Skynner HA, Amos DP, Murray F, Salim K, Knowles MR, Munoz-Sanjuan I, Camargo LM, Bonnert TP, & Guest PC (2006). Proteomic analysis identifies alterations in cellular morphology and cell death pathways in mouse brain after chronic corticosterone treatment. *Brain Res* **1102**, 12-26.

Smith DF & Toft DO (1993). Steroid receptors and their associated proteins. *Mol Endocrinol* **7**, 4-11.

Solit DB & Chiosis G (2008). Development and application of Hsp90 inhibitors. *Drug Discov Today* **13**, 38-43.

Solit DB & Rosen N (2006). Hsp90: a novel target for cancer therapy. *Curr Top Med Chem* **6**, 1205-1214.

Solit DB, Ivy SP, Kopil C, Sikorski R, Morris MJ, Slovin SF, Kelly WK, DeLaCruz A, Curley T, Heller G, Larson S, Schwartz L, Egorin MJ, Rosen N, & Scher HI (2007). Phase I trial of 17-allylamino-17-demethoxygeldanamycin in patients with advanced cancer. *Clin Cancer Res* **13**, 1775-1782.

Solit DB, Osman I, Polsky D, Panageas KS, Daud A, Goydos JS, Teitcher J, Wolchok JD, Germino FJ, Krown SE, Coit D, Rosen N, & Chapman PB (2008). Phase II trial of

17-allylamino-17-demethoxygeldanamycin in patients with metastatic melanoma. *Clin Cancer Res* **14**, 8302-8307.

Solit DB, Zheng FF, Drobnjak M, Munster PN, Higgins B, Verbel D, Heller G, Tong W, Cordon-Cardo C, Agus DB, Scher HI, & Rosen N (2002). 17-Allylamino-17-demethoxygeldanamycin induces the degradation of androgen receptor and HER-2/neu and inhibits the growth of prostate cancer xenografts. *Clin Cancer Res* **8**, 986-993.

Soutschek J, Akinc A, Bramlage B, Charisse K, Constien R, Donoghue M, Elbashir S, Geick A, Hadwiger P, Harborth J, John M, Kesavan V, Lavine G, Pandey RK, Racie T, Rajeev KG, Rohl I, Toudjarska I, Wang G, Wuschko S, Bumcrot D, Koteliansky V, Limmer S, Manoharan M, & Vornlocher HP (2004). Therapeutic silencing of an endogenous gene by systemic administration of modified siRNAs. *Nature* **432**, 173-178.

Sreedhar AS, Kalmar E, Csermely P, & Shen YF (2004). Hsp90 isoforms: functions, expression and clinical importance. *FEBS Lett* **562**, 11-15.

Srinivas PR, Verma M, Zhao Y, & Srivastava S (2002). Proteomics for cancer biomarker discovery. *Clin Chem* **48**, 1160-1169.

Srirangam A, Mitra R, Wang M, Gorski JC, Badve S, Baldridge L, Hamilton J, Kishimoto H, Hawes J, Li L, Orschell CM, Srour EF, Blum JS, Donner D, Sledge GW, Nakshatri H, & Potter DA (2006). Effects of HIV protease inhibitor ritonavir on Akt-regulated cell proliferation in breast cancer. *Clin Cancer Res* **12**, 1883-1896.

Stein CA & Cohen JS (1988). Oligodeoxynucleotides as inhibitors of gene expression: a review. *Cancer Res* **48**, 2659-2668.

Stommel JM, Kimmelman AC, Ying H, Nabioullin R, Ponugoti AH, Wiedemeyer R, Stegh AH, Bradner JE, Ligon KL, Brennan C, Chin L, & DePinho RA (2007). Coactivation of receptor tyrosine kinases affects the response of tumor cells to targeted therapies. *Science* **318**, 287-290.

Stupp R, Hegi ME, van den Bent MJ, Mason WP, Weller M, Mirimanoff RO, & Cairncross JG (2006). Changing paradigms--an update on the multidisciplinary management of malignant glioma. *Oncologist* **11**, 165-180.

Sun W, Xing B, Sun Y, Du X, Lu M, Hao C, Lu Z, Mi W, Wu S, Wei H, Gao X, Zhu Y, Jiang Y, Qian X, & He F (2007). Proteome analysis of hepatocellular carcinoma by two-dimensional difference gel electrophoresis: novel protein markers in hepatocellular carcinoma tissues. *Mol Cell Proteomics* **6**, 1798-1808.

Takahashi M, Hoshi A, Fujii J, Miyoshi E, Kasahara T, Suzuki K, Aozasa K, & Taniguchi N (1996). Induction of aldose reductase gene expression in LEC rats during the development of the hereditary hepatitis and hepatoma. *Jpn J Cancer Res* **87**, 337-341.

Takashi M, Zhu Y, Nakano Y, Miyake K, & Kato K (1992). Elevated levels of serum aldolase A in patients with renal cell carcinoma. *Urol Res* **20**, 307-311.

Takayama S, Reed JC, & Homma S (2003). Heat-shock proteins as regulators of apoptosis. *Oncogene* **22**, 9041-9047.

Takei Y, Kadomatsu K, Yuzawa Y, Matsuo S, & Muramatsu T (2004). A small interfering RNA targeting vascular endothelial growth factor as cancer therapeutics. *Cancer Res* **64**, 3365-3370.

Tatenhorst L, Rescher U, Gerke V, & Paulus W (2006). Knockdown of annexin 2 decreases migration of human glioma cells in vitro. *Neuropathol Appl Neurobiol* **32**, 271-277.

Thakkar D & Shervington A (2008). Proteomics: the tool to bridge the gap between the facts and fables of telomerase. *Crit Rev Oncog* **14**, 203-215.

Thoumine O, Ziegler T, Girard PR, & Nerem RM (1995). Elongation of confluent endothelial cells in culture: the importance of fields of force in the associated alterations of their cytoskeletal structure. *Exp Cell Res* **219**, 427-441.

Tong AW, Jay CM, Senzer N, Maples PB, & Nemunaitis J (2009). Systemic therapeutic gene delivery for cancer: crafting Paris' arrow. *Curr Gene Ther* **9**, 45-60.

Trog D, Fountoulakis M, Friedlein A, & Golubnitschaja O (2006). Is current therapy of malignant gliomas beneficial for patients? Proteomics evidence of shifts in glioma cells expression patterns under clinically relevant treatment conditions. *Proteomics* **6**, 2924-2930.

Tsaytler PA, Krijgsveld J, Goerdayal SS, Rudiger S, & Egmond MR (2009). Novel Hsp90 partners discovered using complementary proteomic approaches. *Cell Stress Chaperones* **14**, 629-638.

Tse AN & Schwartz GK (2004). Potentiation of cytotoxicity of topoisomerase i poison by concurrent and sequential treatment with the checkpoint inhibitor UCN-01 involves disparate mechanisms resulting in either p53-independent clonogenic suppression or p53-dependent mitotic catastrophe. *Cancer Res* **64**, 6635-6644.

Uchida H, Tanaka T, Sasaki K, Kato K, Dehari H, Ito Y, Kobune M, Miyagishi M, Taira K, Tahara H, & Hamada H (2004). Adenovirus-mediated transfer of siRNA against

survivin induced apoptosis and attenuated tumor cell growth in vitro and in vivo. *Mol Ther* **10**, 162-171.

Uehara Y, Hori M, Takeuchi T, & Umezawa H (1986). Phenotypic change from transformed to normal induced by benzoquinonoid ansamycins accompanies inactivation of p60src in rat kidney cells infected with Rous sarcoma virus. *Mol Cell Biol* **6**, 2198-2206.

van Veelen ML, Avezaat CJ, Kros JM, van PW, & Vecht C (1998). Supratentorial low grade astrocytoma: prognostic factors, dedifferentiation, and the issue of early versus late surgery. *J Neurol Neurosurg Psychiatry* **64**, 581-587.

Veltri RW, Partin AW, Epstein JE, Marley GM, Miller CM, Singer DS, Patton KP, Criley SR, & Coffey DS (1994). Quantitative nuclear morphometry, Markovian texture descriptors, and DNA content captured on a CAS-200 Image analysis system, combined with PCNA and HER-2/neu immunohistochemistry for prediction of prostate cancer progression. *J Cell Biochem Suppl* **19**, 249-258.

Vestling MM & Fenselau C (1994). Polyvinylidene difluoride (PVDF): an interface for gel electrophoresis and matrix-assisted laser desorption/ionization mass spectrometry. *Biochem Soc Trans* **22**, 547-551.

Vlassov AV, Korba B, Farrar K, Mukerjee S, Seyhan AA, Ilves H, Kaspar RL, Leake D, Kazakov SA, & Johnston BH (2007). shRNAs targeting hepatitis C: effects of sequence and structural features, and comparision with siRNA. *Oligonucleotides* **17**, 223-236.

Voellmy R & Boellmann F (2007). Chaperone regulation of the heat shock protein response. *Adv Exp Med Biol* **594**, 89-99.

Vorhies JS & Nemunaitis J (2007). Nonviral delivery vehicles for use in short hairpin RNA-based cancer therapies. *Expert Rev Anticancer Ther* **7**, 373-382.

Walsh CT, Garneau-Tsodikova S, & Gatto GJ, Jr. (2005). Protein posttranslational modifications: the chemistry of proteome diversifications. *Angew Chem Int Ed Engl* **44**, 7342-7372.

Wang HC, Liu CS, Chiu CF, Chiang SY, Wang CH, Wang RF, Lin CC, Tsai RY, & Bau DT (2009). Significant association of DNA repair gene Ku80 genotypes with breast cancer susceptibility in Taiwan. *Anticancer Res* **29**, 5251-5254.

Wang N, Butler JP, & Ingber DE (1993). Mechanotransduction across the cell surface and through the cytoskeleton. *Science* **260**, 1124-1127.

Wang X, Wang Q, & Lin H (2010). Correlation between clinicopathology and expression of heat shock protein 72 and glycoprotein 96 in human esophageal squamous cell carcinoma. *Clin Dev Immunol* **2010**, 212537.

Warburg (1956). On the origin of cancer cells. *Science* **123**, 309-314.

Wegele H, Muller L, & Buchner J (2004). Hsp70 and Hsp90--a relay team for protein folding. *Rev Physiol Biochem Pharmacol* **151**, 1-44.

Wegele H, Muschler P, Bunck M, Reinstein J, & Buchner J (2003). Dissection of the contribution of individual domains to the ATPase mechanism of Hsp90. *J Biol Chem* **278**, 39303-39310.

Weigel BJ, Blaney SM, Reid JM, Safgren SL, Bagatell R, Kersey J, Neglia JP, Ivy SP, Ingle AM, Whitesell L, Gilbertson RJ, Krailo M, Ames M, & Adamson PC (2007). A phase I study of 17-allylaminogeldanamycin in relapsed/refractory pediatric

patients with solid tumors: a Children's Oncology Group study. *Clin Cancer Res* **13**, 1789-1793.

Wen PY (2009). New developments in targeted molecular therapies for glioblastoma. *Expert Rev Anticancer Ther* **9**, 7-10.

Whiteley GR (2006). Proteomic patterns for cancer diagnosis--promise and challenges. *Mol Biosyst* **2**, 358-363.

Whitesell L & Lindquist SL (2005). HSP90 and the chaperoning of cancer. *Nat Rev Cancer* **5**, 761-772.

Whitesell L, Mimnaugh EG, De CB, Myers CE, & Neckers LM (1994). Inhibition of heat shock protein HSP90-pp60v-src heteroprotein complex formation by benzoquinone ansamycins: essential role for stress proteins in oncogenic transformation. *Proc Natl Acad Sci U S A* **91**, 8324-8328.

Wilkins MR, Sanchez JC, Gooley AA, Appel RD, Humphery-Smith I, Hochstrasser DF, & Williams KL (1996). Progress with proteome projects: why all proteins expressed by a genome should be identified and how to do it. *Biotechnol Genet Eng Rev* **13**, 19-50.

Wittwer M, Billeter R, Hoppeler H, & Fluck M (2004). Regulatory gene expression in skeletal muscle of highly endurance-trained humans. *Acta Physiol Scand* **180**, 217-227.

Wong KS & Houry WA (2006). Hsp90 at the crossroads of genetics and epigenetics. *Cell Res* **16**, 742-749.

Wood CG & Mulders P (2009). Vitespen: a preclinical and clinical review. *Future Oncol* **5**, 763-774.

Workman P, Burrows F, Neckers L, & Rosen N (2007). Drugging the cancer chaperone HSP90: combinatorial therapeutic exploitation of oncogene addiction and tumor stress. *Ann N Y Acad Sci* **1113**, 202-216.

Wu YC, Yen WY, Lee TC, & Yih LH (2009). Heat shock protein inhibitors, 17-DMAG and KNK437, enhance arsenic trioxide-induced mitotic apoptosis. *Toxicol Appl Pharmacol* **236**, 231-238.

Xie FY, Woodle MC, & Lu PY (2006). Harnessing in vivo siRNA delivery for drug discovery and therapeutic development. *Drug Discov Today* **11**, 67-73.

Yadav AK, Renfrow JJ, Scholtens DM, Xie H, Duran GE, Bredel C, Vogel H, Chandler JP, Chakravarti A, Robe PA, Das S, Scheck AC, Kessler JA, Soares MB, Sikic BI, Harsh GR, & Bredel M (2009). Monosomy of chromosome 10 associated with dysregulation of epidermal growth factor signaling in glioblastomas. *JAMA* **302**, 276-289.

Yamada O, Ikeda R, Ohkita Y, Hayashi R, Sakamoto K, & Akita O (2007). Gene silencing by RNA interference in the koji mold Aspergillus oryzae. *Biosci Biotechnol Bio chem* **71**, 138-144.

Yang J, Yang JM, Iannone M, Shih WJ, Lin Y, & Hait WN (2001). Disruption of the EF-2 kinase/Hsp90 protein complex: a possible mechanism to inhibit glioblastoma by geldanamycin. *Cancer Res* **61**, 4010-4016.

Yano M, Naito Z, Tanaka S, & Asano G (1996). Expression and roles of heat shock proteins in human breast cancer. *Jpn J Cancer Res* **87**, 908-915.

Yates JR, III, Carmack E, Hays L, Link AJ, & Eng JK (1999). Automated protein identification using microcolumn liquid chromatography-tandem mass spectrometry. *Methods Mol Biol* **112**, 553-569.

Yeoh EJ, Ross ME, Shurtleff SA, Williams WK, Patel D, Mahfouz R, Behm FG, Raimondi SC, Relling MV, Patel A, Cheng C, Campana D, Wilkins D, Zhou X, Li J, Liu H, Pui CH, Evans WE, Naeve C, Wong L, & Downing JR (2002). Classification, subtype discovery, and prediction of outcome in pediatric acute lymphoblastic leukemia by gene expression profiling. *Cancer Cell* **1**, 133-143.

Yi R, Qin Y, Macara IG, & Cullen BR (2003). Exportin-5 mediates the nuclear export of pre-microRNAs and short hairpin RNAs. *Genes Dev* **17**, 3011-3016.

Yokota S, Kitahara M, & Nagata K (2000). Benzylidene lactam compound, KNK437, a novel inhibitor of acquisition of thermotolerance and heat shock protein induction in human colon carcinoma cells. *Cancer Res* **60**, 2942-2948.

Young JC, Agashe VR, Siegers K, & Hartl FU (2004). Pathways of chaperone-mediated protein folding in the cytosol. *Nat Rev Mol Cell Biol* **5**, 781-791.

Yu JY, DeRuiter SL, & Turner DL (2002). RNA interference by expression of short-interfering RNAs and hairpin RNAs in mammalian cells. *Proc Natl Acad Sci U S A* **99**, 6047-6052.

Zaarur N, Gabai VL, Porco JA, Jr., Calderwood S, & Sherman MY (2006). Targeting heat shock response to sensitize cancer cells to proteasome and Hsp90 inhibitors. *Cancer Res* **66**, 1783-1791.

Zajchowski DA, Bartholdi MF, Gong Y, Webster L, Liu HL, Munishkin A, Beauheim C, Harvey S, Ethier SP, & Johnson PH (2001). Identification of gene expression profiles that predict the aggressive behavior of breast cancer cells. *Cancer Res* **61**, 5168-5178.

Zhang H, Kolb FA, Brondani V, Billy E, & Filipowicz W (2002). Human Dicer preferentially cleaves dsRNAs at their termini without a requirement for ATP. *EMBO J* **21**, 5875-5885.

Zhang MH, Lee JS, Kim HJ, Jin DI, Kim JI, Lee KJ, & Seo JS (2006). HSP90 protects apoptotic cleavage of vimentin in geldanamycin-induced apoptosis. *Mol Cell Biochem* **281**, 111-121.

Zhang W, Qiu XG, Chen BS, Li SW, Cui Y, Ren H, & Jiang T (2009). Antiangiogenic therapy with bevacizumab in recurrent malignant gliomas: analysis of the response and core pathway aberrations. *Chin Med J (Engl)* **122**, 1250-1254.

Zhang Y, Ye Y, Shen D, Jiang K, Zhang H, Sun W, Zhang J, Xu F, Cui Z, & Wang S (2010). Identification of transgelin-2 as a biomarker of colorectal cancer by laser capture microdissection and quantitative proteome analysis. *Cancer Sci* **101**, 523-529.

Zhao ZG, Ma QZ, & Xu CX (2004). Abrogation of heat-shock protein (HSP)70 expression induced cell growth inhibition and apoptosis in human androgen-independent prostate cancer cell line PC-3m. *Asian J Androl* **6**, 319-324.

Zhong W, Oberley LW, Oberley TD, & St Clair DK (1997). Suppression of the malignant phenotype of human glioma cells by overexpression of manganese superoxide dismutase. *Oncogene* **14**, 481-490.

Zieker D, Konigsrainer I, Tritschler I, Loffler M, Beckert S, Traub F, Nieselt K, Buhler S, Weller M, Gaedcke J, Taichman RS, Northoff H, Brucher BL, & Konigsrainer A (2010). Phosphoglycerate kinase 1 a promoting enzyme for peritoneal dissemination in gastric cancer. *Int J Cancer* **126**, 1513-1520.

Zou J, Guo Y, Guettouche T, Smith DF, & Voellmy R (1998). Repression of heat shock transcription factor HSF1 activation by HSP90 (HSP90 complex) that forms a stress-sensitive complex with HSF1. *Cell* **94**, 471-480.

References for internet links

Ensemble. Hsp90 intron/extron structure (Accessed online, 2009).

Cancer Research, UK. Statistics and outlook for brain tumours (Accessed online, 2010).

The University of Vermount, USA. Standard haemocytometer chamber (Accessed online, 2009).

Sigma Aldrich, UK. siRNA and shRNA pathways (Accessed online, 2009).

Gene Cards. Hsp90α summary page (Accessed online, 2010).

National Centre for Biotechnology Information. Hsp90α summary page (Accessed online, 2009).

Primer3 Plus. Hsp90α primers (Accessed online, 2007).

European Bioinformatic Institute. ClustalW2 Multiple Sequence Alignment (Accessed online, 2008).

Origene. pGFP-V-RS vector map (Accessed online, 2008).

UniProt. EIF3K summary page (Accessed online, 2010).

Gene Cards. Manganese superoxide dismutase summary page (Accessed online, 2010).

National Centre for Biotechnology Information. Transgelin 2 summary page (Accessed online, 2010).

National Centre for Biotechnology Information. Collagen alpha-1 (IV) chain summary page (Accessed online, 2010).

Gene Cards. Apoptosis linked gene 2 summary page (Accessed online, 2010).

Appendix

List of Publications:

Cruickshanks N, Shervington L, Patel R, Munje C, Thakkar D, & Shervington A (2010). Can hsp90alpha-targeted siRNA combined with TMZ be a future therapy for glioma? *Cancer Invest* **28**, 608-614.

List of Abstracts/Conference Proceedings:

Munje C, Mehta A, Shervington L, & Shervington A (2010). Could mimicking cell death be a future treatment for cancer? Faculty of Science Scientific Proceedings **7**: UCLAN

Mehta A, Munje C, Shervington L, & Shervington A (2010). Can we crack the code of caner? Faculty of Science Scientific Proceedings **7**: UCLAN

Munje C, Shervington A, Dawson T & Shervington L (2009). Can *hsp90α* be a potential target in glioma therapy? Faculty of Science Scientific Proceedings **6**: UCLAN